An Investigation into *Helicobacter pylori* Treatment Outcomes and Host Responses

Thesis submitted to the University of Dublin,
Trinity College for the Degree of Doctor of Philosophy

by Rebecca FitzGerald
Supervised by Dr Sinéad Smith

School of Medicine

2024

Declaration of authorship

I declare that details provided above are true and correct.

I declare that this thesis has not been submitted as an exercise for a degree at this or any other university and it is entirely my own work.

I agree to deposit this thesis in the University's open access institutional repository or allow the library to do so on my behalf, subject to Irish Copyright Legislation and Trinity College Library conditions of use and acknowledgement.

Signed: _____ Date: _____

Abstract

Helicobacter pylori (*H. pylori*) is a helical, gram-negative, micro-aerophilic bacterium that infects approximately 50% of the world's population. Although many of those infected will be asymptomatic, *H. pylori* increases the risk of developing peptic ulcers, gastric cancer, and mucosa-associated lymphoid tissue (MALT) lymphoma. *H. pylori* is heavily adapted to colonise the stomach and will persist continuously unless treated. The emergence of antibiotic resistant strains has made treating *H. pylori* more complicated. The European registry on *H. pylori* management (Hp-EuReg) was founded in 2013 to collect real-world clinical treatment and eradication data from 30 different countries across Europe. In Chapter 3, an audit of Irish data in the Hp-EuReg was performed to evaluate *H. pylori* treatment regimens and eradication rates from 2013-2022. Using the modified intention-to-treat (mITT) protocol, 1,000 first line treatments were analysed, with an overall eradication rate of 80.1%. The most prescribed first line treatment was clarithromycin and amoxicillin triple therapy with an eradication rate of 81.4%. Increased treatment duration and high dose PPI were associated with better first line eradication rates. Furthermore, first-line eradication rates significantly increased from 74.5% to 81.6% following publication of the Irish guidelines on the management of *H. pylori* in 2017. The overall eradication rates for second line and rescue therapies were 64.4% (N=90) and 61.9% (N=21), respectively.

Host-directed therapies are treatments that alter the host's biological pathways. To identify potential targets for host-directed therapies, host-pathogen interactions need to be better understood. The aim of Chapter 4 was to investigate the role of the Notch signalling pathway during *H. pylori* infection. The Notch pathway is a highly conserved signalling pathway that participates in cell proliferation, maintenance, and differentiation. It was found that *H. pylori* infection led to downregulated mRNA expression of the Notch associated transcription factor *HES1* in gastric epithelial cells and

gastric biopsy tissue. HES1 protein was also downregulated in gastric epithelial cells infected with *H. pylori*. HES1 was over-expressed in gastric epithelial cells and RNAseq was performed. This identified further genes that are impacted by *H. pylori* mediated *HES1* downregulation, such as *FOS*, *IL-8,* and *CCL20*. In macrophages, *H. pylori* infection was associated with an increase in the expression for the Notch ligands *JAG1* and *DLL4* and the associated transcription factor *HEY1*. These results indicate a cell specific role for Notch signalling factors during *H. pylori* infection.

The aim of Chapter 5 was to investigate the role of histone modifying components and inflammatory caspases in *H. pylori* infection. *H. pylori* down-regulated expression of the polycomb repressive complex 2 component *EED* and upregulated expression of the histone demethylase *KDM6B* in gastric epithelial cells, gastric biopsy tissue and in macrophages. Caspase 4 is an inflammatory caspase that is associated with production of the non-canonical inflammasome. Infection with *H. pylori* led to an increase in *Caspase4* expression in human macrophages. Caspase-11 is the murine homolog of human Caspase 4. Bone marrow derived macrophages from wild-type and caspase 11-deficient ($Casp11^{-/-}$) mice were infected with *H. pylori*. The $Casp11^{-/-}$ cells produced less IL-1ß indicating that Caspase-11 contributes to IL-1ß production in mouse macrophages infected with *H. pylori*.

The main findings of this thesis are that current *H. pylori* treatment regimens are not sufficient to reach the recommended eradication rate of >90% and alternative treatment strategies should be considered in the Irish context. In relation to host-pathogen interactions, *H. pylori*-mediated regulation of the Notch signalling pathway, histone modifying components and inflammatory caspases was identified. Further research into these pathways is warranted.

Acknowledgements

I would like to thank and acknowledge the work of the many people without whom this thesis would not have been possible.

Firstly, I would like to thank my amazing supervisor Dr. Sinéad Smith, who has been such a wonderful mentor throughout the whole process. I have learnt so much working with you. Thank you for your kindness, patience and understanding even when things didn't always go as planned!

I acknowledge the Provost's PhD Project Awards and the TTMI Building Engagements in Health Research Award for funding this project and allowing me to undertake this research.

My sincerest thanks to all the patients who contributed to this study, including those whose data was analysed as part of Hp-EuReg and those who consented to give biopsy tissue to research.

I also wish to thank all the members of the Trinity Academic Gastroenterology Group and in particular, Prof. Deirdre McNamara. Her enthusiasm for research was great motivation (especially during lockdowns)! I would also like to give my appreciation to the TAGG gastroenterologists who collected biopsy samples used in this thesis.

I would like to acknowledge Dr. TJ Butler and Rita Douglas, for all their assistance, from making sure deliveries were collected to organising the TAGG meetings and chatting about our experiments. They also made for great travel companions to conferences in Barcelona, Glasgow, and Vienna. We always managed to sneak in a bit of sightseeing and a lot of coffee and cake!

I would like to thank the members of Prof. Joseph Keane's research group for letting me use their lab space and equipment. In particular, I would like to thank Dr. Mary O' Sullivan for helping me with any questions I had while using the lab in TTMI. I would like to thank Dr. Ewelina Flis and Dr. Michael Freely for their help performing the western blots for Caspase-11 and HES1 respectively. I would like to thank Dr. TJ Butler for his help with uploading HP-EuReg data to the Redcap database and for his help with the pathway enrichment analysis.

Finally, I would like to thank my family and friends for their support and for kindly showing interest in my research. I'm sure you know much more about gut bacteria than any of you ever wanted! I would particularly like to thank my parents Susan and John and my brothers Seán and Ben for being amazingly supportive and encouraging over the past four and a half years!

Thesis Outputs

Book Chapters

- **FitzGerald, R**. and S. M. Smith (2021). 'An Overview of *Helicobacter pylori* Infection' Methods in Molecular Biology (Clifton, NJ) 2283: 1-14.

- **FitzGerald, R**., Devapal, M., Hickey, J, J., McNamara, D., Kelleher, D., Smith, S, M. (2021). 'Purification of Total RNA from Stomach Tissue Biopsies' Methods in Molecular Biology' (Clifton, NJ) 2283: 51-59.

- **FitzGerald, R**., Sinha, C., Yadegar, A., Smith, M, S. (2021). '*Helicobacter pylori* Virulence Factor Genotyping' Methods in Molecular Biology (Clifton, NJ) 2283: 93-106.

Journal article

- **Zaslona, Z**., Flis, E., Nulty, C., Kearney, J., FitzGerald, R., Douglas, A, R., McNamara, D., Smith, S., O'Neill, L, A, J., Creagh, E, M. (2020). 'Caspase-4: A Therapeutic Target for Peptic Ulcer Disease.' ImmunoHorizons 4(10): 627-633.

Presentations

- United European Gastroenterology Week - Barcelona - October 2019 - Oral presentation - Travel grant - National Scholar award "*Helicobacter pylori* Infection Inhibits Notch Signalling in Gastric Epithelial Cells and the Gastric Mucosa".

- Irish Society of Gastroenterology - Dublin - November 2019 - Oral presentation "*Helicobacter pylori* Infection Inhibits Notch Signalling in Gastric Epithelial Cells and the Gastric Mucosa".

- European Helicobacter and Microbiota Study Group - Virtual - September 2020 - ePoster presentation "*Helicobacter pylori* alters expression of Notch pathway components in gastric epithelial cells and macrophages in a cell type- specific manner".

- European Helicobacter and Microbiota Study Group - Virtual - September 2020 - ePoster presentation "Clarithromycin resistance is more common among less virulent *Helicobacter pylori* strains – Data from an Irish centre".United European

- Gastroenterology Week – Virtual - October 2020 - ePoster presentation "Clarithromycin resistance is more common among less virulent Helicobacter pylori strains – Data from an Irish centre".

- European Helicobacter and Microbiota Study Group - Virtual - September 2021 - ePoster presentation "Inhibition of Polycomb Repressive Complex 2 expression and function by *Helicobacter pylori*".

- United European Gastroenterology week - Virtual - October 2021 - ePoster presentation "Helicobacter pylori infection inhibits expression and function of the Polycomb Repressive Complex 2".

- Host Pathogen Communication - Dublin/Virtual - November 2021- ePoster presentation "Inhibition of Polycomb Repressive Complex 2 expression and function by *Helicobacter pylori*".

- Irish Society of Gastroenterology – Dublin/Virtual - December 2021 - Oral presentation "*Helicobacter pylori* Infection Alters Expression of Histone Modification Complex Components".

- Irish Society of Gastroenterology - Belfast - June 2022 - Oral presentation "The Notch pathway transcription factor HES1 regulates expression of the pro-inflammatory cytokine IL-8 during *H. pylori* infection".

- European Helicobacter and Microbiota Study Group - Glasgow - September 2022 - Poster presentation "The Notch pathway transcription factor HES1 regulates expression of the pro-inflammatory cytokine IL-8 during *H. pylori* infection".

- United European Gastroenterology week - Vienna - October 2022 - Moderated poster presentation - Travel grant "The Notch pathway transcription factor HES1 regulates expression of the pro-inflammatory cytokine IL-8 during *H. pylori* infection".

- Irish Society of Gastroenterology - Dublin - November 2022 - Poster presentation - 2nd place prize in audit category "An Audit of First-Line *H. pylori* Treatments and Outcomes from 2019-2021 in Tallaght University Hospital".

Table of Contents

CHAPTER ONE INTRODUCTION 1

1.1. *HELICOBACTER PYLORI* 1
1.2. DISCOVERY OF *H. PYLORI* 2
1.3. STRUCTURE AND VIRULENCE FACTORS OF *H. PYLORI* 3
1.3.1. CAGA 6
1.3.2. VACA 6
1.4. TRANSMISSION OF *H. PYLORI* 8
1.5. PREVALENCE OF *H. PYLORI* 9
1.5.1. PREVALENCE IN EUROPE 10
1.5.2. PREVALENCE IN ASIA AND OCEANIA 12
1.5.3. PREVALENCE IN THE AMERICAS 12
1.5.4. PREVALENCE IN AFRICA 13
1.6. DIAGNOSIS OF *H. PYLORI* 14
1.6.1. NON-INVASIVE DIAGNOSIS OF *H. PYLORI* 15
1.6.1.1. UREA BREATH TEST 15
1.6.1.2. STOOL ANTIGEN TEST 15
1.6.1.3. SEROLOGY 16
1.6.2. INVASIVE DIAGNOSIS OF *H. PYLORI* 17
1.6.2.1. RAPID UREASE TEST 17
1.6.2.2. HISTOLOGY 17
1.6.2.3. CULTURE 18
1.7. TREATMENT FOR *H. PYLORI* INFECTION 19
1.7.1. *H. PYLORI* TREATMENT OPTIONS 19
1.7.2. THE MOST UP-TO-DATE TREATMENT RECOMMENDATIONS 22
1.7.3. THE BENIFITS OF *H. PYLORI* ERADICATION 24
1.7.4. ISSUES WITH THE CURRENT TREATMENT PLANS 25
1.7.5. *H. PYLORI* ANTIBIOTIC RESISTANCE 26
1.7.5.1. ANTIBIOTIC SUSCEPTIBILITY TESTING – CULTURE 27
1.7.5.2. ANTIBIOTIC SUSCEPTIBILITY TESTING – PCR 30
1.7.5.3. ANTIBIOTIC SUSCEPTIBILITY TESTING - NEXT GENERATION SEQUENCING 31
1.8. *H. PYLORI* AND THE INNATE IMMUNE RESPONSE 32

1.8.1. *H. PYLORI* INFECTION RECRUITS MACROPHAGES 32
1.8.2. *H. PYLORI* CAN EVADE THE HOST IMMUNE RESPONSE. 33
1.8.3. *H. PYLORI* AND CYTOKINE RESPONSE 33
1.8.4. *H. PYLORI* AND TLRS 34
1.8.5. *H. PYLORI* AND NLRS 36
1.9. *H. PYLORI* AND THE ADAPTIVE IMMUNE RESPONSE 37
1.10. *H. PYLORI* AND THE MICROBIOME 39
1.11. HOST-DIRECTED THERAPIES 40
1.12. SUMMARY 42
1.13. AIMS AND OBJECTIVES. 43

CHAPTER TWO MATERIALS AND METHODS 44

2.1. HP-EUREG METHODS 44
2.1.1. NATIONAL COORDINATORS AND RECRUITING INVESTIGATORS. 44
2.1.2. DATA EXTRACTION AND ANALYSIS 45
2.1.3. ANALYSIS OF TREATMENT EFFECTIVENESS 45
2.2. *H. PYLORI* 46
2.2.1. GROWTH OF *H. PYLORI* 46
2.2.2. *H. PYLORI* LPS 47
2.2.3. PREPARATION OF HEAT-KILLED *H. PYLORI* 47
2.3. CELL CULTURE 48
2.3.1. CULTURE CONDITIONS 48
2.4. IN VITRO INFECTION WITH *H. PYLORI* 51
2.4.1. SEEDING CELLS 51
2.4.2. PREPARATION OF *H. PYLORI* 52
2.4.3. TREATMENT OF CELLS WITH HEAT-KILLED *H. PYLORI, H. PYLORI* LPS OR *E. COLI* LPS 53
2.4.4. TREATMENT OF CELLS WITH A Γ-SECRETASE INHIBITOR 54
2.4.5. STIMULATION OF CELLS WITH NOTCH LIGAND 54
2.4.6. INHIBITION OF PROTEIN SYNTHESIS USING CYCLOHEXIMIDE PRE-TREATMENT 54
2.5. CELL TRANSFECTION 55
2.5.1. RNA INTERFERENCE 55

2.5.2. PLASMID DNA TRANSFECTION 56
2.5.2.1. TRANSFORMATION OF *E. COLI* WITH PLASMID DNA 56
2.5.2.2. PLASMID PURIFICATION 56
2.5.2.3. AGS CELL TRANSFECTION WITH PLASMID DNA 58
2.6. PATIENT RECRUITMENT FOR GASTRIC BIOPSY TISSUE ANALYSIS 59
2.7. RNA ANALYSIS 60
2.7.1. SAMPLE COLLECTION FOR RNA PURIFICATION 60
2.7.2. CELL LYSIS AND RNA PURIFICATION 60
2.8. RNA QUANTIFICATION 62
2.8.1. RNA QUANTIFICATION USING THE NANODROP 2000 SPECTROPHOTOMETER 62
2.8.2. RNA QUANTIFICATION USING THE QUBIT FLUOROMETER 62
2.8.3. CDNA SYNTHESIS BY REVERSE TRANSCRIPTION (RT) 63
2.8.4. GENE EXPRESSION ANALYSIS BY QPCR 63
2.9. RNASEQ 67
2.9.1. SAMPLE DESCRIPTION 67
2.9.2. LIBRARY PREPARATION AND RNASEQ 68
2.9.3. RNASEQ DATA ANALYSIS 68
2.9.4. DIFFERENTIAL GENE EXPRESSION 71
2.9.5. PATHWAY ANALYSIS 72
2.10. PROTEIN ANALYSIS 73
2.10.1. PREPARATION OF PROTEIN LYSATES 73
2.10.2. SDS POLYACRYLAMIDE GEL ELECTROPHORESIS AND WESTERN BLOT 73
2.10.3. ENZYME-LINKED IMMUNOSORBENT ASSAY 75
2.11. STATISTICAL ANALYSIS 76
2.11.1. STATISTICAL ANALYSIS OF HP-EUREG DATA 76
2.11.2. THE COMPARATIVE CT METHOD FOR GENE EXPRESSION ANALYSIS AND STATISTICS FOR QPCR 76

CHAPTER THREE ANALYSIS OF IRISH DATA IN THE HP-EUREG 78

3.1. INTRODUCTION 78
3.1.1. THE HP-EUREG COLLECTS DATA ON THE MANAGEMENT OF *H. PYLORI* IN EUROPE 78

3.1.2. In 2017 the Irish *H. pylori* Working Group published guidelines for the management of *H. pylori* in Ireland 79
3.1.3. How do Irish guidelines differ from the most recent European guidelines? 81
3.1.4. How can eradication rates be improved in the absence of new treatments? 82
3.2. Aims and objectives. 83
3.3. First line treatment results 84
3.3.1. Treatment-naïve patient characteristics 84
3.3.2. Most treatment-naïve patients were diagnosed with *H. pylori* by an invasive test 85
3.3.3. The duration of first line treatment prescribed increased between 2013-2022 86
3.3.4. The potency of the PPI prescribed in first line treatment increased between 2013-2022 88
3.3.5. Publication of the IHPWG guidelines on the management of *H. pylori* infection led to a significant change in prescription patterns in relation to treatment duration and PPI dose 91
3.3.6. The most prescribed first line treatment was clarithromycin amoxicillin triple therapy 92
3.3.7. The modified intention-to-treat protocol was chosen for eradication analysis in this study. 96
3.3.8. First line treatment effectiveness varies depending on treatment regimen. 97
3.3.8.1. Increased duration of treatment impacted eradication rates for the better. 99
3.3.9. Higher dose PPI impacted eradication rates for the better. 101
3.3.10. The eradication rate improved following the introduction of the Irish guidelines in 2017. 102
3.4. Second line treatment results 105
3.4.1. Second line patient characteristics 105
3.4.2. Most patients were diagnosed with *H. pylori* by an invasive test. 106

3.4.3. THE DURATION OF TREATMENT AND DOSE OF PPI PRESCRIBED IN SECOND LINE TREATMENT INCREASED FOLLOWING THE PUBLICATION OF THE IHPWG GUIDELINES.. 107
3.4.4. THE MOST PRESCRIBED SECOND LINE TREATMENT WAS TRIPLE THERAPY WITH AMOXICILLIN AND LEVOFLOXACIN. 108
3.4.5. SECOND LINE TREATMENT EFFECTIVENESS VARIED DEPENDING ON TREATMENT REGIMEN. 109
3.4.6. LONGER DURATION OF TREATMENT AND HIGHER PPI DOSE WAS NOT ASSOCIATED WITH IMPROVED ERADICATION RATES WITH SECOND LINE THERAPIES..110
3.4.7. THE ERADICATION RATE FOR SECOND LINE TREATMENTS DID NOT IMPROVE FOLLOWING THE INTRODUCTION OF THE IRISH GUIDELINES IN 2017. 113
3.5. RESCUE TREATMENT RESULTS 114
3.5.1. RESCUE TREATMENT PATIENT CHARACTERISTICS. 114
3.5.2. MOST PATIENTS WERE DIAGNOSED WITH *H. PYLORI* BY AN INVASIVE TEST.... 115
3.5.3. THE MOST PRESCRIBED RESCUE TREATMENT WAS BISMUTH QUADRUPLE THERAPY. 116
3.5.4. RESCUE TREATMENT EFFECTIVENESS VARIES DEPENDING ON TREATMENT REGIMEN. 116
3.5.5. REDUCED ERADICATION RATES WERE OBSERVED WITH RESCUE THERAPY..... 118
3.5.6. ERADICATION RATES DECREASED ACCORDING TO THE NUMBER OF THERAPIES. 119
3.6. DISCUSSION 121
3.7. LIMITATIONS OF STUDY 126
3.8. SUMMARY OF CONCLUSIONS 127
3.9. FUTURE WORK 128

CHAPTER FOUR INVESTIGATING THE ROLE OF THE NOTCH SIGNALLING PATHWAY DURING *H. PYLORI* INFECTION.....129

4.1. INTRODUCTION TO NOTCH SIGNALLING 129
4.1.1. THE NOTCH SIGNALLING PATHWAY. 129
4.1.2. HOW DOES THE NOTCH PATHWAY FUNCTION? 129
4.1.3. IMPORTANT NOTCH TARGET GENES. 132
4.1.4. WHAT HAPPENS WHEN NOTCH SIGNALLING IS DYSREGULATED? 132
4.2. HYPOTHESIS 134

4.3. AIMS AND OBJECTIVES 135

4.4. *H. PYLORI* INFECTION ALTERS EXPRESSION OF *HES1* IN THE GASTRIC EPITHELIUM. 136

4.4.1. *H. PYLORI* ALTERS THE EXPRESSION OF NOTCH PATHWAY COMPONENTS IN AGS GASTRIC EPITHELIAL CELLS. 136

4.4.2. *H. PYLORI* DECREASES EXPRESSION OF *JAG2*, *HES1* AND *HEY1* IN THE GASTRIC MUCOSA OF INFECTED PATIENTS. 142

4.4.3. *H. PYLORI* INFECTION DECREASES EXPRESSION OF THE HES1 PROTEIN IN AGS GASTRIC EPITHELIAL CELLS. 146

4.4.4. *H. PYLORI* VIRULENCE FACTORS CAGA AND VACA ARE NOT REQUIRED FOR THE *H. PYLORI*-MEDIATED DOWN-REGULATION OF *HES1* MRNA EXPRESSION. 148

4.4.5. *H. PYLORI* LPS DOES NOT SUPPRESS *HES1* MRNA EXPRESSION IN MKN45 CELLS. 150

4.4.6. NEW PROTEIN SYNTHESIS IS REQUIRED FOR THE *H. PYLORI* -MEDIATED DOWN-REGULATION OF HES1 MRNA EXPRESSION IN AGS GASTRIC EPITHELIAL CELLS 152

4.4.7. Γ-SECRETASE INHIBITION OF NOTCH SIGNALLING DID NOT ENHANCE *H. PYLORI*-MEDIATED *HES1* DOWN-REGULATION IN AGS GASTRIC EPITHELIAL CELLS . 154

4.4.8. *HES1* RNAI DID NOT SUFFICIENTLY ENHANCE *H. PYLORI*-MEDIATED *HES1* DOWN-REGULATION IN AGS CELLS 157

4.4.9. STIMULATION WITH A JAG2 LIGAND WAS NOT SUFFICIENT TO INCREASE NOTCH SIGNALLING IN AGS GASTRIC EPITHELIAL CELLS 159

4.4.10. OVER-EXPRESSION OF *HES1* IN AGS CELLS WAS SUCCESSFULLY ACHIEVED BY PLASMID DNA TRANSFECTION 161

4.5. EVALUATION OF GENOME-WIDE RESPONSES TO *H. PYLORI* BY RNASEQ WITH AND WITHOUT HES1 OVEREXPRESSION 163

4.5.1. PCA PLOTS CLUSTERED THE DUPLICATE RNA-SEQ SAMPLES TOGETHER. 163

4.5.2. RNA-SEQ ANALYSIS OF UN-TRANSFECTED AGS CELLS CONFIRMS CHANGES IN GENE EXPRESSION CHARACTERISTIC OF *H. PYLORI* INFECTION AND IDENTIFIES NEW *H. PYLORI*-REGULATED GENES 165

4.5.3. PATHWAY ENRICHMENT ANALYSIS DEMONSTRATED GENES INVOLVED IN CYTOKINE-CYTOKINE RECEPTOR INTERACTION AND IL-17 SIGNALLING ARE REGULATED IN AGS CELLS DURING *H. PYLORI* INFECTION 169

4.5.4. RNASEQ CONFIRMED OVER-EXPRESSION OF HES1 IN THE HES1 PLASMID-TRANSFECTED CELLS. 173

4.5.5. OVER-EXPRESSION OF HES1 IN AGS CELLS LED TO CHANGES IN GENE EXPRESSION IN UNINFECTED CELLS 175
4.5.6. GENOME WIDE CHANGES IN GENE EXPRESSION IN *H. PYLORI* INFECTED AGS CELLS DUE TO INCREASED HES1 EXPRESSION 179
4.5.7. HES1 SELECTIVELY ENHANCED CYTOKINE INDUCTION IN AGS CELLS IN RESPONSE TO *H. PYLORI* 185
4.5.8. RNASEQ IDENTIFIED ADDITIONAL GENES THAT HES1 MODIFIED DURING *H. PYLORI* INFECTION 187
4.6. *H. PYLORI* INFECTION ALTERS THE EXPRESSION OF NOTCH PATHWAY COMPONENTS IN MACROPHAGES 192
4.6.1. HEAT KILLED AND LIVE *H. PYLORI* ALTER THE EXPRESSION OF *JAG1*, *DLL4* AND *HEY1* IN MACROPHAGES. 192
4.6.2. NEW PROTEIN SYNTHESIS IS REQUIRED FOR *H. PYLORI* MEDIATED INDUCTION OF *DLL4* IN THP-1 MACROPHAGES, BUT NOT FOR *JAG1* AND *HEY1* INDUCTION 195
4.6.3. LPS CAN ALTER THE EXPRESSION *JAG1* AND *DLL4* IN MACROPHAGES. 198
4.7. DISCUSSION 201
4.7.1. *H. PYLORI* DOWNREGULATES HES1 IN THE GASTRIC EPITHELIUM 201
4.7.2. EVALUATION OF GENOME-WIDE RESPONSES TO *H. PYLORI* BY RNASEQ WITH AND WITHOUT HES1 OVEREXPRESSION 206
4.7.2.1. GLOBAL CHANGES IN GENE EXPRESSION IN AGS CELLS IN RESPONSE TO *H. PYLORI* 206
4.7.2.2. HES1 OVER-EXPRESSION REGULATES GENE EXPRESSION IN AGS CELLS .. 210
4.7.2.3. HES1 OVER-EXPRESSION ENHANCES *H. PYLORI*-MEDIATED-UP-REGULATION OF *FOS*, *IL-8* AND *CCL20* IN AGS CELLS 210
4.7.3. *H. PYLORI* INFECTION LED TO UPREGULATION OF *JAG1*, *DLL4* AND *HEY1* IN MACROPHAGES 212
4.8. SUMMARY OF CONLUSIONS 215
4.9. FUTURE WORK 216

CHAPTER FIVE INVESTIGATING THE ROLES OF HISTONE MODIFICATION PROTEINS AND INFLAMMATORY CASPASES DURING *H. PYLORI* INFECTION 217

5.1. INTODUCTION 217
5.1.1. INTRODUCTION TO EPIGENETICS 217

5.1.1.1. How is DNA packaged in the nucleus? 218
5.1.1.2. How does chromatin arrangement impact gene expression? 220
5.1.1.3. Polycomb Group Proteins 222
5.1.1.4. The histone lysine demethylase KDM6B 223
5.1.1.5. Histone modification during *H. pylori* infection 224
5.1.2. Introduction to the Caspase Family 224
5.1.2.1. Caspases and Apoptosis 225
5.1.2.2. Caspases and inflammation 227
5.1.2.3. Inflammasome Complexes 227
5.1.2.4. The non-canonical inflammasome 228
5.1.2.5. Pyroptosis 229
5.1.2.6. IL-1B and *H. pylori* infection 231
5.2. Hypothesis 232
5.3. Aims and Objectives 233
5.4. *H. pylori* Alters the Expression of Histone Modifying Componants 234
5.4.1. *H. pylori* alters the expression of PRC2 components in MKN45 cells 234
5.4.2. Live and heat-killed *H. pylori* alter the expression of the histone demethylase KDM6B in AGS cells 236
5.4.3. *H. pylori* infection is associated with a decrease in *EED* and increase in *KDM6B* in gastric biopsy tissue. 238
5.4.4. New protein synthesis is not required for the *H. pylori*-mediated induction of *KDM6B* in AGS cells 240
241
5.4.5. Live and heat-killed *H. pylori* alter the expression of histone modification components in THP-1 cells 242
5.4.6. Treatment of THP-1 cells with *H. pylori* LPS does not impact PRC2 expression as much as live *H. pylori* 245
5.4.7. New protein synthesis is not required for the *H. pylori*-mediated induction of *KDM6B* in THP-1 cells. 247
5.5. Caspase-11 contributes to IL-1B expression in *H. pylori* infected BMDMs 249
5.5.1. Caspase-4 mRNA expression in gastric epithelial cells and the gastric mucosa is not altered by H. pylori infection. 249

5.5.2. *CASPASE-4* IS UPREGULATED IN MACROPHAGES INFECTED WITH *H. PYLORI*. 251
5.5.3. CASPASE-11 CONTRIBUTES TO IL-1B PRODUCTION IN MURINE MACROPHAGES....253
5.6. DISCUSSION 257
5.6.1. *H. PYLORI* INFECTION DECREASES *EED* EXPRESSION IN GASTRIC EPITHELIAL CELLS, THE GASTRIC MUCOSA, AND THP-1 MACROPHAGES.... 257
5.6.2. *H. PYLORI* INDUCES EXPRESSION OF *KDM6B* IN GASTRIC EPITHELIAL CELLS, THE GASTRIC EPITHELIUM, AND MACROPHAGES.... 259
5.6.3. CASPASE-11 PLAYS A ROLE IN IL-1B EXPRESSION IN *H. PYLORI* INFECTED BMDMS.... 261
5.7. SUMMARY OF CONCLUSIONS 265
5.8. FUTURE WORK....266

CHAPTER SIX GENERAL DISCUSSION....268

6.1. INTRODUCTION 268
6.2. CURRENTLY THE MANAGEMENT OF *H. PYLORI* IN IRELAND FALLS SHORT OF THE RECOMMENDED ERADICATION RATE 269
6.3. *H. PYLORI* DISEASE PROGRESSION IS CORRELATED WITH INFLAMMATION. 272
6.4. *H. PYLORI* ALTERS EXPRESSION OF NOTCH PATHWAY COMPONENTS IN A CELL TYPE SPECIFIC MANNER. 273
THE NOTCH SIGNALLING PATHWAY IS A HIGHLY CONSERVED SIGNALLING PATHWAY....273
6.5. *H. PYLORI* INFECTION DECREASES EXPRESSION OF *EED* AND INCREASES EXPRESSION OF *KDM6B.* 275
6.6. CASPASE-11 IS INVOLVED IN *H. PYLORI* MEDIATED UPREGULATION IN IL-1B. .277
6.7. FUTURE DIRECTIONS 278
6.8. FINAL CONCLUSIONS 280
APPENDIX 298

List of Figures

Figure 1.1 *H. pylori* structure and virulence factors.. 4
Figure 1.2 Disease progression from superficial gastritis to carcinoma is influenced by the host, pathogen and environmental stimuli..... 5
Figure 1.3 Global prevalence of *H. pylori* 10
Figure 1.4 Flow-chart of recommended *H. pylori* treatment options.. 23
Figure 1.5 Rates of *H. pylori* resistance to clarithromycin globally. 27
Figure 1.6 Culture-based methods of antibiotic resistance testing. .. 29
Figure 1.7 The main types of host-directed therapies. 41
Figure 2.1 Cells were counted using a hemocytometer. 52
Figure 2.2 Overview of RT-qPCR methods for gene expression analysis 66
Figure 2.3 RNAseq data analysis overview. 69
Figure 3.1 Countries taking part in the HP-EuReg are coloured in grey. 79
Figure 3.2 Duration of first line treatment prescribed to treatment-naïve patients. 87
Figure 3.3 Percentage of first line prescriptions per year according to duration of treatment. 88
Figure 3.4 PPI potency of first line treatments prescribed to treatment-naïve patients. 89
Figure 3.5 Percentage first line treatments per year broken down by PPI potency. 90
Figure 3.6 Breakdown of treatment regimens as a percentage of all first-line treatments prescribed each year. 95
Figure 3.7 Percentage treatment success and failure broken down by treatment regimen. 99
Figure 3.8 Percentage treatment success and failure broken down by length of treatment. 100

FIGURE 3.9 PERCENTAGE TREATMENT SUCCESS AND FAILURE BROKEN DOWN BY PPI DOSE. 102
FIGURE 3.10 PERCENTAGE TREATMENT SUCCESS AND FAILURE BROKEN DOWN BY YEAR. 104
FIGURE 3.11 TOTAL PERCENTAGE ERADICATION RATE AND PERCENTAGE ERADICATION RATE OF TRIPLE-C+A THERAPY FROM 2013-2022..... 104
FIGURE 3.12 ERADICATION SUCCESS AND FAILURE FOR SECOND LINE TREATMENTS.. 110
FIGURE 3.13 SUCCESS OF SECOND LINE TREATMENTS BROKEN DOWN BY LENGTH OF TREATMENT.. 111
FIGURE 3.14 SUCCESS OF SECOND LINE TREATMENTS BROKEN DOWN BY PPI DOSE. 112
FIGURE 3.15 ERADICATION SUCCESS FOR RESCUE TREATMENTS. 117
FIGURE 3.16 SUCCESS OF RESCUE TREATMENTS BROKEN DOWN BY LENGTH OF TREATMENT. 118
FIGURE 3.17 SUCCESS OF SECOND LINE TREATMENTS BROKEN DOWN BY PPI DOSE. 119
FIGURE 3.18 OVERALL ERADICATION RATES.. 120
FIGURE 4.1 THE NOTCH SIGNALLING PATHWAY.. 131
FIGURE 4.2 EXPRESSION OF NOTCH RECEPTORS IN AGS GASTRIC EPITHELIAL CELLS IN RESPONSE TO *H. PYLORI*. 137
FIGURE 4.3 EXPRESSION OF NOTCH LIGANDS AND *RBP-J* IN AGS GASTRIC EPITHELIAL CELLS IN RESPONSE TO *H. PYLORI*. 139
FIGURE 4.4 EXPRESSION OF NOTCH ASSOCIATED TRANSCRIPTION FACTORS IN AGS GASTRIC EPITHELIAL CELLS IN RESPONSE TO *H. PYLORI*. 141
FIGURE 4.5 EXPRESSION OF NOTCH RECEPTORS IN GASTRIC BIOPSY TISSUE FROM *H. PYLORI* POSITIVE PATIENTS AND UNINFECTED CONTROL PATIENTS.. 143
FIGURE 4.6 EXPRESSION OF NOTCH LIGANDS AND *RBP-J* IN GASTRIC BIOPSY TISSUE FROM *H. PYLORI* POSITIVE PATIENTS AND UNINFECTED CONTROL PATIENTS. 144

FIGURE 4.7 EXPRESSION OF NOTCH ASSOCIATED TRANSCRIPTION FACTORS IN GASTRIC BIOPSY TISSUE FROM *H. PYLORI* POSITIVE PATIENTS AND UNINFECTED CONTROL PATIENTS..... 145
FIGURE 4.8 EXPRESSION OF HES1 PROTEIN IN AGS GASTRIC EPITHELIAL CELLS POST-INFECTION WITH *H. PYLORI*.. 147
FIGURE 4.9 EXPRESSION OF *HES1* IN AGS GASTRIC EPITHELIAL INFECTED WITH WILD TYPE AND MUTANT STRAINS OF *H. PYLORI* 60190. 149
FIGURE 4.10 EXPRESSION OF *HES1* IN MKN45 CELLS TREATED WITH *H. PYLORI* 151
FIGURE 4.11 EXPRESSION OF HES1 MRNA IN AGS CELLS TREATED WITH CYCLOHEXIMIDE AND INFECTED WITH *H. PYLORI.*..... 153
FIGURE 4.12 EXPRESSION OF *HES1* IN AGS CELLS TREATED WITH 4NM EGTA AND A RANGE OF COMPOUND E CONCENTRATIONS..... 155
FIGURE 4.13 EXPRESSION OF *HES1* IN AGS CELLS TREATED WITH COMPOUND E AND INFECTED WITH *H. PYLORI.* 156
FIGURE 4.14 EXPRESSION OF *HES1* IN AGS CELLS TREATED WITH *HES1* SIRNA AND INFECTED WITH *H. PYLORI.* 158
FIGURE 4.15 EXPRESSION OF *HES1 AND HEY1* IN AGS CELLS FOLLOWING STIMULATION WITH JAG2 LIGAND. 160
FIGURE 4.16 EXPRESSION OF *HES1* IN AGS CELLS TRANSFECTED WITH HES1 PLASMID.. 162
FIGURE 4.17 A PCA PLOT COMPARING DUPLICATES OF SAMPLES SENT FOR RNASEQ..... 164
FIGURE 4.18 VOLCANO PLOT OF DIFFERENTIALLY EXPRESSED GENES IN *H. PYLORI* INFECTED AGS CELLS AND UNINFECTED CELLS..... 166
FIGURE 4.19 KEGG PATHWAY FOR CYTOKINE-CYTOKINE RECEPTOR INTERACTION..... 171
FIGURE 4.20 KEGG PATHWAY FOR IL-17 SIGNALLING PATHWAY..... 172
FIGURE 4.21 EXPRESSION OF *HES1* IN AGS CELLS TRANSFECTED WITH HES1 PLASMID. 174
FIGURE 4.22 VOLCANO PLOT OF DIFFERENTIALLY EXPRESSED GENES IN EMPTY-VECTOR TRANSFECTED CELLS COMPARED TO UNINFECTED CELLS. 176

FIGURE 4.23 VOLCANO PLOT OF DIFFERENTIALLY EXPRESSED GENES IN EMPTY-VECTOR TRANSFECTED CELLS COMPARED TO HES PLASMID TRANSFECTED CELLS. 177
FIGURE 4.24 VOLCANO PLOT OF DIFFERENTIALLY EXPRESSED GENES IN HES1 PLASMID TRANSFECTED CELLS INFECTED WITH *H. PYLORI* COMPARED TO EMPTY VECTOR TRANSFECTED CELLS INFECTED CELLS. 180
FIGURE 4.25 HEAT MAP OF THE TOP 20 HES1 DEPENDENT *H. PYLORI* UPREGULATED GENES. 183
FIGURE 4.26 HEAT MAP OF THE TOP 20 HES1 DEPENDENT *H. PYLORI* DOWNREGULATED GENES. 184
FIGURE 4.27 SELECTIVE ENHANCEMENT OF *H. PYLORI* MEDIATED CYTOKINE EXPRESSION IN *HES1* OVEREXPRESSING CELLS. 186
FIGURE 4.28 HES1 OVER-EXPRESSION ENHANCED *H. PYLORI*-MEDIATED INDUCTION OF *FOS* IN AGS CELLS 188
FIGURE 4.29 VALIDATION OF *H. PYLORI* DOWNREGULATED GENES IN *HES1* OVEREXPRESSING CELLS. 191
FIGURE 4.30 EXPRESSION OF NOTCH PATHWAY COMPONENTS IN THP-1 CELLS TREATED WITH HEAT KILLED OR INFECTED WITH LIVE *H. PYLORI*. 194
FIGURE 4.31 EXPRESSION OF NOTCH PATHWAY COMPONENTS IN THP-1 CELLS TREATED WITH CYCLOHEXIMIDE AND INFECTED WITH *H. PYLORI*..... 197
FIGURE 4.32 EXPRESSION OF *JAG1* AND *DLL4* IN THP-1 CELLS TREATED WITH *E. COLI* AND *H. PYLORI* LPS. 200
FIGURE 5.1 DNA IS ORGANISED INTO LEVELS OF STRUCTURAL INTEGRITY. 219
FIGURE 5.2 EUCHROMATIN AND HETEROCHROMATIN. 221
FIGURE 5.3 SCHEMATIC OF THE CORE PRC2 SUBUNITS. 223
FIGURE 5.4 CASPASE DOMAIN STRUCTURE FOR HUMANS AND MICE..... 226
FIGURE 5.5 THE NON-CANONICAL INFLAMMASOME..... 230
FIGURE 5.6 EXPRESSION OF PRC2 AND *KDM6B* COMPONENTS IN MKN45 CELLS INFECTED WITH *H. PYLORI*.. 235
FIGURE 5.7 EXPRESSION OF PRC2 COMPONENTS AND KDM6B IN AGS CELLS TREATED WITH HEAT KILLED *H. PYLORI* OR INFECTED WITH LIVE *H. PYLORI*. 237

FIGURE 5.8 EXPRESSION OF PRC2 COMPONENTS AND *KDM6B* IN GASTRIC BIOPSY TISSUE FROM *H. PYLORI* POSITIVE AND NEGATIVE PATIENTS.. 239
FIGURE 5.9 EXPRESSION OF *KDM6B* IN AGS CELLS TREATED WITH CYCLOHEXIMIDE AND INFECTED WITH *H. PYLORI*. 241
FIGURE 5.10 EXPRESSION OF PRC2 COMPONENTS AND *KDM6B* IN THP-1 CELLS TREATED WITH HEAT KILLED *H. PYLORI* OR INFECTED WITH LIVE *H. PYLORI*. 244
FIGURE 5.11 EXPRESSION OF PRC2 COMPONENTS IN THP-1 CELLS TREATED WITH *H. PYLORI* LPS. 246
FIGURE 5.12 EXPRESSION OF KDM6B IN THP-1 CELLS TREATED WITH CYCLOHEXIMIDE AND INFECTED WITH *H. PYLORI*. 248
FIGURE 5.13 EXPRESSION OF *IL1B* AND *CASPASE-4* IN GASTRIC EPITHELIAL CELLS AND BIOPSY TISSUE FROM *H. PYLORI* POSITIVE PATIENTS AND UNINFECTED CONTROLS..... 250
FIGURE 5.14 EXPRESSION OF *IL1B* AND *CASPASE 4* IN THP-1 CELLS TREATED WITH *E. COLI* LPS OR LIVE *H. PYLORI*. 252
FIGURE 5.15 CASPASE 11, PRO-IL-1B, PRO-CASPASE-1 AND CASPASE 1 EXPRESSION IN WT AND CASPASE $11^{-/-}$ BMDMS FOLLOWING *H. PYLORI* INFECTION. 254
FIGURE 5.16 DENSITOMETRY GRAPHS FOR CASPASE 11, PRO-IL-1B, PRO-CASPASE-1 AND CASPASE 1 EXPRESSION IN WT AND CASPASE $11^{-/-}$ BMDMS FOLLOWING *H. PYLORI* INFECTION. 255
FIGURE 5.17 CASPASE-11 IS INVOLVED IN *H. PYLORI*-MEDIATED SECRETION OF IL-1B FROM BMDMS..... 256

List of Tables

TABLE 1.1 SENSITIVITY AND SPECIFICITY OF THE MOST COMMON INVASIVE AND NON-INVASIVE TESTS FOR *H. PYLORI.* 14
TABLE 1.2 DESCRIPTIONS OF COMMONLY USED TREAMENT REGIMENS FOR *H. PYLORI.*. 21
TABLE 2.1 *H. PYLORI* STRAINS USED IN THE STUDY. 46
TABLE 2.2 CELL LINES USED IN THE STUDY. 50
TABLE 2.3 APPROXIMATE COLONY FORMING UNITS (CFU)/ML AND THEIR CORRESPONDING OD AT 600 NM. 53
TABLE 2.4 SIRNAS USED IN RNAI EXPERIMENTS. 55
TABLE 2.5: LIST OF TAQMAN GENE EXPRESSION ASSAYS USED FOR QPCR..... 65
TABLE 2.6 DESCRIPTION OF SAMPLES ANALYSED BY RNA-SEQ. 67
TABLE 2.7 SOFTWARE USED IN THE DATA ANALYSIS PIPELINE..... 70
TABLE 2.8 FILES RUN IN DESEQ2..... 72
TABLE 2.9 LIST OF ANTIBODIES USED FOR WESTERN BLOTTING. 75
TABLE 3.1 IRISH RECOMMENDATIONS FOR *H. PYLORI* TREATMENT AS PUBLISHED BY THE IHPWG (SMITH ET AL., 2017A)..... 80
TABLE 3.2 NUMBER OF PATIENTS FROM EACH DATA CENTRE INCLUDED IN THE STUDY. 84
TABLE 3.3 BASELINE DEMOGRAPHICS OF PATIENTS INCLUDED IN STUDY. 85
TABLE 3.4 *H. PYLORI* DIAGNOSIS METHOD OF TREATMENT-NAÏVE PATIENTS INCLUDED IN THE STUDY. 86
TABLE 3.5 NUMBER OF FIRST LINE PRESCRIPTIONS PER YEAR ACCORDING TO DURATION OF TREATMENT. 87
TABLE 3.6 NUMBER OF FIRST LINE PRESCRIPTIONS PER YEAR BROKEN DOWN BY PPI POTENCY 89
TABLE 3.7 COMPARISON OF TREATMENT DURATION OF PRESCRIPTIONS PRE- AND POST-PUBLICATION OF THE IHPWG GUIDELINES.. 91
TABLE 3.8 COMPARISON OF PPI DOSE PRESCRIBED PRE- AND POST-PUBLICATION OF THE IHPWG GUIDELINES.. 92
TABLE 3.9 FIRST LINE TREATMENTS PRESCRIBED FROM 2013-2022..... 93

TABLE 3.10 NUMBER OF FIRST LINE TREATMENTS SUB-ANALYSED BY YEAR. 94
TABLE 3.11 NUMBER OF PARTICIPANTS IN EACH GROUP. 97
TABLE 3.12 EFFECTIVENESS OF EACH FIRST LINE TREATMENT IN THE MITT GROUP. 98
TABLE 3.13 PERCENTAGE TREATMENT SUCCESS AND FAILURE BROKEN DOWN BY LENGTH OF TREATMENT. 100
TABLE 3.14 EFFECTIVENESS OF FIRST LINE TREATMENTS BROKEN DOWN BY PPI DOSE. 101
TABLE 3.15 PERCENTAGE ERADICATION RATE BROKEN DOWN BY YEAR FOR TRIPLE C+A AND FOR OVERALL TREATMENTS. 103
TABLE 3.16 COMPARISON OF OVERALL ERADICATION RATES PRE- AND POST-PUBLICATION OF THE IHPWG GUIDELINES. 103
TABLE 3.17 BASELINE DEMOGRAPHICS OF SECOND LINE PATIENTS INCLUDED IN STUDY. 105
TABLE 3.18 *H. PYLORI* DIAGNOSIS METHOD OF SECOND LINE PATIENTS INCLUDED IN THE STUDY. 106
TABLE 3.19 COMPARISON OF TREATMENT DURATION OF 2ND LINE PRESCRIPTIONS PRE- AND POST-PUBLICATION OF THE IHPWG GUIDELINES.. 107
TABLE 3.20 COMPARISON OF PPI DOSE PRESCRIBED IN SECOND LINE THERAPY PRE- AND POST-PUBLICATION OF THE IHPWG GUIDELINES 108
TABLE 3.21 TOTAL SECOND LINE TREATMENTS. 108
TABLE 3.22 ERADICATION SUCCESS FOR SECOND LINE TREATMENTS 109
TABLE 3.23 COMPARISON OF ERADICATION RATES PRE- AND POST-PUBLICATION OF THE IHPWG GUIDELINES. 113
TABLE 3.24 BASELINE DEMOGRAPHICS OF PATIENTS INCLUDED IN STUDY 114
TABLE 3.25 DIAGNOSIS METHOD OF PATIENTS RECEIVING RESCUE TREATMENT FOR *H. PYLORI.* 115
TABLE 3.26 TOTAL RESCUE TREATMENTS. 116
TABLE 3.27 ERADICATION SUCCESS FOR RESCUE TREATMENTS. 117
TABLE 4.1 TOP 20 GENES WITH THE LARGEST INCREASE IN EXPRESSION IN *H. PYLORI* INFECTED AGS CELLS COMPARED TO UNINFECTED CELLS. 167

TABLE 4.2 TOP 20 GENES WITH THE LARGEST DECREASE IN EXPRESSION IN *H. PYLORI* INFECTED AGS CELLS COMPARED TO UNINFECTED CELLS. 168
TABLE 4.3 PATHWAY ANALYSIS IDENTIFIED THE TOP 10 PATHWAYS ALTERED DURING *H. PYLORI* INFECTION IN AGS CELLS. 170
TABLE 4.4 GENES WITH SIGNIFICANT INCREASE OR DECREASE IN EXPRESSION IN HES1 OVEREXPRESSING CELLS COMPARED TO EMPTY VECTOR TRANSFECTED CELLS. 178
TABLE 4.5 TOP 20 GENES WITH THE LARGEST INCREASE IN EXPRESSION IN *H. PYLORI* INFECTED AGS HES1 OVEREXPRESSING CELLS COMPARED TO EMPTY VECTOR TRANSFECTED CELLS INFECTED WITH *H. PYLORI*. 181
TABLE 4.6 TOP 20 GENES WITH THE LARGEST DECREASE IN EXPRESSION IN *H. PYLORI* INFECTED AGS HES1 OVEREXPRESSING CELLS COMPARED TO EMPTY VECTOR TRANSFECTED CELLS INFECTED WITH *H. PYLORI*. 182

Abbreviations

ADAM	A disintegrin and metalloproteinases
AGS	Adenocarcinoma gastric cell line
Apaf1	Apoptotic protease-activating factor-1
BHLH	Basic helix-loop-helix
BID	Bis in die/ twice a day
BMDM	Bone marrow-derived macrophages
BMP	Bone morphogenic proteins
CADASIL	Cerebral autosomal-dominant arteriopathy with subcortical infarcts and leukoencephalopathy
Cag PAI	Cag pathogenicity island
CagA	Cytotoxin-associated gene A
CARD	Caspase recruitment domain
CBA	Columbia blood agar
cDNA	Complementary Deoxyribonucleic acid
CFU	Colony forming unit
CI	Confidence intervals
CT	Cycle threshold
CXCL1	C-X-C motif ligand 1
DAMP	Damage-associated molecular patterns
DED	Death effector domains
DISC	Death induced signalling complex
DLL1/3/4	Delta Like 1/3/4
DMEM	Dulbecco′s modified eagle′s medium
DMSO	Dimethyl sulfoxide
dNTP	Deoxyribonucleotide triphosphate
E. coli	Escherichia coli
EED	Embryonic ectoderm development
EGF	Epidermal growth factor
EGTA	Ethylene glycol tetraacetic acid
EHMSG	European Helicobacter and Microbiota Study Group
ELISA	Enzyme-linked immunosorbent assay
EToH	Ethanol
EUCAST	European Committee on Antimicrobial Resistance
EZH2	Enhancer of zeste homolog 2
FGF	Fibroblast growth factors
GAPDH	Glyceraldehyde 3-phosphate dehydrogenase
H. pylori	Helicobacter pylori
H3K27	Histone 3 lysine 27
HEK	Human embryonic kidney
HEPA	High efficiency particle air
HES1	Hairy and enhancer of split-1
HEY1	HES related Family BHLH transcription factor with YRPW motif 1
HI FBS	Heat inactivated foetal bovine serum
High-dose-A	Dual therapy with amoxicillin and PPI

HP-EuReg	European Registry on Helicobacter pylori management
ICE	Interleukin-1ß converting enzyme
IGV	Integrative genomics viewer
IHPWG	Irish H. pylori working group
IL-1ß	Interleukin 1ß
IL-8	Interleukin 8
IMS	Industrial methylated spirit
ISG	Irish society of Gastroenterology
Jag1/ 2	Jagged 1/ 2
JMJD3	Jumonji domain-containing protein D3
kDa	Kilodalton
KDM6B	Lysine-specific demethylase 6B
LB	Lysogeny broth
LPS	Lipopolysaccharide
MALT	Mucosa-associated lymphoid tissue lymphoma
MIC	Minimum inhibitory concentration
mITT	Modified intention to treat
MOI	Multiplicity of infection
NaDCC	Sodium dichloroisocyanurate
NICD	Notch intracellular domain
NLR	Nod-like-receptor
NLRP	Nucleotide-binding oligomerization domain, leucine rich repeat and pyrin domain containing proteins
NOD	Nucleotide-binding oligomerization domain
NSAID	Nonsteroidal anti-inflammatory drugs
OD600	Optical density 600 nanomolar
ORF	Open reading frame
PAM	Pam2CSK4
PAMP	Pathogen-associated molecular patterns
PBS	Phosphate-buffered saline
PCR	Polymerase chain reaction
PMA	Phorbol 12-myristate 13-acetate
PMSF	Phenylmethysulfonyl fluoride
PPI	Proton pump inhibitor
PRC2	Polycomb repressive complex 2
PRR	Pattern recognition receptors
PYD	Pyrin domain
RAM	RBP-J associated molecule
RBP-J	Recombination signal binding protein for immunoglobulin kappa J region
RCF	Relative centrifugal force
RIPA	Radioimmunoprecipitation assay buffer
RNA	Ribonucleic acid
RNAi	RNA interference
RNAseq	RNA sequencing
RPM	Revolutions per minute
RPMI	Roswell Park memorial institute medium

RT-qPCR	Reverse transcription quantitative polymerase chain reaction
RUT	Rapid urease test
SAT	Stool antigen test
SDS	Sodium dodecyl sulfate
Sequential-C+A+M	Sequential treatment with clarithromycin, amoxicillin, and metronidazole
SNP	Single nucleotide polymorphism
SOC	Super optimal broth with catabolite repression
SUZ12	SUZ12 polycomb repressive complex 2 subunit
Th	T helper cells
THP-1	Immortalized monocyte-like cell line
TIR	Toll/interleukin-1 receptor
TLR	Toll-like receptor
TNF	Tumour necrosis factor
Tregs	T regulatory cells
Triple-A+L	Triple therapy with amoxicillin, levofloxacin, and a PPI
Triple-A+M	Triple therapy with amoxicillin, metronidazole, and a PPI
Triple-C+A	Triple therapy with clarithromycin, amoxicillin, and a PPI
Triple-C+L	Triple therapy with clarithromycin, levofloxacin, and a PPI
Triple-C+M	Triple therapy with clarithromycin, metronidazole, and a PPI
TTMI	Trinity Translational Medicine Institute
UBT	Urea breath test
UEG	United European Gastroenterology
V	Volt
VacA	Vacuolating cytotoxin A
WHO	World health organisation
WNT	Wingless/integrated
WT	Wild type

Chapter One Introduction

Part of this introduction has been published in the following book chapter:

FitzGerald, R. and S. M. Smith (2021). 'An Overview of *Helicobacter pylori* Infection' Methods in Molecular Biology (Clifton, NJ) 2283: 1-14.

1.1. *Helicobacter pylori*

Helicobacter pylori (*H. pylori*) is one of the most extensive and pervasive bacterial infections worldwide, infecting approximately half of the global population (Salama et al., 2013). Even with around ninty percent of *H. pylori* infections being asymptomatic there are still substantial health risks to be considered, particulary in light of increasing antibiotic resistance and decreasing eradication rates (Fallone et al., 2016a). *H. pylori*-infected individuals have a 1-10% risk of developing duodenal or gastric ulcers. In addition, *H. pylori* is categorised as a class 1 carcinogen by the World Health Organisation (WHO) and confers a risk of 0.1-3% of gastric carcinoma and 0.01% risk for mucosa-associated lymphoid tissue lymphoma (MALT) (McColl, 2010). This means that *H. pylori* is one of the leading infectious carcinogens worldwide, corresponding to an estimated 780,000 related cancer cases diagnosed each year, equating to approximately 6.2% of all cancers diagnosed (Plummer et al., 2015). The impact of *H. pylori* infection on human cancer rates, the escalation of antibiotic resistance and the high level of infection in the general public identifies *H. pylori* as a pathogen of great importance for current and future research.

1.2. Discovery of *H. pylori*

When *H. pylori* was initally cultured from gastric tissue in the 1980s by Warren and Marshall, the medical community was doubtful that a bacterium could survive in the harsh and acidic niche of the stomach (Marshall and Warren, 1984). The conventional belief of the time was that peptic ulcers were caused by excess stomach acid (Pincock, 2005). To facilitate Koch's postulates and prove the infectiousness of *H. pylori,* Marshall self-administered a culture of the bacteria and subsequently presented with symptoms of the disease, which was later resolved with antibiotics (Marshall et al., 1985). Since then, there have been huge developments in the techniques used to study bacteria, which has allowed for increased understanding of *H. pylori* and its impact on human health.

1.3. Structure and virulence factors of *H. pylori*

H. pylori is a gram-negative, micro-aerophilic, flagellated, bacterium, which over time has become uniquely adapted to chronically infect the luminal surface of the gastric epithelium (Smith, 2014) (Figure 1.1). *H. pylori* infection triggers both innate and adaptive immune responses, yet these are not sufficient to prevent colonisation by the bacteria, which can persist for decades unless treated (Salama et al., 2013). When *H. pylori* infects the stomach, it must fulfil several obligations before it can colonise its host. *H. pylori* has evolved many adaptations to survive in the acidic niche of the stomach. These adaptations include the production of the enzyme urease, which can convert urea to ammonia and carbon dioxide in order to locally raise pH (Salama et al., 2013). In addition, *H. pylori* possesses a helical shape and uses flagella-mediated chemotaxis to help it breach the mucous layer and evade the low pH of the stomach (Salama et al., 2013, Terry et al., 2005). The bacteria can then attach to the epithelium via adhesion molecules and confer pathogenicity via toxin release (Kao et al., 2016).

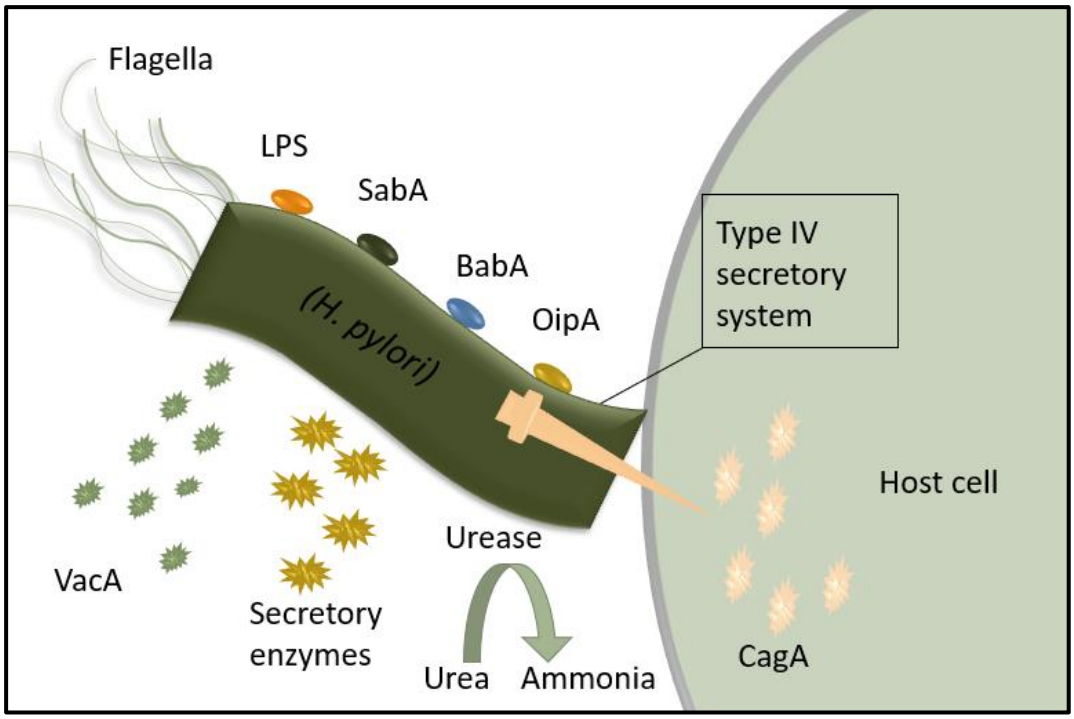

Figure 1.1 *H. pylori* structure and virulence factors. *H. pylori* is a gram-negative bacterium. The *H. pylori* enzyme urease converts urea to ammonia and carbon dioxide to locally raise pH. *H. pylori* persistence and disease progression are associated with several strain-specific virulence factors, including SabA, BabA, OipA and VacA. Strains that contain the *cag* PAI encode a type IV secretion system that injects the virulence factor CagA directly into host cells resulting in changes in host cell signalling. Figure adapted from (FitzGerald and Smith, 2021) and created in PowerPoint.

Gastric cancer occurs in a multi-step process, with disease severity increasing from gastritis followed by intestinal metaplasia, dysplasia and finally carcinoma (Wroblewski et al., 2010). When considering disease progression, several factors need to be taken into consideration; the genotypes of both the host and strain of *H. pylori*, as well as environmental stimuli (Pachathundikandi et al., 2016) (Figure 1.2). Regarding the bacterial genotypes, *H. pylori* isolates are extremely genetically diverse, particularly among their virulence factors. This can lead to strains having different levels of pathogenicity (Su et al., 2016). The most well-studied determinants of *H. pylori* pathogenicity are the virulence factors Cytotoxin-associated gene A (CagA) and the vacuolating cytotoxin gene A (VacA). In the most basic terms, virulence factors are constituents of the bacteria that help it cause disease by fulfilling one or more adaptations, such as helping the

bacteria avoid the host's immune system or allowing the bacteria to attach directly to the host's cells (Salimzadeh et al., 2015).

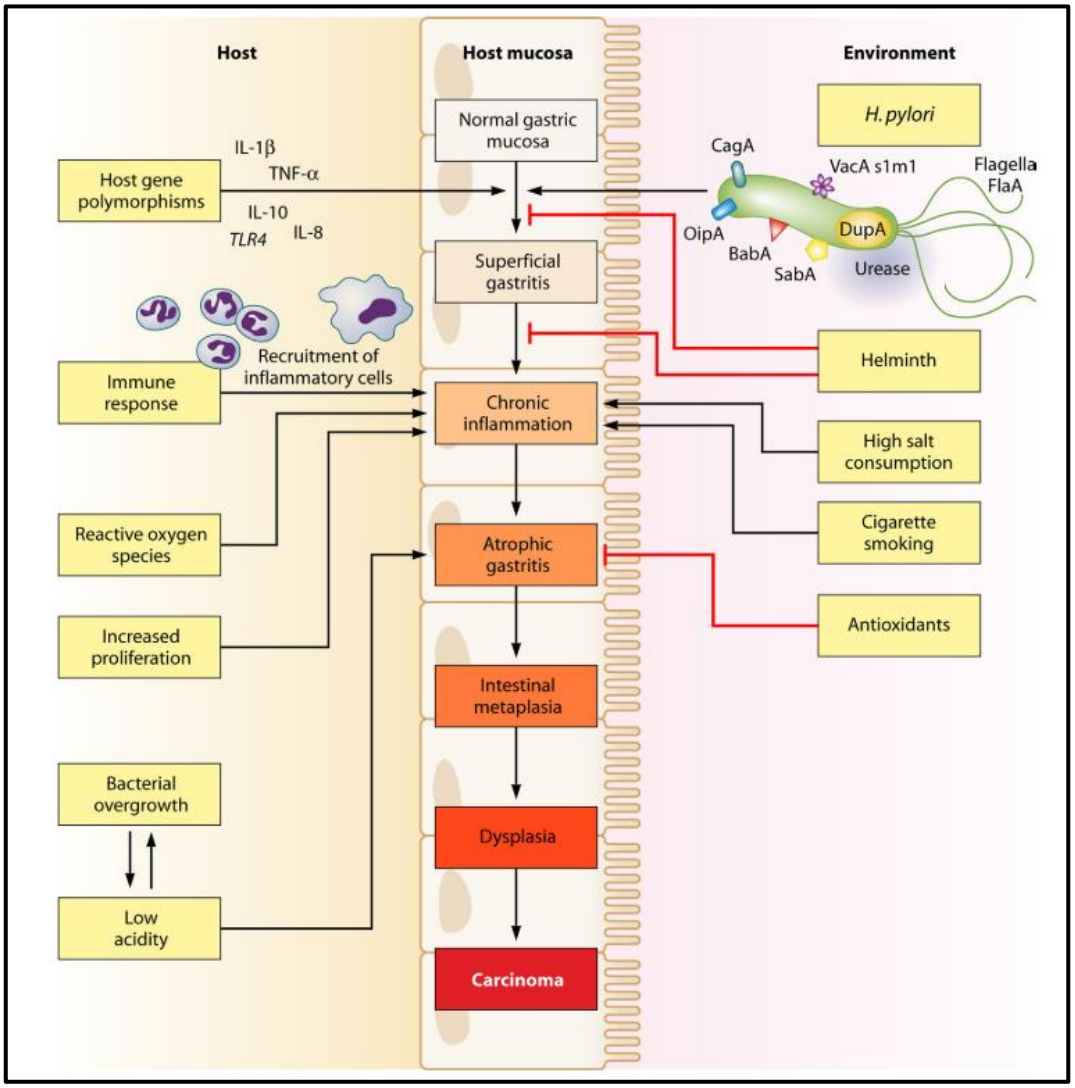

Figure 1.2 Disease progression from superficial gastritis to carcinoma is influenced by the host, pathogen, and environmental stimuli. Adapted from (Wroblewski et al., 2010).

1.3.1. CagA

The *cagA* gene is located in the 40kb cag pathogenicity island (*cag PAI*). It is only present in certain strains and encodes a type IV secretion system which allows for the translocation of the effector protein (CagA) directly into host cells. In the host cells CagA can induce irregular intracellular signalling, as well as aberrant cell motility and proliferation (Matos et al., 2013). While it is unknown why some strains are CagA-positive and some are CagA-negative, there is some evidence that *H. pylori* acquired *cagA* through horizontal gene transfer from an unknown microbe (Hatakeyama, 2014). Importantly, infection with CagA-positive strains is correlated with pronounced inflammation and an increased risk of adverse clinical outcomes by at least one order of magnitude, including a greater risk for gastric cancer (Shiota et al., 2013), (Matos et al., 2013). This is also evidenced by the observation that transgenic mouse models expressing CagA develop gastric epithelial hyperplasia and, in some cases, gastric polyps and adenocarcinomas (Ohnishi et al., 2008).

1.3.2. VacA

The *vacA* gene encodes the VacA vacuolating cytotoxin which causes vacuole formation and tissue damage by embedding into host cell membranes and emitting anions into the cytoplasm (Kao et al., 2016). Originally found to cause toxicity due to this vacuolating ability, numerous other effects have since been observed, such as alteration of autophagy and impediment of immune cells such as T cells, B cells, macrophages and neutrophils (McClain et al., 2017), (Yahiro et al., 2012). VacA can be transported to the mitochondria and activate the BAX and BAK channels releasing cytochrome C, leading to mitochondrial fragmentation and apoptosis (McClain et al., 2017). VacA is found in all strains of *H. pylori* however, there is a substantial amount of variation among toxin activity (McClain et al., 2017).

This is because *vacA* has significant polymorphisms which can impact the cytotoxic activity of the VacA protein. The primary variants of VacA have differences in the signal region, (S1 or S2) and the mid region, (M1 or M2). The signal region influences the formation of membrane channels and the S1 polymorphism has greater toxicity than S2. The M1 subtype produces higher quantities of toxin than M2 (Matos et al., 2013). This means that S1M1 strains are the most cytotoxic, followed by S1M2. On the contrary, S2M2 strains are not as cytotoxic and S2M1 strains are uncommon clinically (Shiota et al., 2013). As would be expected, S1 and M1 genotypes are correlated with higher rates of inflammation and increased risk of peptic ulcers and gastric cancer (Shiota et al., 2013), (McClain et al., 2017). It is important to note that, virulence factors may have a synergistic effect on pathogenesis and strains that contain the *vacA* S1 genotype are more likely to also contain the *cag PAI*, further impacting the strain's pathogenic potential (McClain et al., 2017).

1.4. Transmission of *H. pylori*

The infection rate of *H. pylori* varies regionally and is correlated with age and socioeconomic status (McColl, 2010). Improved standard of living is associated with decreases in infection in many countries (Lim et al., 2013), (Hooi et al., 2017). *H. pylori* prevalence in Europe decreased from 48.8% in 1970-2000 to 39.8% in the years 2000-2016. Similarly, in North America infection fell from 42.7% to 26.6% over the same time period (Hooi et al., 2017). High prevalence in older populations have been attributed to inferior living conditions in previous decades (McColl, 2010). *H. pylori* is often acquired at a young age, despite this, gastric inflammation is significantly lower in paediatric patients even with similar colonisation levels (Razavi et al., 2015).

The means of *H. pylori* transmission are not fully defined. Interpersonal oral-oral transmission is suspected for many cases since intrafamilial cases are common (Eusebi et al., 2014). There have also been studies linking *H. pylori* to a faecal-oral transmission route (Bui et al., 2016). There has been some support for the suggestion un-purified drinking water plays a role in transmission (Leja et al., 2016). Epidemiologic studies have shown a correlation between prevalence of *H. pylori* and water-related sources such as well-water. Other studies have isolated *H. pylori* from water sources (Aziz et al., 2015). It is important to note that while improved hygiene and water safety lowers the risks of contracting *H. pylori*, as of yet there is no clear consensus on the mode of transmission or mechanism of acquisition (Chakrani et al., 2018).

1.5. Prevalence of *H. pylori*

Worldwide the estimate for the number of *H. pylori* infections is 4.4 billion, with large variation in prevalence between regions (Hooi et al., 2017). A recent systemic review and meta-analysis of 184 published articles from 62 countries presents an outline for the global pattern of *H. pylori* worldwide (Hooi et al., 2017). Switzerland had the lowest prevalence (18.9%) followed by Denmark (22.1%) and New Zealand (24.0%) The highest prevalence was found to be in Nigeria (87.7%) followed by Portugal (86.4%) and Estonia (82.5%) (Hooi et al., 2017) (Figure 1.3). Differences in prevalence represent important information regarding future healthcare burdens for *H. pylori*-associated illnesses. Even within countries, studies may have vastly different estimates of prevalence. This may be due to participant inclusion criteria (such as age), the number of individuals that were recruited, the time-period the study took place and within-country geographic differences.

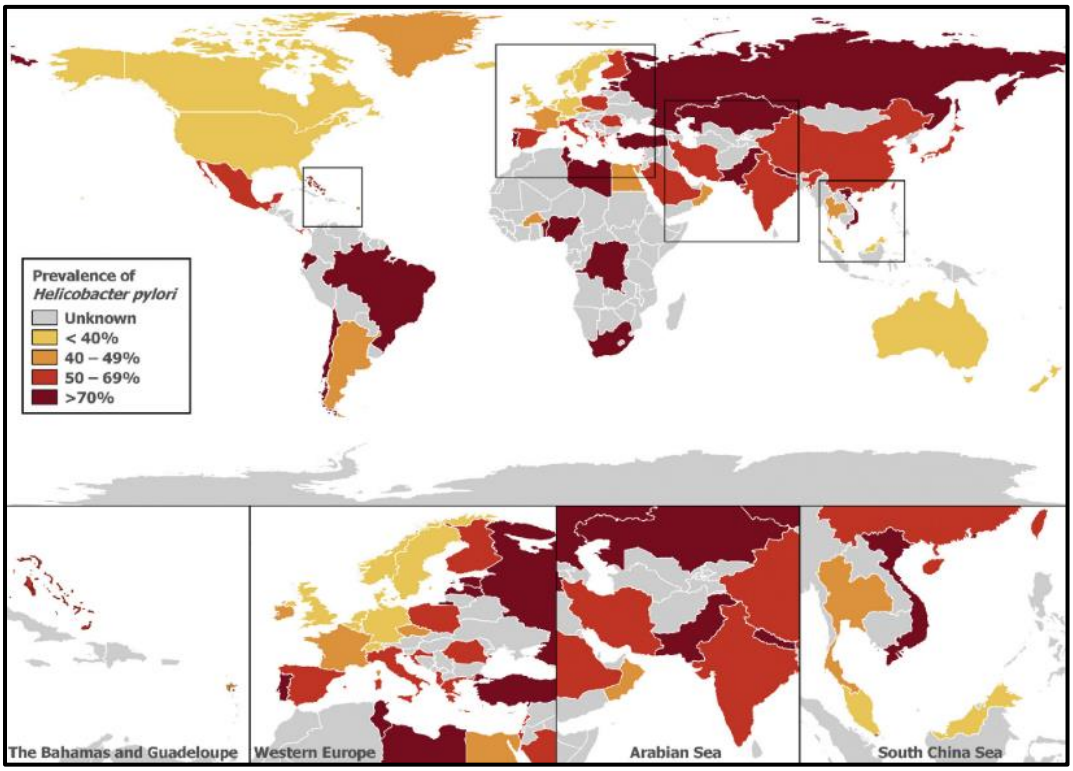

Figure 1.3 Global prevalence of *H. pylori*. Adapted from (Hooi et al., 2017). Hooi et. al. performed meta-analysis on *H. pylori* prevalence data published from 1970-2016. 184 articles from 62 countries were included in the analysis.

1.5.1. Prevalence in Europe

In general, *H. pylori* levels are relatively low in Europe. In the Netherlands a random selection of 1,550 blood donors demonstrated an overall *H. pylori* prevalence of 32% (van Blankenstein et al., 2013). However, patients born between 1935-1946 had a prevalence of 48%, but in patients born between 1977-1987 only 16% were infected. The presence of CagA-positive strains lessened from 38% to 14% over the same time period (Allen and Maillard, 2021). Similar prevalence appears in much of Europe. In Ireland, a study which looked at *H. pylori* seroprevalence in 1,000 patients attending a blood transfusion clinic for non-gastric related issues found that 43% were positive for *H. pylori* IgG antibodies (Buckley et al., 1998). Additionally, it was found that the prevalence of infection was significantly higher in older compared to younger age groups (Buckley et al., 1998). In Northern Ireland a

population based study of 4,742 blood donors found *H. pylori* positive antibodies in 50.5% of those tested (Murray et al., 1997). A more recent study in Ireland found that 33% of patients undergoing a urea breath test (UBT) and 19% of patients undergoing endoscopy tested positive for infection (Brennan et al., 2016). Another study that took place in Cork, found that out of 102 patients attending clinic with dyspeptic symptoms 48 (47%) tested positive for *H. pylori* by UBT (Hooton et al., 2006). These findings would suggest that *H. pylori* prevalence is decreasing in Ireland however, there are some limitations to these studies such as differing methodologies and only recruiting patients from a few centres in Ireland which conceals regional prevalence differences around the country.

In Spain, 47% of 3,426 patients with dyspeptic symptoms tested positive for infection (Morilla et al., 2019). Portugal stands out as an outlier in Europe with unusually high prevalence of *H. pylori*. In the early 1990's some regions reached up to 90% infection (Bastos et al., 2013). Prevalence in these areas is decreasing but still high with 84.2% of a cohort of 2,067 randomly selected adults testing positive in 2013 (Bastos et al., 2013). In association with this, Portugal has the highest rate of gastric cancer mortality in western Europe (Leja et al., 2016). However, along with falling infection rates, gastric cancer mortality rates have also been steadily declining since 1971 by 2.4% per year in males and 2.8% per year in females (Leja et al., 2016). A recent retrospective study of 461 symptomatic paediatric patients indicated an infection rate of 37.3% with a significant trend of decreasing infection rate over time (from 2009 to 2019) (Antunes et al., 2023). Antunes et. al. mentions that over the past several decades, socioeconomic changes, such as improved living standards and better eradication strategies have occurred in Portugal. While Bastos et. al. acknowledge that refrigerator ownership, a marker for higher socioeconomic class, only became available to most people in Portugal in the late 1970's and early 1980's (Bastos et al., 2013). It is projected that these improved living conditions will result in a continued gradual decrease in the prevalence of *H. pylori* infection in Portugal (Antunes et al., 2023). Despite this, it is still not fully understood

why Portugal has a higher infection rate than other southern European countries (Antunes et al., 2023).

1.5.2. Prevalence in Asia and Oceania

A high prevalence of *H. pylori* infection is also seen in Asia. A large multicentre study in Korea demonstrated a seroprevalence of 54.4% for anti-*H. pylori* IgG antibodies in a cohort of 10,796 asymptomatic subjects (Lim et al., 2013). In China, prevalence estimates range from 57.6% to 63.4% (Zhu et al., 2014), (Pan et al., 2015). Metanalysis illustrates a decrease in prevalence over time in China, which may be influenced by rapid urbanisation (Nagy et al., 2016). In Japan, a study of 14,716 individuals showed that infection rates varied by geographic area from 29.4% to 54.5% (Ueda et al., 2014). The infection rate in Australia is estimated to be lower than many other countries with a seroprevalence of 15.5% found in 1,355 community controls reported in 2011 (Pandeya et al., 2011).

1.5.3. Prevalence in the Americas

A high prevalence is observed in Mexico with 52.2% in a cohort of 343 community participants testing positive (Alvarado-Esquivel, 2013). Along the United States-Mexico border, the prevalence was found to be 38.2% (Cardenas et al., 2010). Retrospective testing of serum for *H. pylori* antibodies in Texas found that prevalence varied by age. In total, 24% of those between the ages of 41-60 tested positive for antibodies while only 6% of those aged between 0-20 tested positive (Patterson et al., 2012).

1.5.4. Prevalence in Africa

Data from Africa demonstrates high levels of infection. A study involving 1,388 dyspeptic Ethiopian patients found a seroprevalence of 65.7%, and for patients over the age of 60, 77.0% tested positive for infection (Mathewos et al., 2013). Meta-analysis involving 7 studies and a total of 18,890 patients in Ethiopia found a pooled prevalence of 52.2% (Melese et al., 2019). In Nigeria 89.7% of a cohort of 380 asymptomatic individuals tested positive for anti-*H. pylori* antibodies (Ophori et al., 2011).

1.6. Diagnosis of *H. pylori*

There are several different methods that can be used to detect *H. pylori*. Each test comes with its own advantages and disadvantages, such as varying levels of sensitivity and specificity (Table 1.1). Different tests may be more appropriate depending on circumstances, for example choosing between an invasive or non-invasive test. The test-and-treat strategy recommends that dyspeptic patients without alarm symtoms should be tested for *H. pylori* by non-invasisve means. However, those with a higher risk of malignancy such as older patients, those with alarm symptoms or those who have previously failed *H. pylori* treatment should undergo endoscopy (O'Connor, 2021), (Malfertheiner et al., 2022), (Parihar and McNamara, 2021). It is important that medications used for treating *H. pylori* infection, such PPIs, antibiotics and bismuth compounds should be discontinued several weeks before any test as they can reduce the bacterial load and contribute to false negative results (Malfertheiner et al., 2017).

Test	Type	Sensitivity	Specificity	Reference
UBT	Non-invasive	88-95%	95-100%	(Brennan et al., 2016)
SAT	Non-invasive	94%	97%	(Gisbert et al., 2006)
Serology	Non-invasive	76-84%	79-90%	(Sabbagh et al., 2019)
RUT	Invasive	~90%	95-100%	(Malfertheiner et al., 2017)
Histology	Invasive	80-96%	99-100%	(Sabbagh et al., 2019)
Culture	Invasive	70-80%	100%	(Sabbagh et al., 2019)

Table 1.1 Sensitivity and specificity of the most common invasive and non-invasive tests for *H. pylori*. UBT: urea breath test; SAT; stool antigen test; RUT: rapid urease test.

1.6.1. Non-invasive diagnosis of *H. pylori*

1.6.1.1. Urea breath test

The Urea breath test (UBT) is the most commonly used non-invasive diagnostic method due to its low cost, high sensitivity (88-95%) and specificity (95-100%) (Brennan et al., 2016). The basis of the test is the ability of *H. pylori*-secreted urease to break down an isotope-labelled urea solution (O'Connor, 2021). The test works by having the patient ingest ^{13}C or ^{14}C-labelled urea, which is converted to labelled CO_2 by *H. pylori* urease and absorbed into the blood stream (Makristathis et al., 2019). The labelled CO_2 is measured when exhaled using isotope ratio mass or infared-spectrometry (Wang et al., 2015). A large quantity of labelled CO_2 in the patient's breath denotes a positive test for *H. pylori* (O'Connor, 2021). The principal disadvantage of the UBT test is that certain medications, in particular proton pump inhibitors (PPI), antibiotics and bismuth, can supress *H. pylori* activity leading to false negative results (O'Connor, 2021), (Gatta et al., 2004). While it is recommended patients discontinue use of these medications at least two weeks prior to UBT, this is not always fesable (Malfertheiner et al., 2017). Another negative for the ^{14}C-UBT is that it subjects patients to radiation and so is not certified for use in children or pregnant women (Malfertheiner et al., 2017), (O'Connor, 2021).

1.6.1.2. Stool antigen test

An alternative non-invasive test is the stool antigen test (SAT) which tests for *H. pylori* antigens in a faecal sample (Makristathis et al., 2019). Since strains and thus antigens vary regionally, tests need to be locally validated. Monoclonal antibody tests are generally more accurate than polyclonal antibodies, potentially increasing costs (Malfertheiner et al., 2017). The monoclonal SAT has high sensitivity and specificity, 94% and 97% , respectively (Gisbert et al., 2006).

1.6.1.3. Serology

Serology is a method that measures anti-*H. pylori* antibodies in patient serum (Sabbagh et al., 2019). It has a sensitivity of 76-84% and a specificity of 79-90% (Sabbagh et al., 2019). The benefit of serology it that compared to other methods of *H. pylori* detection, serology is not as impacted by medications used to supress *H. pylori* infection (such as PPIs). This makes it a useful test in scenarios where the patient is not able to discontinue medication prior to testing (Sabbagh et al., 2019). The downside of serology testing is that it can not differentiate between current and previous *H. pylori* infection, meaning it is not acceptable as a post-eradication therapy test (Sabbagh et al., 2019).

1.6.2. Invasive diagnosis of *H. pylori*

1.6.2.1. Rapid urease test

In cases where the patient is above 50 years of age or possesses alarm symptoms such as drastic weight loss, gastrointestinal bleeding or iron deficient anaemia, endoscopy is recommended instead of non-invasive tests (Malfertheiner et al., 2022). The rapid urease test (RUT) is widely used on biopsies taken during endoscopy. Like the UBT, the RUT is based on the activity of the bacteria's urease enzyme. Gastric biopsy tissues collected during endoscopy are placed in a medium containing urea and a pH reagent. If *H. pylori* is present, it will produce urease that will convert the urea in the medium into ammonia and CO_2. This makes the medium more alkaline, which will be detected by the pH reagent and show as a colour change (Parihar and McNamara, 2021). The RUT has a sensitivity of ~90% and specificity between 95-100% (Malfertheiner et al., 2017). The disadvantage of the RUT test is that false negatives may be caused by a low bacterial load and false positives may be caused by other urease producing bacteria such as *Staphylococcus capitis urealyticus* (Godbole et al., 2020). The advantages of the RUT are that it is rapid, inexpensive and largely accurate (Parihar and McNamara, 2021).

1.6.2.2. Histology

Histology can also be used to test for *H. pylori* in gastric biopsy tissue. Stains such as Hematoxylin and Eosin, Giemsa, Hp silver and immunohistochemical stains can be used for detection (Wang et al., 2015). The benefit of histology is that it has good sensitivity and specificity (Table 1.1) and can account for *H. pylori*-associated lesions such as dysplasia and malignancy (Parihar and McNamara, 2021). The disadvandage of histology is that it is costly due to the specialised training required to perform (Parihar and McNamara, 2021).

1.6.2.3. Culture

H. pylori can be cultured from biopsy tissue. This is extremely specific but less sensitive than other tests (Wang et al., 2015). Diagnosing *H. pylori* by culturing the bacteria is time and labour intensive and requires dedicated clinical microbiology facilities. Additionally, since *H. pylori* is a fastidious bacterium, it can be challenging to culture (Brennan et al., 2021). However, culturing the bacteria provides the opportunity to test the sample for antibiotic resistance (See section 1.7.5.1), which may increase eradication rates by tailoring treatment specifically to the patient (Parihar and McNamara, 2021) and is also important for antimicrobial resistance surveillance.

1.7. Treatment for *H. pylori* infection

In 1997, the first Maastricht conference on the management of *H. pylori* infection recommended a standard triple therapy as the first-line treatment for *H. pylori* (Malfertheiner et al., 1997). This included the use of a PPI in combination with the antibiotics clarithromycin and amoxicillin taken twice daily for 7 days, with metronidazole replacing amoxicillin in those with an allergy to penicillin. The effectiveness of this standard first-line triple therapy has fallen in recent years, primarily due to the emergence of antibiotic-resistant bacteria. There have currently been no new drugs developed to replace the standard triple therapy, but extended treatment durations (up to 14 days) and combinations of previously known antibiotics have been used (Smith et al., 2014a). With many treatment combinations and doses available, clinicians deciding on a treatment plan must consider the prevalence of antimicrobial resistance, local eradication rates, patient compliance, adverse effects and antibiotic stewardship when perscribing (Malfertheiner et al., 2022).

1.7.1. *H. pylori* treatment options

The biggest consideration when deciding on a *H. pylori* treatment regimen is the prevalence of local antibiotic resistance. In regions with high primary clarithromycin resistance, first-line therapy can be based on the occurrence of metronidazole and dual clarithromycin and metronidazole resistance (Malfertheiner et al., 2017). In regions with low metronidazole resistance, such as Japan, replacing clarithromycin for metronidazole in standard triple therapy, works well for eradication (Malfertheiner et al., 1997). In regions with high dual clarithromycin and metronidazole resistance, bismuth quadruple therapy is recommended, this includes the use of; a PPI, bismuth salt, tetracycline and metronidazole (Smith et al., 2014b), (Malfertheiner et al., 2017). The number of components in bismuth quadruple therapies may

lead to low compliance in patients. Promisingly, a "3-in-1" capsule of bismuth sub-citrate, tetracycline and metronidazole (Pylera®) has performed well in clinical trials with an overall eradication rate of 90% (Zagari et al., 2018). Unfortunately, bismuth is not available in all regions and in this scenario non-bismuth quadruple and high dual doses of PPI and amoxicillin (Table 1.2) are potential treatment regimens (Malfertheiner et al., 2017). Non-bismuth quadruple therapies involve treating with a PPI, clarithromycin, amoxicillin and metronidazole or tinidazole. This can either be administered as a sequential therapy, where the antibiotics are given successively, or as concomitant therapy, where all the antibiotics are given at the same time (Zagari et al., 2018). While both of these regimens were intended to deal with clarithromycin resistance, their efficacy has been clinically debated (Zagari et al., 2018), particluarly in regions with high dual clarithromycin and metronidzole resistance.

Treatment Regimen	Description
Clarithromycin triple therapy	PPI*, 500 mg clarithromycin, and 1,000 mg amoxicillin (twice daily for 7–14 days)
Metronidazole triple therapy	PPI*, 500 mg clarithromycin, and 400 mg metronidazole (twice daily for 7–14 days)
Bismuth quadruple therapy	PPI* (twice daily), 120–600 mg bismuth salt**, 250–500 mg metronidazole, and 250–500 mg tetracycline (up to four times daily for 7–14 days)
Sequential therapy	PPI* and 1,000 mg amoxicillin (twice daily for 5–7 days) followed by PPI*, 500 mg clarithromycin, and 500 mg metronidazole (twice daily for 5–7 days)
Concomitant therapy	PPI*, 1,000 mg amoxicillin, 500 mg clarithromycin, and 500 mg metronidazole/tinidazole (twice daily for 7–14 days)
Levofloxacin triple therapy	PPI*, 250 mg levofloxacin, and 1,000 mg amoxicillin (twice daily for 7–14 days)
Levofloxacin quadruple therapy	PPI*, 1000 mg amoxicillin, bismuth salt 200 mg bismuth salt twice daily and 500 mg levofloxacin once daily or 200 mg levofloxacin twice daily for 14 days
Rifabutin triple therapy	PPI*, 1,000 mg amoxicillin, and 150 mg rifabutin (twice daily for 7–14 days)
High dose dual therapy	PPI* and 1,000 mg amoxicillin (three times daily for 7-14 days)

Table 1.2 Descriptions of commonly used treament regimens for *H. pylori.* Adapted from (Smith, 2015), (Wong et al., 2003), (Gan et al., 2018), (Öztürk et al., 2020). *PPI dose, one of: 20 mg omeprazole, 20 mg rabeprazole, 30 mg lansoprazole, 40 mg esomeprazole, or 40 mg pantoprazole; **Variations in the dose of bismuth quadruple therapy have been reported.

1.7.2. The most up-to-date treatment recommendations

The most recent Maastricht consensus report (Maastricht VI) was published in 2022 (Malfertheiner et al., 2022). It is now recommended that *H. pylori* is treated as an infectious disease and that positive patients are treated with eradication therapy even in the absence of symptoms (Malfertheiner et al., 2022). First-line clarithromycin triple therapy should only ever be used in areas where primary clarithromycin resistance is known to be below 15% (Figure 1.4.A). If clarithromycin triple therapy is prescribed, it is recommended for 14 days with a high dose PPI (Malfertheiner et al., 2022). Bismuth quadruple therapy is an alternative if available. If first-line clarithromycin triple therapy fails, second-line options include either a bismuth quadruple therapy or a levofloxacin triple or quadruple therapy (Table 1.2). Levofloxacin-based therapy is also the recommended second-line treatment following failure of first-line bismuth quadruple therapy (Figure 1.4A). Third-line treatment depends on the therapies used in second-line treatment and rifabutin triple therapy is the recommended for fourth line therapy (Figure 1.4.A).

Bismuth quadruple therapy is the recommended first-line treatment if individual antibiotic susceptibility testing is unavailable, in areas with >15% clarithromycin resistance or in areas with unknown clarithromycin resistance (Figure 1.4.B). If bismuth is not available, non-bismuth concomitant quadruple therapy is suggested (Malfertheiner et al., 2022) (Table 1.2). However, the report noted that non-bismuth concomitant quadruple therapy exposes patients to several potentially redundant antibiotics, which conflicts with antibiotic stewardship recommendations and may contribute to worsening global resistance rates. In addition, concomitant quadruple therapy should not be used in areas with high dual clarithromycin and metronidazole resistance (>15%) (Malfertheiner et al., 2022). The recommended second-line treatments are bismuth quadruple

therapy, a fluoroquinolone-containing quadruple (or triple) therapy or a PPI-amoxicillin high-dose dual therapy (Malfertheiner et al., 2022).

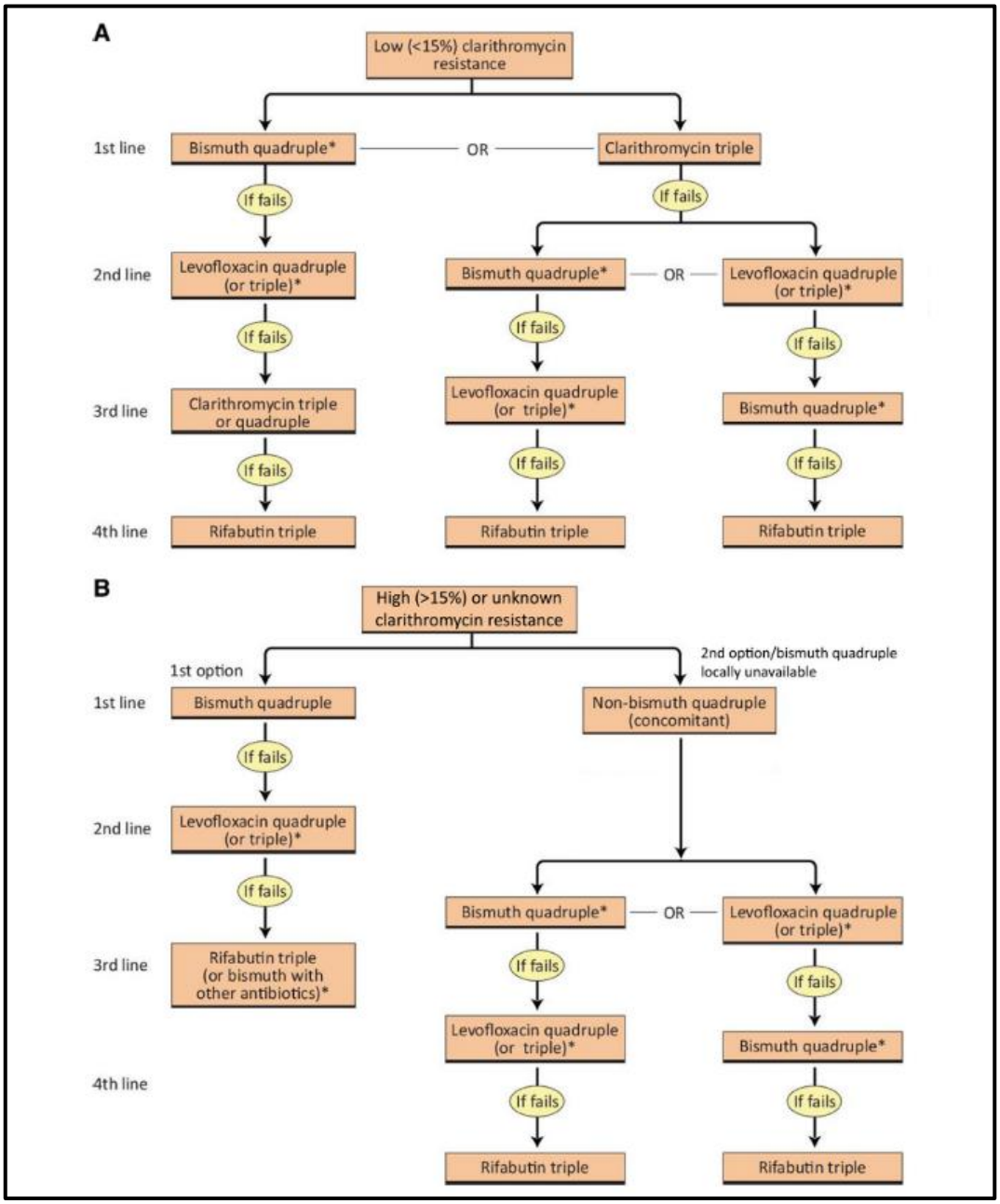

Figure 1.4 Flow-chart of recommended *H. pylori* treatment options. Bismuth quadruple: proton pump inhibitor (PPI), bismuth, tetracycline, and metronidazole. Clarithromycin triple: PPI, clarithromycin, and amoxicillin. Non-bismuth quadruple (concomitant): PPI, clarithromycin, amoxicillin, and metronidazole. Levofloxacin quadruple: PPI, levofloxacin, amoxicillin, and bismuth. Levofloxacin triple: PPI, levofloxacin, and amoxicillin. *High- dose PPI plus amoxicillin may be another option. Figure adapted from (Malfertheiner et al., 2022).

1.7.3. The benifits of *H. pylori* eradication

Meta-analysis has concluded that eradication of *H. pylori* is consistent with considerable improvement in gastritis and gastric atrophy (Malfertheiner et al., 2017). Furthermore, eradication of *H. pylori* provides a long-term cure in 80% of duodenal ulcer patients whose ulcers are not associated with the use of nonsteroidal anti-inflammatory drugs (NSAIDs) (McColl, 2010). Most importantly, eradication of *H. pylori* correlates with reduced incidence of gastric cancer (Savoldi et al., 2018). Complete resolution of symptoms is a strong predictor for sucessful eradication treatment (Gebeyehu et al., 2021, McColl et al., 1998). Treatment is recommended as a preventative measure for those with a high risk of developing gastric cancer and those with un-investigated and functional dyspepsia (Fallone et al., 2016a). Patients with the highest risk of cancer are those who suffer from *H. pylori*-induced inflammation of both the antral and fundic mucosa and those with mucosal atrophy and intestinal metaplasia (McColl 2010). The Maastricht VI consensus report stated that *H. pylori* eradication is an effective preventative measure against gastric cancer at any age, but eradication at a younger age has greater benefits (Malfertheiner et al., 2022).

Eradication of the bacteria in the general public has been proposed as a way to combat the high levels of gastric cancer observed worldwide. Meta-analysis found moderate evidence that *H. pylori* eradication therapy reduces the risk of gastic cancer in both healthy and symptomatic individuals (Ford et al., 2020). Ford et. al. concluded that population screening and treatment programs may be a viable option for reducing gastric cancer rates, particularly in regions with high gastric cancer incidence (Ford et al., 2020).

1.7.4. Issues with the current treatment plans

Eradication success is inversely related to antibiotic resistance, which is often associated with consumption of antibiotics in the population. It is therefore important that resistance rates are determined locally (Thung et al., 2016). As mentioned in Section 1.7.2 above, standard clarithromycin-based triple therapy is now only recommended as a treatment strategy in areas where clarithromycin resistance is known to be less than 15% (Malfertheiner et al., 2022, Malfertheiner et al., 2017). Additionally, patients who have been previously exposed to macrolides and quinolones have a higher potential of carrying strains resistant to those antibiotics, so it is recommended therapies containing clarithromycin or levofloxacin should be avoided in such individuals (Zagari et al., 2018). Treatment options are further limited following an EU review that recommended restricting fluoroquinolone use due to the risk of rare but severe side-effects including tendonitis (EMA, 2018). Additionally, the complexity of some treatment regimens, has resulted in poor patient compliance which in turn may worsen antibiotic resistance.

1.7.5. *H. pylori* antibiotic resistance

In 2017 the WHO declared that clarithromycin resistant *H. pylori* is a high-priority for antibiotic research (Savoldi et al., 2018). Meta-analysis on data published from 2007-2017 found that in most WHO regions *H. pylori* resistance to clarithromycin, metronidazole and levofloxacin was >15% (Savoldi et al., 2018) (Figure 1.5). There have been suggestions that antibiotic resistance testing should be performed on a patient level before therapy is even prescribed, however, this is often impractical (Thung et al., 2016).

Globally clarithromycin resistance appears to be particularly prevalent and is the most extensively studied, with estimated rates of 30% in Japan and Italy, 50% in China and 40% in Turkey (Malfertheiner et al., 2017). Pooled resistance for 18 European countries found clarithromycin resistance to be 21.4% (Megraud et al., 2021). Conversely, in regions with low *H. pylori* seropositivity, such as Sweden, the emergence of antibiotic resistance is significantly slower (Thung et al., 2016). Despite high rates of antibiotic resistance, antimicrobial suceptibility testing prior to treatment is rarely undertaken and isolates from biopsy are often skewed towards more severe cases that have already failed treatment (Domanovich-Asor et al., 2021).

In 2018, primary resistance was collected from 43 treatment naïve patients attending Tallaght University Hospital. Primary resistance for clarithromycin was 25.6%. Primary resistance to levofloxacin was 13.9% and primary resistance to metronidazole was 43% (Megraud et al., 2021). In 2023 primary resistance rates from 103 treatment naïve patients were collected from two urban teaching hospitals (Tallaght University Hospital and St. James's Hospital) and two rural hospitals (Letterkenny University Hospital & Mayo University Hospital) (Butler TJ, 2023). Primary resistance rates for clarithromycin, metronidazole and levofloxacin were found to be 37.9%, 44.7% and 21.4%, respectively (Butler TJ, 2023). These results

indicate that there are considerable antibiotic resistant infections among both rural and urban Irish populations.

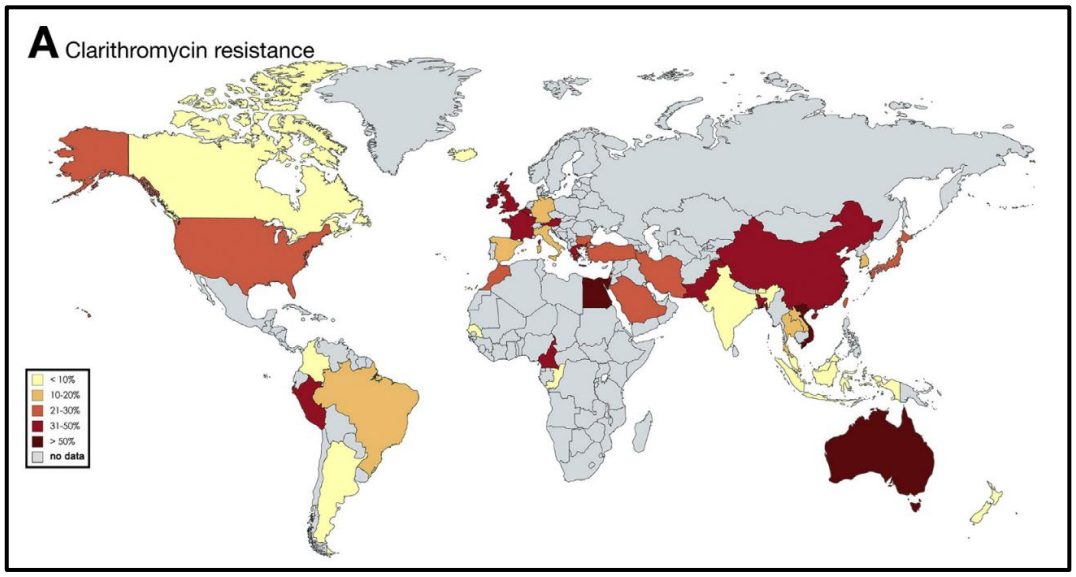

Figure 1.5 Rates of *H. pylori* resistance to clarithromycin globally. Savoldi et. al. performed meta-analysis on 178 studies from 65 different countries published between 2007-2017. Pooled primary and secondary resistance to clarithromycin was found to be greater than the threshold of 15% in the majority of WHO regions. Adapted from (Savoldi et al., 2018).

1.7.5.1. Antibiotic susceptibility testing – Culture

As *H. pylori* antibiotic resistance rates vary from country to country, antimicrobial resistance surveillance is recommended to guide clinicians in the most appropriate therapy in a given population. Culture-based methods are considered the gold standard for *H. pylori* resistance testing and enable susceptibility testing for all the antibiotics used to treat *H. pylori*. However, *H. pylori* is a fastidious microaerophilic bacterium and the culture of *H. pylori* from stomach tissue biopsies requires staff specifically trained in clinical microbiology to work in a biosafety level 2 laboratory and takes approximately 1-2 weeks. Overall, this means that antimicrobial sensitivity testing from cultured bacteria can be costly and time intensive (Li et al., 2022a). In addition, culture of pure isolates of *H. pylori* from tissue biopsies is often unsuccessful.

The four main methods of testing antimicrobial sensitivity from cultured bacteria are the agar dilution test, the disk diffusion test, gradient-E test and broth microdilution test (Li et al., 2022a) (Figure 1.6). The agar dilution test is considered the 'gold standard' test for antibiotic susceptibility testing, however, it is time-consuming as it involves incorporating different concentrations of antibiotics into the Columbia blood agar (CBA) plates prior to inoculation (Li et al., 2022a). The disk diffusion test involves placing a paper disk containing the antibiotic on an agar plate swabbed with bacteria. The antibiotic diffuses into the agar, with agar further from the disc absorbing progressively smaller levels of antibiotics (Li et al., 2022a). The E-test is a commercially available plastic strip that delivers a gradient of antibiotics to the agar (Li et al., 2022a). The broth microdilution method tests the growth of the bacteria in several serial dilutions of the antibiotic in broth (Li et al., 2022a).

The minimum inhibitory concentration (MIC) of antimicrobial required to inhibit *H. pylori* growth can be quantitatively obtained by agar dilution, E-test, and broth microdilution. Clinical MIC breakpoints for resistance to the antibiotics used to treat *H. pylori* are published and annually updated by the European Committee on Antimicrobial Susceptibility Testing (EUCAST; www.eucast.org). By contrast, disc diffusion measurements are qualitative and zone diameter breakpoints have not been published by EUCAST in relation to *H. pylori*.

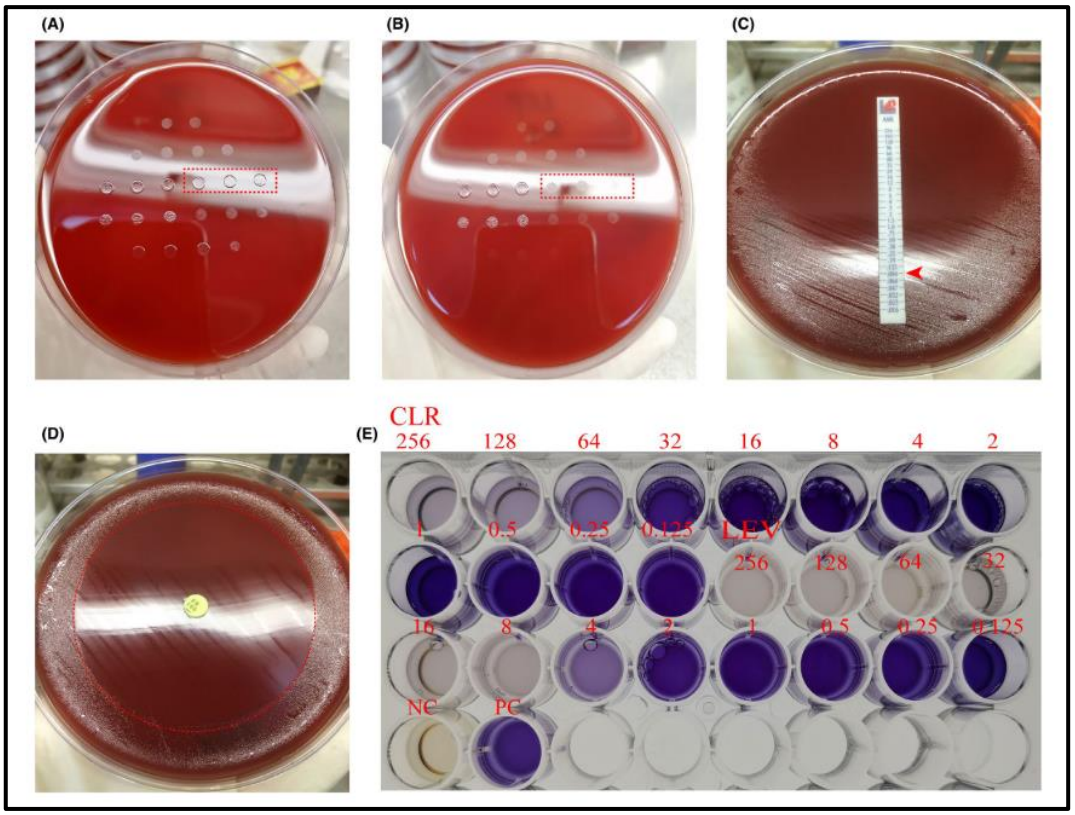

Figure 1.6 Culture-based methods of antibiotic resistance testing. Adapted from (Li et al., 2022a). A) and B) Agar dilution test: Plate A) incorporated 0.25 mg/L of levofloxacin while plate B) incorporated 0.5 mg/L of levofloxacin. The three *H. pylori* isolates highlighted in the red box grew on plate A) but not plate B). This indicates that the levofloxacin MIC for these isolates was judged as 0.5 mg/L. C) E-test: The MIC is read at the barrier of the growth inhibition zone that intersects with the E-test strip and is indicated by a red arrow. D) Disk diffusion test: Measuring the inhibition zone around the antibiotic disk correlates to the MIC and is marked by a red dotted line. E) Broth microdilution test: The amount of *H. Pylori* growth in each well is visualised by the addition of a colour changing oxidase reagent. The MIC for clarithromycin (CLR) is 128 mg/L and the MIC for levofloxacin (LEV) is 8 mg/L. NC – negative control (no bacteria), PC – positive control (bacteria, no antibiotic).

1.7.5.2. Antibiotic susceptibility testing – PCR

Molecular methods such as the polymerase chain reaction (PCR) are extremely accurate for diagnosing *H. pylori* but are more time and cost intensive than some other methods such as the RUT or UBT (Godbole et al., 2020). Additionally, there are several commercial kits that can test for common DNA mutations that confer antibiotic resistance and there is no need to culture the bacteria. However, currently PCR testing can only pick up the most common mutations that confer resistance and will miss less common or yet unknown mutations and/or alternative mechanisms of antibiotic resistance (Brennan et al., 2021). Resistance to clarithromycin is primarily due to mutations in the *23S rRNA* gene, while resistance to levofloxacin is mostly from mutations in the *gyrA* gene (Malfertheiner et al., 2022). Resistance to metronidazole is more complex so can be difficult to predict with PCR testing (Malfertheiner et al., 2022).

PCR is often considered an invasive test as DNA can be isolated from cultured *H. pylori* or collected directly from stomach biopsy tissue (Brennan et al., 2021). However, there is evidence that a non-invasive PCR performed on DNA collected from stool samples has a high agreement with DNA collected from gastric tissue (Moss et al., 2022). Expanded use of PCR from stool samples would reduce the need for endoscopy to identify resistance profiles. The Maastricht VI consensus report strongly recommended clarithromycin sensitivity testing prior to treatment and suggested that the COVID-19 pandemic prepared laboratories around the world to deal with large scale, quick-turnaround PCR tests (Malfertheiner et al., 2022).

1.7.5.3. Antibiotic susceptibility testing - Next generation sequencing

Due to the decreasing cost of sequencing, next generation-sequencing has been proposed as an effective and time conserving measure to detect antibiotic resistance prior to treatment (Argueta et al., 2021). Parrafin-embeded gastric biopsy tissue was used to extract *H. pylori* DNA, which was sequenced and evaluated for mutations associated with resistance to several classes of antibiotics (Argueta et al., 2021). Argueta et. al. reported a 95% success rate for this method with results available within 72 hours. Phenotypic resistance to clarithromycin, levofloxacin and rifampicin were shown to highly correlate with single nucleotide polymorphims (SNPs) identified during whole genome sequencing (Godbole et al., 2020). Another advantage of next-generation sequencing is that it may help identify previously unknown mutations confering antibiotic resistance (Godbole et al., 2020).

1.8. *H. pylori* and the innate immune response

1.8.1. *H. pylori* infection recruits Macrophages

Given the challenges associated with *H. pylori* eradication, understanding how *H. pylori* interacts with the immune system is important to understand disease outcomes and may identify biomarkers predictive of disease progression or targets for therapeutic intervention (Robinson and Lehours, 2020). While gastric epithelial cells represent the first point of contact between *H. pylori* and the host, macrophages are significantly increased in the antrum and the corpus of *H. pylori*-infected patients (Hua-Xiang et al., 2004), (Whitney et al., 2000). The role of macrophages in *H. pylori* colonisation and pathology was examined by transiently depleting macrophages in a mouse model of *H. pylori*. Transient elimination of macrophages reduced the pathogenesis of *H. pylori* SS1 strain but did not affect the bacterial load (Kaparakis et al., 2008). This would suggest macrophages play an important role in *H. pylori*-associated immune and inflammatory responses. Migration of leukocytes and macrophages to an area of inflammation is associated with the formation of active oxygen forms (Cherdantseva et al., 2014). Urease released by *H. pylori* can impact the level of iNOS expression from inflammatory infiltrate cells. *H. pylori*-associated gastritis is accompanied by increases in macrophages and lymphocytes in the gastric mucosa resulting in increased expression of iNOS (Cherdantseva et al., 2014). Although *H. pylori* infects the gastric epithelium, the infection triggers an innate immune response, bringing macrophages to the site of infection. Macrophages are key cells in balancing the pro- and anti-inflammatory response to infections. For this reason, both gastric epithelial and macrophage cell responses to *H. pylori* were investigated during the research studies presented in this thesis.

1.8.2. *H. pylori* can evade the host immune response.

Althougth *H. pylori* triggers an immune response, it accomplishes chronic colonisation of the stomach due to its capacity to evade some host immune responses (Gall et al., 2017). Several of the bacteria's pathogen-associated molecular patterns (PAMPs) avoid recognition by their cognate pattern recognition receptors (PRRs) (Gall et al., 2017). For example, *H. pylori* lipopolysaccharide (LPS) is tetra-acetylated making it a poor ligand for Toll-like receptor 4 (TLR4), it's flagellin monomer sequences are divergent which reduces activation of TLR5 and the O-antigen of it's LPS contains Lewis antigens that mimic the host receptors (Gall et al., 2017). TLR responses to *H. pylori* are discussed in more detail in Section 1.8.4 below.

1.8.3. *H. pylori* and cytokine response

Even with sophisticated evasion methods, *H. pylori* still elicits a robust immune response. One of the most important aspects of the immune system is cytokine signalling. *H. pylori*-infected patients usually have enhanced cytokine levels in their gastric region, in particular, TNFα, INFγ, IL-1, IL6, IL-7, IL-8, IL-10, IL-17, IL-18, IL-23 and IL-1ß (Razavi et al., 2015), (Kameoka et al., 2016). Infection with strains that contain the Cag PAI are more commonly associated with gastric ulcers and cancer. There is evidence that CagA plays a role in the activation of NF-κB and production of IL-8 (Razavi et al., 2015). The Cag type IV secretory system can inject bacterial factors which can activate NF-κB and induce upregulation of inflammatory genes directly into the host cells (Gall et al., 2017). One of the primary cytokines induced by *H. pylori* infection is IL-1ß, the level of which is closely associated with gastric inflammation and carcinogenesis (Kameoka et al., 2016). Evidence for the role of IL-1ß in *H. pylori*-associated inflammation is strengthened by the observation that transgenic mice overproducing Il-1ß in the stomach develop inflammation and cancer. Furthermore,

polymorphisms in the *IL-1β* gene are associated with an increased predisposition to gastric cancers in human patients (Kim et al., 2013).

1.8.4. *H. pylori* and TLRs

TLRs are vital components of the innate immune system. TLRs are a group of cell surface and subcellular transmembrane proteins expressed on immune cells such as macrophages and dendritic cells. There are currently 11 known members of the TLR family, which are part of the interleukin-1 receptor superfamily (Pachathundikandi et al., 2011). They function to detect microorganisms through recognition of the specific molecular motifs referred to as PAMPs (Pachathundikandi et al., 2016). The receptors are composed of a leucine-rich ectodomain, a transmembrane region and the Toll/IL-1 (TIR) domain. Upon activation, TLRs trigger an inflammatory response via signalling cascades, using either a MyD88 dependent pathway (most TLRs except TLR3) or TRAM/TRIF dependent pathway (TLR3 and occasionally TLR4) (Pachathundikandi et al., 2016). The MyD88 pathway recruits members of the IRAK family and TRAF6 which leads to phosphorylation and degradation of the IKK and IkBs, in turn leading to activation of NF-κB, which can bind to the promotor region and upregulate the transcription of cytokines such as IL-6 and TNF-α (Pachathundikandi et al., 2016).

Activation of TLRs by *H. pylori* components has been highly debated and it is not yet fully known which *H. pylori* ligand(s) activate which TLR(s). Generally TLR4 is considered the primary receptor in establishing a response to gram-negative bacteria by responding to bacterial LPS (Pachathundikandi et al., 2016). However, the evidence that *H. pylori* activates this receptor is controversial (Smith, 2014). It has been proposed that the reduced sensitivity to TLR4 is due to modifications of the lipid A core which could in turn be responsible for the reduced innate response to *H. pylori* (Pérez-Pérez et al., 1995).

However, bacterial lipoproteins, lipoteichoic acid and peptidoglycan have all been shown to trigger an immune response when TLR2 heterodimerizes with either TLR1 or TLR6 (Pachathundikandi et al., 2016). *H. pylori* HSP60, NapA, and urease have also been implicated in TLR2 signalling (Smith et al., 2017b). Human embryonic kidney 293 (HEK293) cells are often used as a model in TLR studies as they do not endogenously express TLRs and can thus be stably transfected with different receptors and reporter systems. It was shown that in HEK293 cells, co-transfected with an NF-κB luciferase reporter and expression plasmids for TLR2, TLR4 or TLR5, infection with *H. pylori* induced NF-κB activity in cells transfected with TLR2 and TLR5 but not TLR4 (Smith et al., 2003). This was consistent with an observation in MKN45 gastric epithelial cells that dominant-negative TLR2 and TLR5, but not TLR4 plasmids, ablated NF-κB activation (Smith et al., 2003). Furthermore, Pellino family proteins can interact with downstream TLR signalling molecules. It was shown that Pellino 1 and Pellino 2 positively regulated TLR2 responses to *H. pylori,* while Pellino 3 was a negative regulator. This may be a significant determining factor of the degree of inflammation observed when TLR2 is triggered by *H. Pylori* (Smith et al., 2017b).

TLR5 is ubiquitously expressed on most mammalian epithelial surfaces however, bacterial flagellin is the only ligand identified for TLR5 (Pachathundikandi et al., 2016). Early studies proposed that TLR5 played a role in innate immune response to *H. pylori* (Smith et al., 2003). However, an experiment which replaced amino acids 89-96 of FliC Salmonella flagellin, which potently reacts with TLR5, with the corresponding *H. pylori* flaA sequence abolished TLR5 recognition (Andersen-Nissen et al., 2005). This rationalised the hypothesis that the lack of recognition by TRL5 is an immune evasion utilised by *H. pylori*.

1.8.5. *H. pylori* and NLRs

Nucleotide-binding oligomerization domain (NOD)-like receptors (NLRs) are another subgroup of PRRs that are involved in triggering a *H. pylori*-mediated immune response. Nod1 is an intracellular PRR that is specific for gram-negative peptidoglycan (Viala et al., 2004). An early study demonstrated that HEK293 cells not expressing TLR2 could still activate NF-κB due to NOD1 recognition of peptidoglycan. Furthermore, NOD1-deficient mice showed higher susceptibility to infection by CagA-positive strains than wild type (WT) mice (Viala et al., 2004). NLRs can respond to both PAMPs and damage-associated molecular patterns (DAMPs) in the cytoplasm (Castaño-Rodríguez et al., 2014). The structure of NLRs includes a central nucleotide-binding and oligomerization domain, a C-terminal leucine-rich repeats domain and an N-terminal caspase recruitment (CARD) or pyrin (PYD) domain. Although, it was shown that *H. pylori* peptidoglycan can activate Nod1 resulting in NF-κB activation, Nod1 can also reduce the inflammatory response and promote bacterial persistence by inducing the anti-inflammatory cytokine IL-33. Evidence for this comes from CRISPR/Cas9 Nod1 knockout cells which fail to produce IL-33 in response to *H. pylori* infection (Blosse et al., 2018).

1.9. *H. pylori* and the adaptive immune response

Analysis of human gastric mucosal biopsies revealed that people persistently infected with *H. pylori* show increased levels of infiltrated leukocytes compared with uninfected controls (Razavi et al., 2015). In addtion to innate immune cells such as monocytes, macrophages, mast cells, neutrophils, eosinophils and dendritic cells, T and B lymphocytes are recruited, with CD4+ T and B cells being located in lymphoid follicles indicating ongoing chronic immune response and antigen presentation (Razavi et al., 2015).

T helper (Th) cells are adaptive immune cells that differentiate into four distinct subpopulations of $CD4^+$ cell types. $CD4^+$ cells are fundamental to many aspects of the immune response and since each subtype triggers a unique assembly of cytokine production, each class will elicit a different functional response (Bagheri et al., 2018). These subtypes are Th1 cells, Th2 cells, Th17 cells and regulatory T cells (Tregs). Th1 and Th17 cells are more inflammatory and Tregs are immunosupressive (Robinson and Lehours, 2020). Knockout mice for the inflammatory cytokine IL-21 had a reduced Th1 and Th17 response when infected with *H. pylori* suggesting IL-21 is important for regulating these cells (Robinson and Lehours, 2020). The *H. pylori* protein HP1454 was shown to drive a Th1/Th17 inflammatory response, further evidencing the role of T cell subsets in modulating the outcome of *H. pylori* infection (Capitani et al., 2019).

As previously mentioned, *H. pylori* triggers an immune response but the pathogen is rarely cleared by the host immune system alone. The virulence factor VacA can act on antigen-presenting cells, such as B cells impairing their antigen processing ability (Bagheri et al., 2018), (Molinari et al., 1998). Following infection, the host's innate immune system will work to produce the pro-inflammatory cytokine IL-8, which attracts and activates neutrophils, which in turn produce IL-12. IL-12 is a major component in

driving the subsequent adaptive CD4+ T cell response and along with other cytokines facilitates the maturation of Treg, Th1 and Th17 cells. In general, it has been recognised that *H. pylori* induces a predominantly Th1 cell response, since immunization trials show different *H. pylori* antigens evoke the production of Th1 type cytokines (Bagheri et al., 2018). Th1 cells secret IFN-γ and IL-2 which in turn activate macrophages and T-cells (Mirzaei et al., 2017). However, Th17 cells have also been shown to play an important role in the initial response with the Th17 cytokine IL-17A having enhanced secretion in *H. pylori* infected patients (Bagheri et al., 2018).

1.10. *H. pylori* and the microbiome

Until recently the gastric environment was thought to be sterile with any bacteria that were isolated being thought to come from the intestine and colon (Liatsos et al., 2022). Following the identification of *H. pylori* as a gastric colonising bacteria in the 1980's further research into the gastric microbiome took place (Liatsos et al., 2022). Recently, advanced molecular-based methods have shown that the normal stomach has a far more complex microbiome than previously thought (Thorell et al., 2017). Interestingly, it has been shown that the gastric microbiome is made of 10^1 to 10^3 colony forming units/g (Liatsos et al., 2022). Most isolates from the gastric microbiome belong to the Proteobacteria, Firmicutes, Actinobacteria, Bacteroidetes, and Fusobacteria phyla (Bik et al., 2006). Within these phyla, the main genera are Streptococcus, Lactobacillus, Veillonella, Clostridium, Prevotella, Porphyromonas, Rothia, Neisseria, and Haemophilus (Thorell et al., 2017).

The impact of *H. pylori* infection on the composition of the gastric microbiome is yet to be fully understood (Liatsos et al., 2022). However, there is some data indicating that when *H. pylori* is present it is the dominant bacteria and when *H. pylori* is absent a greater diversity of bacteria is observed (Liatsos et al., 2022), (Jauvain and Bessède, 2023). In addition to *H. pylori*, the composition of the microbiota can be influenced by diet, medication (such as PPI and antibiotic usage) and age among other factors (Liatsos et al., 2022). There has been some evidence that *H. pylori* eradication therapy alters the composition of the gastric microbiome, particularly, decreasing the relative abundance of Bacterioidetes and increasing the abbundance of Firmicutes (Yap et al., 2016). It is now believed that maintaining balance in the gastric microbiome is important. Any alterations as a result of *H. pylori*-infection or eradication, may be clinically important and may influence disease outcome, because of this future studies should evaluate the interaction between *H. pylori* and the microbiome.

1.11. Host-directed therapies

In recent years the continued increase in the emergence of antibiotic-resistant bacteria, including multi-drug resistant bacteria, combined with the lack of new antimicrobial drugs being licenced has ushered in concerns about the future of a 'post-antibiotic era' (Jasovský et al., 2016). This concern has led to an uptake in research into host-directed therapies. Host-directed therapies are treatments that modify host biological pathways to improve clinical outcomes, by boosting host defence mechanisms or curtailing excessive inflammation to improve patient outcomes (Zumla et al., 2016). The main types of host-directed therapies are outlined in Figure 1.7. In the context of *H. pylori* infection, one of the biggest host factors contributing to disease progression is aberrant inflammatory cytokine release (Wroblewski et al., 2010), (Smith et al., 2017b). The use of monoclonal antibodies such as anti-IL-1β or anti-TNFα have been suggested as a means to reduce the impact of host inflammation on disease (Zumla et al., 2016).

Immune dysregulation can impact the severity of an infection and can have many causes including immunosuppressive drugs, stress and malnutrition (Zumla et al., 2016). As vitamin D deficiency is associated with auto-immune and inflammatory diseases (Guo et al., 2014), vitamin D supplementation is another potential approach under investigation during *H. pylori* infection. Gastric epithelial GES-1 cells treated with vitamin D3 and infected with *H. pylori* induced significantly lower amounts of IL-6 and IL-8 compared to *H. pylori* infected cells that were not treated with vitamin D3 (Guo et al., 2014). Studying host-pathogen interactions will give new insights into mechanisms of pathogenesis and host innate and adaptive immune responses that could potentially be manipulated therapeutically.

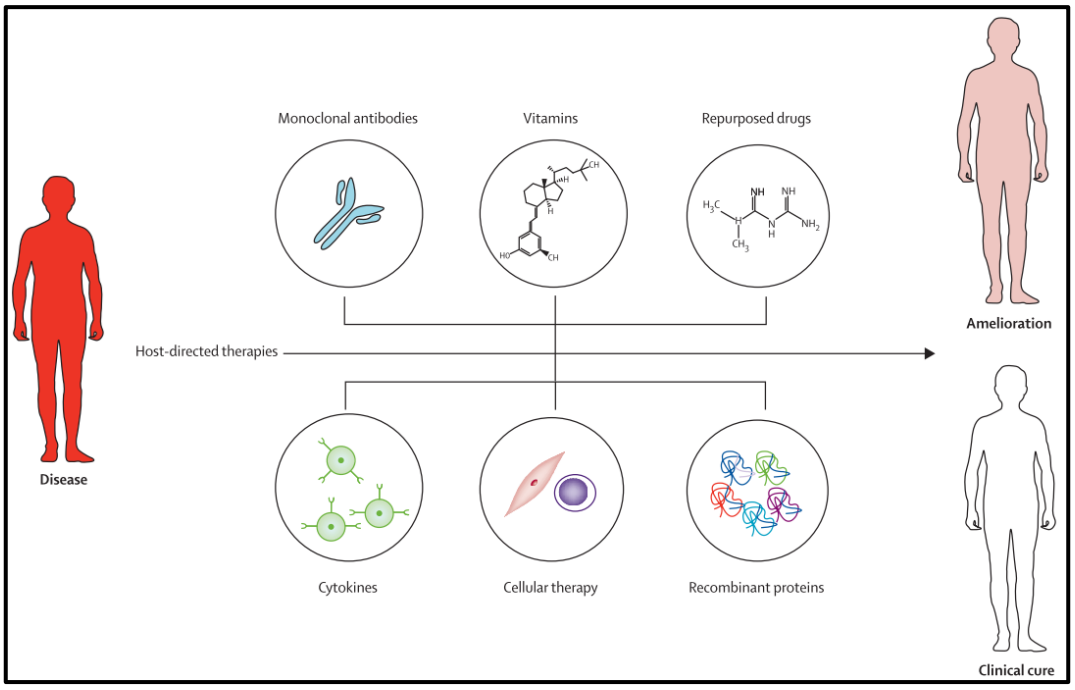

Figure 1.7 The main types of host-directed therapies. The main host-directed therapies are monoclonal antibodies, vitamins, repurposed drugs, cytokines, cellular therapy, and recombinant proteins. Adapted from (Zumla et al., 2016)

1.12. Summary

The global estimate for the number of *H. pylori* infections is 4.4 billion (Hooi et al., 2017). *H. pylori* is considered an infectious disease and eradication is associated with reduced gastric cancer risk (Malfertheiner et al., 2022), (Savoldi et al., 2018). For these reasons, it is important to manage *H. pylori* effectively. The main steps to dealing with *H. pylori* infection are to:

i) Diagnose the bacteria accurately. This means making sure the best and most appropriate test to suit each situation is used. Considerations include availability, cost, sensitivity, specificity, whether to use a non-invasive or invasive test, if the patient is using a PPI, and if antimicrobial susceptibility testing is required.
ii) Treat the infection effectively. Considerations include local antibiotic resistance rates, availability of bismuth, patient's previous exposure to antibiotics, possible side-effects from treatment, patient compliance with treatment and if individual antimicrobial susceptibility testing is possible.

To improve *H. pylori* eradication rates in the short-medium term current treatments should be audited locally to ensure patients are receiving the treatment with the best chance of eradication. In addition, antimicrobial susceptibility testing should be increased at both a population and individual level. However, in the long-term it is clear that new treatments will be required to treat *H. pylori*. Research is needed into new antimicrobial therapies, as well as host-directed therapies. To identify host-directed therapies, an increased understanding of host-pathogen interactions is required.

1.13. Aims and objectives.

The overall objectives of this study were to:

(i) perform an audit on *H. pylori* treatments and outcomes in the Irish healthcare setting and

(ii) investigate host responses to *H. pylori* with a view to identifying potential pathways for host-directed therapies.

These objectives are addressed through the specific aims below.

- To audit *H. pylori* prescription patterns and eradication rates over a 10-year period in Ireland by analysing data from the European Registry on *H. pylori* management (Hp-EuReg) (Chapter 3).
- To investigate the role of the Notch signalling pathway during *H. pylori* infection (Chapter 4).
- To investigate the role of histone modification proteins during *H. pylori* infection (Chapter 5).
- To investigate the role of inflammatory caspases during *H. pylori* infection (Chapter 5).

Chapter Two Materials and methods

2.1. Hp-EuReg methods

The Hp-EuReg is an international multicentre prospective non-interventional registry, collecting information on the management of *H. pylori* infection from over 30 countries since 2013. It was approved by the Research Ethics Committee of La Princesa University Hospital, Madrid, Spain and prospectively registered in ClinicalTrials.gov (NCT02328131). Detailed information on the Hp-EuReg has been previously published (McNicholl et al., 2019), (Nyssen et al., 2021a). The current study is a sub-analysis on a cohort of *H. pylori*-positive adult patients attending gastroenterology out-patient clinics at Tallaght University Hospital and the Beacon Hospital in Dublin, Ireland.

2.1.1. National coordinators and recruiting investigators.

Each country in the Hp-EuReg has a national coordinator. Dr. Sinéad Smith is the national coordinator for Ireland and was responsible for supervising data inclusion. The recruiting investigators were Gastroenterologists and/or members of their teams. Patients were managed and registered following routine clinical practice. Irish recruiting investigators were Rebecca FitzGerald, Dr. Sinéad Smith, Dr. Thomas Butler, Professor Deirdre McNamara, Professor Ashgar Qasim and Professor Colm O'Morain.

2.1.2. Data extraction and analysis

Data were anonymously recorded in an Electronic Case Report Form (e-CRF) using a web-based application RED-Cap (Research Electronic Data Capture), a platform managed and hosted by the non-profit Scientific and Medical Society Asociación Española de Gastroenterología" (AEG; www.aegastro.es). Patient demographics, *H. pylori* treatment history, treatments prescribed and outcomes (eradication rates, reported compliance, reported adverse events and follow-up test) were recorded. PPI data were standardised using the PPI acid inhibition potency (Nyssen et al., 2021a) and classified as low dose (20 mg omeprazole equivalents bis in die [bid]), standard dose (40 mg omeprazole equivalents bid) and high dose (60 mg omeprazole equivalents bid). The main outcome was confirmed *H. pylori* eradication at least 4 weeks after treatment. In this study, Irish data collected from registry inception in 2013 up to December 2022 were analysed.

2.1.3. Analysis of treatment effectiveness

A modified intention-to-treat (mITT) analysis was used to achieve the closest result to those obtained in clinical practice (Gatta et al., 2023), (Rokkas et al., 2022). The mITT includes all cases that completed a follow-up valid confirmatory test at least 4 weeks after their *H. pylori* treatment, regardless of compliance and excluding those lost to follow up. All patients who were empirically treated (in other words, not susceptibility-guided) were included in the effectiveness analysis.

2.2. *H. pylori*

2.2.1. Growth of *H. pylori*

All bacterial culture was performed under aseptic conditions (Appendix A). *H. pylori* strains (Table 2.1) were grown on Columbia blood agar (CBA) plates (Appendix B) under microaerobic conditions at 37°C. Isogenic *cagA* and *vacA* mutant strains of 60190 were grown on selective CBA plates containing 50 µg/ml kanamycin (Appendix B). Microaerobic conditions were generated by placing the CBA plates in a 2.5 L Oxoid Anaerojar (ThermoFisher Scientific) with one CampyGen sachet (ThermoFisher Scientific), which absorbs atmospheric oxygen and generates carbon dioxide. The sealed flask was placed in a 37°C incubator. Bacterial cultures were passaged every 3-4 days. Before infection of cell cultures, bacteria were inoculated into Brain-Heart infusion medium (Sigma) (Appendix B) with 10% Foetal Bovine Serum (FBS; Gibco) and grown under microaerobic conditions at 37°C, 150 RPM overnight.

Strain	Description
NCTC11638	This is a CagA+, VacA S1M1 reference strain. Isolated from human gastric antrum. https://www.dsmz.de/collection/catalogue/details/culture/DSM-10242. (Windle et al., 2000)
60190	This is a CagA+, VacA S1M1 reference strain https://www.culturecollections.org.uk/products/bacteria/detail.jsp?refId=NCTC+13085&collection=nctc. (Kalia et al., 2002)
60190 cagA mutant	CagA-negative isogenic mutant strain of 60190 (Peek et al., 2000)
60190 vacA mutant	VacA-negative isogenic mutant strain of 60190 (Kalia et al., 2002)

Table 2.1 *H. pylori* strains used in the study. All strains were kindly provided by Dr. Henry Windle, School of Medicine, TCD.

2.2.2. *H. pylori* LPS

H. pylori (strain 26695) LPS was a gift from Professor Anthony Moran (NUIG) and was prepared by phenol-water extraction and subsequent enzymatic purification with RNase A, DNase II and proteinase K, as well as by ultracentrifugation, as described previously (Moran et al., 2002).

2.2.3. Preparation of heat-killed *H. pylori*

Following the growth of live *H. pylori*, strain 11638, as outlined in section 2.2.1, the bacteria were pelleted at 4°C, 3,000 relative centrifugal force (RCF) for ten minutes and resuspended in sterile PBS to wash the bacteria. The *H. pylori* were pelleted and resuspended in sterile PBS once again. This was aliquoted and heated to 95°C for thirty minutes and stored at -20°C until use. As a control, the heat killed bacteria were plated on a CBA plate and incubated under optimal growth conditions for several days. No colonies were observed, indicating the bacteria were no longer viable.

2.3. Cell culture

2.3.1. Culture conditions

Cell cultures were handled using aseptic conditions to prevent contamination (Appendix A). The cell lines used in the project are described in Table 2.2. AGS human gastric epithelial cells were maintained in Ham's F-12 Nutrient mix (Gibco) with 10% heat inactivated (HI) FBS and 2mM of L-Glutamine. MKN45 cells were maintained in Roswell Park Memorial Institute Medium (RPMI; Gibco) with 10% HI FBS and 2mM of L-Glutamine. THP-1 human monocytes were maintained in RPMI (Gibco) with 10% HI FBS and 2mM of L-Glutamine and differentiated into macrophages 96 hours prior to experiments (Section 2.4.1). BMDM were maintained in Dulbecco's Modified Eagle's Medium (DMEM; Gibco) with 10% FBS.

All cell lines were maintained in a 5% CO_2, 37°C incubator. Epithelial cells were passaged every 48-72 hours. To passage epithelial cells, the medium was disposed of in Dichloroisocyanurate (NaDCC) solution, and the cells were rinsed with 1X trypsin-EDTA (Gibco). 1X trypsin-EDTA was added to the cells at 1/5th the volume of the growth medium and the cells incubated at 37°C for 5-10 minutes, checking under the microscope every few minutes until the cells started to detach. When the cells detached, fresh medium was added to deactivate the trypsin. The cells were spun for 5 minutes at 800 RCF. The supernatant was disposed of, and the cell pellet was resuspended in fresh medium. Typically, cells were sub-cultured at ratios from 1:3-1:10.

Macrophage cells were maintained by medium renewal every 48-72 hours. Typically, ¼ to ¾ of the medium was removed and replaced with fresh medium. Macrophage cells were sub-cultured once a week. The cells were

spun at 100 RCF for 5 minutes and the pellet was resuspended in fresh medium. Typically, cells were sub-cultured at ratios from 1:4-1:10.

Working stocks for each cell line were made at a low passage number and stored in 1ml aliquots at either -80°C or in liquid nitrogen. To make epithelial cell working stocks, cells were pelleted and resuspended in culture medium containing 10% DMSO. Monocyte working stocks were resuspended in culture medium containing 5% DMSO. When cells reached a passage number >30 a new working stock of cells was defrosted for use. The vial of cells was defrosted quickly in a 37°C water bath and added directly to a T25 flask containing the appropriate medium for epithelial cells and 50% the appropriate medium and 50% HI FBS for monocyte cell lines. Cells were sub-cultured twice before being used in experiments to allow the cells to reach optimum health.

Cell Line	Species	Description	Medium
AGS	Human	AGS is a cell line with gastric epithelial morphology that was isolated from a female patient with gastric adenocarcinoma. These are adherent cells. (AGS (ATCC CRL-1739))	Ham's F-12 Nutrient mix (Gibco), 10% HI FBS, 2mM of L-Glutamine.
MKN45	Human	MKN45 is a cell line that was isolated from the stomach of a female patient with poorly differentiated gastric adenocarcinoma. These are adherent cells. (cellbank.nibiohn.go.jp; JCRB0254 MKN45)	RPMI (Gibco), 10% HI FBS, 2mM of L-Glutamine.
THP-1	Human	THP-1 is a monocyte cell line that was isolated from the peripheral blood of a male patient with acute monocytic leukaemia. These are suspension cells. (HP-1 (ATCC TIB-202))	RPMI (Gibco), 10% HI FBS, 2mM of L-Glutamine.
Wild type BMDM	Mouse	Bone-marrow-derived macrophages from wild type C57BL/6J mice (Zasłona et al., 2020a), (Zasłona et al., 2020b),	DMEM (Gibco), 10% HI FBS.
Casp11$^{-/-}$ BMDM	Mouse	Bone-marrow derived macrophages from caspase 11-deficient C57BL/6J mice (Zasłona et al., 2020a), (Zasłona et al., 2020b)	DMEM (Gibco), 10% HI FBS.

Table 2.2 Cell lines used in the study. THP-1 cells were kindly provided by Dr. Thomas Butler -Technical University Dublin. WT and Casp11$^{-/-}$ BMDM cells were kindly provided by Dr. Ewelina Flis - Trinity College Dublin.

2.4. In vitro infection with *H. pylori*

2.4.1. Seeding cells

The cells were counted using a hemocytometer (Figure 2.1). AGS cells were seeded 24 hours prior to infection at $1x10^6$ cells/well in 6 well plate, $3x10^5$ cells/well in a 12 well plate or $1.5x10^5$ cells/well in a 24 well plate. THP-1 cells were seeded at $1x10^6$ cells/well in a 6 well plate or $0.7\text{-}0.75x10^6$ cells/well in a 12 well plate. Monocytes were differentiated macrophages using RPMI with 10% FBS in the presence of 100 nM phorbol 12-myristate 13-acetate (PMA; Sigma Aldrich) for 72 hours. Cells were cultured for a further 24 hours in the absence of PMA before infection with *H. pylori*. Murine bone marrow-derived macrophages (BMDM) were isolated from wild-type and caspase 4-deficient mice by Ewelina Flis in TBSI and transported to TTMI the day before infection.

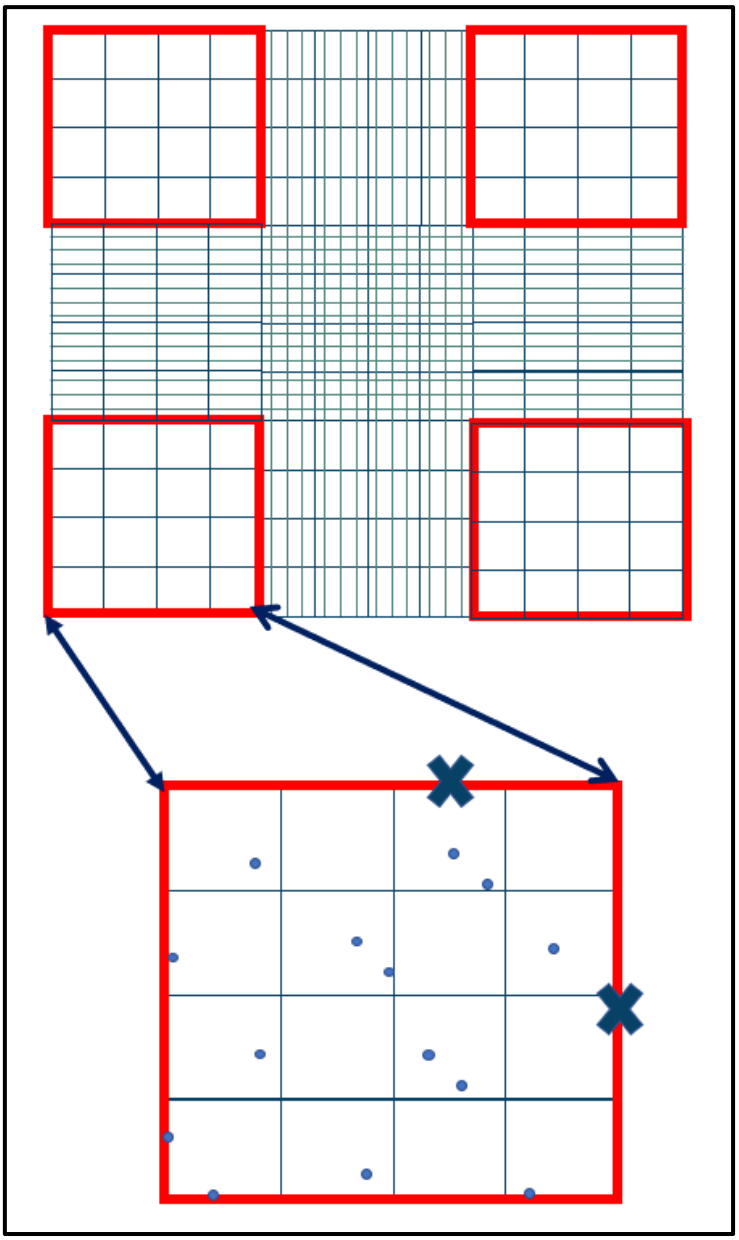

Figure 2.1 Cells were counted using a hemocytometer. The number of cells in the outer four quadrants were counted and the average was found. Cells that were found on the edge of the quadrants were counted on two sides of the quadrant only. The average number of cells per quadrant was multiplied by 10^4 to estimate the number of cells/ml. Figure created in PowerPoint.

2.4.2. Preparation of *H. pylori*

Using overnight cultures of *H. pylori* grown in brain heart infusion broth containing 10% FBS (Appendix B), bacterial cell numbers were calculated by measuring the optical density (OD) at 600 nm with a spectrophotometer and a standardised growth curve (Table 2.3). The required volume of

bacteria to obtain a multiplicity of infection (MOI) of 100:1 was spun in the centrifuge at 4°C, 3,000 RCF for ten minutes and resuspended in fresh medium for the appropriate cell line. This step was repeated first to wash the bacteria and then to resuspend in desired volume of appropriate medium and added to the cells. Cells were cultured in the presence of *H. pylori* in a 5% CO_2 incubator at 37°C for various time-points. To collect samples following infection, the cells were washed with PBS and RNA, or protein lysates were collected in the wells as described in sections 2.7.1 and 2.10.1.

OD600nm	**0.08-0.1**	**0.257**	**0.451**	**0.582**
CFUX10^8/ml	1.5	3	6	9

Table 2.3 Approximate colony forming units (CFU)/ml and their corresponding OD at 600 nm.

2.4.3. Treatment of cells with Heat-killed *H. pylori, H. pylori* LPS or *E. coli* LPS

Cells were seeded as described in Section 2.4.1. Heat killed bacteria were diluted in appropriate cell culture medium and added to cells at a concentration corresponding to a multiplicity of infection (MOI) of 100:1. *H. pylori* LPS (2.2.2) was diluted in appropriate cell culture medium and added to cells for a final concentration of 10ng/ml, 100ng/ml or 1µg/ml.
E. coli LPS (Alexis) was diluted in appropriate cell culture medium and added to cells for a final concentration of 1µg/ml. At several time-points, the cells were washed with PBS and RNA lysates were collected as described in section 2.7.1.

2.4.4. Treatment of cells with a γ-secretase inhibitor

The γ-secretase inhibitor, Compound E (Abcam) was dissolved in Dimethyl sulfoxide (DMSO) to make a concentration of 1mM. Aliquots were stored at -20°C until needed. Cells were treated with either 500nM, 1 μM Compound E or an equal volume of DMSO and were incubated at 37°C in a CO_2 incubator for 18 hours before infection with *H. pylori* or treatment with Heat killed *H. pylori* as indicated in sections 2.4.2 and 2.4.3 respectively. As a positive control for Notch signalling, cells were treated with 4nM Ethylene glycol tetraacetic acid (EGTA; Sigma) in the presence of 0, 100nM, 500nM and 1μM Compound E. Following treatment, the cells were washed with PBS and RNA lysates were collected as described in Section 2.7.1.

2.4.5. Stimulation of cells with Notch Ligand

In a 24 well plate, wells were coated with 10 μg/ml JAG2 ligand (R&D Systems; 1726-JG) that had been diluted in a volume of 250μl of sterile phosphate buffered saline (PBS). The same volume of sterile PBS was added in the control wells. The plates were stored at 4°C overnight. The next day AGS cells were seeded as described in Section 2.4.1. RNA lysates were collected at several timepoints as described in 2.7.1.

2.4.6. Inhibition of protein synthesis using Cycloheximide pre-treatment

Cells were seeded as described in section 2.4.1. The next day, cells were treated for 1 hour with 20μg/ml cycloheximide that was diluted in the appropriate cell culture medium (Sigma). Following this, infection with *H. pylori* or treatment with heat killed *H. pylori* was performed as indicated in section 2.4.2 and 2.4.3.

2.5. Cell transfection

2.5.1. RNA interference

AGS cells were reverse transfected with siRNA using Lipofectamine 2000. For each transfection sample, a small interfering RNA (siRNA) oligomer-Lipofectamine 2000 (Invitrogen; 11668-019) complex was prepared. The siRNA: lipofectamine complexes were prepared by diluting 6µl of siRNA (20 µM stock) in 100 µl Opti-MEM (so that the final concentration when added to the cells is 100 nM) and mixed gently (Table 2.4).
The lipofectamine was mixed before use. Then 2 µl was diluted into 100 µl of Opti-MEM medium and mixed gently. The lipofectamine-Opti-MEM mixture was allowed to incubate at room temperature for 5 minutes.
After the 5 minutes incubation, the diluted siRNA was mixed with the diluted lipofectamine and incubated for 20 minutes. In each well of a 12-well plate, 200 µl of siRNA: lipofectamine complex was added. AGS cells were prepared as described in section 2.4.1. Cells were resuspended at a dilution of $4x10^5$cells/ml and 1 ml of cells was added to each well. After they had been seeded for 48-hours the cells were infected with the 11638 strain of *H. pylori* as described in section 2.4.2.

siRNA	Assay ID
Invitrogen stealth siRNA HES1	HSS179374
Invitrogen stealth siRNA non-targeting control	12935-400

Table 2.4 siRNAs used in RNAi experiments.

2.5.2. Plasmid DNA transfection

2.5.2.1. Transformation of *E. coli* with plasmid DNA

The plasmids, pCMV6-HES1 (NM_005524) Human Tagged ORF Clone (OriGene) and pCMV6-AC-GFP Mammalian Expression Vector (OriGene) were briefly spun by centrifugation and placed on ice. A vial of One Shot® TOP10 Competent Cells (Invitrogen) for each transformation was defrosted on ice. 1µl of each plasmid was added to each vial of competent cells and mixed by tapping gently. The reactions were incubated on ice for thirty minutes. The cells were heated to 42°C for exactly 30 seconds and then placed on ice. 250µl of room-temperature Super Optimal broth with Catabolite repression (SOC medium) was added to each vial and cells were incubated at 37°C for one hour at 225 rpm. On separate labelled LB agar plates (Appendix B) with selective antibiotic (ampicillin, Fisher 10193433), 40µl from each transformation was plated out. The plates were inverted and incubated overnight at 37°. The following day a single colony from each plate was selected and inoculated into a starter culture containing 3ml of LB medium (Appendix B) with selective antibiotic (ampicillin) and incubated for 6 hours at 37°C, 270 rpm. The starter culture was diluted 1/1000 by adding 100µl of starter culture to 100ml of selective LB medium and incubated at 37°C, 270 rpm for approximately 16 hours.

2.5.2.2. Plasmid purification

Plasmids were prepared using the EndoFree® Plasmid Maxi Kit (Qiagen) according to the manufacturer's instructions. Before commencing, RNase A solution and LyseBlue were added to Buffer P1 and stored at 4°C. Buffer P3 was stored at 4°C. A solution of 70% ethanol was prepared. Bacterial cells were harvested by centrifuging at 6,000 RCF for 15 minutes at 4°C. The supernatant was discarded, and the pellet was completely lysed in 10ml of Buffer P1. 10ml of Buffer P2 was added and the tube inverted 4-6 times to

mix. The tubes were incubated for 5 minutes at room temperature. 10ml of Buffer P3 was added and mixed by inversion. The lysate was poured into the QIAfilter Cartridge and incubated at room temperature for 10 minutes. The plunger was used to filter the cell lysate into a 50ml tube and 2.5ml of Buffer ER was added to the filtered lysate. The lysate was mixed by inversion 10-12 times and then incubated on ice for 30 minutes. A QIAGEN-tip 50 column was equilibrated with 10ml of Buffer QBT and allowed to empty by gravity flow. The filtered lysate was added to the QIAGEN-tip 50 column and allowed to flow through. The QIAGEN-tip 50 column was washed with 2 X 30ml of Buffer QC. The DNA was eluted with 15ml of Buffer QN and precipitated with 10.5ml (0.7 volumes) of room temperature isopropanol and mixed. Each prep was split into 17, 1.5ml Eppendorf tubes. The tubes were spun at 15,000 RCF, 4°C for 30 minutes in a refrigerated microcentrifuge. The supernatants were disposed of and a sterile 200µl tip was used to remove any remaining liquid around the pellet. To each pellet, 294µl of 70% sterile filtered EtOH was added, and the tubes were spun at 15,000 RCF, 4°C for 10 minutes in a refrigerated microcentrifuge. The supernatant was removed with a sterile P200 tip and allowed to air dry for 10-15 minutes. To each tube 30µl of sterile nuclease-free water was added. The samples were left for 5 minutes at room temperature to allow the DNA to dissolve. The samples were vortexed to mix and centrifuged briefly before they were pooled. The DNA concentration was determined by spectrophotometry using the NanoDrop 2000 (Thermo Fisher Scientific). 1µl of RNase-free water was loaded onto the pedestals to initialise the spectrophotometer and act as a blanking buffer. Following the measurement of the reference spectrum the pedestals were wiped clean and the DNA-50 application was selected. 1µl of the samples were loaded onto the pedestals and measured. Once all the samples were measured the pedestals were cleaned with water. The plasmid was diluted to a stock of 100ng/ml with sterile nuclease-free water. The samples were kept at -30°C until required.

2.5.2.3. AGS cell transfection with plasmid DNA

AGS cells were transfected with either pCMV6-HES1 (NM_005524) Human Tagged ORF Clone (ORIGENE) or with the empty control vector, pCMV6-AC-GFP (ORIGENE). AGS cells were counted and seeded at $4.5x10^5$ cells per well in a 6 well plate. The following day, 2.5µg of DNA was diluted in 500 µl of Opti-MEM® I Reduced Serum Media without serum (Gibco, Cat No./ID: 31985062). For each well 11.2µl per well of Lipofectamine LTX® Reagent (Invitrogen, Cat No./ID: A12621) was added into the diluted Opti-MEM®:DNA solution and mixed by pipetting. 500µl of the DNA-Lipofectamine LTX® Reagent complexes were added directly to each well. Cells were incubated at 37°C in a CO_2 incubator for 18 hours before infection with *H. pylori* as indicated in section 2.4.2 followed by RNA isolation as described in section 2.7.1.

2.6. Patient recruitment for gastric biopsy tissue analysis

Stomach tissue biopsies from *H. pylori*-infected and uninfected patients were analysed in the study. Ethical permission was granted by the Joint Research Ethics Committee of Tallaght University Hospital and St. James's Hospital (Research Ethics Committee reference numbers: 2013/23/04 and 2020-03 List 9 Amendment (18)). Patients attending Tallaght University Hospital, Department of Gastroenterology Outpatient Clinics and requiring gastroscopy as part of their routine care, were invited to participate in this study. Inclusion criteria were ability and willingness to participate in the study and to provide informed consent. Participants were excluded from the study if they fulfilled any of the following criteria: aged less than 18 years old or greater than 80 years old, were unable to give informed consent, had taken antibiotics four weeks in advance or proton pump inhibitors two weeks in advance of gastroscopy, were pregnant or breastfeeding, had a significant co-existing illness, coagulopathy or current use of dual anti-platelet therapy or warfarin.

Hard-copy consent forms were stored in locked cabinets in the research offices. All personal data of the study participants were pseudonymised and stored in encrypted and password protected files. Confirmation of the participants' *H. pylori* status was determined by rapid urease test, histopathologic examination of the biopsy specimens and culture of the bacteria. The patients were considered infected if 2/3 tests were positive. Patients were considered negative if they tested negative in both rapid urease test and histology. Patients testing negative in these tests did not have culture testing. Patients who tested positive for one test only were excluded from analysis.

2.7. RNA analysis

2.7.1. Sample collection for RNA purification

Samples were harvested and total RNA was purified from cell culture experiments using the Monarch Total RNA Miniprep Kit as described below. An alternative protocol for RNA purification using the RNeasy Mini Kit (Qiagen, Cat No./ID: 74104) was utilised depending on the availability of the RNA isolation kits. The Qiagen protocol is described in Appendix C.

Following in vitro infection or cell treatment experiments, cells were harvested at various time-points. Cell culture medium was removed, and the cells were washed by addition and subsequent removal of sterile PBS. Cells were collected in 1X Monarch DNA/RNA protection reagent that was diluted from 2X with nuclease free water (Monarch Total RNA Miniprep Kit; NEB, Cat No./ID: T2010). In a 6 well plate the cells were collected in 600µl of 1X Monarch DNA/RNA protection reagent, and in either 12 well or 24 well plates 300µl of the 1X Monarch DNA/RNA protection reagent was used.

Antral biopsies from recruited patients were collected and stored in 500µl of RNAlater (Life Technologies) at 4°C overnight and at -80°C until processed for RNA purification.

2.7.2. Cell lysis and RNA purification

Before commencing, the lyophilized DNase I from the Monarch RNA Miniprep Kit was dissolved in 275µl of RNase-free water and mixed gently. The DNase I was aliquoted and stored at -20°C. 100ml ethanol (98%) was added to the 25ml RNA Wash Buffer concentrate. Samples were removed

from the freezer and brought to room temperature. All further steps were performed at room temperature to prevent precipitation of buffers. As the samples were stored in DNA/RNA Protection Reagent, an equal volume of lysis buffer was added to each tube. Up to 800µl of the sample was added to a gDNA removal column fitted with a collection tube. The samples were spun for 30 seconds at >8,000 RCF to remove most of the gDNA. The flow-through was saved and an equal volume of 98% ethanol was added and mixed by pipetting. The samples were added to the RNA purification column fitted with a collection tube and spun for 30 seconds at >8,000 RCF. The flow-through was discarded. 500µl of RNA wash buffer was added to the column and spun for 30 seconds at >8,000 RCF. For each sample, 5µl DNase I was combined with 75µl DNase I Reaction Buffer and 75µl of the mixture was pipetted directly to the top of the matrix. The samples were incubated at room temperature for 15 minutes. 500µl of priming buffer was added to the columns and spun for 30 seconds at >8,000 RCF, flow-through was discarded. 500µl of wash buffer was added to the columns and spun for 30 seconds, flow-through was discarded. Another 500µl of wash buffer was added to the columns and spun for 2 minutes, flow-through was discarded. The columns were spun for a further minute to dry the membrane. The column was transferred to a 1.5ml microfuge tube. 50-100µl of RNase free water was added directly onto each membrane. The samples were incubated at room temperature for 5 minutes for the elution buffer to absorb into the membrane. The columns were spun for 60 seconds at >8,000 RCF. The purified RNA samples were kept at -80°C until required.

RNA lysates from biopsy tissues were prepared by firstly removing the tissue samples from RNAlater and then homogenizing each tissue biopsy in 600µl of buffer RLT from the Qiagen RNeasy Mini Kit (Qiagen Cat No./ID: 74104) using a TissueRuptor (Qiagen). For RNA purification from biopsy tissue samples, the Qiagen RNeasy Mini Kit was used (Appendix C).

2.8. RNA quantification

2.8.1. RNA quantification using the Nanodrop 2000 Spectrophotometer

The RNA concentration and purity were determined by spectrophotometry to measure absorbances at 230, 260 and 280nm using the NanoDrop 2000 platform (Thermo Fisher Scientific). 1µl of RNase-free water was loaded onto the pedestals to initialise the spectrophotometer and act as a blanking buffer. Following the measurement of the reference spectrum the pedestals were wiped clean and the RNA-40 application was selected using the NanoDrop 2000 software. 1µl of the sample was loaded onto the pedestals and measured. Once all the samples were measured the pedestals were cleaned with water. Only samples with an A260/A280 ratio >1.8 were used in subsequent analyses.

2.8.2. RNA quantification using the Qubit Fluorometer

Alternatively, RNA concentration was determined using the Qubit® RNA assay kit (Thermo Fisher Scientific). An assay tube for the two standards and each of the samples were labelled and set aside. The Qubit® Working Solution was prepared by diluting the Qubit® RNA Reagent 1:200 in Qubit® RNA Buffer. The standards contained 10µl of standard and 190µl of working solution. The samples contained 2µl of RNA and 198µl of working solution. The samples and standards were mixed by vortex for 2–3 seconds and incubated at room temperature for at least 2 minutes. The RNA BR Assay program on the Qubit® 2.0 Fluorometer was used to calibrate the fluorometer with the standards and read the concentration of the samples.

2.8.3. cDNA synthesis by reverse transcription (RT)

RNA was reverse transcribed to cDNA using the RevertAid First Strand cDNA Synthesis Kit (Thermo Fisher Scientific, Cat no. K1621) according to the manufacturer's instructions. Firstly, up to 1µg of total RNA was diluted to a volume of 11µl with RNase-free water so that each sample had the same concentration of RNA. To each reaction, the following reagents were added: 4µl of reaction buffer, 1µl of RiboLock RNase inhibitor, 2µl of 10mM dNTP mix, 1µl RevertAid M-MulV reverse transcriptase and 1µl of a random hexamer primer. A master mix with enough reagents for each sample and an additional 10% was prepared. 9µl of master mix was then added to each diluted RNA sample. The RT thermal cycling conditions used were 25°C for 5 minutes to initiate the reaction, 42°C for 60 minutes to allow the reaction to progress and 70°C for 5 minutes to terminate the reaction. The RiboLock RNase inhibitor provided in the kit was used to prevent RNA degradation by RNase. The samples were stored at -20°C until required for quantitative PCR (qPCR).

2.8.4. Gene Expression analysis by qPCR

mRNA expression was analysed using TaqMan gene expression assays (Applied Biosystems) and the Taqman Universal PCR mastermix (Applied Biosystems) on the QuantStudio 5 platform. TaqMan gene expression assays used in the project are listed in Table 2.5. Firstly, the cDNA was diluted by adding nuclease free water to give a concentration of approximately 5µg/ml of cDNA. Then a mastermix of reagents was prepared for each gene of interest so that each qPCR reaction contained 0.5µl of Taqman gene expression assay and 5µl of the Taqman Universal PCR mastermix. 5.5µl of the mastermix for each gene of interest was added to wells of a microamp optical 96-well reaction plate. 4.5µl of diluted cDNA was also added to the wells. The plate was sealed using a Microamp Optical

Adhesive film and spun in the centrifuge at 1,000 RCF for 10 seconds. The comparative CT analysis was run on the Quantstudio 5 platform. The thermal cycling conditions used were 50°C for 2 minutes and 95°C for 10 minutes to activate the enzyme, followed by 40 cycles of denaturing at 95°C for 15 seconds and extension and annealing at 60°C for 1 minute. Results were normalised to the housekeeping gene GAPDH and expressed relative to uninfected patients or cells using the $2^{-\Delta\Delta ct}$ method (Livak and Schmittgen, 2001) as described in Section 2.11.2 below.

Gene Name	Assay ID
Caspase-4	Hs01031951_m1
CCL20	Hs00535829_s1
CXCL1	Hs00236937_m1
Delta Like 1	HS00194509_m1
Delta Like 3	HS01085096_m1
Delta Like 4	HS00184092_m1
EED	Hs00537777_m1
EZH2	Hs01016789_m1
FOS	Hs00170630_m1
GAPDH	HS99999905_m1
HES1	HS00172878_m1
HEY1	HS01114113_m1
IL-1β	Hs00174097_m1
IL-8	HS00174103_m1
Jagged 1	HS00164982_m1
Jagged 2	HS00171432_m1
KDM6B	Hs00996325_g1
Notch 1	HS01062014_m1
Notch 2	Hs00225747_m1
Notch 3	HS01128537_m1
Notch 4	HS009685889_m1
RBP-J	HS01068138_m1
RTL10	Hs00535829_s1
SLX1B-SULT1A4	Hs00225232_m1
SOX9	Hs00165814_m1
SUZ12	Hs00248742_m1
TNF	Hs00174128_m1
TRAF1	Hs01090170_m1

Table 2.5: List of TaqMan gene expression assays used for qPCR

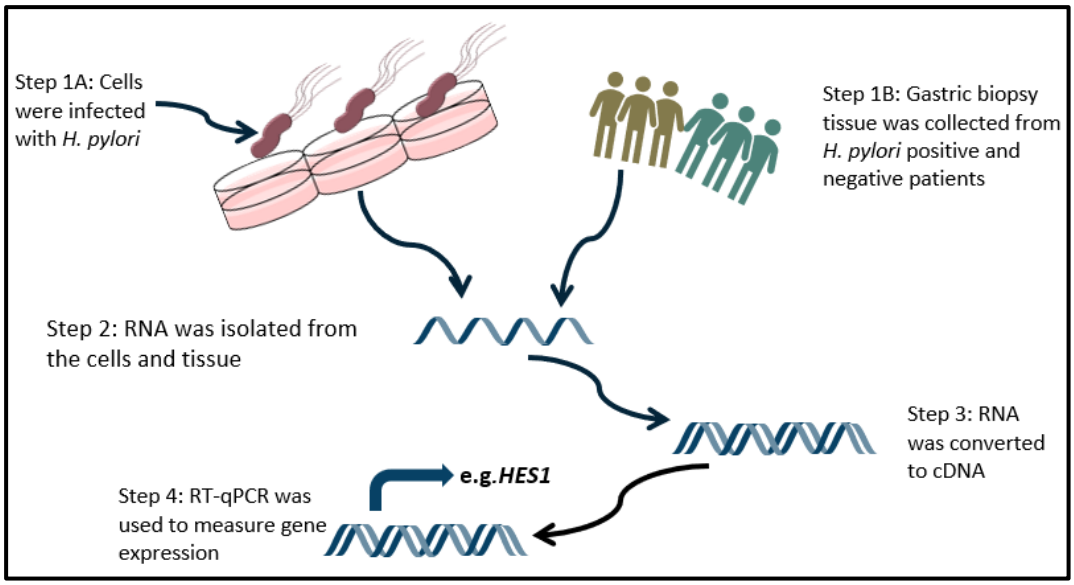

Figure 2.2 Overview of RT-qPCR methods for gene expression analysis. Firstly (Step 1A), cell lines were cultured and seeded at appropriate concentrations and infected with *H. pylori* (or treated with various stimuli). Alternatively (Step 1B), gastric biopsy tissue was collected from *H. pylori* positive and negative control patients. In both cases RNA was purified (Step 2), converted to cDNA (Step 3) and gene expression was measured by qPCR (Step 4) prior to statistical analysis to identify significant changes in gene expression. Figure created in PowerPoint.

2.9. RNAseq

2.9.1. Sample description

Total RNA was purified from the samples listed in Table 2.6 below and the RNA concentration and quality assessed using the Nanodrop spectrophotometer as described in section 2.8.1. The samples were diluted to 30ng/µl with nuclease free water, packaged in dry ice and shipped to Eurofins Genomics, Germany for RNAseq.

Sample Name	Description
Un-transfected/ No plasmid A & B	Duplicate samples of un-transfected AGS cells in the absence of *H. pylori.*
Un-transfected/ No plasmid + *H. pylori* A & B	Duplicate samples of un-transfected AGS cells infected with *H. pylori* for 3 hours.
Control plasmid A & B	Duplicate samples of AGS cells transfected with pCMV6-AC-GFP in the absences of *H. pylori.*
Control plasmid + *H. pylori* A & B	Duplicate samples of AGS cells transfected with pCMV6-AC-GFP infected with *H. pylori* for 3 hours.
HES1 plasmid A & B	Duplicate samples of AGS cells transfected with pCMV6-HES1 in the absences of *H. pylori.*
Hes1 plasmid + *H. pylori* A& B	Duplicate samples of AGS cells transfected with pCMV6-Hes1 infected with *H. pylori* for 3 hours.

Table 2.6 Description of samples analysed by RNA-seq.

2.9.2. Library preparation and RNAseq

Samples were processed by Eurofins Genomics using their Inview Transcriptome Discover Service. Briefly, this package involved checking the quality of the RNA samples, purification of poly-A containing mRNA molecules, mRNA fragmentation, random primed cDNA synthesis (strand specific), adapter ligation and adapter specific PCR amplification. The resulting samples were then sequenced on the Illumina NovaSeq platform using paired end sequencing with a read length of 2 x 150 bp.

2.9.3. RNAseq data analysis

Initial data analysis including sequence quality control, mapping, alignment, and transcript quantification were performed by Eurofins Genomics. The analysis workflow is summarised in Figure 2.3 below and the corresponding software packages listed in Table 2.7.

During sequence quality control, raw sequencing data was pre-processed using fastp software (Table 2.7) to clean the data for down-stream analysis. The quality of the raw sequencing was checked and filtered so that only high-quality bases were retained. The high-quality sequence reads were then aligned to the reference genome (*Homo sapiens* UCSC genome version hg38) using the alignment tool STAR (Spliced Transcripts Alignment to a Reference, Table 2.7) and the Sentieon framework (Table 2.7). The alignments were inspected using the RSEM tool (Table 2.7) to quantify the transcripts, which are reported as fragments per kilobase per million (FPKM). Using the files provided by Eurofins genomics, principal component analysis was then performed using Deseq2 (Table 2.7) to evaluate patterns and variations in the datasets.

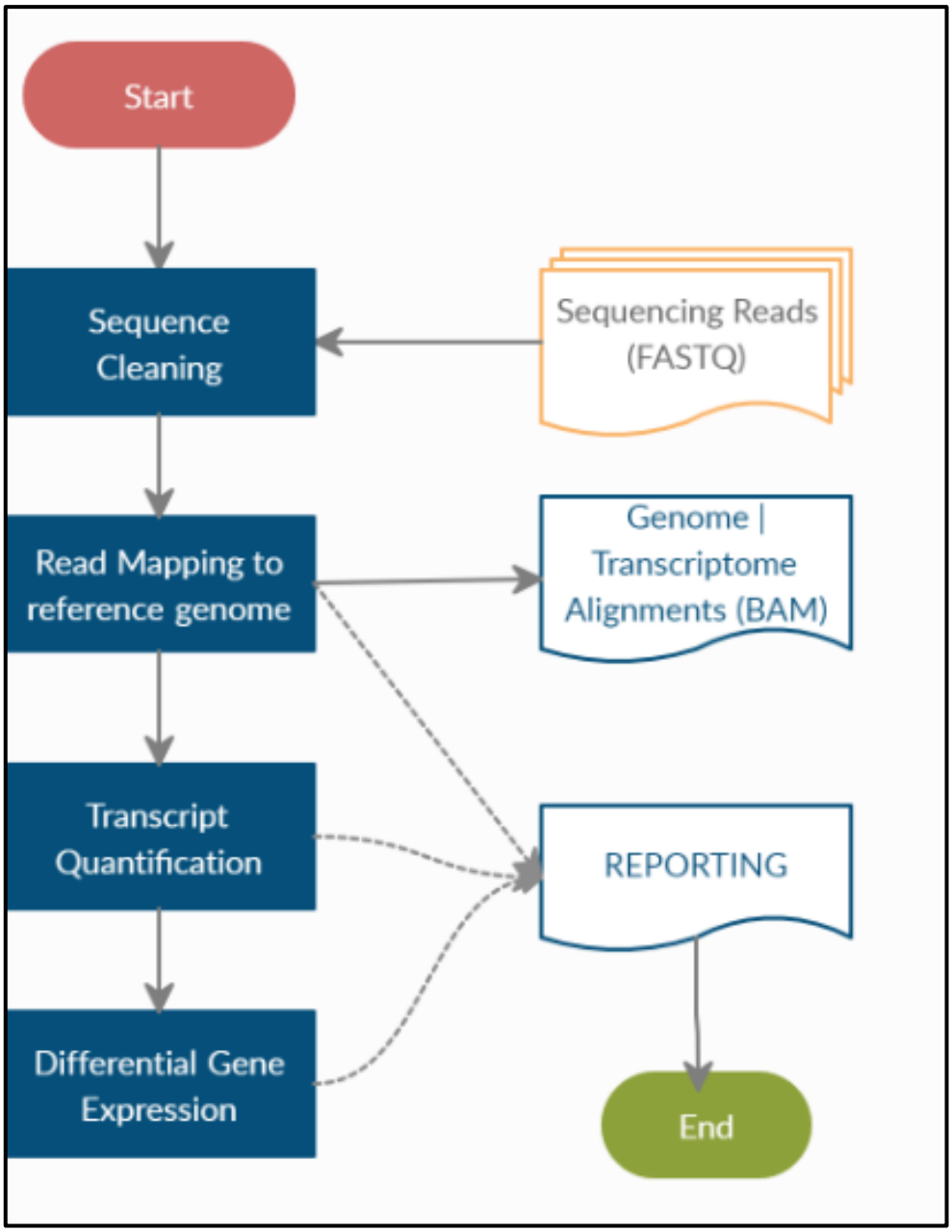

Figure 2.3 RNAseq data analysis overview. Adapted from Eurofins Expression analysis report.

Tool	Version	Description	Reference
fastp	0.20.0	Fastp is a tool which can provide fast pre-processing (such as quality control, adapter trimming, quality filtering and per-read quality pruning) for FastQ files.	(Chen et al., 2018)
STAR	2.7.8a	Spliced Transcripts Alignment to a Reference (STAR) is a fast RNAseq read mapper, that aligns hight-throughput RNAseq data to a reference genome. STAR has support for splice-junction and fusion read detection.	(Dobin et al., 2013)
Sentieon	202112.02	Sentieon® provides for secondary RNA analysis and for calling variants from next-generation sequence data.	(Freed et al., 2017)
RSEM	1.3.3	RSEM is a software tool for measuring gene and isoform abundances from RNAseq data.	(Li and Dewey, 2011)
Deseq2	2.11.40.7+galaxy2	Verifies differentially expressed features from count tables to calculate fold change.	(Love et al., 2014), (Afgan et al., 2018)
GAGE	Bioconductor version 3.17	Generally Applicable Gene-set Enrichment (GAGE) is a method of analysing a gene set based on pathway knowledge.	(Luo et al., 2009)
Pathview	Bioconductor version 3.17	A tool to integrate and visualise pathway data. Maps data onto relevant pathway graphs.	(Luo and Brouwer, 2013)

Table 2.7 Software used in the data analysis pipeline.

2.9.4. Differential Gene Expression

To identify differential gene expression between conditions, the gene counts calculated by Eurofins Genomics were analysed using the Deseq2 package on the Galaxy Europe server (Table 2.8), (Love et al., 2014), (Afgan et al., 2018). The gene counts for each individual treatment were converted to .txt files and uploaded to the Galaxy Europe platform. The Deseq2 package was used to determine differentially expressed features by comparing the duplicates of each treatment against the duplicate of the un-transfected control sample according to the layout in Table 2.8. The resulting .txt files that were produced in Deseq2 were copied into excel files. Gene IDs that did not have corresponding gene names and genes that had 'NA' for log2 fold difference were filtered out. To find significantly upregulated genes, the $\log_2$ fold difference column was filtered for values >0 and the adjusted p value column for values <.05. To find significantly downregulated genes, the $\log_2$ fold difference column for values <0 was filtered and the adjusted p value column for values <.05.

Deseq2 analysis	Factor 1	Factor 2
1	- Un-transfected, *H. pylori* A And - Un-transfected, *H. pylori* B	- Un-transfected A And - Un-transfected B
2	- Control plasmid A And - Control plasmid B	- Un-transfected A And - Un-transfected B
3	- Control plasmid, *H. pylori* A And - Control plasmid, *H. pylori* B	- Un-transfected A And - Un-transfected B
4	- HES1 plasmid A And - HES1 plasmid B	- Un-transfected A And - Un-transfected B
5	- HES1 plasmid, *H. pylori* A And - HES1 plasmid, *H. pylori* B	- Un-transfected A And - Un-transfected B
6	- HES1 plasmid A And - HES1 plasmid B	- Control plasmid A And - Control plasmid B
7	- HES1 plasmid, *H. pylori* A And - HES1 plasmid, *H. pylori* B	- Control plasmid, *H. pylori* A And - Control plasmid, *H. pylori* B

Table 2.8 Files run in Deseq2.

2.9.5. Pathway analysis

Pathway analysis was performed with help from Dr Thomas Butler, Smith laboratory. The GAGE tool (Table 2.7) in Bioconductor was used to perform pathway enrichment analysis on the files generated using Deseq2. Pathview (Table 2.7) was used to map the GAGE results onto KEGG pathways.

2.10. Protein Analysis

2.10.1. Preparation of protein lysates

Cells were washed with ice-cold sterile PBS. Cells seeded in a 24 well plate were collected in 90µl of ice-cold radioimmunoprecipitation assay (RIPA) buffer (Sigma; R0278). Cells seeded in a 6 well plate were collected in 500µl of RIPA buffer. Directly before use 100 X protease inhibitor cocktail (Thermo Fisher; 78440) was added to the RIPA buffer for a final volume of 1X. Adherent cells were scraped from the wells. The appropriate volume of 5X Lamelli buffer (0.25M Tris-HCl, (pH 6.8), 10% sodium dodecyl sulphate (SDS), 50% glycerol, 0.5% bromophenol blue with 10% 1M dithiothreitol (DTT)) was added to each sample for a final concentration of 1X and boiled for 7 minutes at 90°C to denature the proteins. The samples were stored at -20°C until use.

2.10.2. SDS polyacrylamide gel electrophoresis and Western blot

SDS polyacrylamide gel electrophoresis (PAGE) and Western blots were performed in collaboration with Dr Ewelina Flis from Prof. Emma Creagh's laboratory, School of Biotechnology, and Immunology TBSI and Prof. Michael Freeley, School of Biotechnology, Dublin City University.

Samples were transported to DCU and TBSI on ice. Before commencing, 15ml of a 10% resolving gel was prepared: 5.9ml H_2O, 5.0ml 30% acrylamide mix, 3.8ml 1.5M Tris (pH 8.8), 0.15ml 10% SDS, 0.15ml 10% ammonium persulfate, 0.006ml TEMED. The percentage of the gel used is dependent on the molecular weight of the proteins of interest. 10% gels can be used for proteins between 15-100 kDa. The gel was poured into the cassette leaving a

space of ~5cm. A small amount of propanol was poured on top. When the gel was polymerised, the propanol was poured off and 5ml of stacking gel was prepared and poured on top of the resolving gel: 3.4ml H_2O, 0.38ml 30% acrylamide mix, 0.63ml 1.0M Tris (pH 6.8), 0.05ml 10% SDS, 0.05ml 10% ammonium persulfate, 0.005ml TEMED, and the comb was put in place.

The gels were fitted into the electrophoresis rig. The gels were covered in 1L of running buffer adjusted to pH 8.3: 25mM Tris base, 190mM glycine, 0.1% SDS. 5µl of protein ladder was run in one of the wells. 20µl of each sample was loaded into each well of the gels. The gels were run at 90V until the dye reached the bottom of the gel and there was clear separation of the ladder.

The nitrocellulose membrane was activated in transfer buffer (25mM Tris base (pH 8.3), 190mM glycine 20% methanol) for 5 minutes. The gels were removed from the rig and the glass slides, and a "Sandwich" was prepared in the following order: clear side of cassette, sponge, filter paper x2, nitrocellulose membrane, gel, filter paper x2, sponge, black side of cassette. Air bubbles were removed with a roller and the cassette was placed in the transfer rig, covered in transfer buffer, and run overnight at 40mAmps. Following transfer, the membrane was washed briefly in TBST (10mM Tris, 150mM NaCL, 0.05% Tween20). The membrane was submerged in blocking buffer (5% dried milk dissolved in TBST) for 1 hour on a rocker.

Primary antibodies used in the study are listed in (Table 2.9). The primary antibody was diluted according to Table 2.9 in 5ml of blocking buffer and the membrane was incubated in the primary antibody overnight rotating in a cold room. The membrane was washed 3 times for 10 minutes each with TBST. The corresponding secondary antibody was diluted according to the manufacturer's instruction in blocking buffer, and the membrane was incubated for 1 hour on a rocker. The membrane was washed with TBST. The ECL solution was prepared in the ratio 1:1:2 ECLA: ECLB: Deionised water. The ECL mix was poured on top of the membrane and incubated for

1 minute and imaged. Band intensities were quantified using ImageJ software (National Institute of Health, Bethesda, MD, USA).

Primary Antibody	Source	Dilution
Hes1 (D6P2U) rabbit monoclonal antibody	Cell Signalling (#11988)	1:1000
Caspase 11 (17D9) rat monoclonal antibody	Sigma Aldrich (#MABF265)	1:1000
Pro-IL-1β (AF401) goat polyclonal antibody	R&D Systems (#AF401-SP)	1:1000
Pro-caspase 1 (p45) (A-19) rabbit polyclonal antibody	Santa Cruz (#sc-622)	1:2000
Cleaved caspase 1 (Asp297) (D57A2) rabbit monoclonal antibody	Cell Signalling (#4199)	1:1000
β-actin (AC-74) mouse monoclonal antibody	Sigma Aldrich (#A2228)	1:15000
β-tubulin	Cell signalling (#2146)	1:1000

Table 2.9 List of antibodies used for western blotting.

2.10.3. Enzyme-linked immunosorbent assay

The enzyme-linked immunosorbent assay (ELISA) was performed in collaboration with Dr Ewelina Flis from Prof. Emma Creagh's laboratory, School of Biotechnology, and Immunology TBSI.

Cell culture supernatant was spun in a microcentrifuge for 10 minutes at top speed. The supernatant was transferred to a fresh tube making sure not to disturb the pellet. The samples were stored at -20°C until use and transported to TBSI on ice. IL-1ß concentrations in supernatants were measured by ELISA (R&D Systems) according to the manufacturer's instructions.

2.11. Statistical analysis

2.11.1. Statistical analysis of HP-EuReg data

Continuous variables are presented as arithmetic means and standard deviations. Qualitative variables are presented as proportions with 95% confidence intervals (CI). The statistical analysis of results was calculated using the Fisher's exact test or a Chi-square test when more than 20% of the cells had expected frequencies < 5. Two-sided tests were used for analyses and the P-value cut-off for significance was set to 0.05. The analysis was carried out using, Excel and Graphpad.

2.11.2. The comparative CT method for gene expression analysis and statistics for qPCR

Gene expression was calculated using the comparative CT method. The ΔCT value was determined by subtracting the average GAPDH CT value from the average gene of interest CT value. The standard deviation of the difference was calculated from the standard deviations of both the gene of interest and GAPDH using the formula:
$\sqrt{(Standard\ deviation\ GAPDH)^2 + (Standard\ deviation\ gene\ of\ interest)^2}$.
To calculate the ΔΔCT, the ΔCT calibrator value (uninfected/untreated value) was subtracted from the ΔCT treated/infected value. Subtraction of an arbitrary constant makes sure the standard deviation of ΔΔCT is the same as the standard deviation of the ΔCT value. The fold difference was calculated using the formula: $2^{-\Delta\Delta CT}$. The negative error bar was calculated by subtracting the fold difference value from the fold difference plus the ΔΔCT standard deviation. The positive error bar was calculated by subtracting the fold difference minus the ΔΔCT standard deviation from the fold difference (Livak and Schmittgen, 2001).

Statistical analysis to identify significant changes in relative gene expression was performed using GraphPad Prism version 9.00 for Windows. A one-tailed, Mann-Whitney U-test was used to compare results from biopsies of *H. pylori*-infected versus uninfected patients. A P value of <.05 was considered significant. A One-way ANOVA followed by a post-hoc test was used to determine whether there were any statistically significant differences between the means of three or more independent groups on a single dependent variable. A Two-way ANOVA followed by a post-hoc test was used to determine how the mean of a dependent variable changes depending on two separate independent variables in more than three independent groups. The post-hoc (multiple comparison) tests used were Tukey, Dunnett's or Šídák depending on the type of multiple comparisons performed. The Tukey method was used when comparing every mean with every other mean. The Dunnett's method was used to compare every mean with a control mean. The Šídák was used when a group of means were selected to be compared. A summary of the methods used for qPCR is found in Figure 2.2.

Chapter Three Analysis of Irish data in the Hp-EuReg

3.1. Introduction

Although *H. pylori* has been a recognised pathogen since the 1980s a universally agreed upon method for diagnosis and treatment does not yet exist. The effectiveness of a treatment can be impacted by choice of antibiotics, duration of therapy, administration in relation to food and number of doses a day (Graham et al., 2014). The main concern with *H. pylori* treatment is growing antibiotic resistance, particularly to clarithromycin, which has impacted *H. pylori* eradication rates in recent years (Boltin et al., 2021).

3.1.1. The HP-EuReg collects data on the management of *H. pylori* in Europe.

The European registry on *H. pylori* management (Hp-EuReg) was set up in 2013 to collect real-world clinical treatment and eradication data from 30 different countries in Europe (Nyssen et al., 2021b) (Figure 3.1). Study data was collected and uploaded to REDCap Electronic Data Capture tools hosted at "Asociación Española de Gastroenterología" (www.aegas tro.es) (McNicholl et al., 2019). The aim of the Hp-EuReg is to audit *H. pylori* treatment and patient outcomes and compare them to the most up-to-date international guidelines. There are many variations of treatment for *H. pylori*, in fact an audit of the Hp-EuReg from 2013-2018 found that over 100 different first-line regimens were prescribed across Europe (Nyssen et al., 2021a). Additionally, a benefit of auditing these treatments using the Hp-EuReg is that it collects real-world data instead of controlled clinical trials which show how effective these treatments are in practice.

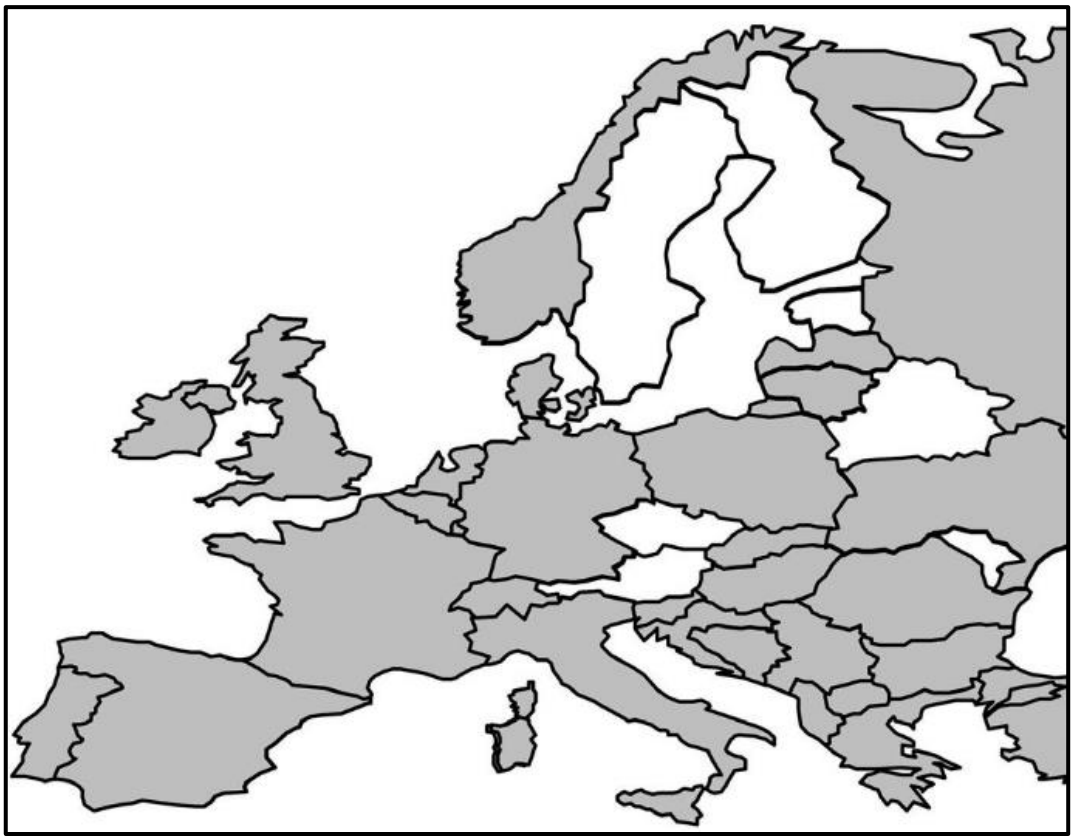

Figure 3.1 Countries taking part in the HP-EuReg are coloured in grey. Adapted from (McNicholl et al., 2019).

3.1.2. In 2017 the Irish *H. pylori* Working Group published guidelines for the management of *H. pylori* in Ireland.

H. pylori can be a challenging pathogen to treat. The ideal treatment regimen for *H. pylori* eradication depends on many factors, including local antibiotic resistance rates, patient compliance and possible side effects from treatment. Since the rates of antibiotic resistance can vary greatly between regions it is important to have local treatment guidelines to support international recommendations (Megraud et al., 2013). The Irish *Helicobacter pylori* Working Group (IHPWG) was set up to offer recommendations on *H. pylori* treatment in Ireland (Smith et al., 2017a). The aim of the IHPWG was to review literature and to fine-tune the available international guidelines to best fit the Irish population (Smith et

al., 2017a), (Malfertheiner et al., 2017). Following review of the available data at the time, the IHPWG recommended 15 statements with regard to diagnosis and treatment of *H. pylori* in Ireland (Smith et al., 2017a). The statements are outlined in Table 3.1.

1	All patients with upper gastrointestinal tract symptoms should be tested for *H. pylori.*
2	The recommended non-invasive test for *H. pylori* is the C^{13} UBT.
3	The recommended invasive test for *H. pylori* is combined histology and RUT.
4	Corpus and antrum biopsies should be used for RUT.
5	When culture of *H. pylori* is required corpus and antrum biopsies should be collected.
6	It is necessary to perform post-eradication testing. If gastroscopy is not required, the recommendation is to use C^{13} UBT.
7	PPIs should be stopped 14 days before testing for *H. pylori* due to PPIs increasing the risk of false negative results.
8	Standard Triple-C+A therapy for 7 days can no longer be recommended due to low eradication rates.
9	14-day Triple-C+A with a high-dose proton pump inhibitor is recommended. Bismuth quadruple therapy for 14 days is an alternative if available.
10	At present, antimicrobial susceptibility testing prior to first line treatment in not recommended.
11	Molecular methods (PCR) can be used to monitor clarithromycin resistance rates.
12	Second line treatment should be different to first line treatment. The recommended second line treatments are either a) 14 days of levofloxacin-based therapy with high-dose PPI, b) 14 days of Triple-C+A therapy with high-dose PPI or c) bismuth quadruple therapy for 14 days.
13	Antimicrobial susceptibility testing by culture should be performed following two failed treatments.
14	Due to the risk of severe side effects, rifabutin should be reserved for third line or subsequent rescue treatments.
15	Sequential therapy is not recommended for rescue therapy.

Table 3.1 Irish recommendations for *H. pylori* treatment as published by the IHPWG (Smith et al., 2017a). Abbreviations: UBT: Urea breath test, RUT: Rapid urease test, PPI: Proton pump inhibitor, Triple-C+A: Triple therapy consisting of clarithromycin, amoxicillin, and PPI.

3.1.3. How do Irish guidelines differ from the most recent European guidelines?

The most recent Maastricht guidelines were published in 2022 (Malfertheiner et al., 2022). These guidelines recommended that clarithromycin susceptibility testing, using culture or PCR, should be performed before any treatment containing clarithromycin is prescribed. In the absence of individual testing, areas with unknown or >15% clarithromycin resistance should not prescribe Triple-C+A as a first line treatment. Instead bismuth quadruple therapy or non-bismuth concomitant quadruple therapy (PPI, amoxicillin, clarithromycin, nitroimidazole) is recommended (Malfertheiner et al., 2022). These new European guidelines would suggest an audit of treatment patterns and eradications rates in Ireland should be performed. Depending on the outcome, Irish guidelines may need to be updated to consider the findings of the audit as well as the latest international guidelines for the management of *H. pylori*.

3.1.4. How can eradication rates be improved in the absence of new treatments?

It may take a long time before new antibiotics/host directed therapies are developed to replace the current therapies for *H. pylori* . In the absence of new treatments there are two methods to better improve the management of *H. pylori*.

1) Adapt treatments so they align with up-to-date and local antibiotic susceptibility and/or treatment efficacy.
2) Specifically, tailor treatment to an individual patient via antimicrobial susceptibility testing.

Performing antimicrobial susceptibility testing often requires an invasive test which is not favourable for many patients. Furthermore, antimicrobial testing can be challenging, costly and time consuming. For these reasons susceptibility testing is not recommended for treatment naïve patients in the IHPWG guidelines (Smith et al., 2017a). Considering this, having an extensive local audit of first line, second line and rescue treatments is extremely important to make sure patients receive a treatment that gives them the best possible likelihood of *H. pylori* eradication.

3.2. Aims and objectives.

The aim of this chapter was to audit *H. pylori* prescription patterns and cure rates over a 10-year period from 2013-2022 using data collected in the Hp-EuReg. The objectives are listed below.

- Objective 1: To describe *H. pylori* first line treatment patterns and eradication rates in Ireland from 2013-2022.
- Objective 2: To describe *H. pylori* second line treatment patterns and eradication rates in Ireland from 2013-2022.
- Objective 3: To describe *H. pylori* rescue treatment patterns and eradication rates in Ireland from 2013-2022.

3.3. First line treatment results

3.3.1. Treatment-naïve patient characteristics.

Due to variations in antibiotic usage, antibiotic resistance and treatment availability, local audits of prescription and eradication patterns are necessary to find the optimal treatment regimen. Irish data from the Hp-EuReg was analysed. Variables assessed included PPI dose, length of treatment and antibiotics used. Two sites were included in the Irish analysis. These were the public hospital, Tallaght University Hospital Dublin, and the private hospital, Beacon Hospital Dublin. A combined 1,006 patients were included in the first line treatment cohort (Table 3.2). Descriptive demographic analysis on these patients found they had a mean age of 49.9 years and 53.3% (N=536) were female (Table 3.3). Most patients had no recorded drug allergy (N=992, 98.6%) but 1.4% (N=14) had a recorded penicillin allergy. No other drug allergies were recorded in the database. The percentage of patients not taking any known concurrent medication was 90.2% (N=907). However, 9% (N=91) were taking PPIs and 8.9% (N=90) were taking acetylsalicylic acid, NSAIDs and statins each (Table 3.3). The most common indications were dyspepsia (91.9%; N=925) and peptic ulcer (3%; N=30) (Table 3.3).

	Number of patients (N)	Percentage
Tallaght University Hospital	788	78.3
Beacon Hospital	217	21.6
Unknown	1	0.1
Total (N)	1006	100.0

Table 3.2 Number of patients from each data centre included in the study.

Number of patients		**1,006**
Age: Mean (SD)		49.9 (15.5)
Female*: N (%)		536 (53.3)
Indication: N (%)	Dyspepsia Peptic ulcer Other	925 (91.9) 30 (3.0) 51 (5.1)
Concurrent medication: N (%)	None Unknown Proton pump inhibitors Acetylsalicylic acid NSAIDs Statins	907 (90.2) 6 (0.6) 91 (9) 90 (8.9) 90 (8.9) 90 (8.9)
Drug allergies: N (%)	None Penicillin	992 (98.6) 14 (1.4)

Table 3.3 Baseline demographics of patients included in study. Abbreviations: SD: standard deviation, NSAID: non-steroidal anti-inflammatory drugs. * One patient had unrecorded gender.

3.3.2. Most treatment-naïve patients were diagnosed with *H. pylori* by an invasive test.

The three most common methods of diagnosis were the RUT (46.8%; N=471), histology (37.2%; N=374) and the C^{13}-UBT (35.6%; N=353) (Table 3.4). Only 33 patients had *H. pylori* culture and antibiotic susceptibility testing performed. Of these 7 cultured strains were resistant to clarithromycin, 13 were resistant to metronidazole and 1 each resistant to levofloxacin and amoxicillin (Table 3.4). Overall, data indicates that most patients receiving first line *H. pylori* treatment were diagnosed by an invasive test.

Test	Description	N	Percentage
^{13}C- UBT	Non-invasive	353	35.6
Histology	Invasive	374	37.2
RUT	Invasive	471	46.8
Culture	Invasive	33	3.3
Resistance	Clarithromycin Metronidazole Levofloxacin Amoxicillin	7 13 1 1	31.8 59.1 4.5 4.5
Other		6	0.6

Table 3.4 *H. pylori* diagnosis method of treatment-naïve patients included in the study.

3.3.3. The duration of first line treatment prescribed increased between 2013-2022.

Overall, most first line treatment prescriptions were for 14 days (N=870, 86.5%) followed by 7 days (N=89, 8.8%) (Figure 3.2) (Table 3.5). Analysis of first line treatment duration over time indicated that prescriptions for shorter durations were more common in 2013 and 2014 (Table 3.5) (Figure 3.3). In 2013, 65.9% (N=29) of prescriptions were for 7 days while only 31.8% (N=14) were for 14 days. The length of treatment prescribed increased over time. In 2017 and 2018 only two patients received 7-day treatment each year and from 2019 onwards all patients were prescribed 14-day treatment (Table 3.5) (Figure 3.3). In 2017 the IHPWG stated that "standard triple therapy for a duration of 7 days can no longer be recommended" (Smith et al., 2017a). The dominance of 14-day treatment regimens post-2017 indicates good clinical compliance with this recommendation.

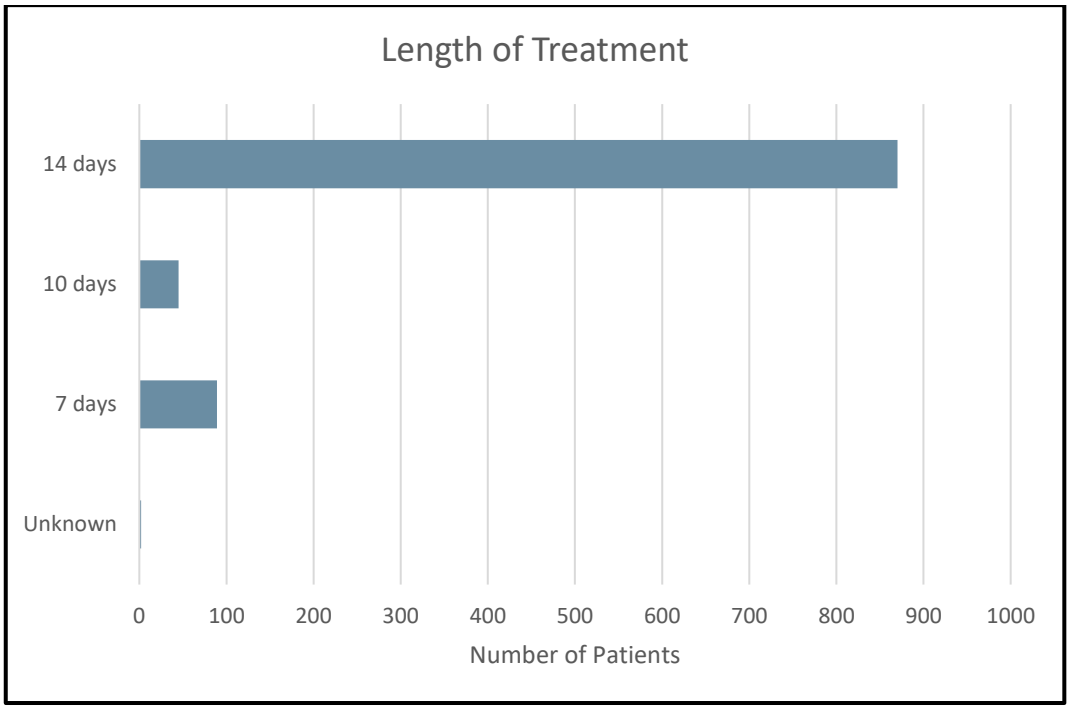

Figure 3.2 Duration of first line treatment prescribed to treatment-naïve patients.

	Year										
	2013	**2014**	**2015**	**2016**	**2017**	**2018**	**2019**	**2020**	**2021**	**2022**	**Total**
7 days	29	52	0	4	2	2	0	0	0	0	89
10 days	1	44	0	0	0	0	0	0	0	0	45
14 days	14	14	29	26	54	114	232	141	159	87	870

Table 3.5 Number of first line prescriptions per year according to duration of treatment. N = 1004. 2 patients had unknown treatment length and are not included in the table.

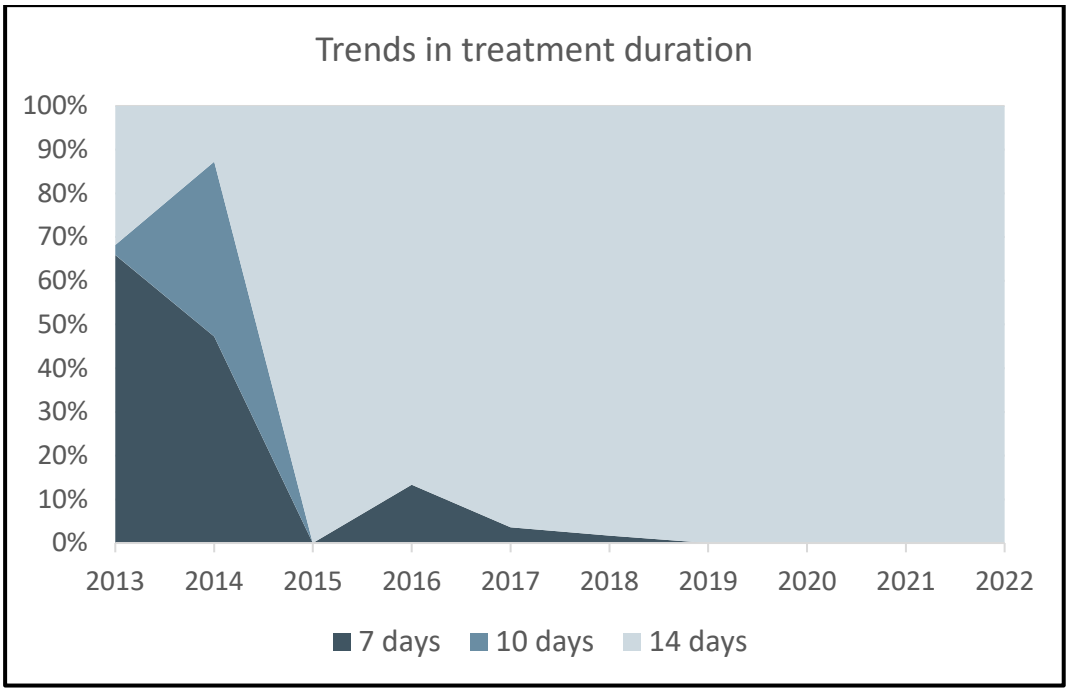

Figure 3.3 Percentage of first line prescriptions per year according to duration of treatment. N = 1004. 2 patients had unknown treatment length and are not included in graph.

3.3.4. The potency of the PPI prescribed in first line treatment increased between 2013-2022.

In total, most first line prescriptions (N=861, 85.6%) (Figure 3.4) (Table 3.6) were for a high dose PPI, as defined as between 54 to 128 mg omeprazole equivalents (Nyssen et al., 2021a). In 2013 and 2014, 88.6% (N=39) and 87% (N=94) respectively of PPI prescriptions were low doses (Table 3.6) (Figure 3.5). However, a sharp change in prescription patterns was observed from 2015 onwards and every year from 2015-2022 PPI dosage was high >98% of the time. Several metanalyses have shown that increased PPI dose enhances *H. pylori* eradication (Vallve et al., 2002), (Villoria et al., 2008). Additionally in 2016 the Maastricht V/Florence Consensus Report recommended that the "use of high dose PPI twice daily increases the efficacy of triple therapy" (Malfertheiner et al., 2016). The sharp decline in prescriptions for low dose PPI from 2015 onwards is consistent with these European recommendations. Changes in treatment duration and PPI dose

also correspond to recommendations from the IHPWG published in 2017 (Smith et al., 2017a) (Figure 3.5).

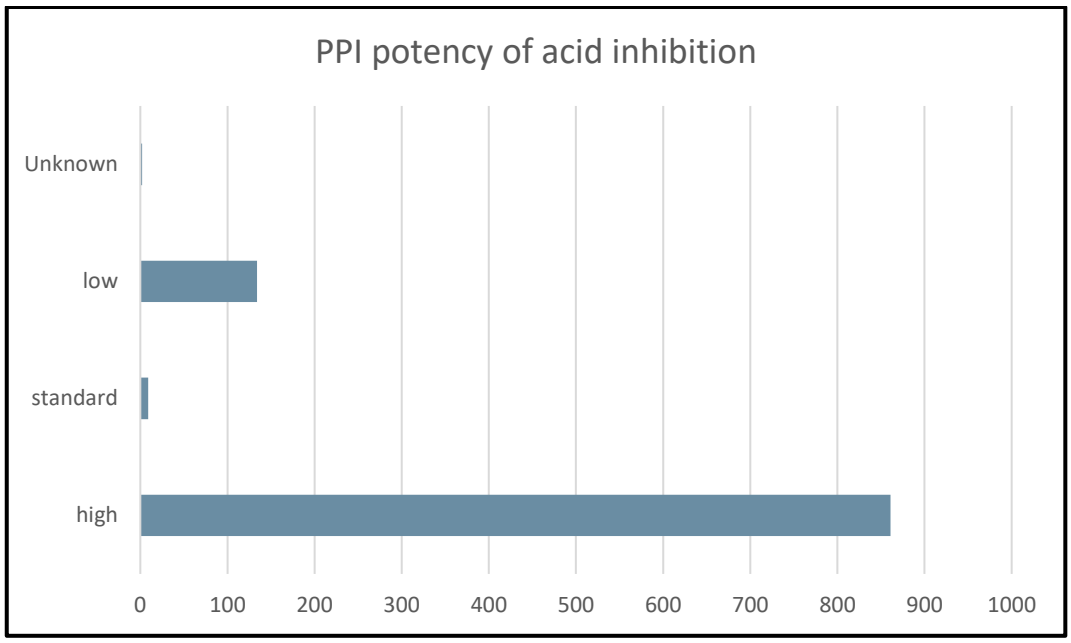

Figure 3.4 PPI potency of first line treatments prescribed to treatment-naïve patients. Low dose PPI: ranging from 4.5 to 27 mg omeprazole equivalents. Standard dose PPI: ranging from 32 to 40 mg omeprazole equivalents. High dose PPI: ranging from 54 to 128 mg omeprazole equivalents. N = 1006. 2 patients had unknown PPI dose.

	Year										
	2013	**2014**	**2015**	**2016**	**2017**	**2018**	**2019**	**2020**	**2021**	**2022**	**Total**
Low	39	94	0	0	0	0	1	0	0	0	134
Standard	1	0	0	0	0	2	5	1	0	0	9
High	4	14	29	30	56	114	226	142	159	87	861

Table 3.6 Number of first line prescriptions per year broken down by PPI potency. Low dose PPI: ranging from 4.5 to 27 mg omeprazole equivalents. Standard dose PPI: ranging from 32 to 40 mg omeprazole equivalents. High dose PPI: ranging from 54 to 128 mg omeprazole equivalents. N = 1004. 2 patients had unknown PPI dose and are not included in table.

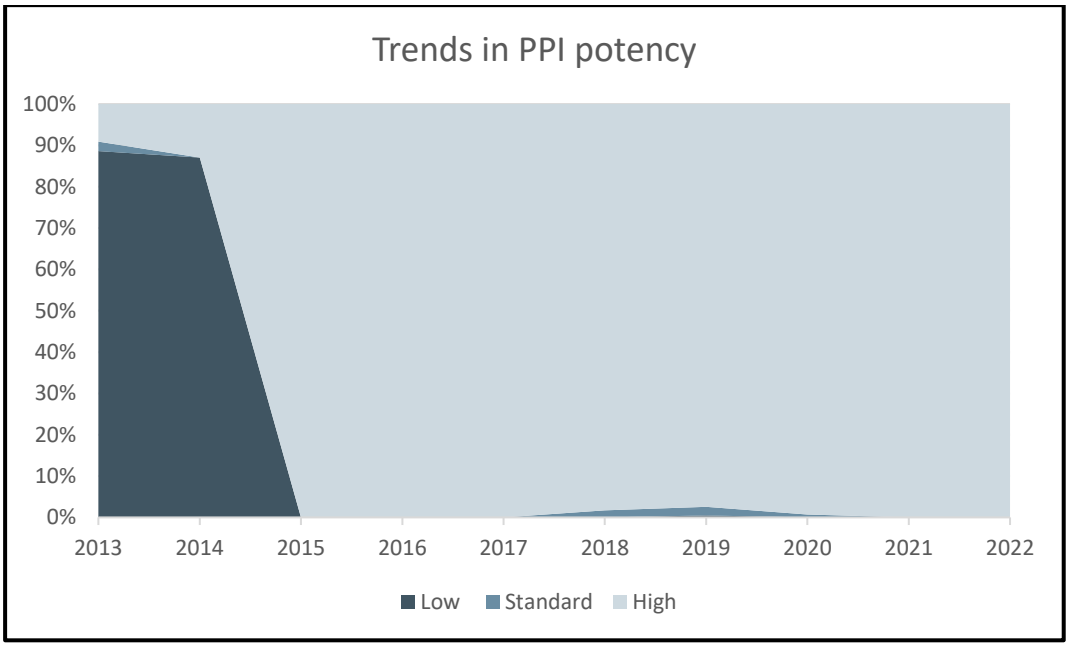

Figure 3.5 Percentage first line treatments per year broken down by PPI potency. Low dose PPI: ranging from 4.5 to 27 mg omeprazole equivalents. Standard dose PPI: ranging from 32 to 40 mg omeprazole equivalents. High dose PPI: ranging from 54 to 128 mg omeprazole equivalents. N = 1004. 2 patients had unknown PPI dose and are not included in graph.

3.3.5. Publication of the IHPWG guidelines on the management of *H. pylori* infection led to a significant change in prescription patterns in relation to treatment duration and PPI dose.

To directly evaluate the impact of the IHPWG Guidelines on first line treatment patterns, treatment duration and PPI doses prescribed were compared before and after their publication. There was a significant decrease in the prescription of 7 day therapies following publication of the guidelines; 7 day therapy represented 39.9% of all treatments prescribed pre-2017 compared to just 0.5% post-2017 ($p<.001$), while 14 day treatment increased from 39% of treatments prescribed pre-2017 to 99.2% afterwards ($p<.001$) (Table 3.7).

Similarly, the use of low dose PPI decreased following the publication of the guidelines, with an increase in high dose PPI prescriptions from 36.2% of *H. pylori* treatments in the period 2013-2016 to 98.9% of therapies prescribed between 2017-2022 (Table 3.8).

Duration	Pre-Irish guidelines 2013-2016 N=213		Post-Irish guidelines 2017-2022 N=793		*P value
	N	%	N	%	
7 days	85	39.9	4	0.5	<.001
10 days	45	21.1	0	0	<.001
14 days	83	39.0	787	99.2	<.001
Unknown	0	0	2	0.3	N/A

Table 3.7 Comparison of treatment duration of prescriptions pre- and post-publication of the IHPWG Guidelines. Irish recommendations for *H. pylori* treatment were published in 2017 (Smith et al., 2017a). P value was calculated by a 2-tailed Chi Square test.

PPI Dose	2013-2016 N=213		2017-2022 N=793		*P value
	N	%	N	%	
Low	133	62.4	1	0.1	<.001
Standard	1	0.5	8	1	.458
High	77	36.2	784	98.9	<.001
Unknown	2	0.9	0	0	N/A

Table 3.8 Comparison of PPI dose prescribed pre- and post-publication of the IHPWG Guidelines. Irish recommendations for *H. pylori* treatment were published in 2017 (Smith et al., 2017a). P value was calculated by a 2-tailed Chi Square test.

3.3.6. The most prescribed first line treatment was clarithromycin amoxicillin triple therapy.

Next, the antibiotics prescribed to the 1,006 patients that received empirical first line treatment was investigated. The most frequently prescribed treatment was triple therapy consisting of clarithromycin, amoxicillin, and a PPI (Triple-C+A) (Table 3.9) Triple-C+A was prescribed 88% of the time (N=885). The other first line treatments prescribed were sequential treatment with clarithromycin, amoxicillin and metronidazole (Sequential-C+A+M) (N=43), triple therapy with clarithromycin and metronidazole (Triple-C+M) (N=27), triple therapy with amoxicillin and levofloxacin (Triple-A+L) (N=23), bismuth quadruple therapy (N=17), triple therapy with amoxicillin and metronidazole (Triple-A+M) (N=10) and triple therapy with clarithromycin and levofloxacin (Triple-C+L) (N=1).

	Frequency (N)	Percentage
Triple-C+A	885	88.0
Sequential-C+A+M	43	4.3
Triple-C+M	27	2.7
Triple-A+L	23	2.3
BQT	17	1.7
Triple-A+M	10	1.0
Triple-C+L	1	0.1
Total	1006	100.0

Table 3.9 First line treatments prescribed from 2013-2022. C=clarithromycin, A=amoxicillin, M=metronidazole, L=levofloxacin, BQT=bismuth quadruple therapy.

The prescription patterns were then sub-analysed by year. The number of each treatment prescribed per year is shown in Table 3.10 and the percentage of each treatment prescribed per year is shown in Figure 3.6. In all years except for 2014 Triple-C+A was >85% of all first line prescriptions (Table 3.10) (Figure 3.6). In 2014, 54.5% (N=60) of patients received Triple-C+A and 39.1% (N=43) received Sequential-C+A+M therapy. The reason for the increase in sequential therapy in 2014 was due to a prospective randomized–controlled study that took place that year at Tallaght University Hospital (Haider et al., 2015). The study found that sequential therapy was not significantly more effective compared to standard triple therapy. For this reason, Triple-C+A therapy regained usage in 2015. In 2016, 100% of all first line treatments recorded were Triple-C+A (Table 3.10) (Figure 3.6). Triple-C+M was between 0-3.5% of prescriptions depending on the year (Table 3.10) (Figure 3.6); this is often used as an alternative treatment to Triple-C+A therapy for patients who have a penicillin allergy.

	Year										
	2013	**2014**	**2015**	**2016**	**2017**	**2018**	**2019**	**2020**	**2021**	**2022**	**Total**
Triple-C+M	1	0	1	0	2	4	7	5	5	2	27
Triple-C+L	0	0	0	0	0	0	1	0	0	0	1
Triple-C+A	40	60	26	30	53	110	215	128	143	80	885
Triple-A+M	1	0	1	0	1	0	0	1	6	0	10
Triple-A+L	1	6	1	0	0	2	6	2	1	4	23
Sequential-C+A+M	0	43	0	0	0	0	0	0	0	0	43
BQT	1	1	0	0	0	0	3	7	4	1	17
Total	44	110	29	30	56	116	232	143	159	87	1,006

Table 3.10 Number of first line treatments sub-analysed by year.
C=clarithromycin, A=amoxicillin, M=metronidazole, L=levofloxacin, BQT=bismuth quadruple therapy.

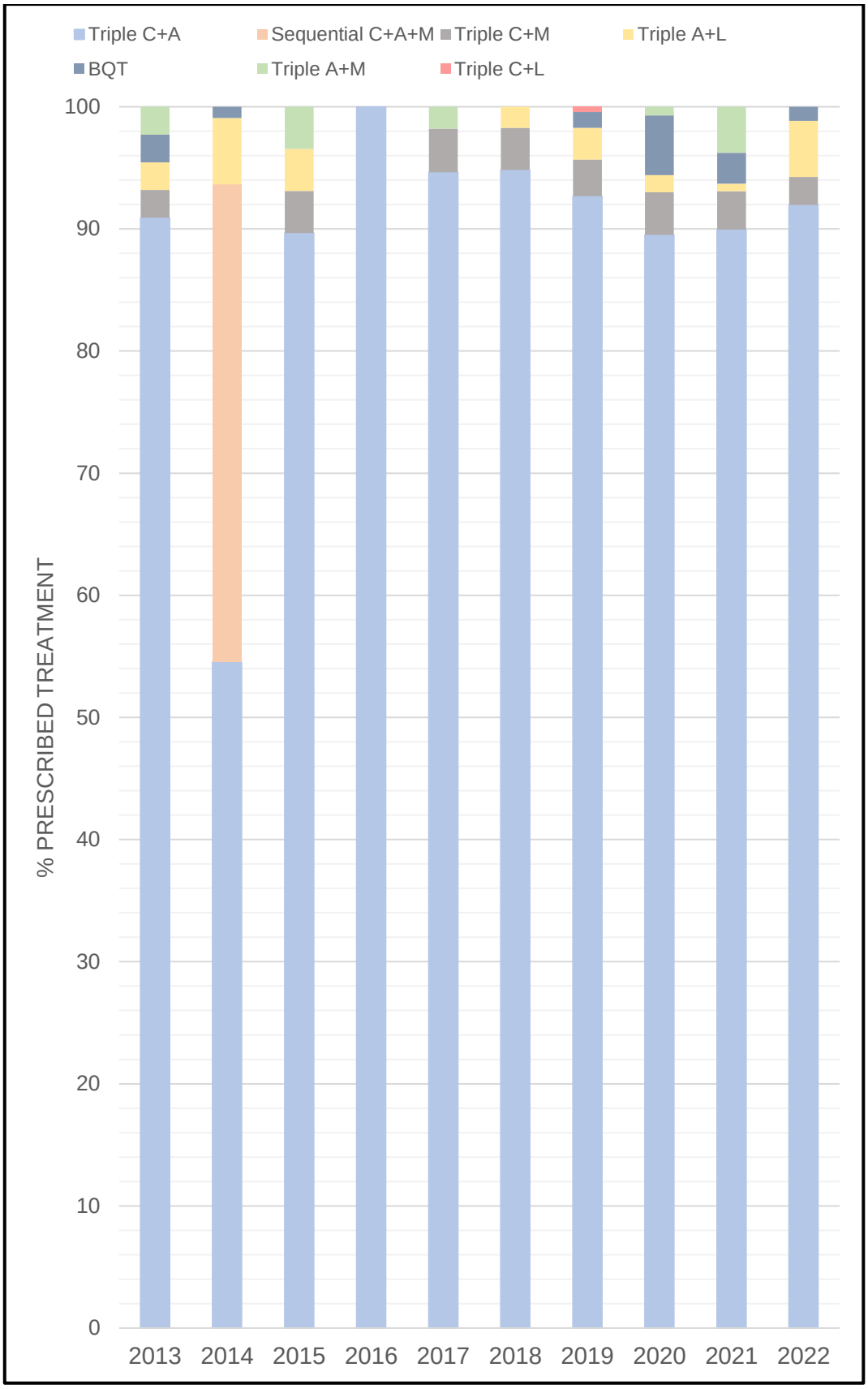

Figure 3.6 Breakdown of treatment regimens as a percentage of all first-line treatments prescribed each year. C=clarithromycin, A=amoxicillin M=metronidazole, L=levofloxacin, BQT=bismuth quadruple therapy.

3.3.7. The modified intention-to-treat protocol was chosen for eradication analysis in this study.

When evaluating treatment outcomes, data can be anlaysed by either the intention-to-treat (ITT) principle or the per-protocol (PP) analysis. Both analyses are valid and can offer complementary interpretations of the data. The ITT principle aims to understand the impact of assigning a drug whereas the PP analysis investigates the effect of receiving the treatment (Tripepi et al., 2020). With the ITT analysis, patients who do not comply with the protocol (for example, the patient does not finish the course of antibiotics perscribed) are still considered as belonging to the treatment group they were originlaly assigned. The benefit of ITT is that it reflects the daily clinical practice where non-compliance and deviations from protocol can occur often. In contrast the PP analysis looks at the effect of actually receiving the full treatments as outlined in the protocol. In other words the PP group is a subgroup of the ITT group who completed the treatment and follow up without deviating from the protocol.

Three different patient groupings were considered for analysing eradication rates in this study. Firstly, an ITT group that included all patients prescribed first line treatment to allow for at least a 6-month follow up. In this group, patients where confirmation of eradication was unknown were considered treatment failures. Secondly, a PP group for whom success or failure of eradication was known and for patients that complied with >90% of the treatment regimen.Thirdly, a modified-intention-to-treat (mITT) protocol that included all patients who had a confirmatory test following treatment regardless of compliance (Nyssen et al., 2022), (Nyssen et al., 2021a). The number of patients included or excluded in each group is shown in Table 3.11. The group with the largest number of valid participants was the mITT) group with 1,000 valid patients. The ITT and PP groups had 991 and 999 valid participants, respectively. Since the mITT group, most closely resembles what is observed in a clinical setting (Rokkas et al., 2022),

(Burgos-Santamaría et al., 2022) and there was little difference between the patient numbers across the three sub-groups, the rest of the analysis in this chapter was performed using the mITT group. For mITT analysis, 6 patients were lost to follow up, so analysis was performed on 1,000 patients.

		Intention-to-treat	Modified intention-to-treat	Per protocol
N	**Valid**	991	1000	999
	Excluded	15	6	7

Table 3.11 Number of participants in each group.

3.3.8. First line treatment effectiveness varies depending on treatment regimen.

Combining all the first line treatment regimens in the mITT group showed an overall eradication rate of 80.1% (N=801/100) with a 95% confidence interval (95% CI) of 77.5% - 82.5% (Table 3.12). The percentage of successful eradication with each first-line treatment regimen showed that bismuth quadruple therapy was the superior treatment with a mITT eradication rate of 94.2% (95% CI 71.1%-99.9%) (Table 3.12), (Figure 3.7). However, bismuth quadruple therapy was only given to 1.7% (N=17/ 1,000) patients receiving first line treatment. The small number of prescriptions for bismuth quadruple therapy may be due to issues sourcing bismuth in Ireland. As shown in Table 3.9 in Section 3.3.6 above, Triple-C+A was the most prescribed treatment over the time-period of 2013-2022. Triple-C+A had a mITT eradication rate of 81.4% (95% CI 78.7%-83.3%). Some treatments, such as triple-A+M (N=10) were prescribed in low numbers meaning wide margins for the 95% confidence intervals were observed.

	Failure (N)	Success (N)	Total (N)	mITT %	95% CI
Triple-C+M	12	15	27	55.6	37.3-72.4
Triple-C+L	1	0	1	0	
Triple-C+A	164	716	880	81.4	78.7-83.8
Triple-A+M	2	8	10	80	47.9-95.4
Triple-A+L	6	16	22	72.7	49.8-89.3
Sequential-C+A+M	13	30	43	69.8	54.8-81-5
BQT	1	16	17	94.2	71.1-99.9
Overall	199	801	1000	80.1	77.5-82.5

Table 3.12 Effectiveness of each first line treatment in the mITT group.
C=clarithromycin, A=amoxicillin M=metronidazole, L=levofloxacin, BQT=bismuth quadruple therapy.

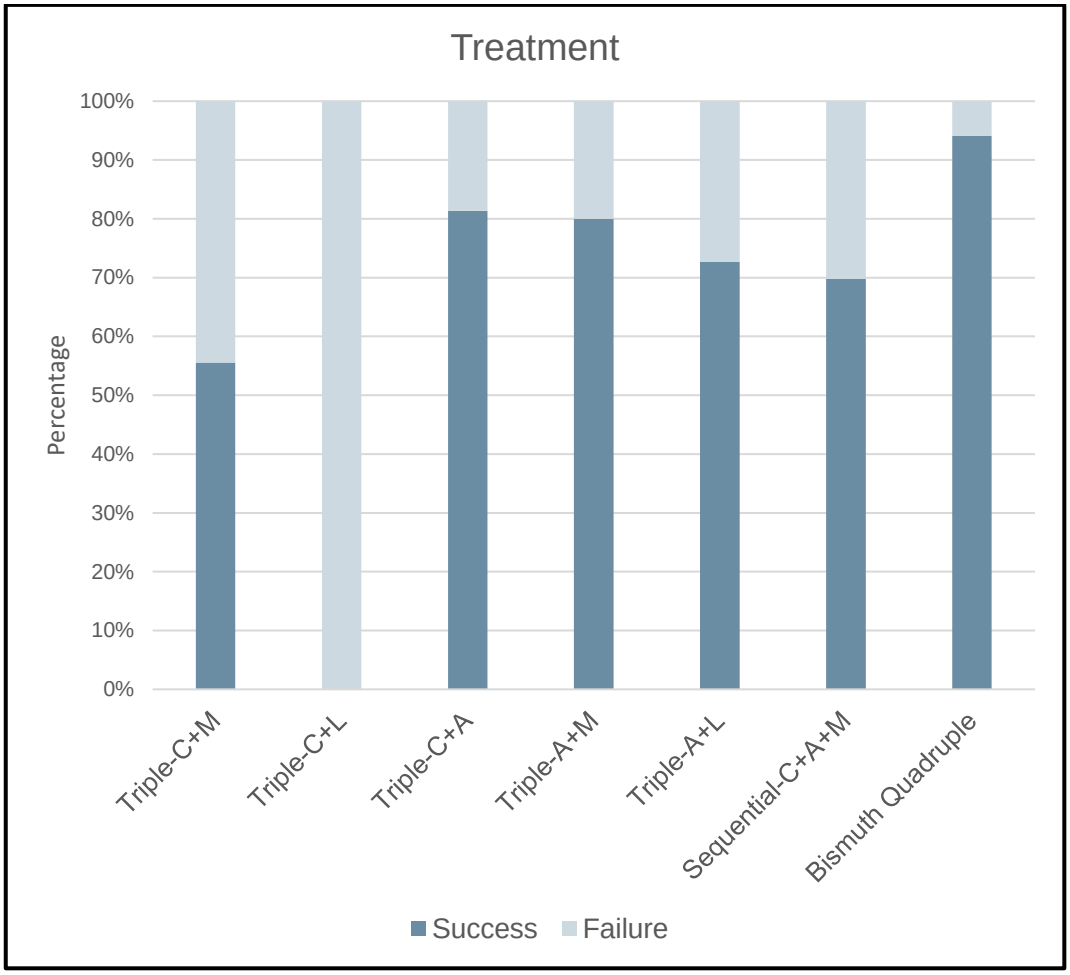

Figure 3.7 Percentage treatment success and failure broken down by treatment regimen. C=clarithromycin, A=amoxicillin M=metronidazole, L=levofloxacin, BQT=bismuth quadruple therapy.

3.3.8.1. Increased duration of treatment impacted eradication rates for the better.

Over the course of the audit most treatments were prescribed for 14 days. With 14 days treatment, 158 patients failed first line treatment and *H. pylori* was successfully eradicated in 710 patients (Table 3.13). For 7- and 10-day long treatments 28 and 13 patients respectively failed treatment and 57 and 32 respectively were successfully eradicated (Table 3.13). The percentage mITT eradication rate increased according to treatment duration, with a statistically significant increase in eradication when 14

days treatment was prescribed compared to 7 days therapy (83.4% vs 67.1%, p=.001) (Table 3.13) (Figure 3.8).

	Failure	Success	Overall	mITT %	95% CI
7-days	28	57	85	67.1	56.5-76.2
10-days	13	32	45	71.1	54.3-80.6
14-days	158	710	868	83.4	79.1-84.2
Total	199	799	998	80.1	77.5-83.1

Table 3.13 Percentage treatment success and failure broken down by length of treatment.

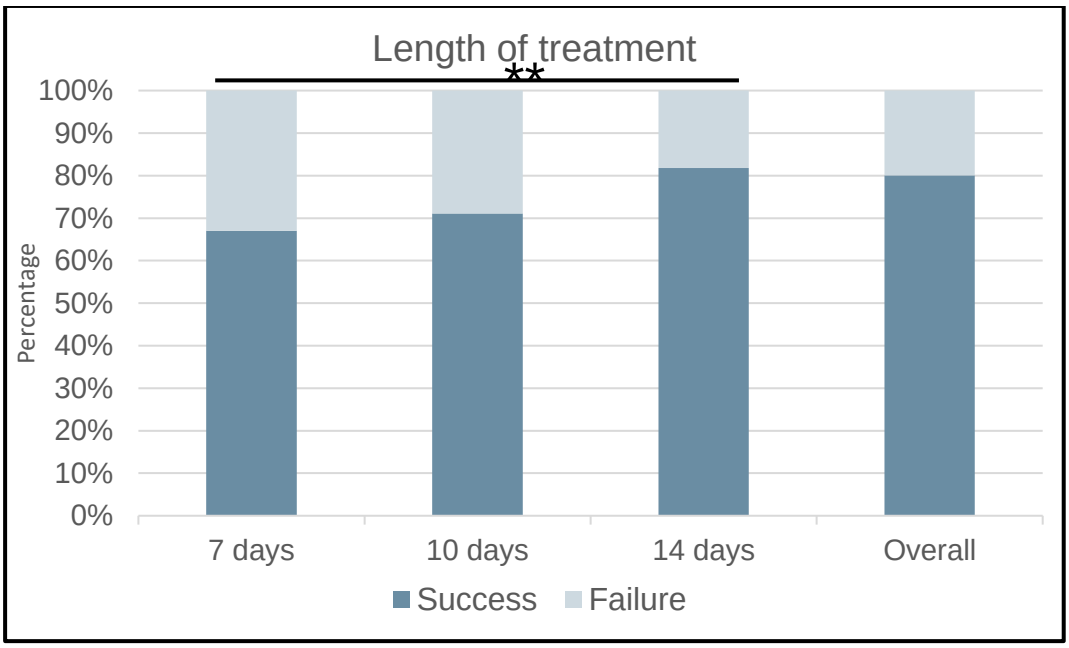

Figure 3.8 Percentage treatment success and failure broken down by length of treatment. Two tailed Chi Square tests were performed on the data: 10 days vs 7 days (p=.636), 14 days vs 7 d days (p=.001) and 14 days vs 10 days (p=.073).

3.3.9. Higher dose PPI impacted eradication rates for the better.

The majority of treatments over the 10-year period were prescribed with a high dose of PPI. With the high dose of PPI, 154 patients failed first line treatment and *H. pylori* was successfully eradicated in 706 patients (Table 3.14). For low and standard dosage, 42 and 3 patients respectively failed treatment and 88 and 6 patients respectively were successfully eradicated (Table 3.14). There was an increase in the mITT eradication rate when high dose PPI was prescribed compared to either low or standard dose (Figure 3.9).

	Failure	Success	Overall	mITT %	95% CI
Low dose	42	88	130	67.7	59.2-75.1
Standard dose	3	6	9	66.7	35.1-88.3
High dose	154	706	860	82.1	79.4-84.5
Total	199	800	999	80.1	77.5-83.1

Table 3.14 Effectiveness of first line treatments broken down by PPI dose. Low dose PPI: ranging from 4.5 to 27 mg omeprazole equivalents. Standard dose PPI: ranging from 32 to 40 mg omeprazole equivalents. High dose PPI: ranging from 54 to 128 mg omeprazole equivalents.

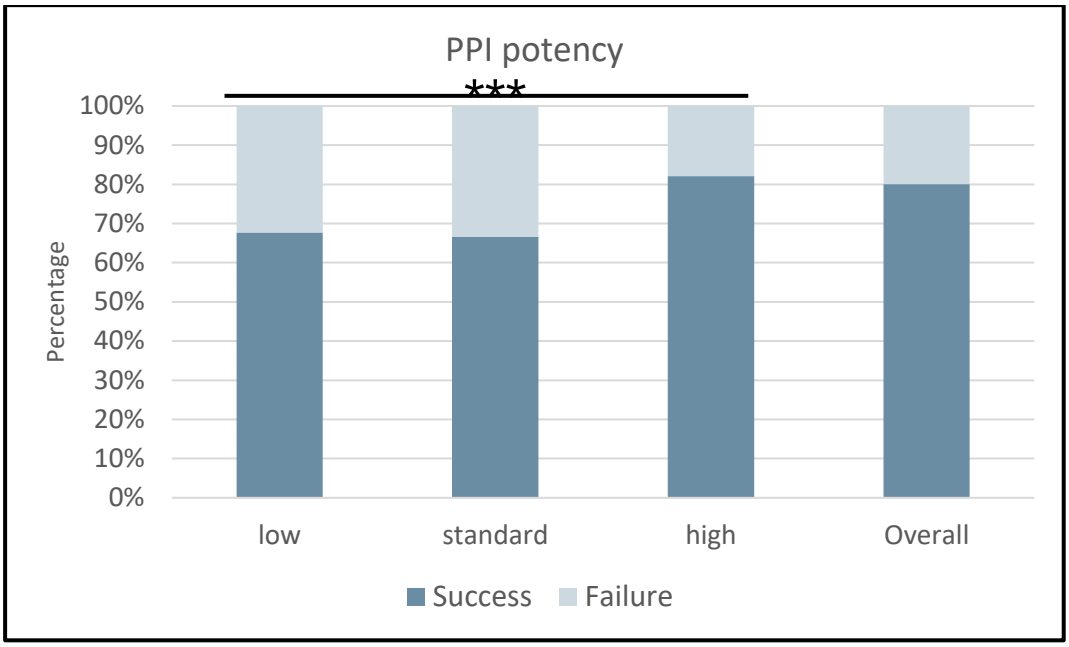

Figure 3.9 Percentage treatment success and failure broken down by PPI dose. Low dose PPI: ranging from 4.5 to 27 mg omeprazole equivalents. Standard dose PPI: ranging from 32 to 40 mg omeprazole equivalents. High dose PPI: ranging from 54 to 128 mg omeprazole equivalents. Two tailed Chi square tests were performed on the data: low vs standard (p=.949), low vs high (p<.001) and standard vs high (p=.232).

3.3.10. The eradication rate improved following the introduction of the Irish guidelines in 2017.

Next, trends in eradication rates over time were analysed. The lowest successful eradication rate was observed in 2014 at 69.4% followed by 2013 with 70.7% (Figure 3.10) (Table 3.15). The low eradication rates observed during 2013-2014 are likely due to the number of prescriptions for 7-day treatment with a low dosage PPI that were prescribed during those two years. The best eradication rates were from 2015-2016, with rates of 86.2% and 86.7% recorded respectively. The most recent four years of the audit shows that eradication rates have held stable with 81.9%, 84.5%, 82.4% and 81.6% eradication for 2019, 2020, 2021 and 2022 respectively. Comparing the overall eradication rates pre- and post- publication of the IHPWG Guidelines (Smith et al., 2017a) found that there was a significant

improvement in recorded eradication rates following the introduction of the guidelines (p=.024), (Table 3.16). Triple-C+A is the most frequently prescribed treatment across all 10 years. Since so much of the total first line treatment data is made of Triple-C+A the overall eradication rates each year is similar to the eradication rate for Triple-C+A only (Figure 3.11). The number of prescriptions and cases with treatment success for each first line treatment were broken down by year and are graphed in Appendix D.

mITT Eradication Year	Triple C+A % (N Eradicated/N total)	Overall % (N Eradicated/N total)
2013	70 (26/37)	71 (29/41)
2014	68 (40/59)	69 (75/108)
2015	88 (23/26)	86 (25/29)
2016	87 (26/30)	87 (26/30)
2017	85 (45/53)	82 (46/56)
2018	76 (84/110)	76 (88/116)
2019	84 (180/215)	82 (190/232)
2020	85 (108/127)	85 (120/142)
2021	83 (118/143)	82 (131/159)
2022	83 (66/80)	82 (71/87)

Table 3.15 Percentage Eradication rate broken down by year for Triple C+A and for overall treatments.

Duration	2013-2016 N=208		2017-2022 N=792		*P value
	N	%	N	%	
Failure	53	25.5	146	18.4	
Success	155	74.5	646	81.6	0.024

Table 3.16 Comparison of overall eradication rates pre- and post-publication of the IHPWG Guidelines. Irish recommendations for *H. pylori* treatment were published in 2017 (Smith et al., 2017a). P value was calculated by a 2-tailed Chi square test.

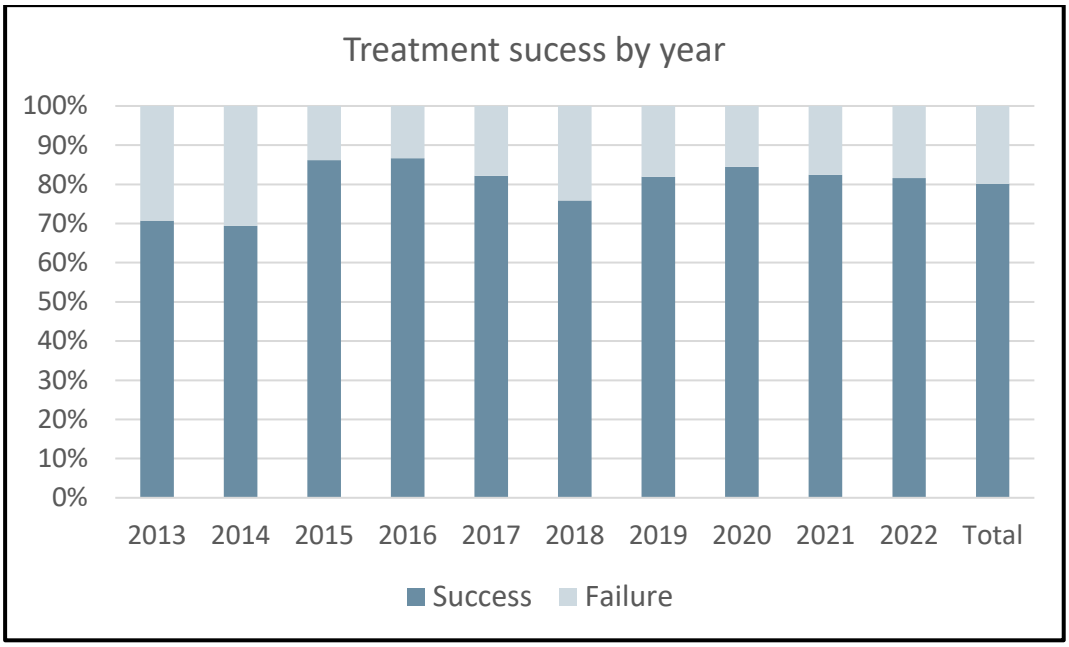

Figure 3.10 Percentage treatment success and failure broken down by year.

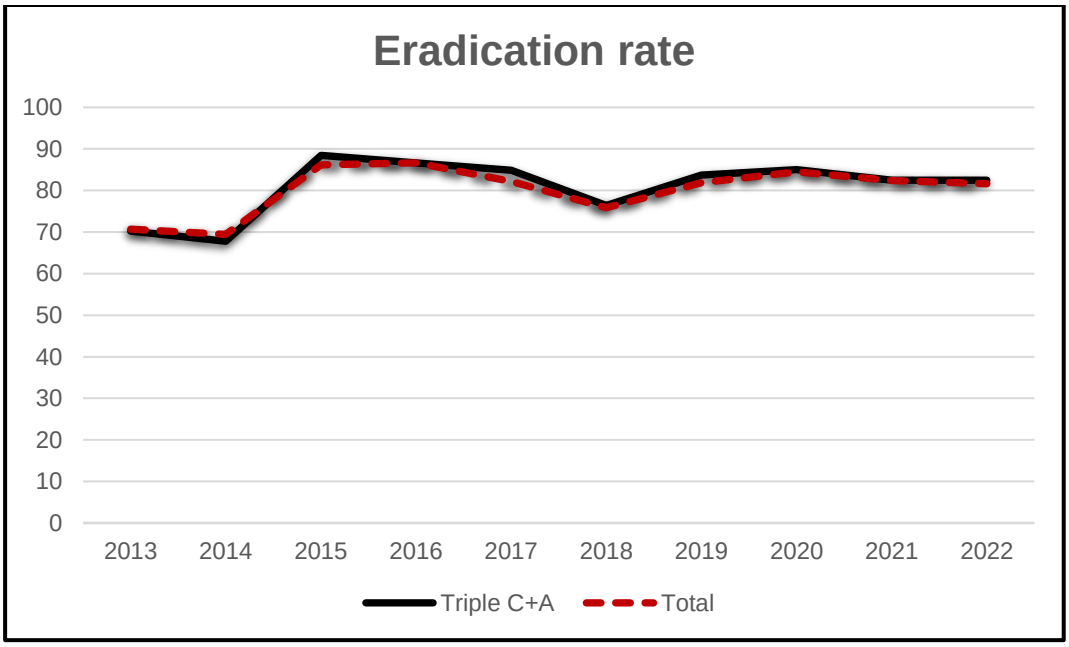

Figure 3.11 Total percentage eradication rate and percentage eradication rate of Triple-C+A therapy from 2013-2022.

3.4. Second line treatment results

3.4.1. Second line patient characteristics

Patients who fail first line eradication therapy are referred for second line therapy. Patients receiving second line therapy in Tallaght University Hospital between 2013 and 2022 were audited for prescription and eradication rates. There were 90 patients included in the second line treatment cohort (Table 3.17). Descriptive demographic analysis on these patients found they had a mean age of 50 and 65.6.% (N=59) were female (Table 3.17). Most patients had no recorded drug allergy, however, 2.2% (N=2) had a recorded penicillin allergy. No other drug allergies were recorded in the database. The percentage of patients not taking any known concurrent medication was 97.8%. However, 2.2% (N=2) were taking proton-pump inhibitors (Table 3.17). The most common indication was dyspepsia (62.2%; N=56 (Table 3.17).

Number of patients		90
Age: Mean (SD)		50 (14.6)
Female*: N (%)		59 (65.6)
Indication: N (%)	Dyspepsia Peptic ulcer Other	56 (62.2) 3 (3.3) 31 (34.4)
Concurrent medication: N (%)	None Proton pump inhibitors	88 (97.8) 2 (2.2)
Drug allergies: N (%)	None Penicillin	88 (97.8) 2 (2.2)

Table 3.17 Baseline demographics of second line patients included in study. SD: standard deviation.

3.4.2. Most patients were diagnosed with *H. pylori* by an invasive test.

Similar to the treatment-naïve patients (Section 3.3.2), the three most common methods of diagnosis were the RUT (32.2%; N=29), histology (31.1%; N=28) and C^{13} UBT (44.4%; N=40) (Table 3.18). These data indicate that the majority of patients receiving second line *H. pylori* treatment were diagnosed by an invasive test. Despite this, only 11% (N=10) of patients had antibiotic susceptibility testing performed by culture. Of these, 7 were resistant to clarithromycin, 5 were resistant to metronidazole and 2 were resistant to Levofloxacin (Table 3.18). This shows that antibiotic resistance is high in patients who have already failed one treatment for *H. pylori*. However, the small sample size is noted.

Test	Description	N	Percentage
^{13}C- UBT	Non-invasive	40	44.4
Histology	Invasive	28	31.1
RUT	Invasive	29	32.2
Culture	Invasive	10	11.1
Resistance	Clarithromycin Metronidazole Levofloxacin	7 5 2	70 50 20
Other		1	1.1

Table 3.18 *H. pylori* diagnosis method of second line patients included in the study.

3.4.3. The duration of treatment and dose of PPI prescribed in second line treatment increased following the publication of the IHPWG guidelines.

To directly evaluate the impact of the IHPWG Guidelines on second line treatment patterns, treatment duration and PPI doses prescribed were compared before and after their publication. There was a significant decrease in the prescription of 7 day therapies following publication of the guidelines; 7 day therapy represented 100% of all treatments prescribed pre-2017 compared to just 1.2% post-2017 (p<.001), while 14 day treatment increased from 0% of treatments prescribed pre-2017 to 98.8% afterwards (p<.001) (Table 3.19).

Similarly, the use of low dose PPI decreased following the publication of the guidelines, with an increase in high dose PPI prescriptions from 0% of *H. pylori* treatments in the period 2013-2016 to 98.9% of therapies prescribed between 2017-2022 (Table 3.20).

Duration	2013-2016 N=10		2017-2022 N=80		P value
	N	%	N	%	
7 days	8	80	1	1.25	<.001
14 days	2	20	79	98.75	<.001

Table 3.19 Comparison of treatment duration of 2nd line prescriptions pre- and post-publication of the IHPWG Guidelines. P value calculated by two tailed Chi square test.

PPI Dose	2013-2016 N=10		2017-2022 N=80		*P value
	N	%	N	%	
Low	7	70	0	0	<.001
Standard	1	10	1	1.25	0.77
High	2	20	79	98.75	<.001

Table 3.20 Comparison of PPI dose prescribed in second line therapy pre- and post-publication of the IHPWG Guidelines. P value calculated by two tailed Chi square test.

3.4.4. The most prescribed second line treatment was triple therapy with amoxicillin and levofloxacin.

Out of the 90 patients who received second line therapy in Tallaght University Hospital between the years 2013-2022 more than half (56.7%) received Triple-A+L therapy (Table 3.21). The second most prescribed second line therapy was Triple-A+M at 23.3%. This was followed by bismuth quadruple therapy at 6.5%.

	Frequency (N)	Percentage
Triple-C+A	4	4.4
Triple-C+M	4	4.4
Triple-A+L	51	56.7
BQT	6	6.7
Triple-M+L	2	2.2
Triple-A+M	21	23.3
Triple-C+L	1	1.1
High-dose-A	1	1.1
Total	90	100

Table 3.21 Total Second line treatments. C=clarithromycin, A=amoxicillin, M=metronidazole, L=levofloxacin, BQT=bismuth quadruple therapy.

3.4.5. Second line treatment effectiveness varied depending on treatment regimen.

Overall, second line treatments only successfully eradicated the infection 64.4% (95% CI 54.1-73.6%) (Table 3.22). Triple-A+L was the most prescribed second line treatment over the time-period of 2013-2022 and had an eradication rate of 68.6% (95% CI 54.9.7-79.7%) (Table 3.22) (Figure 3.12). The second most common second line treatment, Triple-A+M therapy, was less effective compared to Triple-A+L and had an eradication rate of 57.1% (95% CI 36.5-75.6%). Bismuth quadruple therapy was the most effective first line treatment with an eradication rate of 94.2%. However, eradication rate dropped at second line. Only 66.7% of patients treated with bismuth quadruple therapy for second line were successfully eradicated. This discrepancy may be due to the small number of prescriptions (N=6) for bismuth quadruple therapy, as illustrated by the large 95% CI of 29.6-90.8%.

	Failure	Success	Total	mITT %	95% CI
Triple-C+A	2	2	4	50	15-85
Triple-C+M	1	3	4	75	28.9-96.6
Triple-A+L	16	35	51	68.6	54.9-79.7
BQT	2	4	6	66.7	29.6-90.8
Triple-M+L	1	1	2	50	9.5-90.6
Triple-A+M	9	12	21	57.1	36.5-75.6
Triple-C+L	0	1	1	100	-
High-dose-A	1	0	1	0	-
Total	32	58	90	64.4	54.1-73.6

Table 3.22 Eradication success for second line treatments. C=clarithromycin, A=amoxicillin, M=metronidazole, L=levofloxacin, BQT=bismuth quadruple therapy.

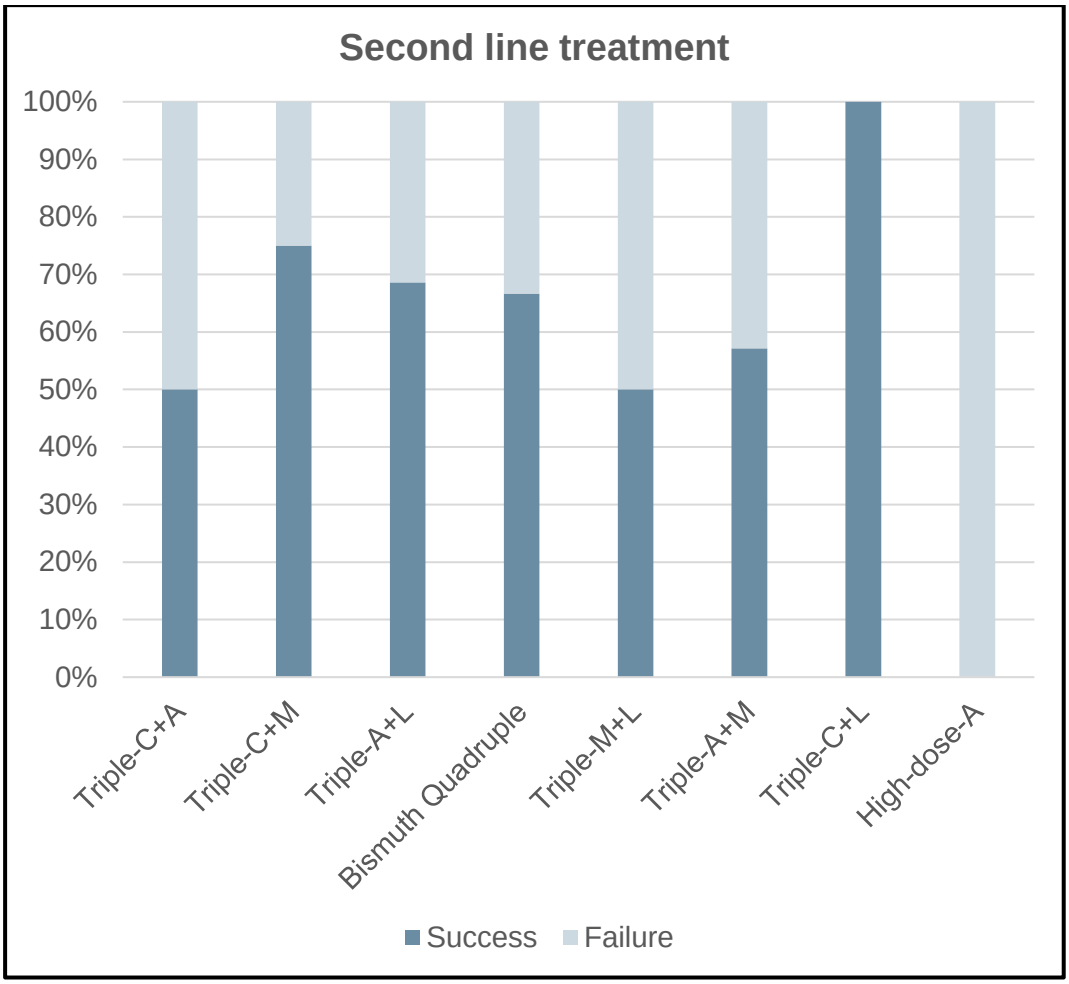

Figure 3.12 Eradication success and failure for second line treatments.
C=clarithromycin, A=amoxicillin, M=metronidazole, L=levofloxacin.

3.4.6. Longer duration of treatment and higher PPI dose was not associated with improved eradication rates with second line therapies.

Over the course of the audit the majority of second line treatments were prescribed for 14 days. With 14 days treatment 31 patients failed second line treatment and 50 successfully eradicated *H. pylori*. For 7-day long treatments only 1 patient failed treatment and 8 were successfully eradicated (Figure 3.13).

Likewise, the majority of second line treatments were prescribed with high dose PPI. With low dose treatment 1 patient failed second line treatment and 6 successfully eradicated Only 2 patients received standard dose and they both successfully eradicated *H. pylori*. For the high dose 31 patients failed treatment and 50 were successfully eradicated (Figure 3.14).

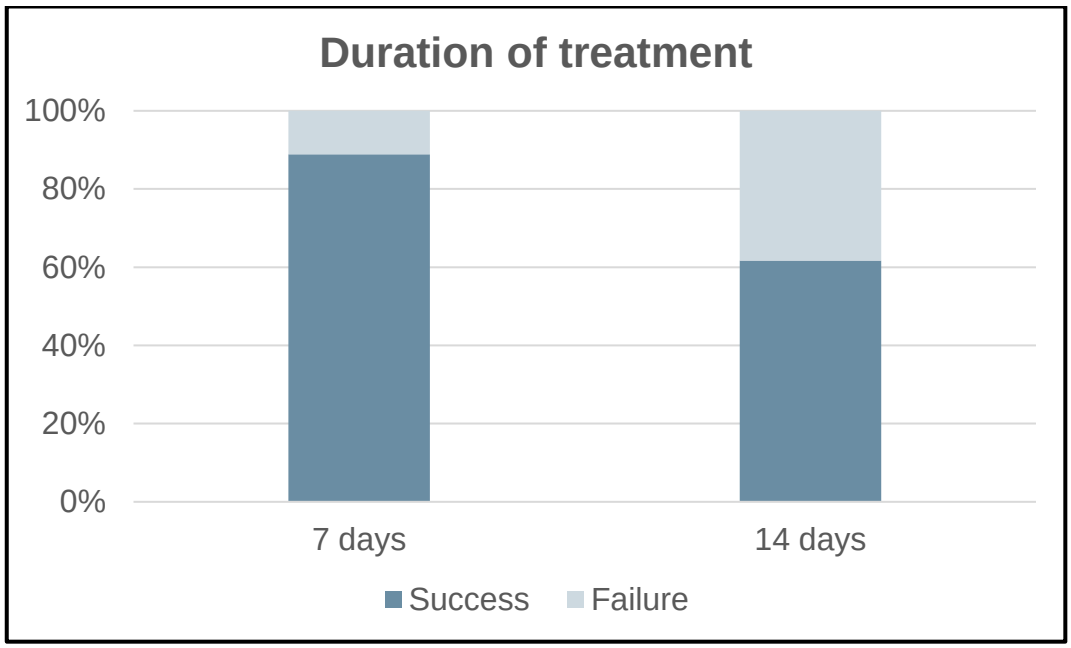

Figure 3.13 Success of second line treatments broken down by length of treatment. Two tailed Chi square tests were performed on the data: 7 days vs 14 days (p=.106).

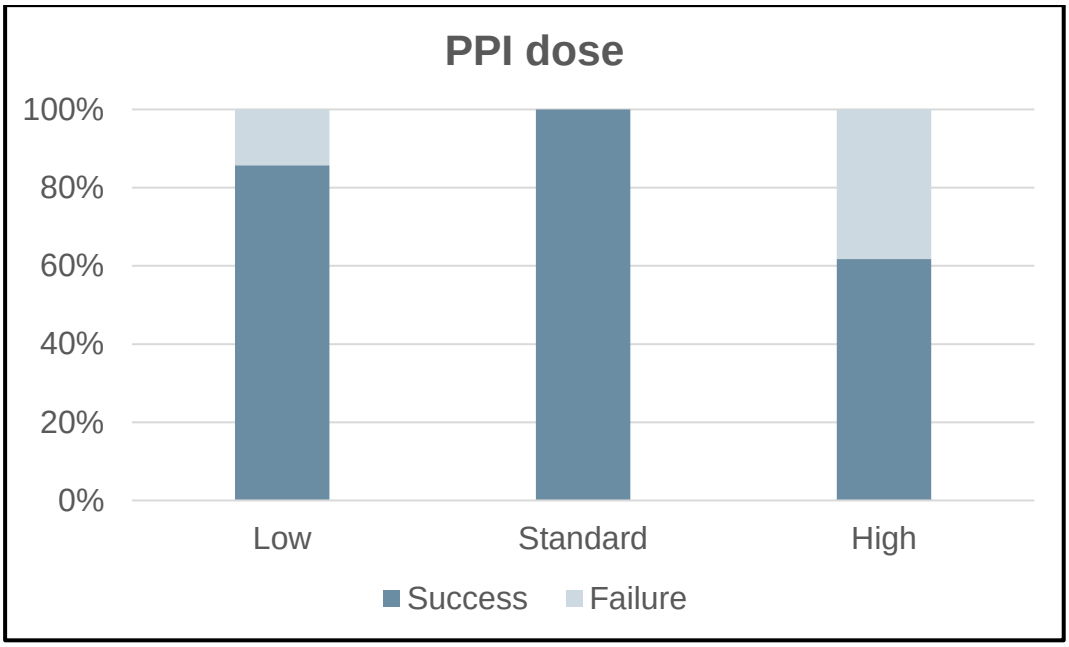

Figure 3.14 Success of second line treatments broken down by PPI dose. Low dose PPI: ranging from 4.5 to 27 mg omeprazole equivalents. Standard dose PPI: ranging from 32 to 40 mg omeprazole equivalents. High dose PPI: ranging from 54 to 128 mg omeprazole equivalents. Two tailed Chi square tests were performed on the data: low vs standard (p=.57), low vs high (p=.206) and standard vs high (p=.269).

3.4.7. The eradication rate for second line treatments did not improve following the introduction of the Irish guidelines in 2017.

Comparing the eradication rates pre- and post- publication of the IHPWG Guidelines found that there was no significant change in recorded eradication rates for second line treatment following the introduction of the guidelines (p=.485), (Table 3.23), (Smith et al., 2017a).

Duration	2013-2016 N=10		2017-2022 N=80		*P value
	N	%	N	%	
Failure	2	20	30	37.5	
Success	8	80	50	62.5	.276

Table 3.23 Comparison of eradication rates pre- and post-publication of the IHPWG Guidelines. Irish recommendations for *H. pylori* treatment were published in 2017 (Smith et al., 2017a). P value was calculated by a 2-tailed Chi square test.

3.5. Rescue treatment results

3.5.1. Rescue treatment patient characteristics.

Patients who failed eradication therapy more than twice between 2013 and 2022 at Tallaght University Hospital were grouped into the rescue treatment group. Together the rescue treatment group was made up of just 21 patients, 17 of whom had received two previous treatments, 3 who received three previous treatments and one patient who received four previous treatments. Descriptive demographic analysis on these patients found they had a mean age of 47 and 76.2.% were female (Table 3.24). Most patients had no recorded drug allergy but 9.5% (N=2) had a recorded penicillin allergy. No other drug allergies were recorded in the database. The percentage of patients not taking any known concurrent medication was 76.2%. However, 19.1% were taking PPIs. 4.8% were taking statins and acetylsalicylic acid respectively (Table 3.24). The jump in concurrent medications, in particular PPIs in the rescue treatment group may suggest more progressed disease symptoms. The most common indication was dyspepsia (76.2%) (Table 3.24).

Number of patients		**21**
Age: Mean (SD)		47 (12.7)
Female*: N (%)		16 (76.2)
Indication: N (%)	Dyspepsia Other	16 (76.2) 5 (23.8)
Concurrent medication: N (%)	None Proton pump inhibitors Statin Acetylsalicylic acid	16 (76.2) 4 (19.1) 1 (4.8) 1 (4.8)
Drug allergies: N (%)	None Penicillin	19 (90.5) 2 (9.5)

Table 3.24 Baseline demographics of patients included in study. Abbreviations: SD: standard deviation.

3.5.2. Most patients were diagnosed with *H. pylori* by an invasive test.

The three most common methods of diagnosis were RUT (47.6%), histology (33.3%) and C^{13} UBT (38.1%) (Table 3.25). This data indicates that most patients receiving rescue *H. pylori* treatment are diagnosed by an invasive test. Despite patients receiving at least 2 previous treatments only 19% (N=4) patients had antibiotic susceptibility testing performed by culture. Of these, 100% were resistant to clarithromycin and 75% were resistant to metronidazole (Table 3.25). This shows that patients who fail multiple therapies are likely to have resistant strains of bacteria. The use of Triple-C+A therapy as the most common first line therapy likely selects for rescue patients that are resistant to clarithromycin treatment.

Test	Description	N	Percentage
^{13}C- UBT	Non-invasive	8	38.1
Histology	Invasive	7	33.3
RUT	Invasive	10	47.6
Culture	Invasive	4	19.0
Resistance	Clarithromycin Metronidazole	4 3	100.0 75.0

Table 3.25 Diagnosis method of patients receiving rescue treatment for *H. pylori.*

3.5.3. The most prescribed rescue treatment was bismuth quadruple therapy.

Out of the 21 patients who received rescue therapy in Tallaght University Hospital between the years 2013-2022 almost half (47.6%) received bismuth quadruple therapy (Table 3.26). The second most prescribed rescue therapy was Triple-A+L at 23.8%. This was followed by Triple-C+A and Triple-C+M at 9.5% each.

	Frequency (N)	Percentage
Triple-C+A	2	9.5
Triple-C+M	2	9.5
Triple-A+L	5	23.8
BQT	10	47.6
Triple-A+M	1	4.8
High-dose-A	1	4.8
Total	21	100

Table 3.26 Total rescue treatments. C=clarithromycin, A=amoxicillin, M=metronidazole, L=levofloxacin, BQT=bismuth quadruple therapy.

3.5.4. Rescue treatment effectiveness varies depending on treatment regimen.

Combining all the rescue treatment regimens in the mITT group showed an overall eradication rate of 61.9%. Bismuth quadruple therapy, which was the most prescribed rescue treatment, had an eradication rate of 70% (95% CI 39.2-89.7%) (Table 3.27) (Figure 3.15). The second most common rescue treatment, Triple-A+L therapy, was less effective compared to bismuth quadruple with an eradication rate of 60% (95% CI 22.9-88.4%). Only a very small number of patients received a treatment other than bismuth quadruple or Triple-A+L as a rescue therapy so the 95% confidence intervals for the other treatments are very large.

	Failure	Success	Total	mITT %	95% CI
Triple-C+A	1	1	2	50	9.5-90.6
Triple-C+M	1	1	2	50	9.5-90.6
Triple-A+L	2	3	5	60	22.9-88.4
BQT	3	7	10	70	39.2-89.7
Triple-A+M	1	0	1	0	-
High-dose-A	0	1	1	100	-
Total	8	13	21	61.9	40.8-79.3

Table 3.27 Eradication success for rescue treatments. C=clarithromycin, A=amoxicillin, M=metronidazole, L=levofloxacin, BQT=bismuth quadruple therapy.

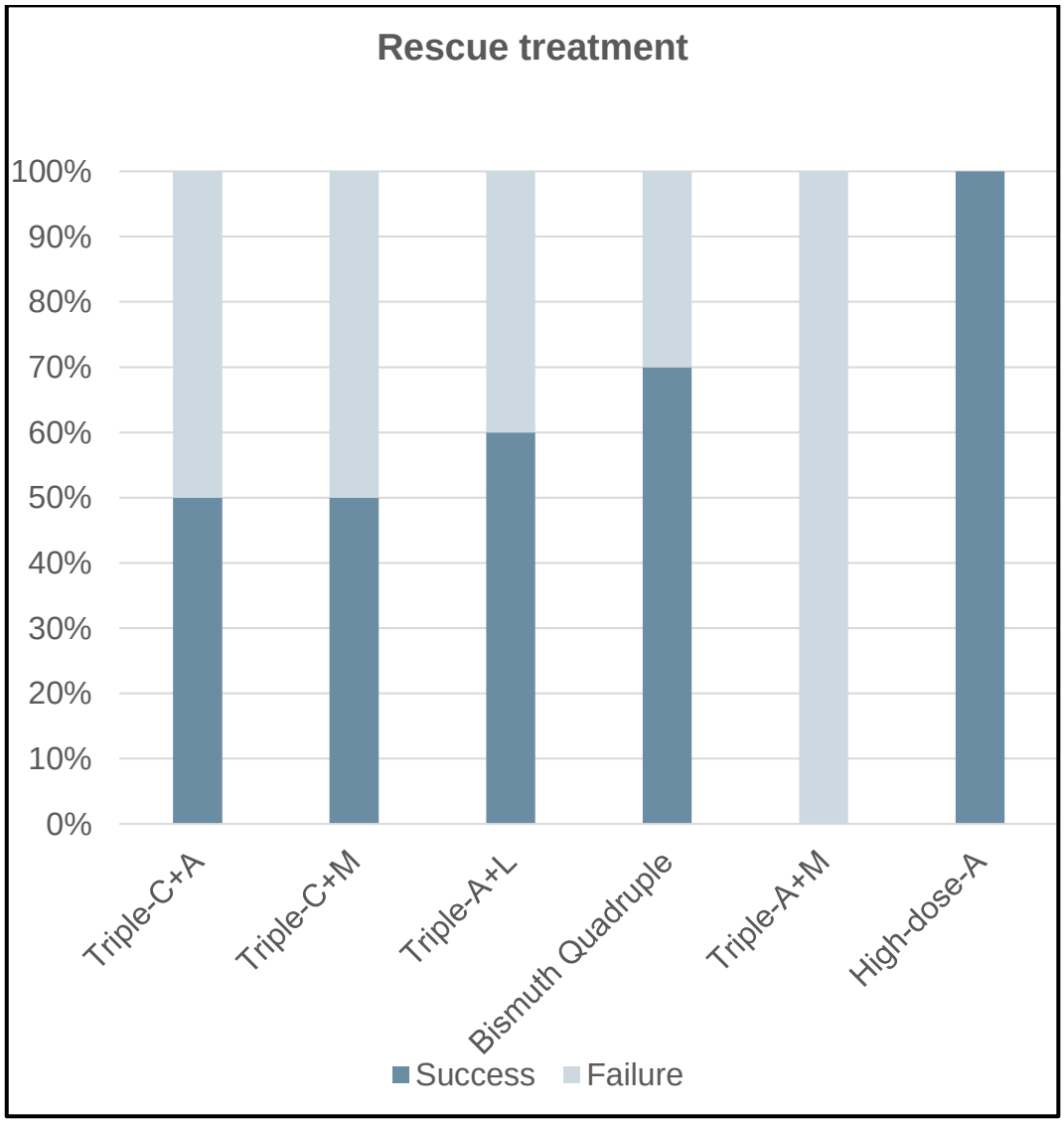

Figure 3.15 Eradication success for rescue treatments. C=clarithromycin, A=amoxicillin, M=metronidazole, L=levofloxacin, Tc=tetracycline, B=bismuth.

3.5.5. Reduced eradication rates were observed with rescue therapy.

Over the course of the audit most rescue treatments were prescribed for 14 days. With 14-day treatments, 5 patients failed rescue treatment and 10 were successfully eradicated. For 10-day long treatments only 2 patients had successful treatment but 3 had failed treatments. Only 1 patient was prescribed a 7-day rescue treatment and this treatment was successful (Figure 3.16).

Likewise, the majority of rescue treatments were prescribed with high dose PPI. With low dose treatment, 3 patients failed second line treatment and 3 successfully eradicated. For the high dose, 5 patients failed treatment and 10 were successfully eradicated (Figure 3.17).

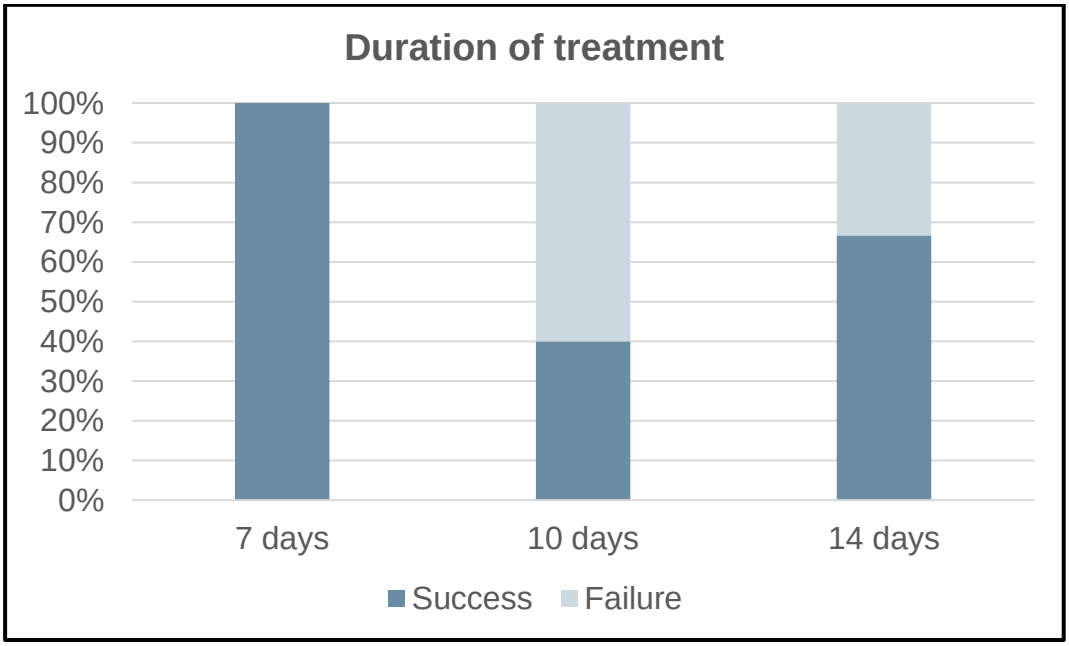

Figure 3.16 Success of rescue treatments broken down by length of treatment. Two tailed Fishers exact tests were performed on the data: low vs standard (p=1), low vs high (p=1) and standard vs high (p=.347).

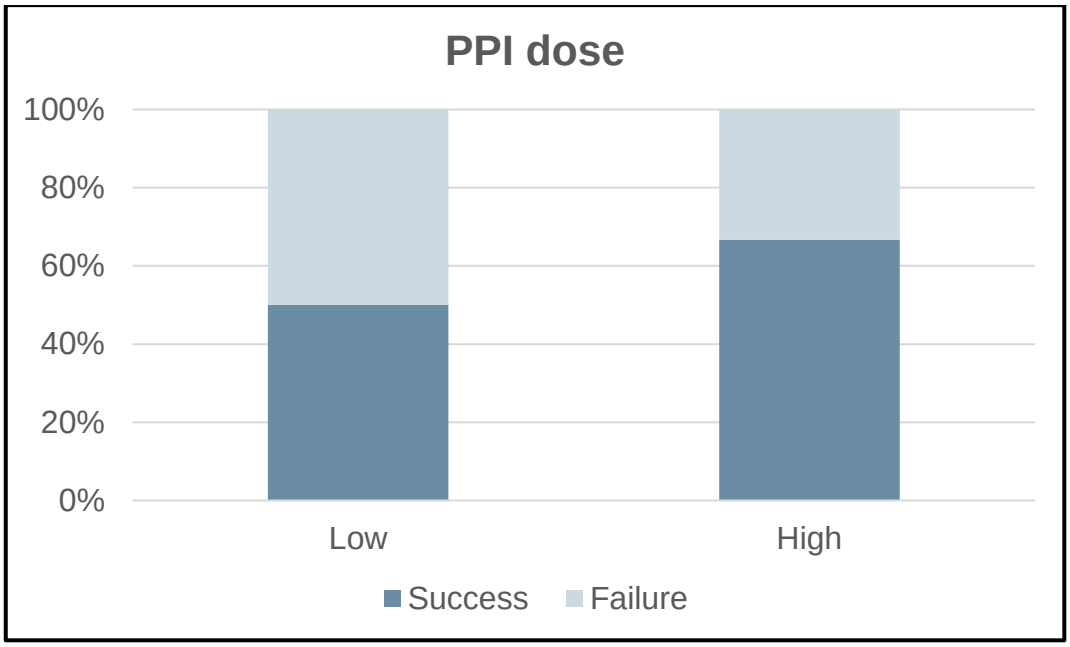

Figure 3.17 Success of second line treatments broken down by PPI dose. Low dose PPI: ranging from 4.5 to 27 mg omeprazole equivalents. Standard dose PPI: ranging from 32 to 40 mg omeprazole equivalents. High dose PPI: ranging from 54 to 128 mg omeprazole equivalents. Two tailed Fishers exact tests were performed on the data: low vs high (p<.631)

3.5.6. Eradication rates decreased according to the number of therapies.

First line eradication had a total successful eradication rate of 80.1%, second line treatments only successfully eradicated the infection 64.4% of the time and rescue treatments eradicated *H. pylori* only 61.9% of the time (Figure 3.18). The reduction in effectiveness is likely due to patients that fail multiple therapies are more likely to be infected with an antibiotic resistant strain making it more difficult to treat.

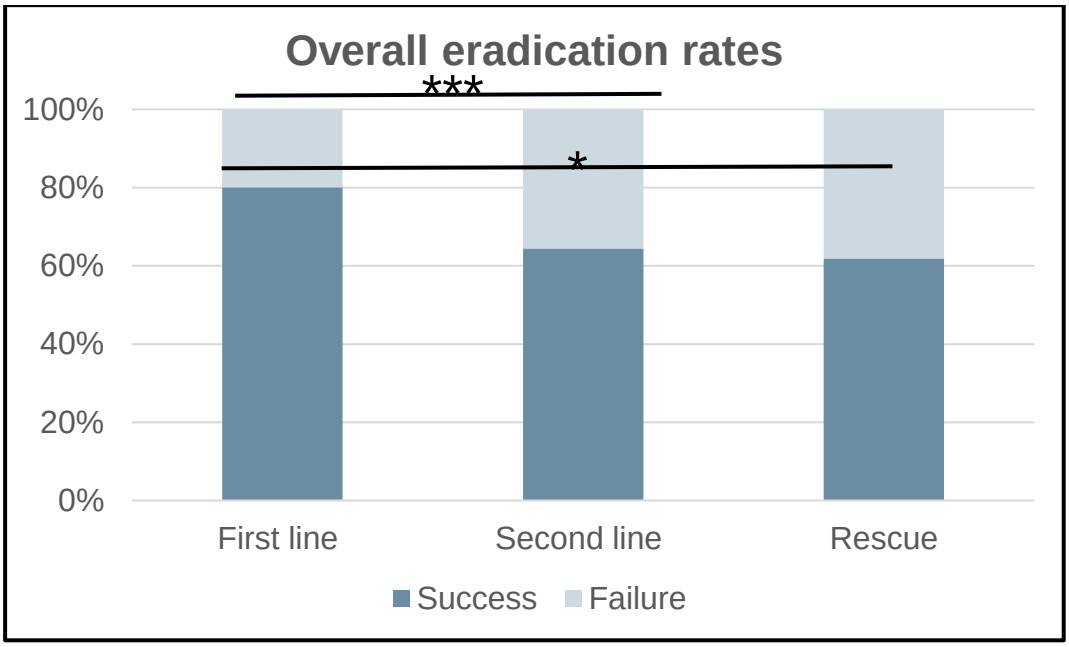

Figure 3.18 Overall eradication rates. Two tailed Chi square tests were performed on the data: First line vs Second line (p<.001), Second line vs Rescue (p=.827), First line vs Rescue (p=.04).

3.6. Discussion

There are many possible treatments for *H. pylori* which vary in efficacy, availability, complexity, and side effects. The best method for deciding on an empirical therapy is to choose a locally audited reliable and effective regimen which takes into account local antimicrobial susceptibility and clinical data (Graham et al., 2014). The Hp-EuReg aims to provide continuous analysis of routine clinical practice for *H. pylori* diagnosis, treatment and eradication across Europe (McNicholl et al., 2019). The WHO and the EU council recommend cautious use of antibiotics to prevent accelerating antibiotic resistance (Malfertheiner et al., 2022). Auditing *H. pylori* treatment will hopefully aid in selecting therapies that have the best chance of eradicating the bacteria, preventing the need for unnecessary rounds of treatment.

In total, first line treatment was successful 80.1% (N=801/1000) of the time with a 95% CI of 77.5-82.5%. Triple-C+A therapy was used in most (88%) of first line treatments and successfully eradicated *H. pylori* 81.4% (95% CI 78.7-83.8) of the time. Analysis of 21,533 fist line treatments in the HP-EuReg found that Triple-C+A therapy was the most used first line treatment in Europe. Triple-C+A was found to be 38% of all first line treatments in the registry with a mITT eradication rate of 81.5% (Nyssen et al., 2021a). Generally, the effectiveness of Triple-C+A as a first line treatment is similar in Ireland and Europe as a whole, with eradication rates of 81.4% and 81.5% respectively.

The Irish data showed a clear signal that both longer treatment duration (14 days) and higher proton-pump inhibitor dosage were associated with higher efficacy of first line treatments. This finding corresponds with what was observed in other countries across Europe (Caldas et al., 2020) (Nyssen et al., 2021a). The use of 14-day, high dose PPI treatments was almost ubiquitous following the release of the IHPWG guidelines in 2017 (Smith et

al., 2017a), demonstrating good clinical compliance with local guidance. This change in clinical practice in response to the IHPWG guidelines is reflected in the enhanced eradication rates from 74.5% (N=155/208) for the period 2013-2016 to 81.6% (N=646/792; p=.031) following their publication.

The most likely explanation for failed eradication therapy is the presence of *H. pylori* that is resistant to one or more of the antibiotics used (Graham et al., 2014). In 2018, primary resistance was collected from 43 treatment naïve patients attending Tallaght University Hospital. Primary resistance for clarithromycin was 25.6%. Primary resistance to levofloxacin was 13.9% and primary resistance to metronidazole was 43% (Megraud et al., 2021). Although the N=43 is small, it shows that there are considerable antibiotic resistant infections among the population attending Tallaght University Hospital. The high resistance to clarithromycin can explain the low first line eradication rate of 81% for Triple-C+A seen in this audit. An analysis of 1,211 patients from 18 European countries found average resistance rates of 21.4% for clarithromycin, 15.8% for levofloxacin and 38.9% for metronidazole in Europe (Megraud et al., 2021).

Although, Triple-C+A therapy for 14 days with a high dose PPI is in agreement with the current IHPWG guidelines, its usage resulted in less than the >90% eradication threshold that is recommended for first line treatments (Smith et al., 2017a), (Nyssen et al., 2021a). The Maastricht consensus guidelines recommend that areas that have unknown clarithromycin resistance or resistance >15% should not use Triple-C+A as a first line treatment (Malfertheiner et al., 2022), (Malfertheiner et al., 2017). Considering, the results of this audit, the 25.6% primary clarithromycin resistance rate among Irish patients published in the pan-European study (Megraud et al., 2021) and the most up-to-date Maastricht guidelines (Malfertheiner et al., 2022), there is substantial evidence that the current IHPWG guidelines should be updated and Triple-C+A therapy should be phased out as a first line treatment.

In total, second line treatments were successful 64.4% (N=58/90) of the time with a 95% CI of 54.1-73.6%. Triple-A+L was the most used second line treatment and was used in 56.7% of patients. The Irish data analysis found Triple-A+L to have a second line effectiveness of 68.6% (N=35/51) with a 95% CI of 54.9-79.7%. Triple-A+L was also found to be the most common second line treatment in Europe with 33% of the 5,055 second line patients in the HP-EuReg receiving Triple-A+L treatment with an eradication rate of 81% (Nyssen et al., 2021b). Comparatively, Triple-A+L treatment is much less effective as a second line treatment in an Irish context compared to its use in the rest of Europe. This may be caused by population differences such as resistance patterns among the infecting strains or poor patient compliance. The low eradication rate observed in this study would suggest that Triple-A+L is not an optimal second line treatment in an Irish context and should ideally be replaced with a more effective therapy. Adding bismuth to Triple-A+L therapy has been recommended by the recent Maastricht guidelines to enhance eradication rates for second line levofloxacin-based therapy (Malfertheiner et al., 2022).

The more times a patient fails treatment the effectiveness of subsequent treatment decreases. This is because patients who have failed more than two treatments are likely to have multi-resistant *H. pylori* (Burgos-Santamaría et al., 2022). In accordance with this, eradication rates fell from 80.1% in first line therapy to 64.4% in second line therapy, and third, fourth- and fifth-line rescue treatments had a combined eradication rate of only 61.9% (N=13/21). This highlights the importance of aiming to eradicate *H. pylori* infection first time around by choosing the most appropriate therapy.

Bismuth quadruple therapy was the most used rescue treatment in 47.6% of cases and successfully eradicated *H. pylori* 70% (N=7/10) of the time with a 95% CI of 39.2-89.7%, albeit with a very small sample size analysed.

Across Europe, usage of bismuth containing quadruple therapies for rescue treatment increased from 33%–35% in 2013–2014 to 64%–75% in 2018–2021 (Burgos-Santamaría et al., 2022). The single bismuth containing three-in-one capsule had good effectiveness as a rescue treatment in Europe with an eradication rate of 84.8% observed (Burgos-Santamaría et al., 2022). The IHPWG guidelines say that antimicrobial susceptibility testing by culture should be performed following two failed treatments (Smith et al., 2017a). However, only 19% of patients in this audit received susceptibility testing prior to receiving rescue treatments. This is one area that compliance with the Irish guidelines is lacking and may be due to the time and cost involved in antimicrobial susceptibility testing by culture.

Other countries taking part in the HP-EuReg study have shown that therapies containing bismuth have a high eradication rate. Pylera® a single capsule containing tetracycline, metronidazole and bismuth salts combined with high dose PPI had a 95% eradication rate in 1,660 first line Spanish patients and an 88% eradication rate as a second line treatment on 454 patients (Caldas et al., 2020). Across Europe, the single capsule bismuth treatment had mITT effectiveness rates of 94.5% and 90% as first and second line treatments respectively (Nyssen et al., 2021a), (Nyssen et al., 2021b). Since Pylera® is a single capsule, it simplifies the complicated quadruple treatment, which should help combat any issues of compliance with the treatment. Additionally, Pylera® does not contain clarithromycin making it a good option for clarithromycin resistant patients. If possible increased usage of bismuth in first- or second-line treatment would be recommended in the Irish healthcare setting. Access to bismuth is limited in Ireland and this likely explains the low usage of bismuth in Irish treatments (Smith et al., 2017a). Improving access to bismuth should be prioritised to benefit eradication rates and improve patient outcomes.

The recent Maastricht VI report concluded that the Covid19 pandemic had a negative impact of *H. pylori* diagnosis and treatment globally (Malfertheiner

et al., 2022). This was due to periods when UBTs, endoscopy and gastroenterology consultations were halted. Despite this, the data from this audit shows there was still a large number of patients in Ireland who received first line treatment during the height of the pandemic. In 2020 and 2021, 123 and 159 patients respectively received first line treatment.

For first line treatment 53.3% of patients were female. This percentage increased to 65.6% in second line treatments and 76.2% of patients who received rescue treatment were female. This may suggest female patients are failing *H. pylori* eradication treatment and are requiring second line and rescue treatments more often than male patients. These findings are in line with previous studies which have observed that female gender is predictive of eradication failure (Cai et al., 2009), (Chang et al., 2019), (Caldas et al., 2020). It is possible that biological, behavioural, or environmental reasons may contribute to this observation. However, there has been some research showing that *H. pylori* isolates from female patients were more likely to be clarithromycin and/or metronidazole resistant (Osato et al., 2001). Further research is required to identify how these variables impact *H. pylori* treatment and eradication.

3.7. Limitations of study

While this analysis represents the largest audit of *H. pylori* treatment undertaken in Ireland to date and included patients from both the public and private healthcare setting, there are some limitations to the study. Although a large study population was achieved for first line treatment analysis, the sample size for second line and rescue therapy were considerably smaller making it more difficult to perform powered statistical analysis or draw solid conclusions from these groups, in particular in relation to rescue therapy. Another limitation was that patients from only two centres were included in the first line Irish data analysis and just one centre in the second line and rescue therapy analysis. Both centres, Tallaght University Hospital and the Beacon Hospital are located in Dublin so, there is no accounting for any differences in population or treatment management outside of Dublin. Additionally, the low percentage of patients who received antimicrobial susceptibility testing, even at second line and recue therapy stage, makes it difficult to draw strong conclusions on resistance rates of the study population.

3.8. Summary of conclusions

The results from this chapter found that 88% of prescriptions for first line treatment were for Triple-C+A therapy. The first line eradication rate is largely influenced by the overwhelming usage of Triple-C+A, with the eradication rate for overall first line treatments at 80.1% and for Triple-C+A at 81%. Current first line treatments in Ireland are failing to reach the recommended >90% eradication (Fallone et al., 2016b).

Most clinicians appear to be are following the IHPWG recommendations (Smith et al., 2017a) by prescribing high dose PPI, Triple-C+A for 14 days as a first-line therapy. We found that both high dose PPI and 14-day treatment were associated with significantly improved first line eradication rates.

Overall, second line treatments were successful 64.4% of the time. Triple-A+L was the most used second line treatment and was used in 56.7% of patients and had an eradication rate of 68.6%.

Bismuth quadruple therapy was the most used rescue treatment and was used in 47.6% of rescue cases. It successfully eradicated *H. pylori* in 70% of cases, albeit with a very small sample size (N=10) analysed.

3.9. Future work

While it is heartening to see that first line eradication rates significantly improved following the introduction of the IHPWG guidelines in 2017, the rate of first line eradication is still below the recommended 90%. Currently, the Irish guidelines recommend either Triple C+A or bismuth quadruple therapy for first line *H. pylori* treatment. The data presented herein would suggest that current Triple C+A therapy is not sufficient, and the guidelines may need to be updated. Bismuth quadruple therapy represents a valid alternative and has shown good eradication rates in other countries in Europe (Nyssen et al., 2021a), (Nyssen et al., 2021b) and exhibited an eradication rate >90% in the small subset of patients prescribed it as first line therapy in this study. Although it is difficult to source in Ireland more efforts should be made to obtain bismuth for *H. pylori* treatment.

Based on the low second line eradication rate for Triple L+A reported in this study, updated Irish second line recommendation should also be considered. The recent Maastricht guidelines have recommended adding bismuth to Triple L+A therapy to enhance its efficacy (Malfertheiner et al., 2022), an option which should be considered here. For rescue therapy, antimicrobial susceptibility testing could be increased to be consistent with the Irish guidance to perform antimicrobial susceptibility testing following two failed treatments. Although rifabutin triple therapy is now the recommended rescue therapy in the Maastricht guidelines, none of the patients analysed in this study were prescribed rifabutin. It would be interesting to evaluate the efficacy of this rescue therapy in the Irish setting going forward.

Finally, the addition of other treatment centres, particularly those outside of Dublin, to recruit patients and collect data for the Hp-EuReg would give a larger study population and provide a more representative country wide overview of the management of *H. pylori* infection in Ireland.

Chapter Four Investigating the Role of the Notch Signalling Pathway During *H. pylori* Infection

4.1. Introduction to Notch signalling

4.1.1. The Notch Signalling pathway.

The Notch pathway is one of the fundamental signalling pathways within invertebrate and vertebrate biology. The highly conserved pathway is well known for its role in pattern formation during development, particularly during neurogenesis (Shang et al., 2016b), (Bray, 2016). Notch, along with wingless/integrated (WNT), fibroblast growth factors (FGF), Hedgehog and bone morphogenic proteins (BMP) make up the primary stem cell signalling pathways in the body. Together these pathways work to regulate renewal, proliferation, maintenance and differentiation in both stem and progenitor cells (Katoh and Katoh, 2007b). The Notch pathway is effective in varied contexts. Dysregulation of the Notch signalling pathway has been shown to play a key part in the development of numerous human cancers; including T-cell leukaemia, lymphoma, colorectal, pancreatic, ovarian and lung (Giakoustidis et al., 2015).

4.1.2. How does the Notch Pathway function?

The significance of the Notch pathway is underpinned by its high evolutionary conservation which is characterised by its similar function across invertebrate and vertebrate species. *Drosophila melanogaster* have one Notch receptor and two ligands (Delta and Serrate), while mammals have a total of four Notch receptors (Notch 1-4) and five ligands (Jagged1, Jagged2 (JAG1, -2), Delta-like -1, -3, -4 (DLL1, -3, -4)) (Bray, 2016). These

receptors in both invertebrates and mammals are single pass type I transmembrane proteins and are responsible for transducing specific extracellular signals to the nucleus when activated by their respective ligands (Bray, 2016).

The Notch protein is formed from a single mRNA transcript. While in the Golgi apparatus the protein is proteolytically cleaved at site S1 by a furin-like convertase, but it is later restored to a functional heterodimeric receptor at the cell surface (Shang et al., 2016b). This Notch molecule has a transmembrane domain and a separate extracellular domain. The extracellular domain contains 29-36 tandem epidermal growth factor (EGF) – like repeats that prevent ligand- independent activation (Shang et al., 2016b). Lateral inhibition, by which cells prevent adjacent cells from adopting the same fate, is an essential component of Notch signalling (Bray, 2016). This initial bias would be reinforced by a negative-feedback loop so that ligand expression becomes repressed in signal-receiving cells (Bray, 2016).

Canonical Notch signalling is initiated by the binding of the extracellular domain of the Notch receptor to Notch ligands on adjacent cells (Bray, 2016). Binding of Notch ligands to their receptors results in a sequence of proteolytic events initiating with cleavage at the S2 site by a disintegrin and metalloprotease (ADAM) protease (Figure 4.1). The extracellular domain is subsequently released and endocytosed by the ligand-expressing cell. Following this, the protease γ-secretase cleaves at the S3 site in the transmembrane domain. This results in the Notch intracellular domain (NICD) being released and translocated into the nucleus (Shang et al., 2016b). Within the nucleus the RBP-J associated molecule (RAM) domain of NICD interacts with the DNA-binding protein recombinant recognition sequence binding protein at the Jκ site (RBP-J) (also known as CSL or CBF1) (Shang et al., 2016b). Binding of NICD causes displacement of transcriptional corepressors and histone deacetylases from the

transcriptional repressor RBP-J. Recruitment of mastermind proteins (MAML1-3) and transcription activation complex follows, initiating transcription of Notch target genes. Finally NICD is degraded within the nucleus by the ubiquitin-proteosome system (Shang et al., 2016b).

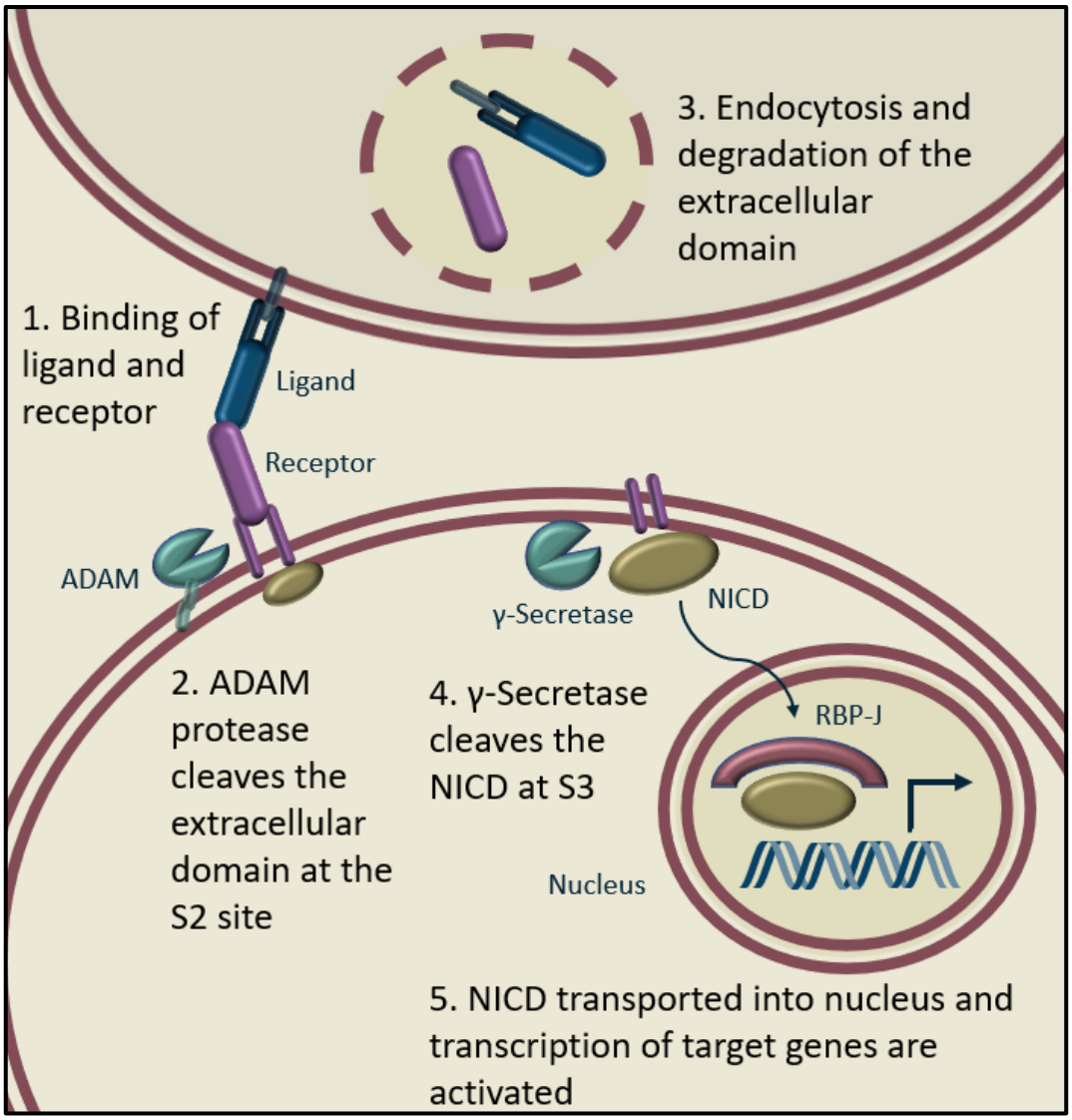

Figure 4.1 The Notch Signalling pathway. Mammals have a total of four Notch receptors (Notch 1-4) and five ligands (Jagged1, Jagged2, Delta-like -1, -3, -4). The binding of the receptor and ligand on adjacent cells triggers a canonical signalling pathway where γ-secretase releases the Notch intracellular domain (NICD). The NICD is translocated to the nucleus where it interacts with RBP-J to initiate transcription. Notch target genes include members of the basic-helix-loop-helix transcription factors belonging to the hairy and enhancer of split (HES) and hairy and enhancer of split with YRPW motif (HEY) families. Diagram created in PowerPoint.

4.1.3. Important Notch target genes.

The best described canonical Notch target genes in mammals are members of the basic-helix-loop-helix transcription factors belonging to the hairy and enhancer of split (HES) and hairy and enhancer of split with YRPW motif (HEY) families, consisting of HES1, HES5, HES7, HEY1, HEY2, and HEYL. Further targets include DELTEX1, IL2RA, GATA3 and MYC (Shang et al., 2016b). While the Notch signalling pathway is predominantly regulated at the transcriptional level, microRNAs also contribute, notably the members of the miR-200 family which target the 3' untranslated regions of Serrate and JAG1 in *D. melanogaster* and mammals respectively (Bray, 2016). Even though each ligand and receptor results in the same action (production of the NICD) they illicit a different overall response, likely due to the strength or duration of intracellular signals produced by different ligands (Bray, 2016). In humans, mutations in different paralogues can cause different diseases, for example, only defects in Notch3 cause the disease cerebral autosomal-dominant arteriopathy with subcortical infarcts and leukoencephalopathy (CADASIL) (Bray, 2016).

4.1.4. What happens when Notch signalling is dysregulated?

One of the most important and well known functions of the Notch signalling pathway is its role in embryonic development, however, the pathway is also essential in the immune system and works in the differentiation of lymphoid T and B cell lineages, T cell activation, regulatory T cell function, and T helper (Th) cell differentiation (Shang et al., 2016b). In particular, Notch signalling is a necessary component dictating the selection of $CD4^+$/$CD8^+$ T cells and in regulating the effector functions of these cells (Wei et al., 2016). Interestingly, Notch can function as either an oncogene or a tumour suppressor gene, dependent on context and tissue (Giakoustidis et al., 2015).

As an example, Notch1 activating mutations are observed in 60 percent of all T-cell acute lymphoblastic leukaemia and lymphoma (Tosello and Ferrando, 2013). Contrary to this, deletion of Notch can lead to an increase in epidermal hyperplasia and active Notch signalling is involved in cell growth suppression via p21WAF/Cip1 expression in the epidermis (Rangarajan et al., 2001). It is likely the varied effects of Notch signalling on diverse cell types is partly due to the observation that RBP-J recruits different activation and repression complexes depending on the cell context (Vázquez-Ulloa et al., 2018). Thus, the role of Notch signalling to turn on expression of target genes is dependent on proteins that are already expressed in the cell and can vary on cell and tissue type (Vázquez-Ulloa et al., 2018). While the role of Notch signalling has been extensively studied in the aspects of development, cell fate control, adaptive immune regulation and carcinogenesis, it is only more recently that the role of Notch signalling in innate immunity and inflammation has become appreciated (Shang et al., 2016b). Notch signalling has been shown to be regulated in the context of bacterial or viral infection (Castro et al., 2021). Furthermore, dysregulation of Notch signalling has been associated with gastric cancer (Katoh and Katoh, 2007a), (Piazzi et al., 2011), (Brzozowa et al., 2013), (Du et al., 2014), (Hsu et al., 2016a), (Sun et al., 2011), (Konishi et al., 2016).

4.2. Hypothesis

As Notch signalling is regulated in infectious disease and is associated with gastric cancer, it was hypothesised that the Notch signalling pathway and its associated transcription factor HES1 are involved in *H. pylori*-mediated pathogenesis.

4.3. Aims and Objectives

The aim of this chapter was to investigate the role of the Notch signalling pathway during *H. pylori* infection through the objectives below.

- Objective 1: To characterise Notch pathway component expression in gastric epithelial cells in response to *H. pylori*.
- Objective 2: To characterise Notch pathway component expression in gastric biopsy tissue from *H. pylori* positive and negative patients.
- Objective 3: To investigate the role of virulence factors and LPS in the *H. pylori*-mediated down-regulation of *HES1*.
- Objective 4: To evaluate loss- and gain-of-function approaches for studying Notch signalling in gastric epithelial cells.
- Objective 5: To investigate the role of *HES1* in *H. pylori*-infected gastric epithelial cells using a gain-of-function approach.
- Objective 6: To characterise Notch pathway component expression in THP-1 macrophages in response to *H. pylori*.

4.4. *H. pylori* infection alters expression of *HES1* in the gastric epithelium.

4.4.1. *H. pylori* alters the expression of Notch pathway components in AGS gastric epithelial cells.

To investigate whether components of the Notch signalling pathway are differentially expressed in response to *H. pylori*, AGS gastric epithelial cells were treated with either live or heat killed *H. pylori* and mRNA expression was investigated over time. *IL-8* and *CXCL1* mRNA expression was monitored as a positive readout for *H. pylori* stimulation. As expected, *H. pylori* infection led to significant upregulation of *IL-8* at all time-points (Figure 4.2.A). At every time point, live *H. pylori* led to significantly more *IL-8* production than heat killed *H. pylori*. Live *H. pylori* significantly upregulated *CXCL1* at 1, 3 and 6-hours. Heat killed *H. pylori* only increased *CXCL1* at 24-hours expression (Figure 4.2.B).

Firstly, the impact of *H. pylori* infection on Notch receptor expression was evaluated. Live *H. pylori* led to a significant decrease in *Notch1* expression at the 23-hour time-point (p=.004). Heat killed bacteria led to significant decreases in *Notch1* expression at the 1-hour time point (p=.013) (Figure 4.2.C). Live *H. pylori* led to significant downregulation of *Notch2* at 24-hours, while heat killed *H. pylori* led to significant downregulation of *Notch2* at 1 and 24-hours. Live and heat killed bacteria had significantly different impacts on *Notch2* expression at 1, 6 and 24-hour time-points (Figure 4.2.D). Similarly, *Notch3* expression was upregulated at 3-hours but downregulated significantly at 24 hours with live *H. pylori* and was significantly downregulated at 1 and 24-hours with heat killed bacteria (Figure 4.2.E). *Notch4* was not expressed well in these cells and had average CT values >35 or undetermined. Subsequently *Notch4* was excluded from analysis in AGS cells.

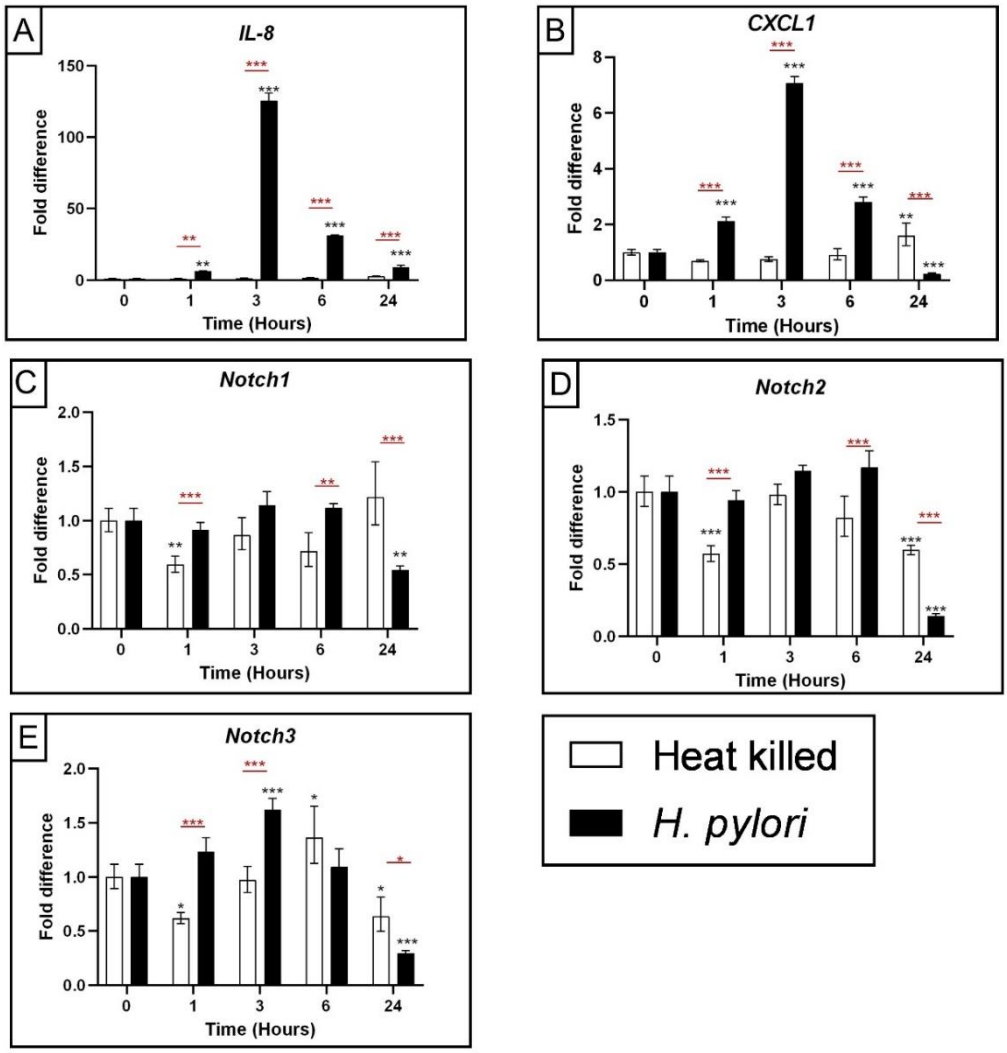

Figure 4.2 Expression of Notch receptors in AGS gastric epithelial cells in response to *H. pylori*. AGS gastric epithelial cells were seeded at $0.3x10^6$ cells/well in 12-well plate 24-hours prior to infection with 100 MOI of 11638 strain of *H. pylori* or the equivalent number of heat killed *H. pylori* for the time points indicated underneath the graphs. Total RNA was isolated and changes in *IL-8* (A), *CXCL1* (B), *Notch1* (C), *Notch2* (D) and *Notch3* (E) gene expression was evaluated by RT-qPCR using the comparative cycle threshold method. Results were normalised to *GAPDH* levels and expressed relative to uninfected cells at each time point. Data shown are means ± SD. A two-way Anova was performed for each gene. Šidák multiple comparison tests were used to compare mean values of treated samples with untreated samples (black asterisk) and to compare mean values between live and heat-killed samples (red asterisk). * $P \leq 0.05$, ** $P \leq 0.01$, *** $P \leq 0.001$. Graphs are representative of three independent experiments.

Next, the impact of *H. pylori* infection on Notch ligands and *RBP-J* mRNA expression were evaluated. Live *H. pylori* led to significant upregulation of *JAG1* at 6-hours but significant downregulation at 24-hours (Figure 4.3.A). Heat killed *H. pylori* led to significant downregulation at 1-hour. Significant differences between the effects of live and heat killed *H. pylori* on *JAG1* expression were observed at 1, 6 and 24-hours (Figure 4.3.A). Live bacteria led to significant upregulation of *JAG2* at all time points (Figure 4.3.B). Neither live nor heat killed bacteria led to significant changes in *DLL1* expression (Figure 4.3.C). A significant increase in *DLL3* expression was seen at 24-hours post infection with *H. pylori*. Heat killed bacteria did not lead to significant upregulation of *DLL3* (Figure 4.3.D). An increase in *DLL4* expression was seen at 3-hour with live *H. pylori* ($p<.001$) (Figure 4.3.E). Significant upregulation of *RBP-J* was observed when infected with live *H. pylori* at 24-hours (Figure 4.3.F).

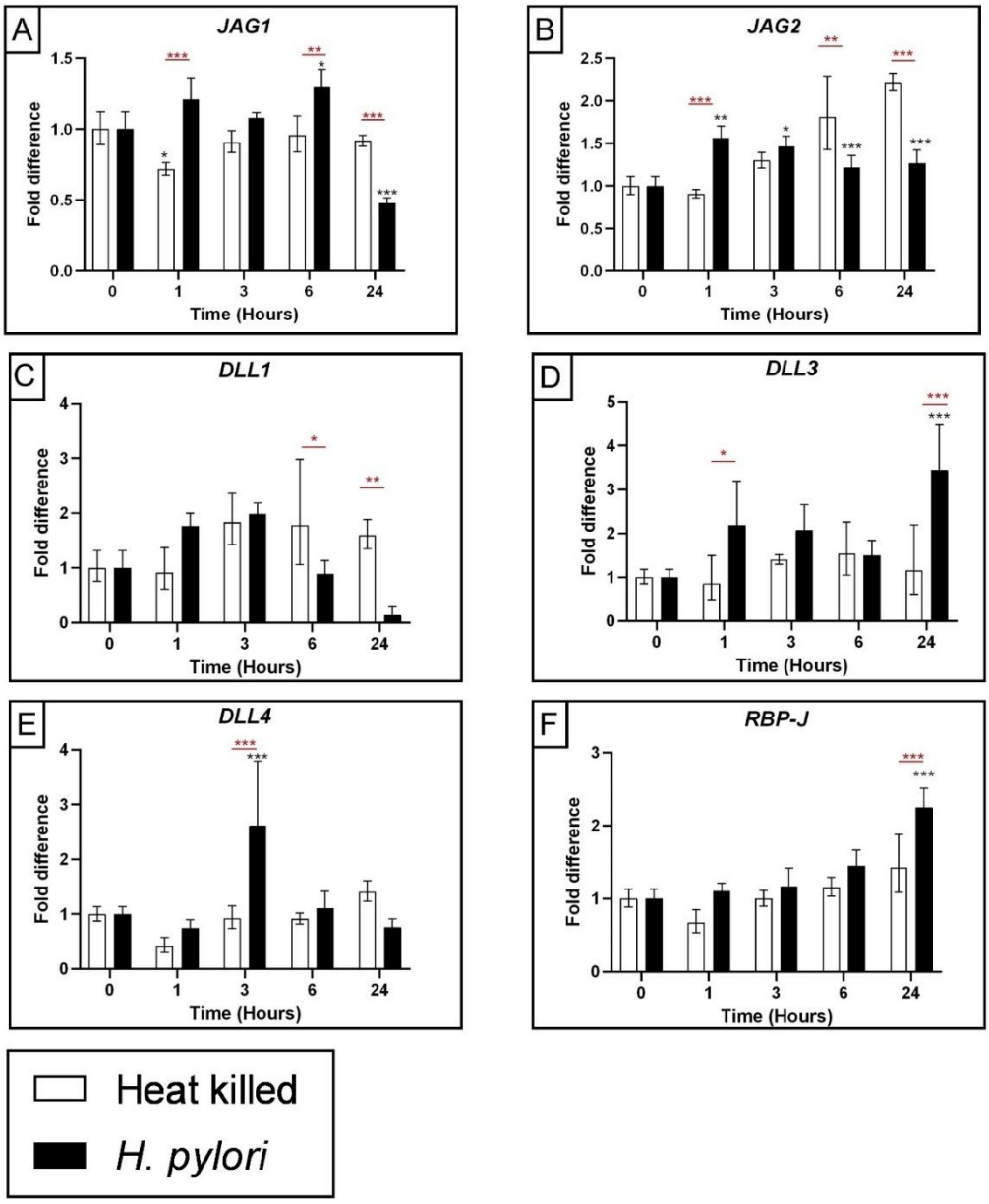

Figure 4.3 Expression of Notch ligands and *RBP-J* in AGS gastric epithelial cells in response to *H. pylori*. AGS gastric epithelial cells were seeded at $0.3x10^6$ cells/well in 12-well plate 24-hours prior to infection with 100 MOI of 11638 strain of *H. pylori* or the equivalent number of heat killed *H. pylori* for the time points indicated underneath the graphs. Total RNA was isolated and changes in *JAG1* (A), *JAG2* (B), *DLL1* (C), *DLL3* (D), *DLL4* (E) and *RBP-J* (F) gene expression was evaluated by RT-qPCR using the comparative cycle threshold method. Results were normalised to *GAPDH* levels and expressed relative to uninfected cells at each time point. Data shown are means ± SD. A two-way Anova was performed for each gene. Šidák multiple comparison tests were used to compare mean values of treated samples with untreated samples (black asterisk) and to compare mean values between live and heat-killed samples (red asterisk). * $P \leq 0.05$, ** $P \leq 0.01$, *** $P \leq 0.001$. Graphs are representative of three independent experiments.

Finally, the impact of *H. pylori* infection on Notch pathway associated transcription factors was evaluated. Live *H. pylori* led to significant decreases in *HES1* expression at 3, and 24-hour time points (0.7-fold, p=.005, 0.4-fold, p<.001 respectively). Live *H. pylori* was significantly better at reducing *HES1* expression compared to heat killed *H. pylori* at the 24-hour time point (p<.001) (Figure 4.4.A). Live *H. pylori* led to significant increases in *HEY1* expression at 6 and 24-hour time points. The largest increase was seen at 24 hours post infection (7-fold, p<.001). Heat killed bacteria did not impact *HEY1* expression in a similar manner as live bacteria and significant differences in expression were seen between live and heat killed *H. pylori* at 1, 6 and 24-hour time points (Figure 4.4.B).

Taken together, these results show that *H. pylori* increases expression of *JAG2, DLL3, RBP-J* and *HEY1* in AGS cells. Infection increased expression of *JAG1, DLL1, DLL4* and *Notch 1-3* in AGS cells at early time points, followed by decreased expression at 24 hours. Expression of *HES1* was decreased at early and late time points. For the most part, live *H. pylori* was required for these effects.

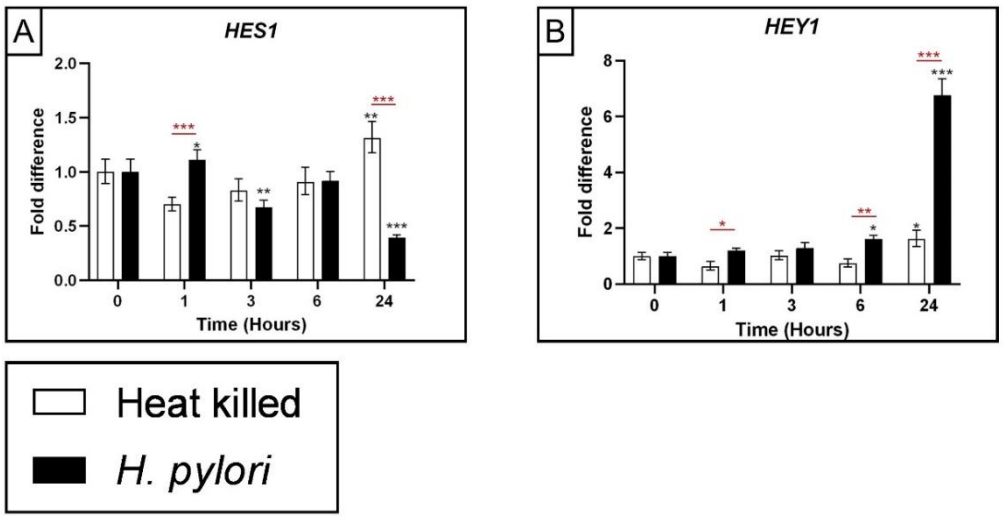

Figure 4.4 Expression of Notch associated transcription factors in AGS gastric epithelial cells in response to *H. pylori*. AGS gastric epithelial cells were seeded at $0.3x10^6$ cells/well in 12-well plate 24-hours prior to infection with 100 MOI of 11638 strain of *H. pylori* or the equivalent number of heat killed *H. pylori* for the time points indicated underneath the graphs. Total RNA was isolated and changes in *HES1* (A) and *HEY1* (B) gene expression was evaluated by RT-qPCR using the comparative cycle threshold method. Results were normalised to *GAPDH* levels and expressed relative to uninfected cells at each time point. Data shown are means ± SD. A two-way Anova was performed for each gene. Šidák multiple comparison tests were used to compare mean values of treated samples with untreated samples (black asterisk) and to compare mean values between live and heat-killed samples (red asterisk). * P≤0.05, ** P≤0.01, *** P≤0.001. Graphs are representative of three independent experiments.

4.4.2. *H. pylori* decreases expression of *JAG2*, *HES1* and *HEY1* in the gastric mucosa of infected patients.

To identify if *H. pylori* mediates gene expression changes in Notch pathway components in the gastric epithelium, RT-qPCR was performed on RNA isolated from gastric biopsy tissue. Patients were recruited following ethical approval in Tallaght University Hospital. Antral biopsy tissue was collected from 33 *H. pylori*-infected and 19 uninfected control patients. Patients were considered infected if they tested positive for two out of three diagnostic tests. The diagnostic tests considered were the rapid urease test (RUT), histopathologic examination of the biopsy specimen and culture of the bacteria.

Significant upregulation of the cytokines *IL-8* and *CXCL1* was seen in the *H. pylori*-infected group ($p<.001$ and $p<.001$ respectively) (Figure 4.5.A,B). Despite a downward trend in Notch receptor expression, there was no statistically significant difference between *H. pylori* infected versus uninfected patients (Figure 4.5.C-F). When comparing expression of the Notch ligands between *H. pylori* infected and uninfected patients, only *JAG2* had a significantly lower median expression level ($p=.014$) (Figure 4.6.B). Lastly, the Notch target genes *HES1* and *HEY1* had significantly downregulated median expression levels in the *H. pylori* infected group ($p=.047$ and $p=.015$ respectively) (Figure 4.7.A,B). Taken together, these findings show decreased expression of *JAG2*, *HES1* and *HEY1* in the gastric mucosa of *H. pylori*-infected compared to uninfected patients.

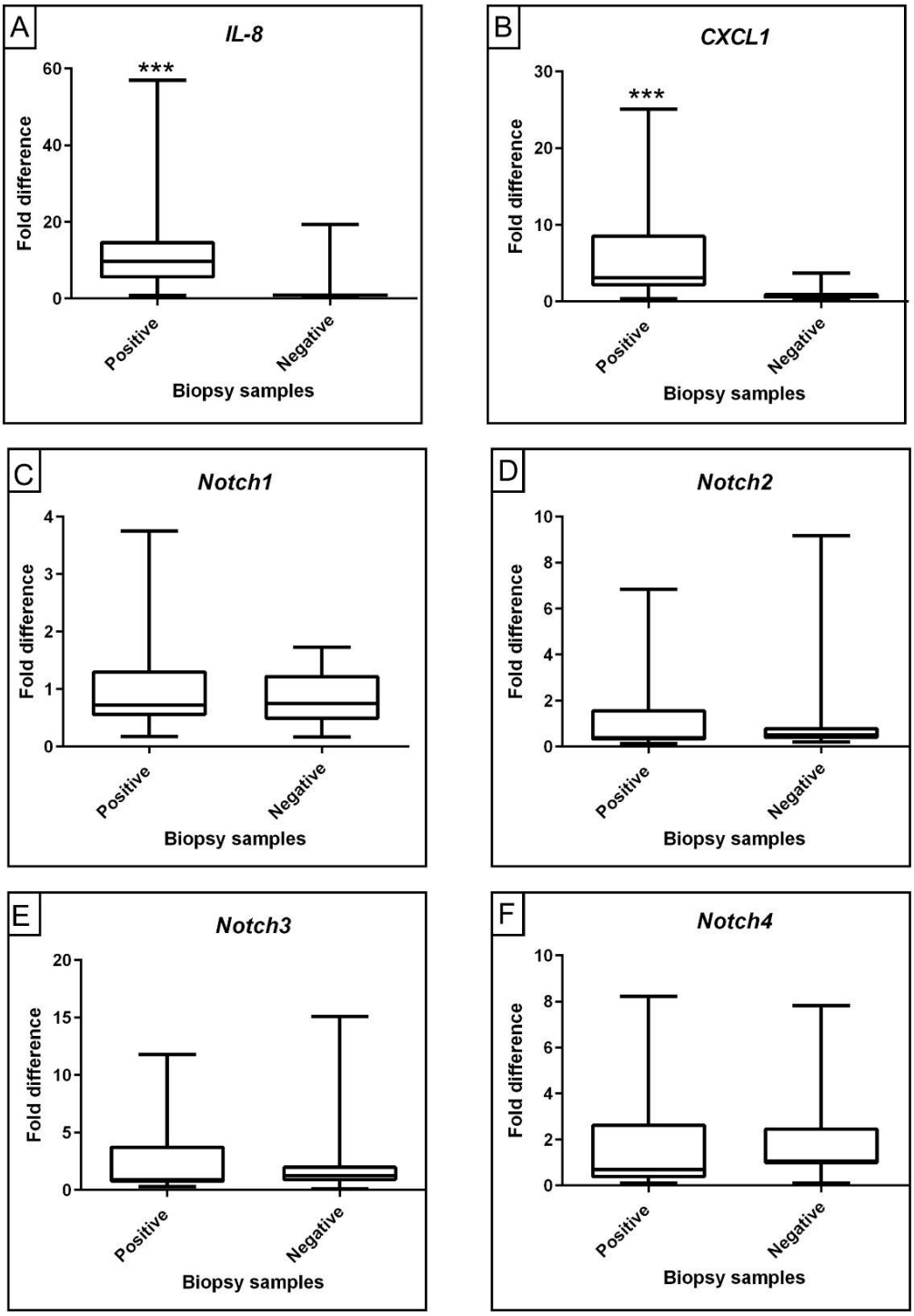

Figure 4.5 Expression of Notch receptors in gastric biopsy tissue from *H. pylori* positive patients and uninfected control patients. Total RNA was purified from antral biopsies of 33 *H. pylori*- infected patients (positive) and 19 uninfected controls (negative). Changes in *IL-8* (A), *CXCL1* (B), *Notch1* (C), *Notch2* (D), *Notch3* (E) and *Notch4* (F) mRNA expression were evaluated by RT-qPCR using the comparative cycle threshold method. Results were normalised to *GAPDH* levels and are expressed relative to a sample in the uninfected control group. The Mann-Whitney U-test was used to compare results from positive and negative groups. *** $P \leq 0.001$.

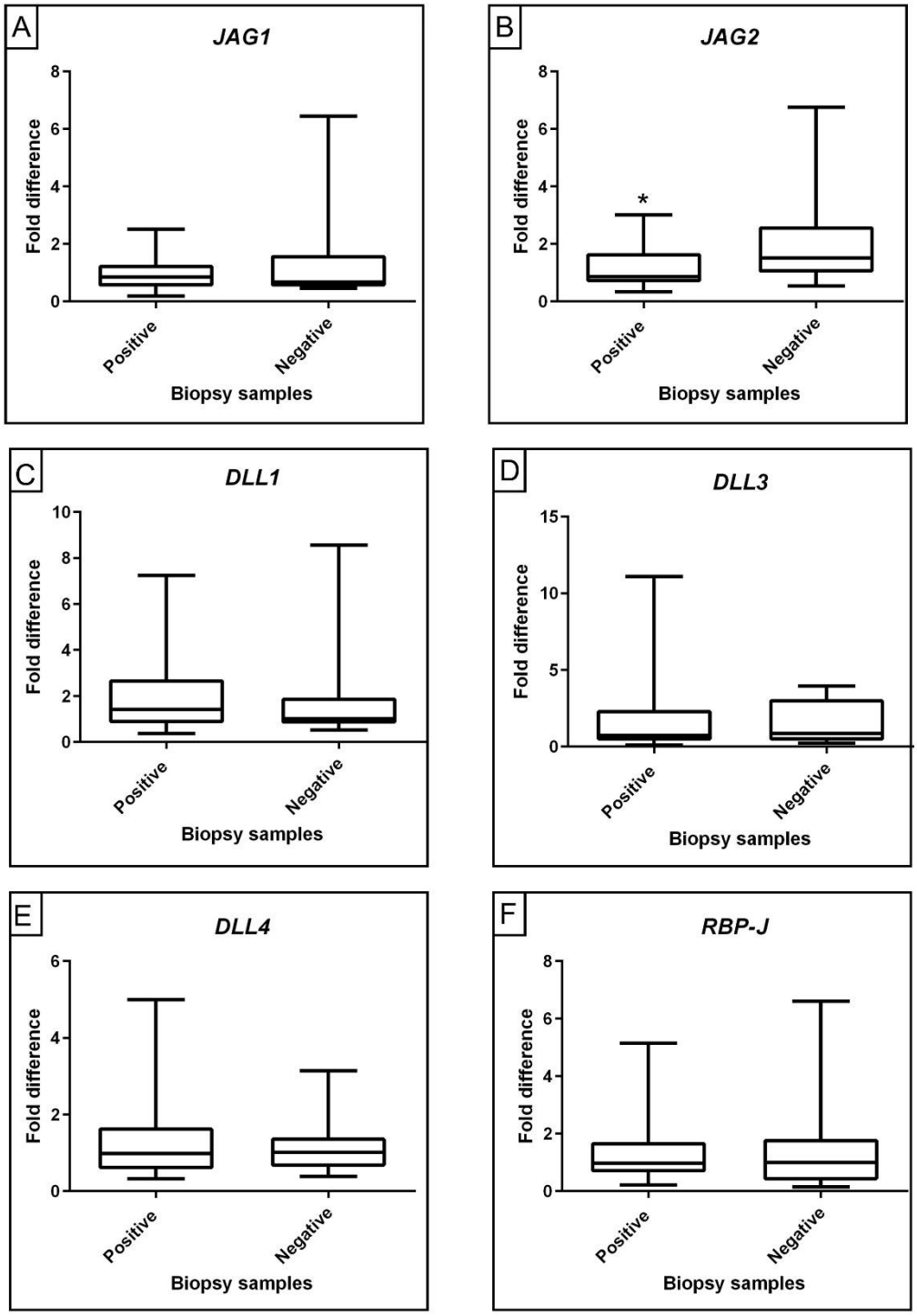

Figure 4.6 Expression of Notch ligands and *RBP-J* in gastric biopsy tissue from *H. pylori* positive patients and uninfected control patients. Total RNA was purified from antral biopsies of 33 *H. pylori*- infected patients (positive) and 19 uninfected controls (negative). Changes in *JAG1* (A), *JAG2* (B), *DLL1* (C), *DLL3* (D), *DLL4* (E) and *RBP-J* (F) mRNA expression were evaluated by RT-qPCR using the comparative cycle threshold method. Results were normalised to *GAPDH* levels and are expressed relative to a sample in the uninfected control group. The Mann-Whitney U-test was used to compare results from positive and negative groups. * $P \leq 0.05$.

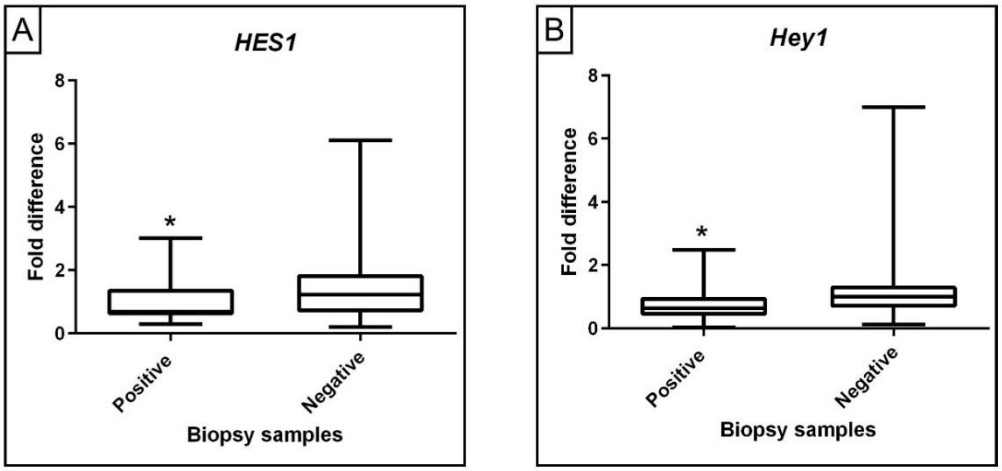

Figure 4.7 Expression of Notch associated transcription factors in gastric biopsy tissue from *H. pylori* positive patients and uninfected control patients. Total RNA was purified from antral biopsies of 33 *H. pylori*- infected patients (positive) and 19 uninfected controls (negative). Changes in *HES1* (A) and *HEY1* (B) mRNA expression were evaluated by RT-qPCR using the comparative cycle threshold method. Results were normalised to *GAPDH* levels and are expressed relative to a sample in the uninfected control group. The Mann-Whitney U-test was used to compare results from positive and negative groups. * $P \leq 0.05$.

4.4.3. *H. pylori* infection decreases expression of the HES1 protein in AGS gastric epithelial cells.

As expression of the Notch pathway target gene *HES1* was consistently downregulated in both AGS cells and stomach tissue biopsy samples in response to *H. pylori*, it was chosen for further investigation. Western blots were performed to confirm that the reduction in *HES1* mRNA expression that was seen with *H. pylori* infection in AGS gastric epithelial cells was seen at the protein level. There was a downregulation of HES1 protein particularly at 3 and 6-hours post infection (Figure 4.8). As a positive control for immunoblotting, transfection of AGS cells with pCMV-Hes1 plasmid increased the expression of HES1 protein.

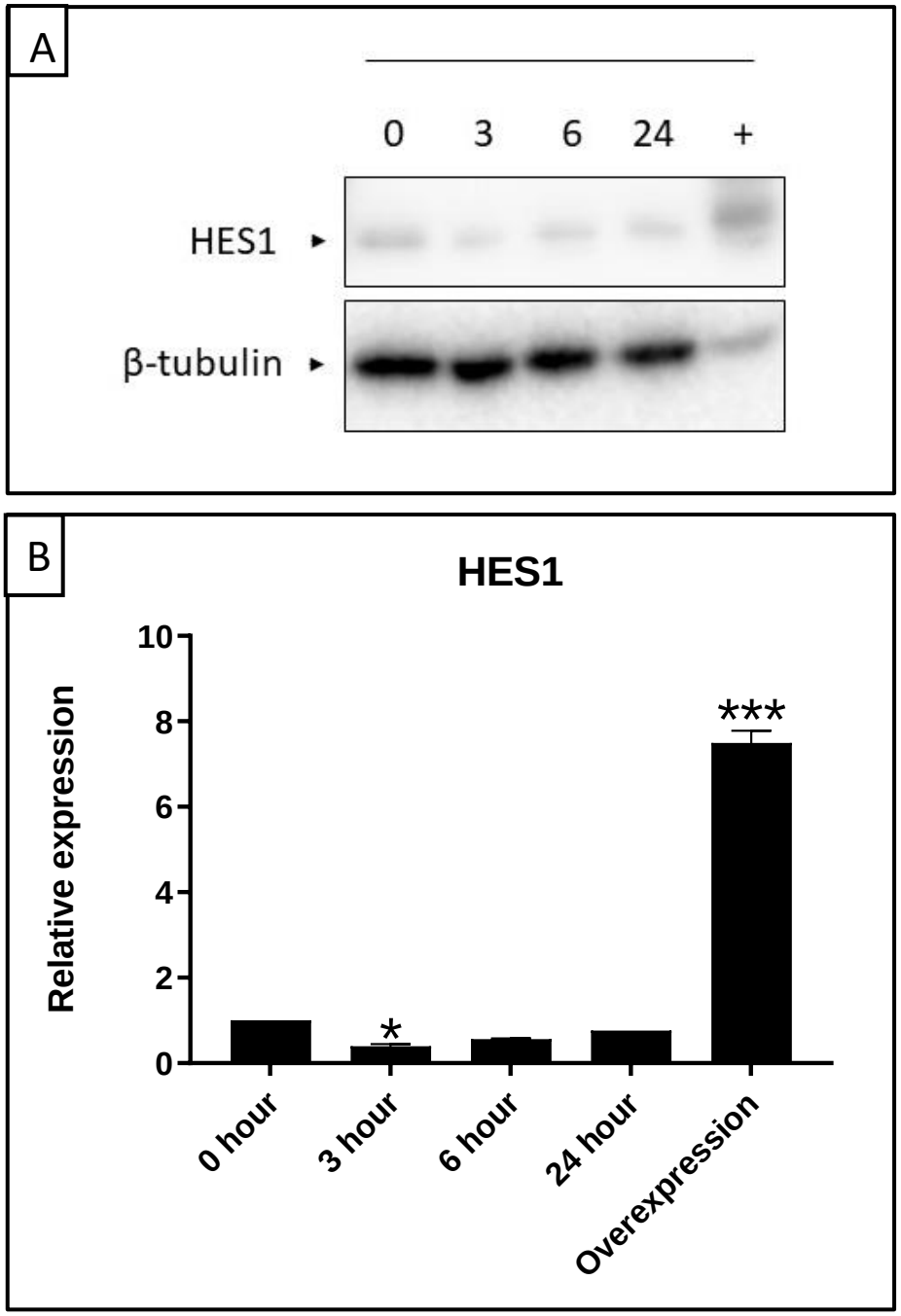

Figure 4.8 Expression of HES1 protein in AGS gastric epithelial cells post-infection with *H. pylori*. AGS cells were seeded at $1X10^6$ cells per well in a 6 well plate 24-hours prior to infection. The cells were infected with 100 MOI of 11638 strain of *H. pylori* for the time points indicated above the image. As a positive control for HES1, AGS cells were transfected with 25µg of pCMV-Hes1 plasmid (+) for 18-hours. Protein lysates were collected in RIPA buffer with protease inhibitor cocktail. ß-tubulin was used as a loading control. Protein size for HES1 30 kDa, protein size for ß-tubulin 55 kDa. A) Western blots were performed by Dr. Michael Freeley, School of Biotechnology, DCU. B) HES1 band intensities were quantified using ImageJ software, normalised to B-tubulin band intensities, and expressed relative to time 0. Results shown are mean values and SD from 2 independent experiments. One-way Anova with Dunnett's multiple comparisons test was performed. * $P \leq 0.05$, *** $P \leq 0.001$.

4.4.4. *H. pylori* virulence factors CagA and VacA are not required for the *H. pylori*-mediated down-regulation of *HES1* mRNA expression.

Next, to identify if the *H. pylori* virulence factors CagA and VacA contribute to *H. pylori*-mediated down-regulation of *HES1* mRNA expression, AGS cells were infected with either a wild-type (WT) *H. pylori* strain 60190 or it's isogenic CagA or VacA mutant strains. Similar to results obtained in AGS cells infected with *H. pylori* NCTC11638 (Figure 4.9), *H. pylori* WT strain 60190 significantly up-regulated expression of *IL-8* (Figure 4.9.A) and *CXCL1* (Figure 4.2.B). Infection with the isogenic CagA mutant strain resulted in significantly less induction of *CXCL1* at 3 and 6-hours (Figure 4.9.B) compared to the WT strain, indicating that CagA plays a role in the *H. pylori*-mediated induction of *CXCL1*. The VacA mutant significantly reduced expression of *CXCL1* compared to the WT strain. Unexpectedly, the isogenic VacA mutant induced a higher expression of *IL-8* than the WT strain (Figure 4.9.A,B). This suggests that VacA is involved in *CXCL1*, but not *IL-8* induction.

In line with the findings using strain NCTC11638 (Section 4.4.1. above), WT strain 60190 also down-regulated *HES1* mRNA expression in AGS cells (Figure 4.9.C). Down-regulation of *HES1* was also observed in response to the *H. pylori* CagA and VacA mutant strains, indicating that the virulence factors CagA and VacA are not required for *H. pylori*-mediated *HES1* suppression.

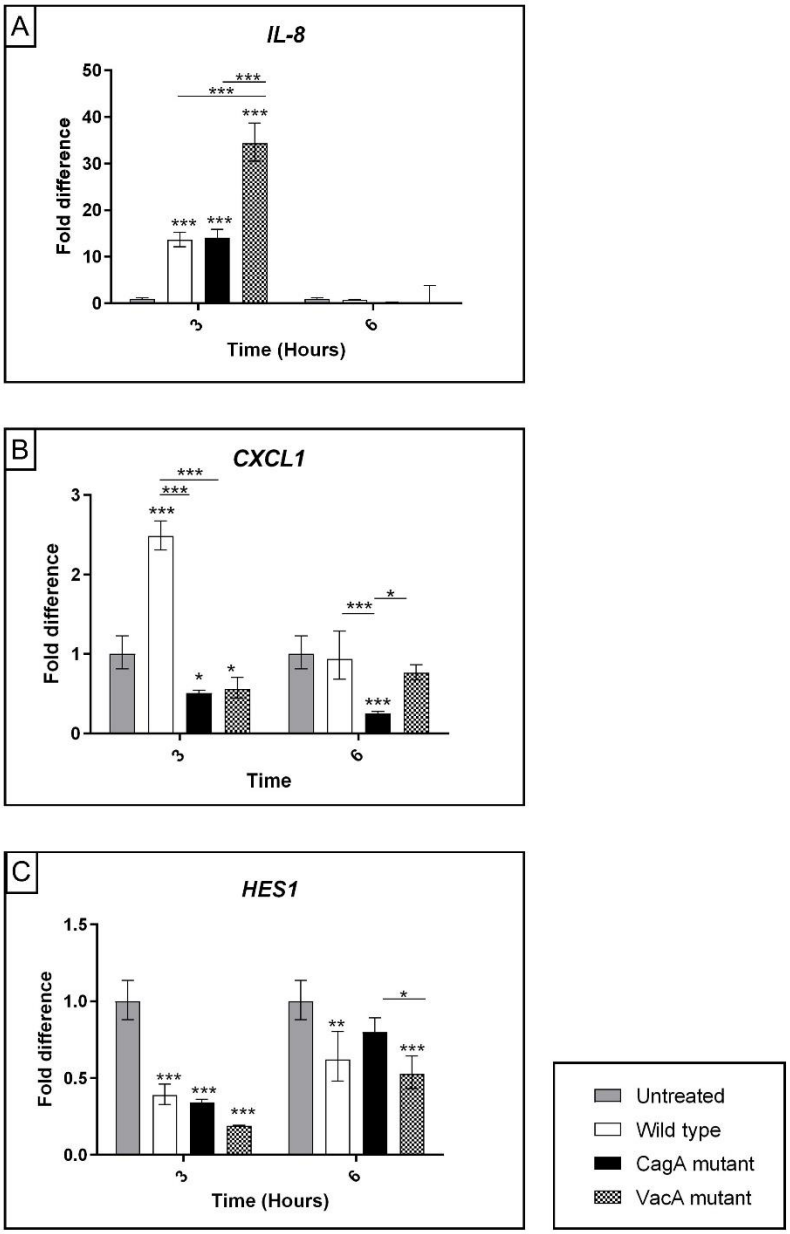

Figure 4.9 Expression of *HES1* in AGS gastric epithelial infected with wild type and mutant strains of *H. pylori* 60190. Cells were seeded at $1x10^6$ cells/well in 6-well plate 24-hours prior to infection. AGS gastric epithelial cells were infected with 100 MOI of WT 60190 strain of *H. pylori* or isogenic CagA and VacA mutants for the time points indicated underneath the graphs. Total RNA was isolated and changes in *IL-8* (A), *CXCL1* (B) and *HES1* (C) gene expression were evaluated by RT-qPCR using the comparative cycle threshold method. Results were normalised to *GAPDH* levels and expressed relative to uninfected cells at each time point. Data shown are means ± SD. A two-way Anova test was performed for each gene. Tukey's multiple comparisons test was used to compare each treatment mean with every other treatment mean at each time point. * P≤0.05, ** P≤0.01, *** P≤0.001. Graphs are representative of two independent experiments.

4.4.5. *H. pylori* LPS does not suppress *HES1* mRNA expression in MKN45 cells.

The role of *H. pylori* LPS in the downregulation of *HES1* was also investigated. MKN45 gastric epithelial cells were used in these experiments as they express functional TLR2 (unlike AGS cells) and previous findings from our laboratory have demonstrated that TLR2 responds to *H. pylori* LPS in epithelial cells (Smith et al., 2011). The synthetic TLR2 ligand Pam_2CSK_4 (PAM) was used in these experiments as a positive control for TLR2 stimulation. MKN45 cells were infected with 100 MOI of *H. pylori* or treated with 100 ng/ml PAM or 10 μg/ml *H. pylori* LPS. Infection with *H. pylori* led to significant increases in *TNF* mRNA expression at 3 and 6-hour time points (Figure 4.10.A). Infection with *H. pylori* led to significant reduction in *HES1* expression at both 3 and 6-hours post infection ($p<.001$, $p=.013$ respectively). In contrast to infection with live *H. pylori,* neither PAM not LPS inhibited *HES1* mRNA expression in MKN45 cells (Figure 4.10.B). These findings indicate that *H. pylori* LPS is not involved in the *H. pylori*-mediated reduction in *HES1*.

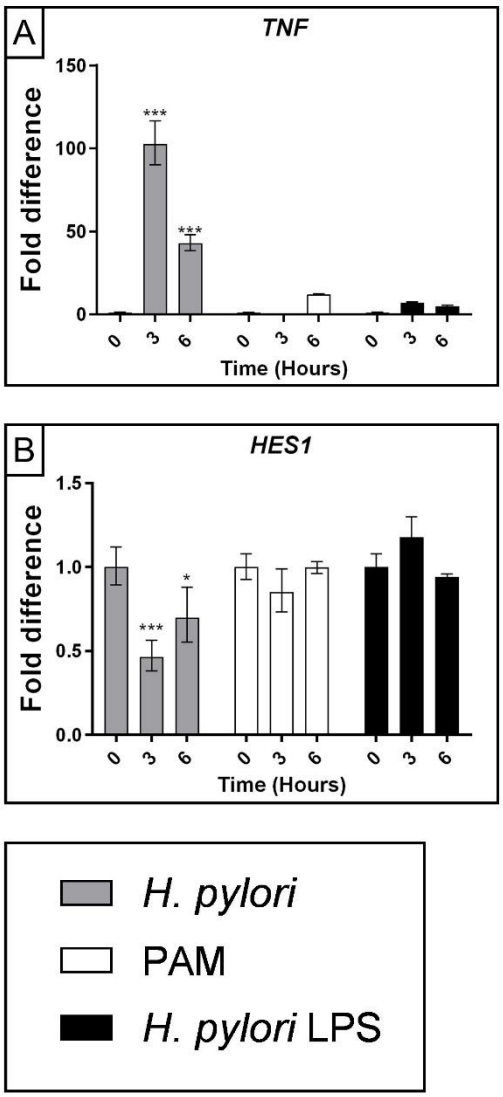

Figure 4.10 Expression of *HES1* in MKN45 cells treated with *H. pylori* LPS, Pam2CSK4 or infected with *H. pylori*. MKN45 cells were infected with 100 MOI of *H. pylori* or treated with 100 ng/ml of the TLR2 ligand Pam2CSK4 (PAM) or 10 µg/ml *H. pylori* LPS for the time points indicated underneath the graphs. Total RNA was isolated and changes in *TNF* (A) and *HES1* (B) gene expression was evaluated by RT-qPCR using the comparative cycle threshold method. Results were normalised to *GAPDH* levels and expressed relative to uninfected cells at the 0-hour time point. Data shown are means ± SD. A two-way Anova was performed for each gene. Dunnett's multiple comparison tests were used to compare each sample mean with the mean of the control (*H. pylori* 0-hour). $P \leq 0.05$, *** $P \leq 0.001$. Graphs are representative of three independent experiments. Data presented were analysed from in vitro infection experiments performed by James Lamb.

4.4.6. New protein synthesis is required for the *H. pylori*-mediated down-regulation of *HES1* mRNA expression in AGS gastric epithelial cells.

To investigate whether new protein synthesis is required for the *H. pylori*-mediated suppression of *HES1*, AGS cells were treated with the protein synthesis inhibitor, cycloheximide before infection. Cycloheximide combined with *H. pylori* infection led to significant increases in expression of *IL-8* and *CXCL1* compared to either *H. pylori* infection alone or cycloheximide treatment alone at 3 and 6-hours (Figure 4.11.A,B).

As previously reported in the literature, cycloheximide treatment alone significantly increased the expression of *HES1* mRNA at all time points tested (Revollo et al., 2013), (Hirata et al., 2002). In the presence of cycloheximide, *H. pylori* no longer inhibited *HES1* mRNA expression in AGS cells (Figure 4.11.C). Since blocking new protein synthesis blocks *H. pylori*-mediated downregulation of *HES1,* this would suggest that *H. pylori* induces a protein that inhibits *HES1* mRNA expression.

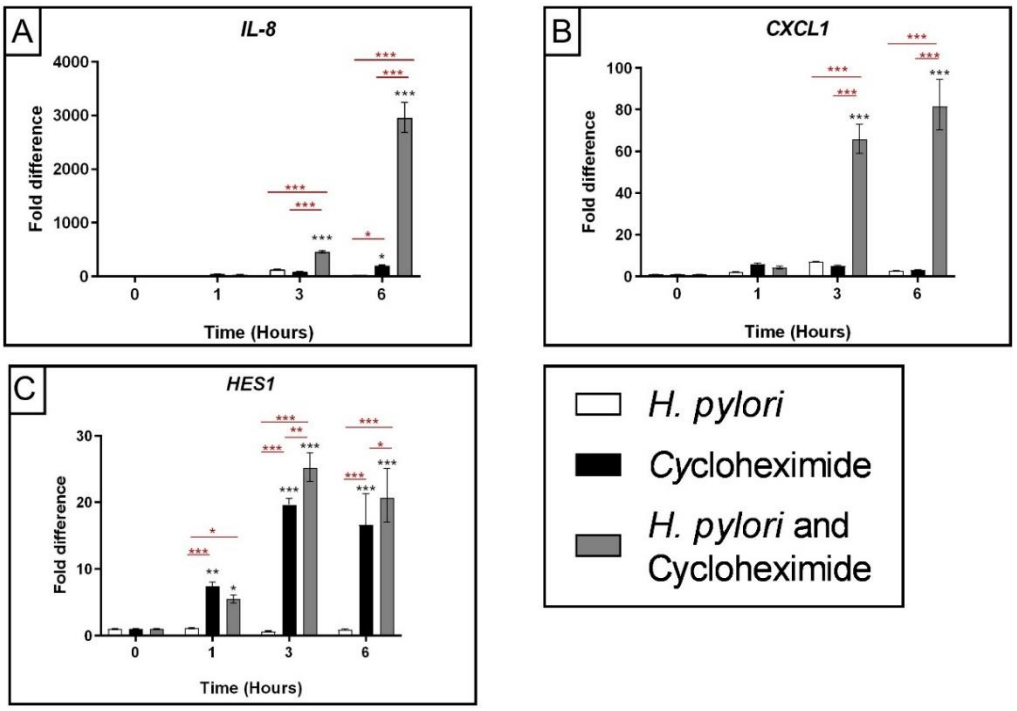

Figure 4.11 Expression of Hes1 mRNA in AGS cells treated with cycloheximide and infected with *H. pylori*. AGS cells were seeded at 0.3x106 cell per well. The following day the cells were treated for 1 hour with 20 μg/ml cycloheximide and infected with 100 MOI of *H. pylori* strain 11638 for the time points indicated underneath the graphs. Total RNA was isolated and changes in Gene expression for *IL-8* (A), *CXCL1* (B) and *HES1* (C) was evaluated by RT-qPCR using the comparative cycle threshold method. Results were normalised to *GAPDH* levels and expressed relative to uninfected cells at each time point. A two-way Anova was performed for each gene. Dunnett's multiple comparison test was used to compare mean values of each sample with the untreated sample (*H. pylori* 0-hour) (black asterisk). Tukey's multiple comparison test was used to compare mean values of each treatment to every other treatment at each time-point (red asterisk). P≤0.05, ** P≤0.01, *** P≤0.001. Graphs are representative of three independent experiments.

4.4.7. γ-secretase inhibition of Notch signalling did not enhance *H. pylori*-mediated *HES1* down-regulation in AGS gastric epithelial cells.

Since *H. pylori* reduces expression of *HES1* in gastric epithelial cells (both AGS and MKN45) and the gastric mucosa of infected patients, a loss-of-function approach was next attempted to identify downstream effects. The enzyme γ-secretase processes the Notch receptor at the S3 site in the transmembrane domain allowing for Notch signalling to progress through translocation of the cleaved NICD to the nucleus to activate transcription of Notch target genes, including *HES1* (Shang et al., 2016b). Commercially available γ-secretase inhibitors that bind to presenilin 1, the catalytic site of γ-secretase, prevent Notch signalling (Yang et al., 2008). To confirm the ability of the γ-secretase inhibitor (Compound E; Abcam) to inhibit *HES1* expression, a control experiment was carried out on AGS cells stimulated with the ion chelator, Ethylene glycol-bis(ß-aminoethyl ether)-N,N,N′,N′-tetraacetic acid (EGTA), which can mimic activation of Notch signalling to an equivalent degree as ligand binding (Rand et al., 2000).

AGS cells were treated with the γ-secretase inhibitor for 16 hours and EGTA for 1 hour. As expected, stimulation of Notch signalling with EGTA significantly increased the expression of *HES1* compared to untreated cells (Fold difference 2.8, $p<.001$; Figure 4.12). All concentrations of Compound E (100 nM, 500 nM and 1000 nM) significantly reduced the expression of *HES1* in EGTA treated AGS cells (Figure 4.12). However, Compound E treatment on cells that were not stimulated with EGTA did not significantly reduce *HES1* expression compared to baseline levels.

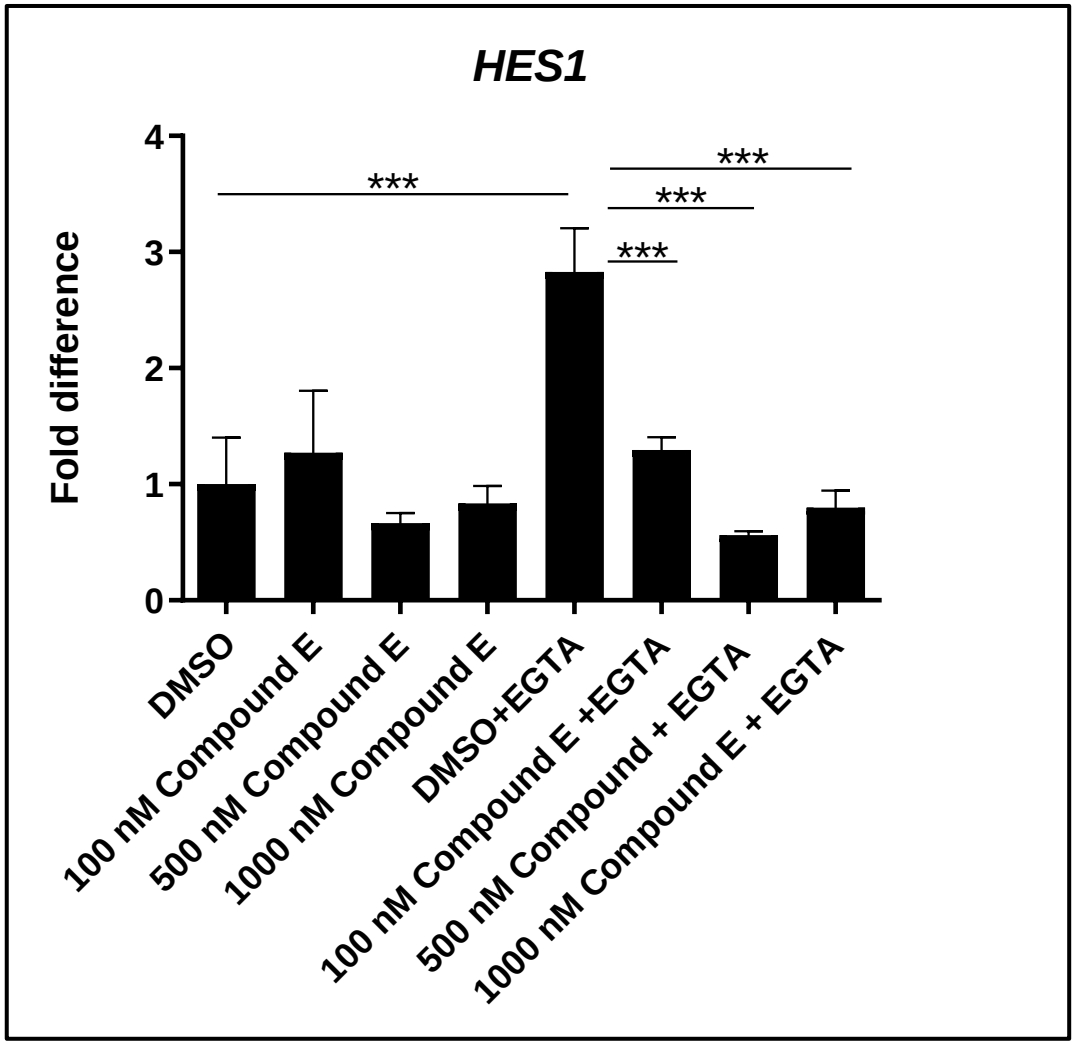

Figure 4.12 Expression of *HES1* in AGS cells treated with 4nM EGTA and a range of Compound E concentrations. AGS cells were seeded at $1x10^6$ cells/well in a 6-well plate and incubated for 24 hours. Cells were then incubated with 100nM, 500nM or 1000nM of Compound E for 16 hours. Subsequently they were stimulated with 4mM EGTA for 1 hour or with DMSO as a control. An equivalent volume of DMSO was used as a control since Compound E is dissolved in DMSO. *HES1* expression was measured by RT-qPCR using the comparative cycle threshold method. Results were normalised to *GAPDH* levels and expressed relative to the DMSO sample. Data shown are means ± SD. A one-way Anova with Tukey's multiple comparison test was used to calculate significance between each of the samples. * $P \leq 0.05$, ** $P \leq 0.01$, *** $P \leq 0.001$.

Next, the ability of Compound E to further suppress *HES1* in the context of *H. pylori* infection was tested. As anticipated, *H. pylori* infection alone led to significant decreases in *HES1* expression at 3 and 6-hours post infection ($p<.001$, and $p<.001$ respectively, not marked on graph) (Figure 4.13). However, treatment with Compound E did not significantly reduce *HES1* expression to levels lower than what was experienced with *H. pylori* alone. This makes it difficult to use Compound E as a loss-of-function method for measuring the impact of decreased *HES1* expression during *H. pylori* infection in gastric epithelial cells.

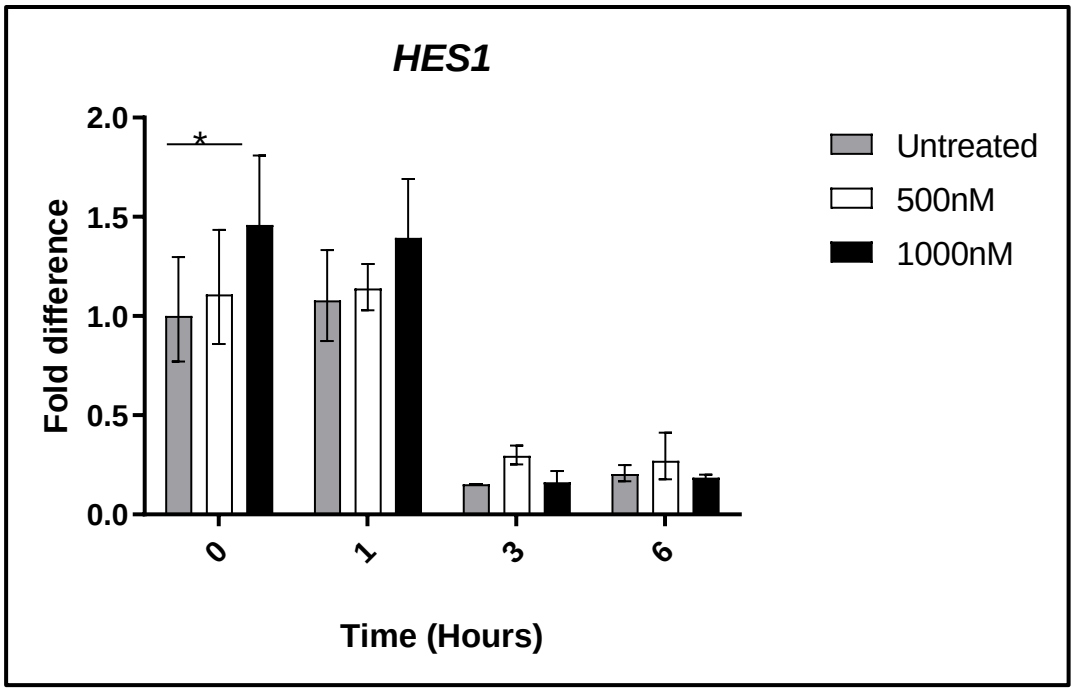

Figure 4.13 Expression of *HES1* in AGS cells treated with Compound E and infected with *H. pylori*. AGS cells were seeded at $1x10^6$ cells per well in a 6 well plate 48 hours prior to infection. After they had been seeded for 24-hours, the cells were treated with 500nM or 1000nM of Compound E, 16-hours later the cells were infected with the 11638 strain of *H. pylori* for the time points indicated under the graph. Total RNA was isolated and changes in *HES1* gene expression was evaluated by RT-qPCR using the comparative cycle threshold method. Results were normalised to *GAPDH* levels and expressed relative to uninfected cells at the 0-hour time point. Data shown are means ± SD. A two-way Anova with Tukey's multiple comparison test was used to compare each treatment mean with every other treatment mean at each time point. * $P\leq0.05$, ** $P\leq0.01$, *** $P\leq0.001$. Graph is representative of three independent experiments.

4.4.8. *HES1* RNAi did not sufficiently enhance *H. pylori*-mediated *HES1* down-regulation in AGS cells.

Next, the ability of a *HES1* siRNA to further suppress *HES1* in the context of *H. pylori* infection was tested. *H. pylori* infection alone led to significant decreases in *HES1* expression at 3 and 6-hours post infection ($p<.001$) (Figure 4.14). In the absence of *H. pylori,* the *HES1* siRNA decreased the expression of *HES1* to 0.57-fold, ($p<.001$). However, the *HES1* siRNA did decrease the expression of *HES1* to a significantly greater extent than *H. pylori* alone, hence, the fold difference was not stark enough to use the *HES1* siRNA as a loss-of-function method for measuring the impact of decreased *HES1* expression during *H. pylori* infection in gastric epithelial cells.

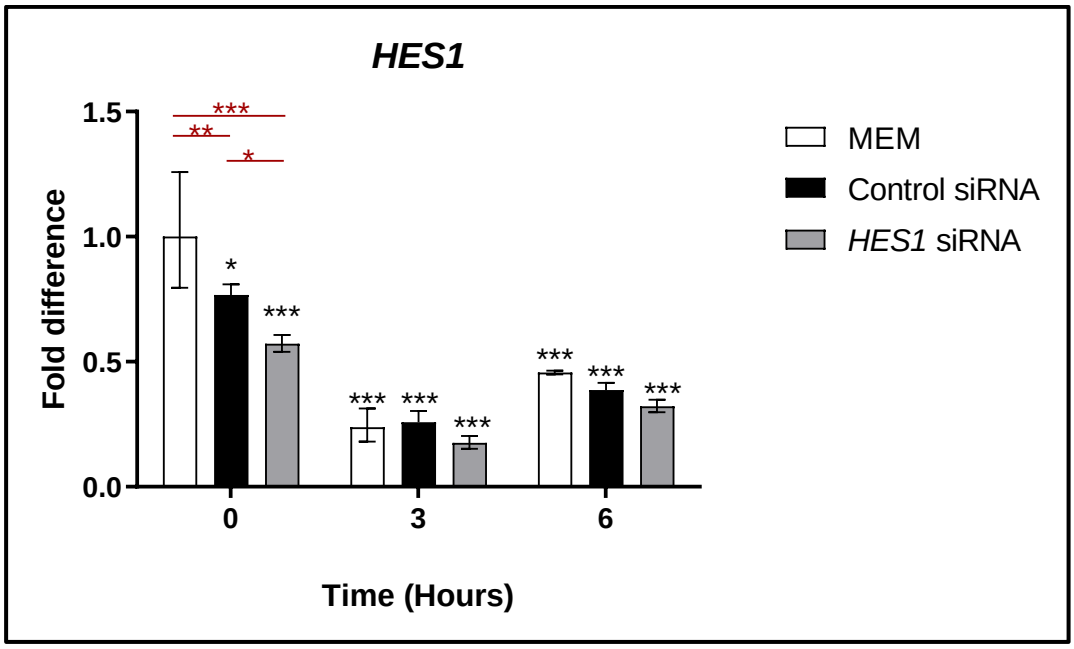

Figure 4.14 Expression of *HES1* in AGS cells treated with *HES1* siRNA and infected with *H. pylori*. 100nM of *HES1* siRNA (Invitrogen 1299001; ID: HSS179374) or a non-targeting control siRNA (Invitrogen 12935-400) were transfected into AGS cells using Lipofectamine 2000. AGS cells were resuspended and combined with the RNA:lipofectomine complexes with $4x10^5$ cells seeded per well in a 12 well plate. Cells that were not transfected with an siRNA had an equivalent volume of Opti-MEM I Reduced Serum Medium added to the well (MEM). After they had been seeded for 48-hours the cells were infected with the 11638 strain of *H. pylori* for the time points indicated under the graph. Total RNA was isolated and changes in *HES1* gene expression was evaluated by RT-qPCR using the comparative cycle threshold method. Results were normalised to GAPDH levels and expressed relative to un-transfected cells (MEM) at the 0-hour time point. Data shown are means ± SD. A two-way Anova test was performed with a Dunnett's multiple comparison test to compare all the samples to the MEM 0-hour sample (black asterisk) and Tukey's multiple comparison test to compare the mean of each sample against every other sample at that time point (red asterisk). * $P \leq 0.05$, ** $P \leq 0.01$, *** $P \leq 0.001$. Graphs are representative of three independent experiments.

4.4.9. Stimulation with a JAG2 ligand was not sufficient to increase Notch signalling in AGS gastric epithelial cells.

The next step was to see if a gain-of-function approach could be used to identify the role of Notch pathway activation during *H. pylori* infection. For this reason, Notch signalling was attempted to be triggered using a JAG2 ligand. A recombinant human JAG2 protein or PBS were added to cell culture plates overnight. The following day, AGS cells were added and harvested at later time points for evaluation of Notch pathway activation by measuring expression of the Notch target genes *HES1* and *HEY1*. The JAG2 ligand did not significantly increase *HES1* or *HEY1* expression in AGS cells at either 15 or 21-hours (Figure 4.15). Collecting at other time points also did not increase *HES1* or *HEY1* expression (not shown). Additionally, adding the JAG2 ligand directly to the cell culture medium of pre-seeded cells did not lead to significant increases in *HES1* expression (not shown).

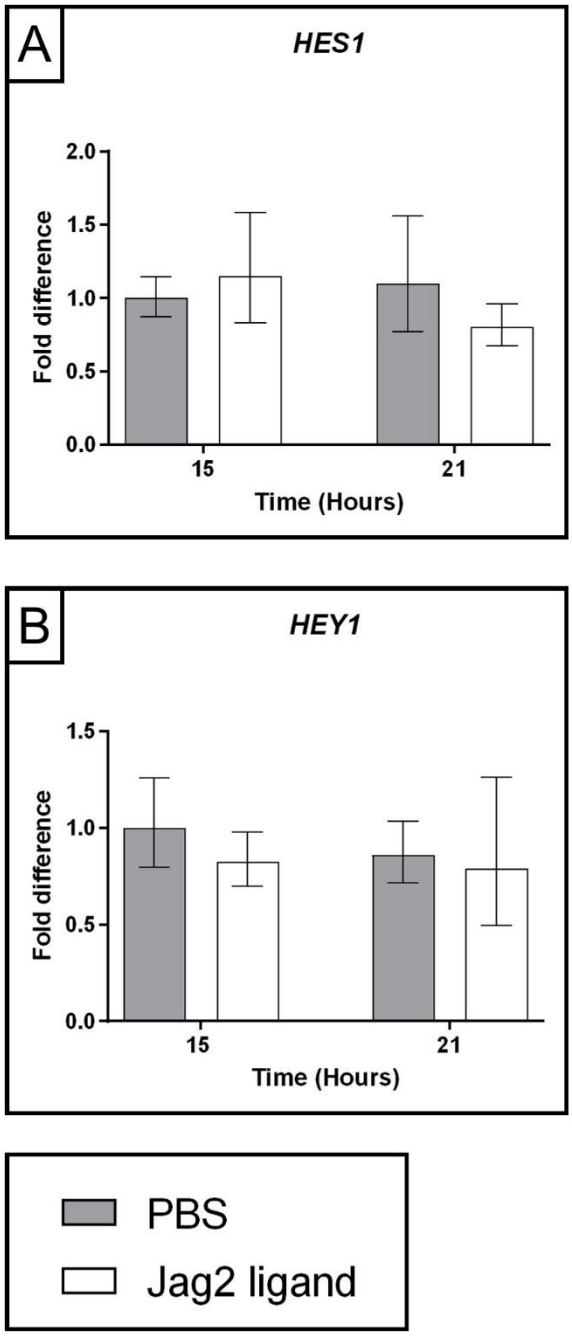

Figure 4.15 Expression of *HES1 and HEY1* in AGS cells following stimulation with JAG2 ligand. Cell culture plates were coated with 10µg/ml JAG2 ligand (R&D Systems; 1726-JG) that had been diluted in a volume of 250µl of sterile phosphate buffered saline (PBS). The same volume of sterile PBS was added in the control wells. The plates were stored at 4°C overnight. AGS cells were seeded the following day and collected 15 or 21 hours later. RNA lysates were collected and *HES1* (A) and *HEY1* (B) expression was measured by RT-qPCR using the comparative cycle threshold method. Results were normalised to *GAPDH* levels and expressed relative to wells pre-treated with sterile PBS. Data shown are means ± SD. A two-way Anova test with Tukey's multiple comparisons was performed for each gene. No statistically significant differences were found. Graphs are representative of three independent experiments.

4.4.10. Over-expression of *HES1* in AGS cells was successfully achieved by plasmid DNA transfection.

As an alternative gain-of-function approach to characterise the role of HES1 during *H. pylori* infection, AGS cells were transfected with an expression vector for HES1 (pCMV6-HES1 plasmid). To control for the impact of transfection, cells were transfected with an empty control vector (pCMV6-AC-GFP).

When measured with RT-qPCR, transfection with the HES1 plasmid significantly upregulated *HES1* mRNA expression in the absence and presence of *H. pylori* compared to the un-transfected and samples transfected with the empty control plasmid (Figure 4.16). *H. pylori* infection led to the expected downregulation of *HES1* expression in the un-transfected (0.15-fold) and empty vector transfected (0.88-fold) samples however, this was not significant. Additionally, overexpression of *HES1* corresponded to an increase in HES1 protein (Figure 4.8). Having successfully achieved HES1 overexpression at the mRNA and protein level, the impact of increased HES1 expression on genome-wide responses to *H. pylori* in AGS cells was measured by RNAseq (see Section 4.5 below).

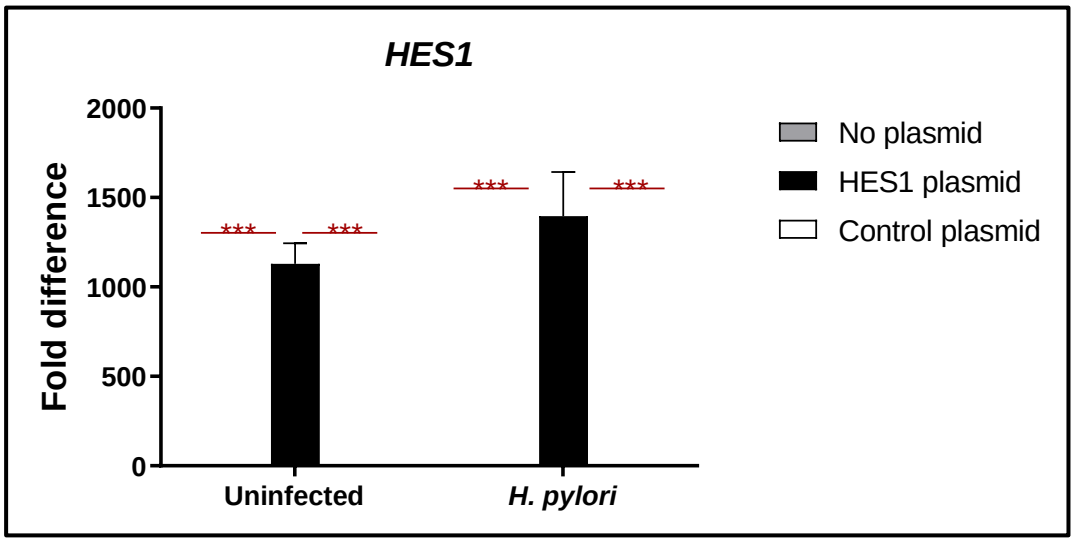

Figure 4.16 Expression of *HES1* in AGS cells transfected with HES1 plasmid. AGS cells were transfected with either pCMV6-HES1 (NM_005524) Human Tagged ORF Clone (ORIGENE) or with the empty control vector, pCMV6-AC-GFP (ORIGENE). AGS cells were seeded at $4.5x10^5$ cells per well in a 6 well plate. The following day, 2.5 µg of DNA was transfected per well using Lipofectamine LTX® Reagent. 18 hours later the cells were infected with *H. pylori* strain 11638 for 3-hours. Total RNA was isolated and changes in Gene expression for *HES1* was evaluated by RT-qPCR using the comparative cycle threshold method. Results were normalised to *GAPDH* levels and expressed relative to uninfected cells at each time point. A two-way Anova was performed with Tukey's multiple comparisons test to compare every sample to each other at each time point. ** $P \leq 0.01$. Graphs are representative of three independent experiments.

4.5. Evaluation of genome-wide responses to *H. pylori* by RNAseq with and without HES1 overexpression.

In short, RNA sequencing (RNAseq) involves deeply sequencing the transcriptome and counting how frequently each gene is represented in the sequenced sample (Mortazavi et al., 2008). RNAseq produces large volumes of data that can be interpreted and analysed in many ways. In this study, RNAseq was utilised to investigate the impact of increased HES1 expression on genome-wide transcriptional responses of AGS cells to *H. pylori* infection. RNAseq was performed on duplicate samples of (i) un-transfected AGS cells in the absence and presence of *H. pylori*, (ii) control plasmid (empty vector pCMV6-AC-GFP) transfected AGS cells in the absence and presence of *H. pylori* and (iii) AGS cells overexpressing HES1 in the absence and presence of *H. pylori*.

4.5.1. PCA Plots clustered the duplicate RNA-seq samples together.

PCA plots show which samples are clustered together and can help identify patterns in the data and/or outlier samples (Marini and Binder, 2019). PCA analysis of the RNAseq data showed that most duplicate samples clustered very close together (Figure 4.17). There was some variation in the two samples transfected with the HES1 plasmid which may reflect technical error. The samples infected with *H. pylori* cluster on one side of the plot while the uninfected samples cluster on the other, demonstrating the large impact *H. pylori* infection has on gene expression in gastric epithelial cells. The distance between the un-transfected duplicates and the empty-vector transfected duplicates indicate that transfection alone had an impact on gene expression.

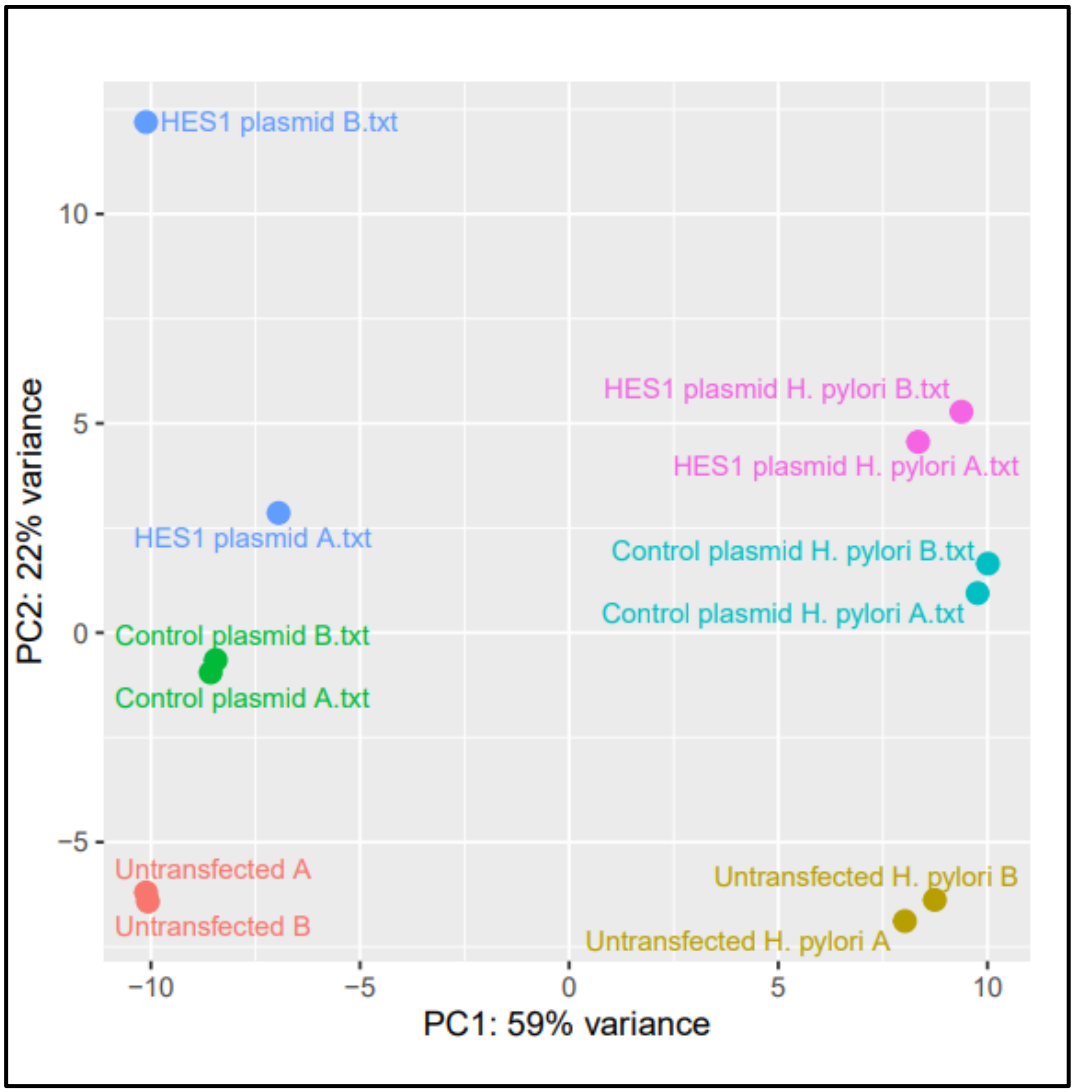

Figure 4.17 A PCA plot comparing duplicates of samples sent for RNAseq. Gene count data was analysed by Deseq2. Each of the 12 samples sent for sequencing are represented on the graph. Un-transfected sample A and B (Red), Empty vector plasmid A and B (Green), HES1 plasmid A and B (Blue), Un-transfected, infected with *H. pylori* A and B (yellow), Empty vector plasmid, infected with *H. pylori* (turquoise), HES1 plasmid, infected with *H. pylori* A and B (pink).

4.5.2. RNA-seq analysis of un-transfected AGS cells confirms changes in gene expression characteristic of *H. pylori* infection and identifies new *H. pylori*-regulated genes.

To confirm expected *H. pylori* mediated changes in gene expression and identify new changes, genome-wide differential expression was compared between uninfected AGS cells and AGS cells infected with *H. pylori* for 3 hours. A volcano scatterplot was generated to enable visualisation of significantly differentially expressed genes (Figure 4.18). The X-axis represents the $\log_2$-transformed fold changes and the y-axis represents -log10(adjusted P value) (Zhao and Wang, 2022). In the volcano plot, the most upregulated genes are to the right, the most down regulated genes are to the left and the most statistically significant genes (*KDM6B*, *PHLDA1* and *PLAUR*) are to the top of the plot.

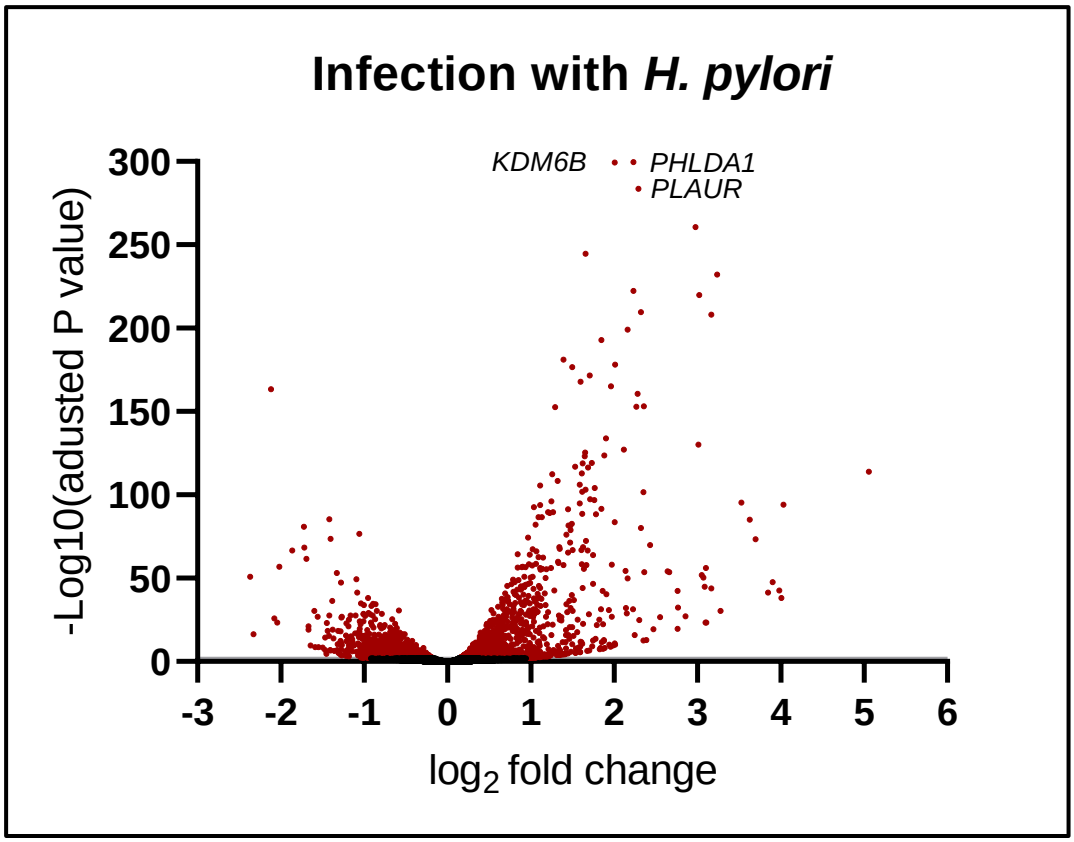

Figure 4.18 Volcano plot of differentially expressed genes in *H. pylori* infected AGS cells and uninfected cells. AGS cells were infected with 100 MOI of *H. pylori* strain 11638 for 3 hours. Duplicate samples were analysed by RNAseq. The gene lists from Deseq2 were ordered by highest -$\log_{10}$ adjusted P value and graphed against the corresponding $\log_2$ fold change. Genes that have an adjusted P value of <.01 (>2 -$\log_{10}$ of the adjusted P value) are marked as red dots on the plot. Genes that have an adjusted P value of >.01 (<2 -$\log_{10}$ of the adjusted P value) are marked as black dots on the graph. The three genes with the largest -$\log_{10}$(adjusted P value) are labelled on the graph.

The gene lists from Deseq2 were then filtered to exclude values with a P>.05 and were ordered by highest $\log_2$ fold change. 1,804 genes had increased expression in AGS cells following *H. pylori* infection and 1,992 genes had decreased expression. The 20 genes with the largest increase in expression ($\log_2$ fold change) following *H. pylori* infection are represented in Table 4.1. The 20 genes with the largest decrease in expression following *H. pylori* infection are represented in Table 4.2. In line with the published literature, the RNAseq identified significant up-regulation in the chemokines *IL-8* (*CXCL8*) and *CCL20* (Yoshida et al., 2009), (Eftang et al., 2012), demonstrating the validity of our in vitro infection model.

Gene ID	Log2 fold change	Gene name
ENSG00000169429	5.055003	*CXCL8 (IL-8)*
ENSG00000196611	4.030248	*MMP1*
ENSG00000122641	4.007443	*INHBA*
ENSG00000115009	3.980046	*CCL20*
ENSG00000162892	3.900121	*IL24*
ENSG00000056558	3.847355	*TRAF1*
ENSG00000008516	3.698093	*MMP25*
ENSG00000164949	3.62786	*GEM*
ENSG00000049249	3.527022	*TNFRSF9*
ENSG00000163082	3.279562	*SGPP2*
ENSG00000184371	3.236329	*CSF1*
ENSG00000023445	3.168869	*BIRC3*
ENSG00000160712	3.166353	*IL6R*
ENSG00000273590	3.106929	*SMIM11B*
ENSG00000185338	3.100104	*SOCS1*
ENSG00000134070	3.097868	*IRAK2*
ENSG00000172602	3.086533	*RND1*
ENSG00000179674	3.070455	*ARL14*
ENSG00000248323	3.051928	*LUCAT1*
ENSG00000057657	3.021074	*PRDM1*

Table 4.1 Top 20 genes with the largest increase in expression in *H. pylori* infected AGS cells compared to uninfected cells. AGS cells were infected with 100 MOI of *H. pylori* strain 11638 for 3 hours. Duplicate samples were analysed by RNAseq. The gene lists from Deseq2 were filtered to exclude values with a P>.05 and were ordered by highest $\log_2$ fold change.

Gene ID	Log2 Fold change	Gene name
ENSG00000120093	-1.46666	*HOXB3*
ENSG00000180884	-1.4989	*ZNF792*
ENSG00000175087	-1.54772	*PDIK1L*
ENSG00000136122	-1.5577	*BORA*
ENSG00000197050	-1.58592	*ZNF420*
ENSG00000132669	-1.59854	*RIN2*
ENSG00000090447	-1.64196	*TFAP4*
ENSG00000120696	-1.66556	*KBTBD7*
ENSG00000175538	-1.66656	*KCNE3*
ENSG00000163513	-1.6947	*TGFBR2*
ENSG00000149474	-1.71956	*KAT14*
ENSG00000108375	-1.72281	*RNF43*
ENSG00000204335	-1.86496	*SP5*
ENSG00000115738	-2.01906	*ID2*
ENSG00000181449	-2.04335	*SOX2*
ENSG00000165572	-2.07623	*KBTBD6*
ENSG00000168646	-2.11611	*AXIN2*
ENSG00000164056	-2.3262	*SPRY1*
ENSG00000215012	-2.36566	*RTL10*

Table 4.2 Top 20 genes with the largest decrease in expression in *H. pylori* infected AGS cells compared to uninfected cells. AGS cells were infected with 100 MOI of *H. pylori* strain 11638 for 3 hours. Duplicate samples were analysed by RNAseq. The gene lists from Deseq2 were filtered to exclude values with a P>.05 and were ordered by lowest $\log_2$ fold change.

4.5.3. Pathway enrichment analysis demonstrated genes involved in cytokine-cytokine receptor interaction and IL-17 signalling are regulated in AGS cells during *H. pylori* infection.

Sequencing analysis often leads to a long list of differently expressed genes that can be difficult to manage and interpret. Pathway enrichment analysis is a method of making sequencing data more understandable by compressing a large list of genes into a smaller list of pathways (Reimand et al., 2019). To better interpret the impact of *H. pylori* mediated changes in gene expression, pathway analysis was performed to identify biological pathways enriched with genes whose expression was altered in *H. pylori* infected AGS cells. The top 10 pathways containing genes whose expression was significantly altered in response to *H. pylori* are shown in Table 4.3. Two pathways of interest are the cytokine-cytokine receptor interaction pathway and the IL-17 signalling pathway. The KEGG diagrams for these pathways are found in Figure 4.19 and Figure 4.20 respectively. On the KEGG diagrams genes associated with *H. pylori* mediated upregulation are marked in red, genes associated with *H. pylori* mediated downregulation are marked in green and genes not impacted by *H. pylori* are marked in white. Genes that were in the top 20 up or downregulated lists from Table 4.1 and Table 4.2 are marked by a yellow box.

Direction	Pathways	Gene number	Adjusted p value
Down	Herpes simplex virus 1 infection	346	3.30E-09
Up	Cytokine-cytokine receptor interaction	100	0.0025
Up	TNF signalling pathway	90	0.013
Up	Rheumatoid arthritis	42	0.015
Up	Coronavirus disease	163	0.013
Up	Osteoclast differentiation	79	0.015
Up	IL-17 signalling pathway	62	0.015
Up	Complement and coagulation cascades	33	0.017
Up	Lipid and atherosclerosis	146	0.026
Up	PI3K-Akt signalling pathway	211	0.026

Table 4.3 Pathway analysis identified the top 10 pathways altered during *H. pylori* infection in AGS cells. AGS cells were infected with 100 MOI of *H. pylori* strain 11638 for 3 hours. Duplicate samples were analysed by RNAseq. The GAGE tool in Bioconductor was used to perform pathway enrichment analysis on the files generated using Deseq. Pathview was used to map the GAGE results onto KEGG pathways.

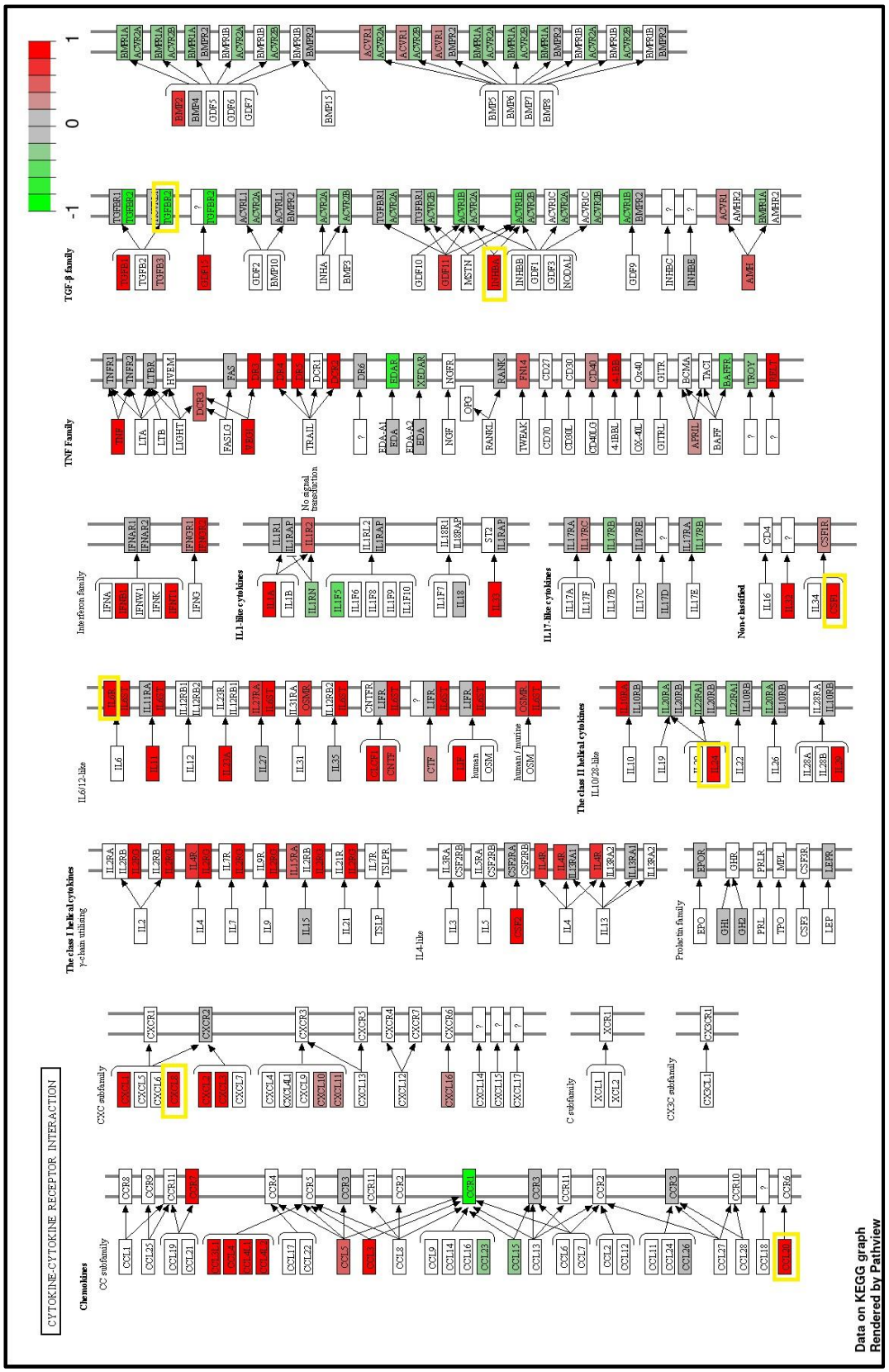

Figure 4.19 KEGG pathway for cytokine-cytokine receptor interaction.

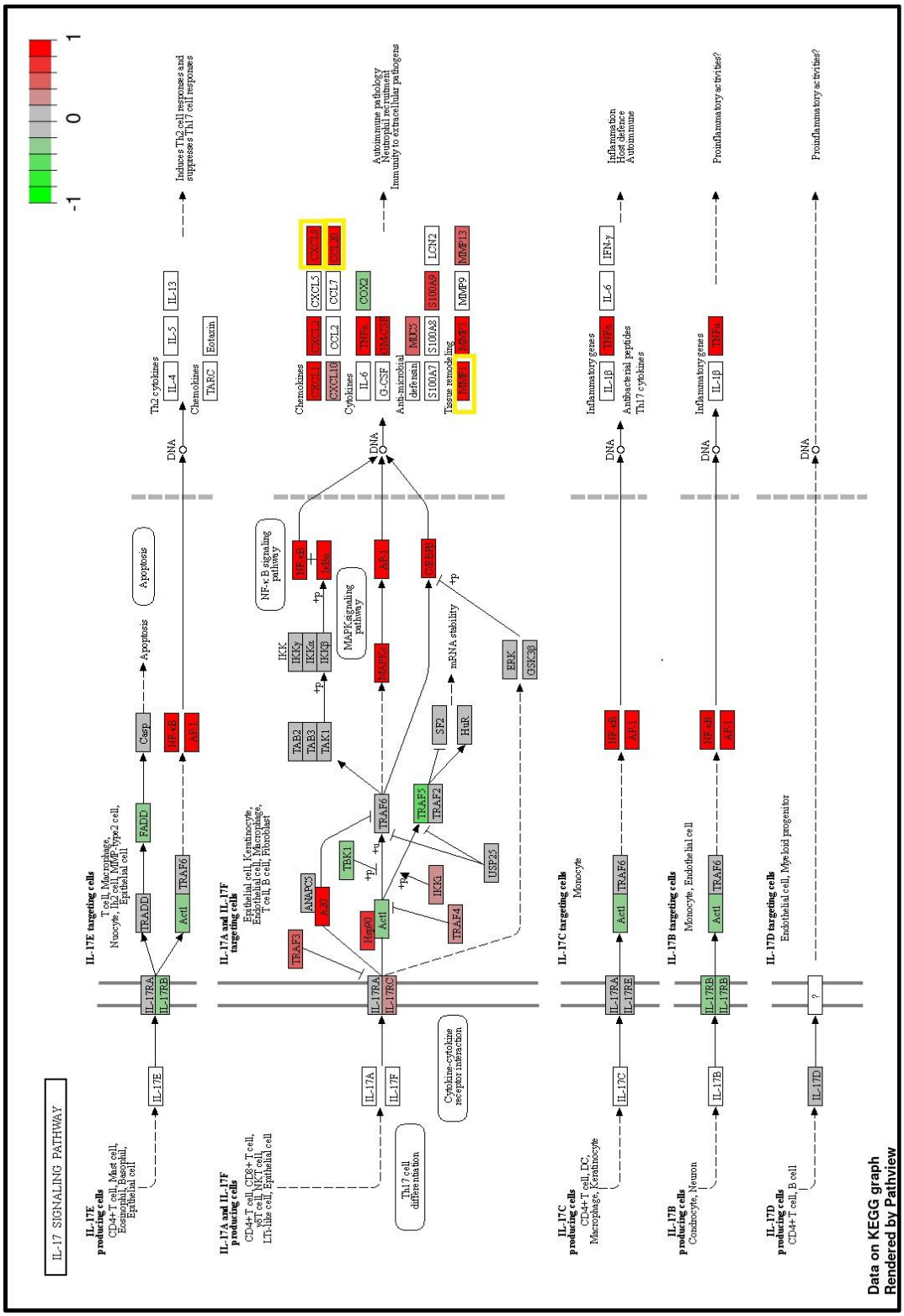

Figure 4.20 KEGG pathway for IL-17 signalling pathway.

4.5.4. RNAseq confirmed over-expression of HES1 in the HES1 plasmid-transfected cells.

To confirm over-expression in the *HES1* plasmid transfected cells, the level of *HES1* in each of the samples was measured by both RT-qPCR (

Figure 4.21.A) and by RNAseq (Figure 4.21.B). For the RNAseq analysis, quality control, mapping, alignment, and transcript quantification were performed by Eurofins. To identify differential gene expression, the gene counts calculated by Eurofins were analysed using Deseq2 package on the Galaxy Europe server (Love et al., 2014), (Afgan et al., 2018).

When measured with RT-qPCR, transfection with the *HES1* plasmid significantly upregulated *HES1* mRNA expression in the absence and presence of *H. pylori* compared to both the un-transfected samples and the samples transfected with the empty control plasmid (Figure 4.21.A). *H. pylori* infection led to the expected downregulation of *HES1* expression in the un-transfected (0.4-fold) and empty vector transfected (0.8-fold). When measured by RNAseq there was a similar expression pattern, with the *HES1* plasmid successfully upregulating expression of *HES1* (Figure 4.21B). Additionally, *H. pylori* infection led to a decrease in *HES1* expression in the un-transfected and control vector samples.

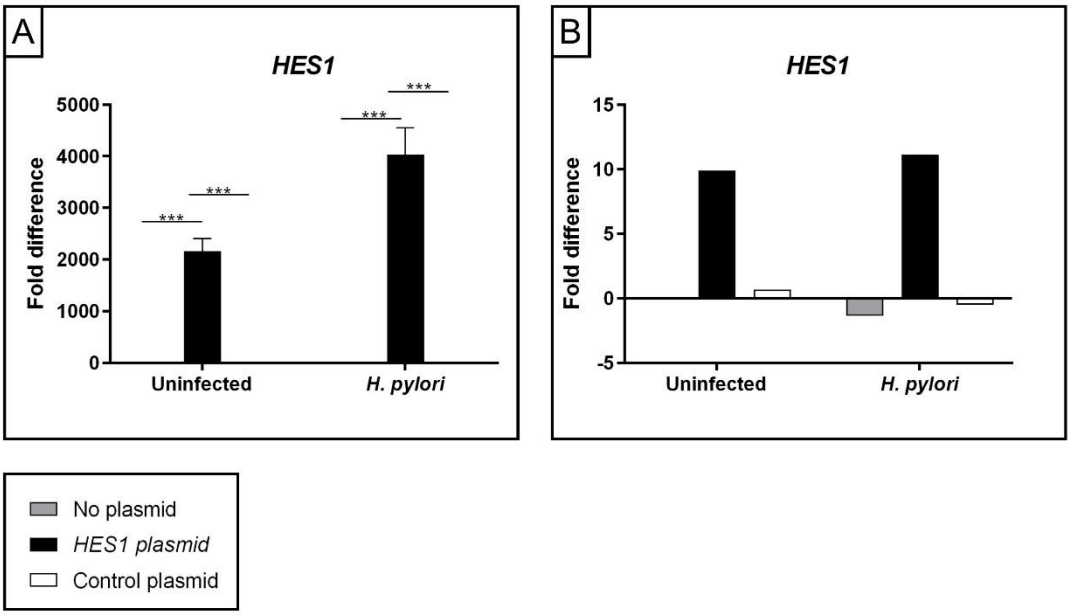

Figure 4.21 Expression of *HES1* in AGS cells transfected with HES1 plasmid. AGS cells were transfected with either pCMV6-HES1 (NM_005524) Human Tagged ORF Clone or with the empty control vector, pCMV6-AC-GFP. AGS cells were seeded at $4.5x10^5$ cells per well in a 6 well plate. The following day, 2.5 µg of DNA was transfected per well using Lipofectamine LTX® Reagent. 18 hours later the cells were infected with *H. pylori* strain 11638 for 3-hours. Total RNA was isolated and changes in gene expression for *HES1* was evaluated by RT-qPCR (A) using the comparative cycle threshold method. Results were normalised to *GAPDH* levels and expressed relative to uninfected cells at each time point. A two-way Anova with Tukey's multiple comparisons compared No plasmid with *HES1* plasmid, No plasmid with Control plasmid and *HES1* plasmid with Control plasmid in the absence (uninfected) and presence of *H. pylori*. The level of *HES1* in the RNA was also measured by RNAseq (B). ** $P \leq 0.01$. RT-qPCR graphs are representative of three independent experiments. RNAseq graphs represent the average of duplicate samples.

4.5.5. Over-expression of HES1 in AGS cells led to changes in gene expression in uninfected cells.

1,467 genes were up-regulated and 1,329 were downregulated in empty vector plasmid-transfected AGS cells compared to un-transfected cells, indicating that the transfection process itself alters gene expression (Figure 4.22). To control for the effects of plasmid transfection, gene expression in cells transfected with the HES1 plasmid was compared with the empty vector-transfected cells (Figure 4.23). This shows the genes with the significantly different expression in response to HES1 over-expression in AGS cells. Transfection with the HES1 plasmid compared to transfection with the empty vector identified 8 significantly upregulated genes (including *HES1*) and one significantly downregulated gene. Notably, overexpression of HES1 was associated with higher *FOS* and *CXCL8* expression (Table 4.4).

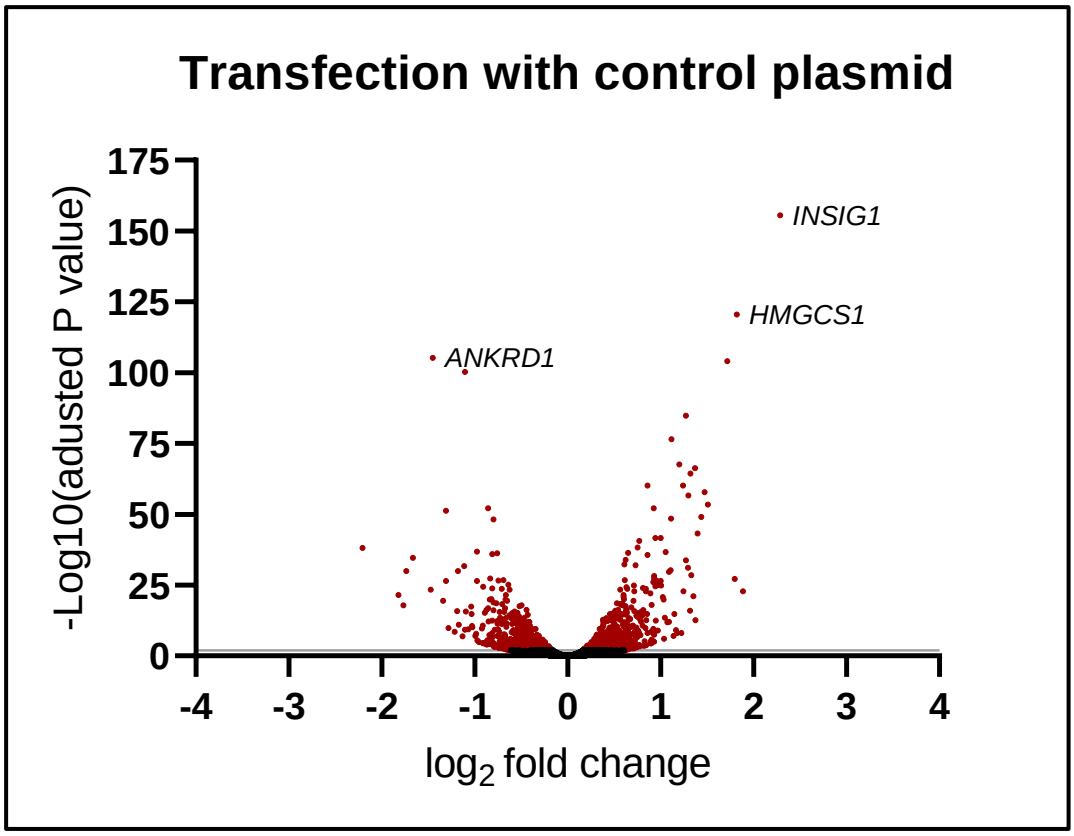

Figure 4.22 Volcano plot of differentially expressed genes in empty-vector transfected cells compared to uninfected cells. Each well of AGS cells was transfected with 2.5 µg of the empty plasmid, pCMV6-AC-GFP or left un-transfected. Duplicate samples were analysed by RNAseq. The gene lists from Deseq2 were ordered by highest $-\log_{10}$ adjusted P value and graphed against the corresponding $\log_2$ fold change. Genes that have an adjusted P value of <.001 (>2 $-\log_{10}$ of the adjusted P value) are marked as red dots on the plot. Genes that have an adjusted P value of >.001 (<2 $-\log_{10}$ of the adjusted P value) are marked as black dots on the graph. The three genes with the largest $-\log_{10}$(adjusted P value) are labelled on the graph.

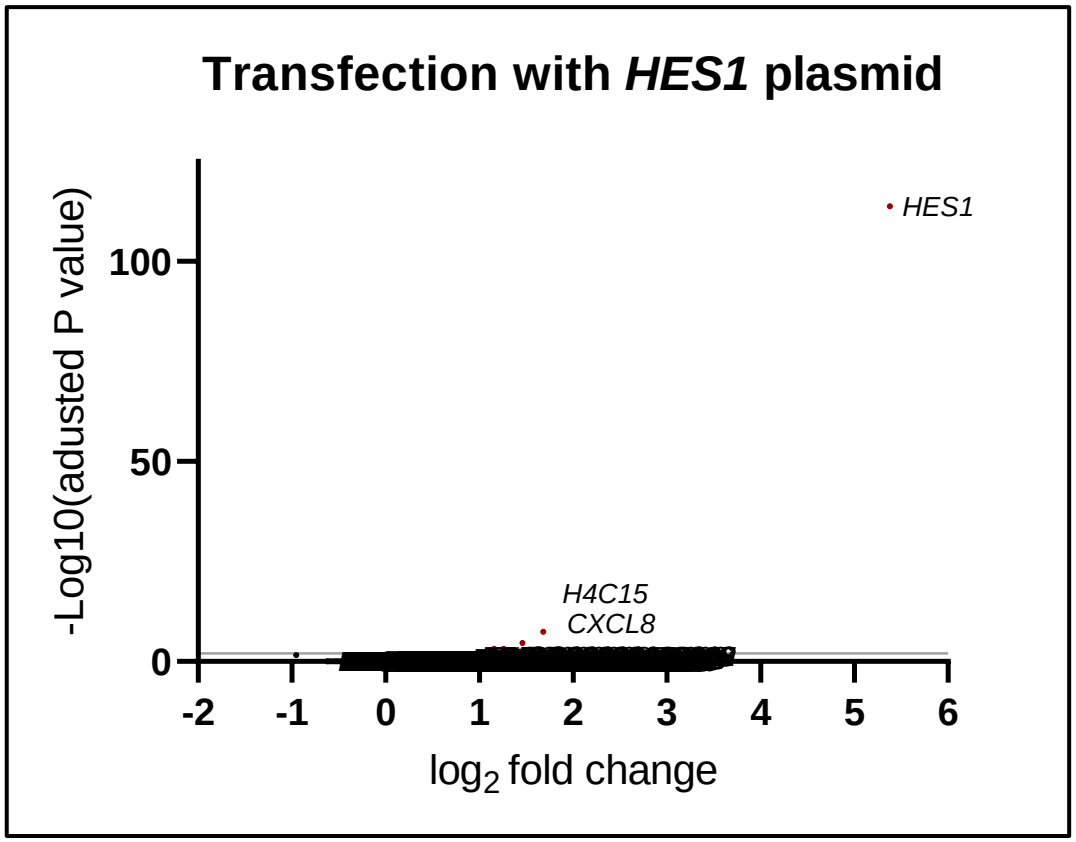

Figure 4.23 Volcano plot of differentially expressed genes in empty-vector transfected cells compared to HES plasmid transfect cells. Each well of AGS cells was transfected with 2.5 µg of the empty plasmid, pCMV6-AC-GFP or with pCMV6-HES1 (NM_005524) Human Tagged ORF Clone. Duplicate samples were analysed by RNAseq. The gene lists from Deseq2 were ordered by highest $-\log_{10}$ adjusted P value and graphed against the corresponding $\log_2$ fold change. Genes that have an adjusted P value of <.001 (>2 $-\log_{10}$ of the adjusted P value) are marked as red dots on the plot. Genes that have an adjusted P value of >.001 (<2 $-\log_{10}$ of the adjusted P value) are marked as black dots on the graph. The three genes with the largest $-\log_{10}$(adjusted P value) are labelled on the graph.

Gene ID	Log2 fold change	Gene name
ENSG00000114315	5.379853	*HES1*
ENSG00000270276	1.684039	*H4C15*
ENSG00000169429	1.458163	*CXCL8 (IL-8)*
ENSG00000173110	1.258732	*HSPA6*
ENSG00000170345	1.157304	*FOS*
ENSG00000253227	1.154508	*Novel transcript*
ENSG00000120738	1.116354	*EGR1*
ENSG00000189056	1.054642	*RELN*
ENSG00000288683	-0.95304	*PEX26-TUBA8*

Table 4.4 Genes with significant increase or decrease in expression in HES1 overexpressing cells compared to empty vector transfected cells. Each well of AGS cells was transfected with 2.5 µg of the empty plasmid, pCMV6-AC-GFP or HES1 plasmid. Duplicate samples were analysed by RNAseq. The gene lists from Deseq2 were filtered to exclude values with a P>.05 and were ordered by highest $\log_2$ fold change.

4.5.6. Genome wide changes in gene expression in *H. pylori* infected AGS cells due to increased HES1 expression.

Next, to identify the role HES1 plays during *H. pylori* infection, the HES1 overexpressing samples infected with *H. pylori* were compared to the empty plasmid transfected cells infected with *H. pylori*. In all 310 genes were significantly up-regulated and 452 genes were significantly down-regulated following HES1 over-expression in *H. pylori*-infected AGS cells compared to *H. pylori* infected control plasmid cells. The volcano plot is shown in Figure 4.24. The most significantly differentially expressed genes were members of the heat-shock protein family (*HSPA1A*, *HSPA1B* and *HSPA6*).

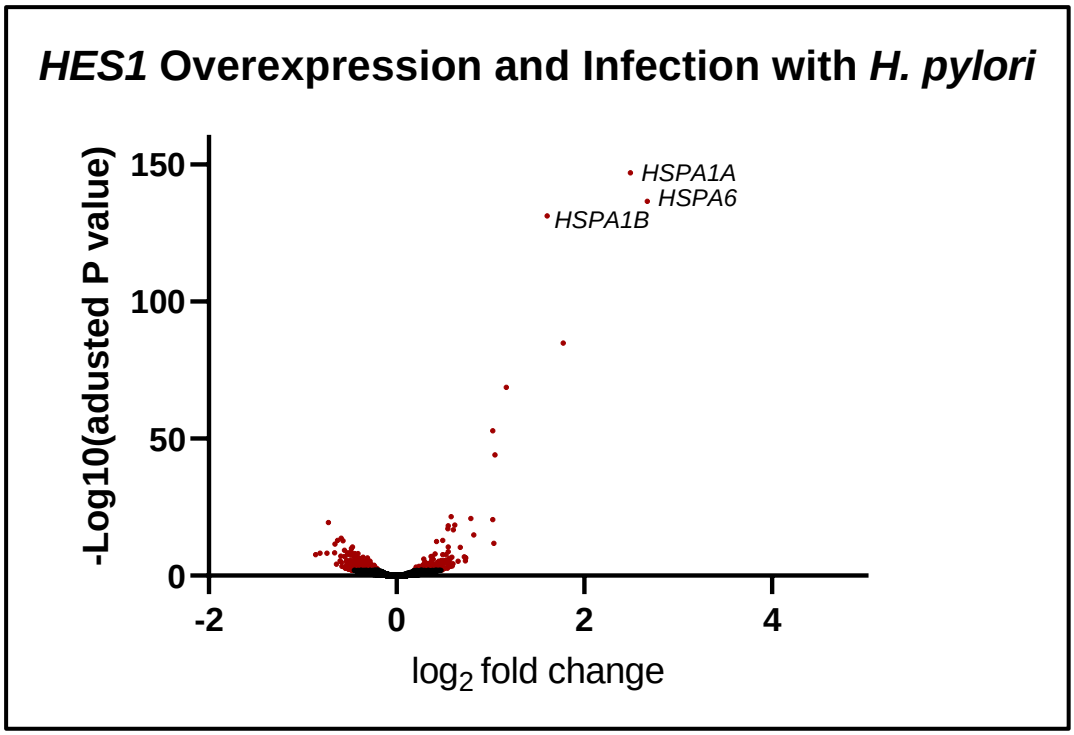

Figure 4.24 Volcano plot of differentially expressed genes in HES1 plasmid transfected cells infected with *H. pylori* compared to empty vector transfected cells infected cells. Each well of AGS cells was transfected with 2.5 µg of the empty plasmid, pCMV6-AC-GFP or HES1 plasmid. 18 hours following transfection the cells were infected with 100 MOI of *H. pylori* strain 11638 for 3 hours. Duplicate samples were analysed by RNAseq. The gene lists from Deseq2 were ordered by highest $-\log_{10}$ adjusted P value and graphed against the corresponding $\log_2$ fold change. Genes that have an adjusted P value of <.001 (>2 $-\log_{10}$ of the adjusted P value) are marked as red dots on the plot. Genes that have an adjusted P value of >.001 (<2 $-\log_{10}$ of the adjusted P value) are marked as black dots on the graph. The three genes with the largest $-\log_{10}$(adjusted P value) are labelled on the graph. Note: due to the large $\log_2$ fold change of HES1 (10.3-fold) it is not visible on the volcano plot.

The top 20 genes with the largest increase in expression in response to *H. pylori* in HES1-transfected compared to AGS control plasmid transfected cells are shown in Table 4.5. The top 20 genes with the largest decrease in expression in response to *H. pylori* in HES1-transfected compared to AGS control plasmid transfected cells are shown in Table 4.6. To visualise expression of these genes across all conditions, heat-maps of the genes presented in Table 4.5 and Table 4.6 were generated (Figure 4.25 and Figure 4.26 respectively).

Pathway analysis was performed on the *H. pylori* infected AGS HES1 overexpressing cells controlled against the empty vector transfected cells infected with *H. pylori*. While two pathways were shown to be enriched (ribosome and oxidative phosphorylation) neither were significant (p=.17 and p=.17 respectively).

Gene ID	Log2 fold change	Gene name
ENSG00000114315	10.79305	*HES1*
ENSG00000173110	2.66827	*HSPA6*
ENSG00000204389	2.489232	*HSPA1A*
ENSG00000170345	1.773725	*FOS*
ENSG00000204388	1.604495	*HSPA1B*
ENSG00000148677	1.169015	*ANKRD1*
ENSG00000120738	1.04546	*EGR1*
ENSG00000253227	1.036093	*Novel transcript*
ENSG00000118523	1.025262	*CCN2*
ENSG00000169429	1.022916	*CXCL8 (IL-8)*
ENSG00000119922	0.820146	*IFIT2*
ENSG00000125740	0.789123	*FOSB*
ENSG00000257524	0.736603	*SIAT7-F*
ENSG00000232133	0.732022	*IMPDH1P10*
ENSG00000189056	0.731192	*RELN*
ENSG00000162616	0.721847	*DNAJB4*
ENSG00000114019	0.676811	*AMOTL2*
ENSG00000115009	0.654156	*CCL20*
ENSG00000115963	0.620792	*RND3*
ENSG00000143322	0.603182	*ABL2*

Table 4.5 Top 20 genes with the largest increase in expression in *H. pylori* infected AGS HES1 overexpressing cells compared to empty vector transfected cells infected with *H. pylori*. AGS cells were infected with 100 MOI of *H. pylori* strain 11638 for 3 hours. Duplicate samples were analysed by RNAseq. The gene lists from Deseq2 were filtered to exclude values with a P>.05 and were ordered by highest $\log_2$ fold change.

Gene ID	Log2 fold change	Gene name
ENSG00000269955	-0.8618	*FMC1-LUC7L2*
ENSG00000213599	-0.81609	*SLX1A0SULT1A3*
ENSG00000165655	-0.74043	*ZNF503*
ENSG00000069399	-0.72741	*BCL3*
ENSG00000205420	-0.65959	*KRT6A*
ENSG00000183779	-0.65463	*ZNF703*
ENSG00000056558	-0.6416	*TRAF1*
ENSG00000100311	-0.62752	*PDGFB*
ENSG00000197261	-0.60085	*C6orf141*
ENSG00000125968	-0.59571	*ID1*
ENSG00000168209	-0.59153	*DDIT4*
ENSG00000135596	-0.58457	*MICAL1*
ENSG00000203896	-0.58395	*LIME1*
ENSG00000177426	-0.57118	*TGIF1*
ENSG00000168646	-0.55705	*AXIN2*
ENSG00000168264	-0.5557	*IRF2BP2*
ENSG00000286219	-0.54785	*NOTCH2NLC*
ENSG00000284969	-0.54168	*Q6FHM9*
ENSG00000095752	-0.54133	*IL11*
ENSG00000240053	-0.54128	*LY6G5B*

Table 4.6 Top 20 genes with the largest decrease in expression in *H. pylori* infected AGS HES1 overexpressing cells compared to empty vector transfected cells infected with *H. pylori*. AGS cells were infected with 100 MOI of *H. pylori* strain 11638 for 3 hours. Duplicate samples were analysed by RNAseq. The gene lists from Deseq2 were filtered to exclude values with a P>.05 and were ordered by lowest $\log_2$ fold change.

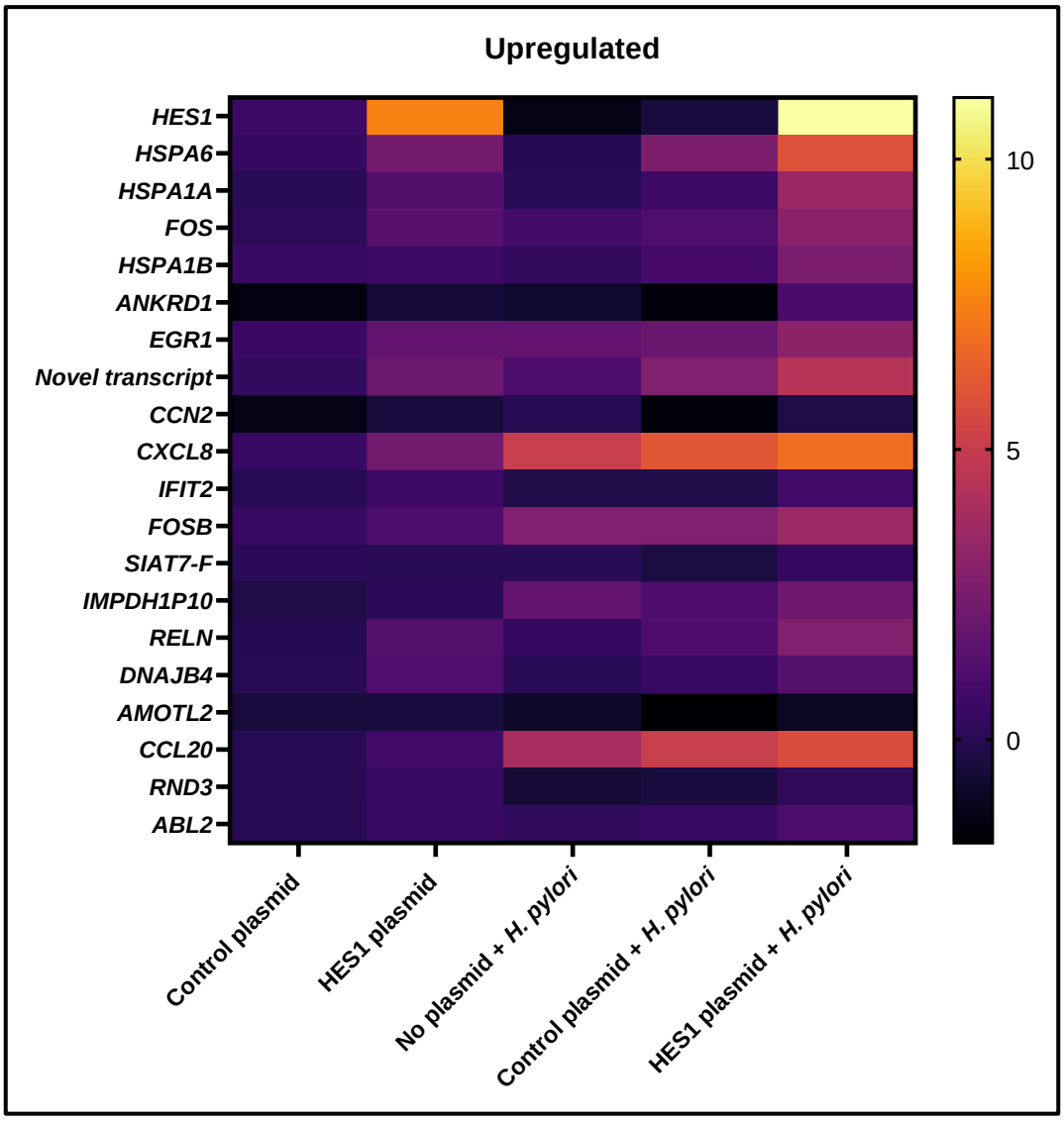

Figure 4.25 Heat map of the top 20 HES1 dependent *H. pylori* upregulated genes. The expression of the top 20 genes (Table 4.5) were calculated for all conditions by comparing each condition with the un-transfected, uninfected samples.

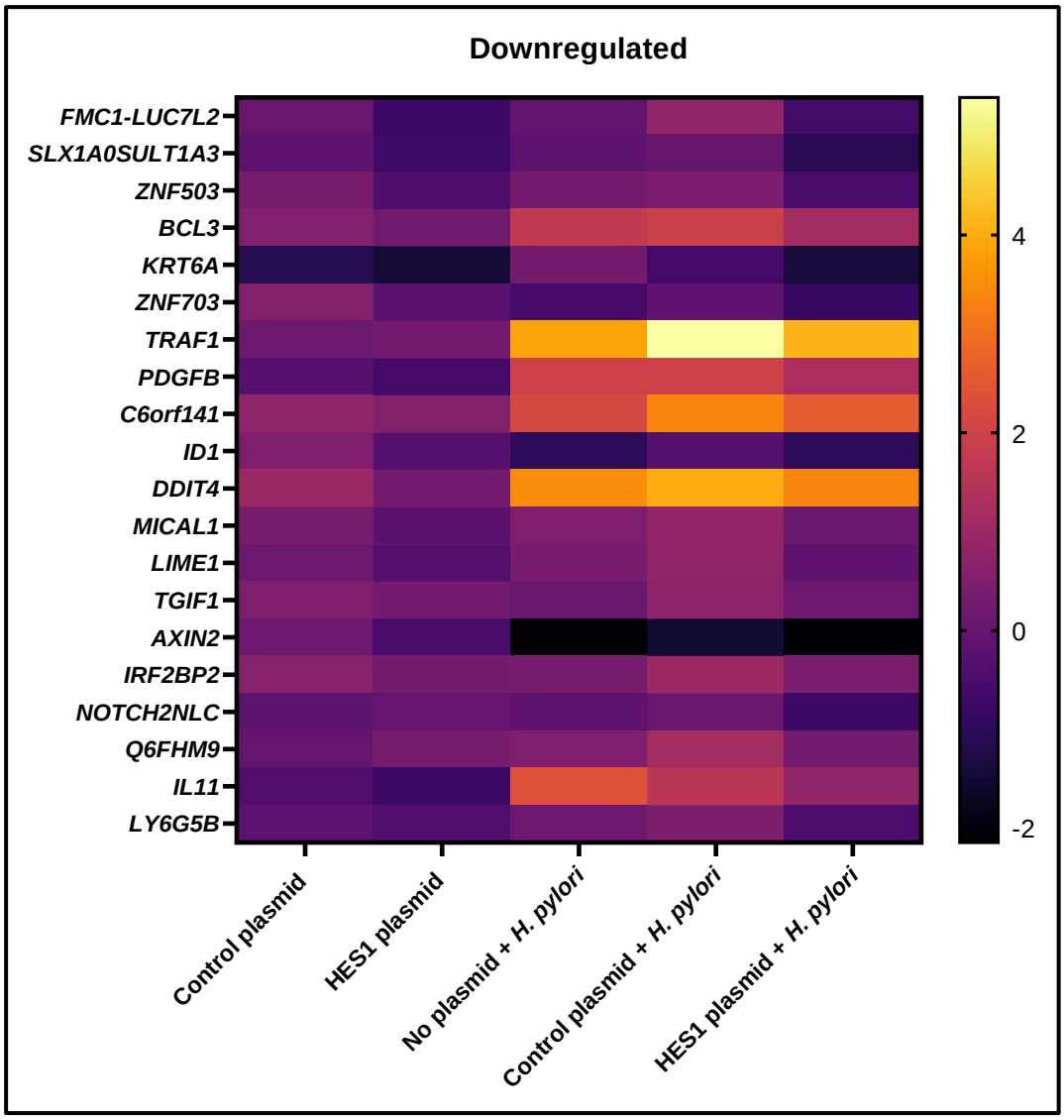

Figure 4.26 Heat map of the top 20 HES1 dependent *H. pylori* downregulated genes. The expression of the top 20 genes (Table 4.6) were calculated for all conditions by comparing each condition with the un-transfected, uninfected samples.

4.5.7. HES1 selectively enhanced cytokine induction in AGS cells in response to *H. pylori.*

Some genes that were regulated by *H. pylori* in HES1-overexpressing cells were chosen for validation by RT-qPCR. Firstly, *IL-8* and *CCL20* were chosen for validation as they were identified in Table 4.15 as exhibiting increased expression in HES1-overexpressing cells in response to *H. pylori* compared to *H. pylori* infected control vector-transfected cells. *IL-8* was significantly augmented in *H. pylori* infected cells over-expressing *HES1* (224-fold) compared to un-transfected (91-fold, $p<.001$) or control vector transfected cells (105-fold, $p<.001$) (Figure 4.27.A.B). Infection with *H. pylori* led to upregulation of *CCL20* expression. Transfection with the HES1 plasmid following infection with *H. pylori* led to increased expression of *CCL20* (226-fold). This was significantly higher than its expression in un-transfected cells or empty vector transfected cells (104-fold $p<.001$ and 159-fold $p=.001$ respectively) (Figure 4.27.C.D). In contrast, *H. pylori* did not significantly increase *CXCL1* expression in *HES1* over-expressing cells (6-fold) compared to un-transfected (4-fold) and control vector transfected cells (7-fold) (Figure 4.27.E.F). Similarly, HES1 over-expression did not change *H. pylori*-mediated TNF induction (data not shown). Taken together, these findings show that increased HES1 expression selectively enhanced the *H. pylori*-mediated induction of *IL-8* and *CCL20*, implying that the downregulation of HES1 by *H. pylori* observed in AGS under un-transfected conditions restrains induction of these 2 cytokines. This suggests that *H. pylori* mediated *HES1* downregulation may be preventing maximum increases in *CCL20* and *IL-8,* but not *CXCL1* or *TNF* expression.

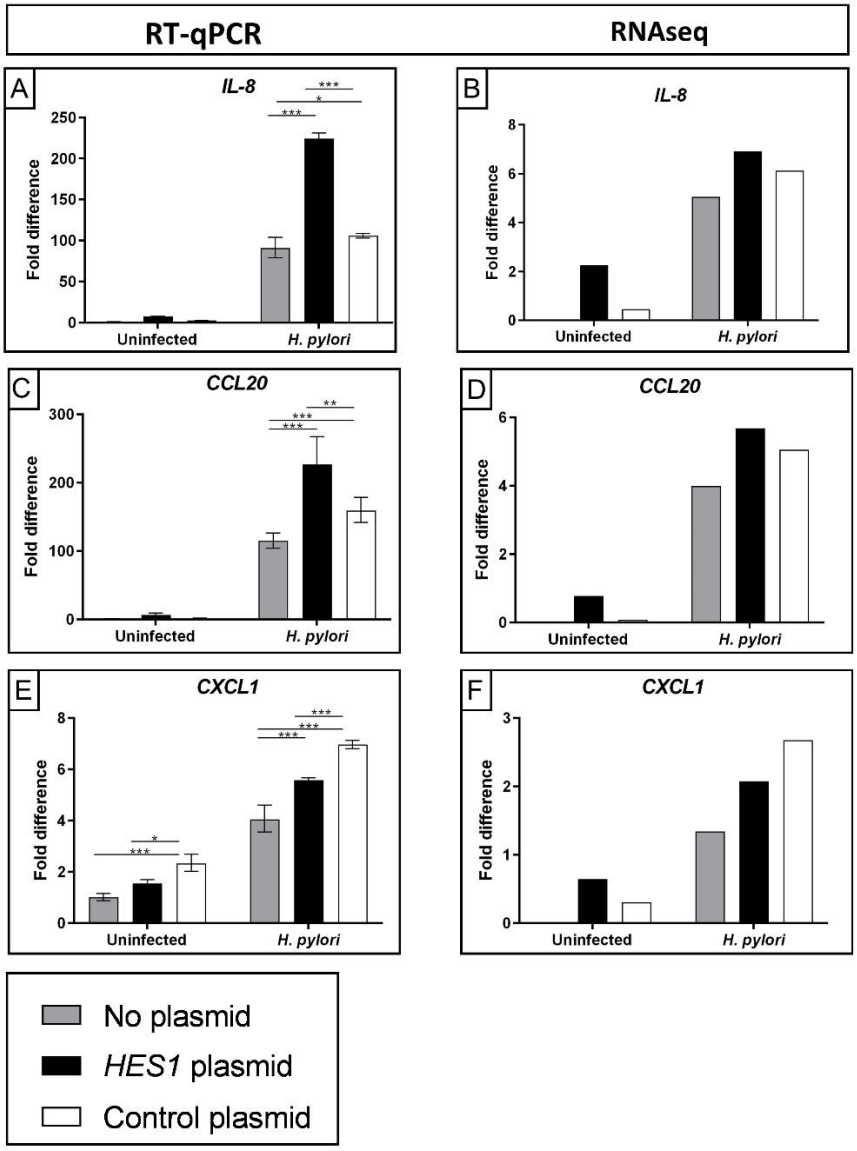

Figure 4.27 Selective enhancement of *H. pylori* mediated cytokine expression in *HES1* overexpressing cells. AGS cells were transfected with either pCMV6-HES1 (NM_005524) Human Tagged ORF Clone or with the empty control vector, pCMV6-AC-GFP. AGS cells were seeded at $4.5x10^5$ cells per well in a 6 well plate. The following day, 2.5 µg of DNA was transfected per well using Lipofectamine LTX® Reagent. 18 hours later the cells were infected with *H. pylori* strain 11638 for 3-hours. Total RNA was isolated and changes in Gene expression for *IL-8* (A), *CCL20* (C) and *CXCL1* (E) were evaluated by RT-qPCR using the comparative cycle threshold method. Results were normalised to *GAPDH* levels and expressed relative to uninfected cells at each time point. Two-way Anova tests with Tukey's multiple comparisons were used to calculate difference between No plasmid with *HES1* plasmid, No plasmid with Control plasmid and *HES1* plasmid with Control plasmid in the absence (uninfected) and presence of *H. pylori*. The levels of *IL-8* (B), *CCL20* (D) and *CXCL1* (F) in the RNA were also measured by RNAseq (Eurofins). $P \leq 0.05$, ** $P \leq 0.01$, *** $P \leq 0.001$. RT-qPCR graphs are representative of three independent experiments. RNAseq graphs represent the average of duplicate samples.

4.5.8. RNAseq identified additional genes that HES1 modified during *H. pylori* infection.

Additional genes were chosen for follow-up validation by RT-qPCR. Overall, the patterns observed when expression was measured by RT-qPCR corresponded to the measurements by RNAseq. TRAF1 is a signalling adapter that is part of the TNF receptor superfamily (Edilova et al., 2018). Infection with *H. pylori* led to upregulation of *TRAF1. TRAF1* was chosen to be validated by PCR because it was identified in Table 4.1 as being in the top 20 most upregulated genes following *H. pylori* infection. Additionally, *TRAF1* was found to be in the top 20 list of genes with decreased expression in *H. pylori* infected HES1 overexpressing cells compared to empty vector transfected cells infected with *H. pylori* (Table 4.6). However, transfection with the empty control vector led to the highest increase in *TRAF1* which would indicate *HES1* is not involved in *TRAF1* regulation during *H. pylori* infection (Figure 4.28.A.B).

The leucine zipper protein, FOS, can dimerise with Jun to form the activator protein 1 complex (AP-1) which acts as a transcription factor and can regulate cell processes including cell cycle, apoptosis and differentiation (Szalóki et al., 2015). Infection with *H. pylori* led to upregulation of *FOS* expression. FOS was chosen to be validated because it was also found to be in the list of genes with significant increase in expression in HES1 overexpressing cells compared to empty vector transfected cells (Table 4.4) and in the list of genes with the largest increase in expression in *H. pylori* infected HES1 overexpressing cells compared to empty vector transfected cells infected with *H. pylori* (Table 4.5). Transfection with the HES1 plasmid led to expression of *FOS* that was significantly higher than un-transfected cells or empty vector transfected cells (Figure 4.28.C,D). This would suggest that the *H. pylori* mediated HES1 decrease under normal conditions may be restraining increases in *FOS* expression.

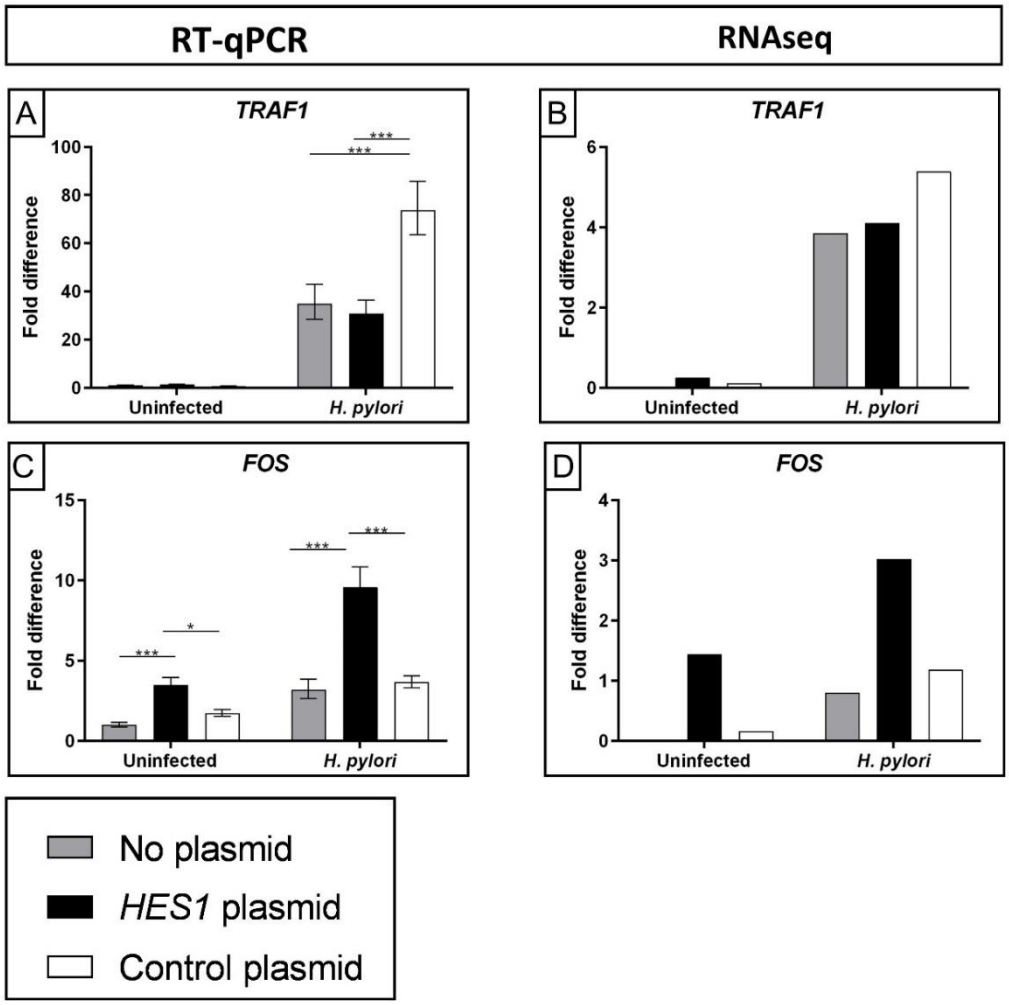

Figure 4.28 Hes1 over-expression enhanced *H. pylori*-mediated induction of *FOS* in AGS cells *H.* AGS cells were transfected with either pCMV6-HES1 (NM_005524) Human Tagged ORF Clone or with the empty control vector, pCMV6-AC-GFP. AGS cells were seeded at $4.5x10^5$ cells per well in a 6 well plate. The following day, 2.5 µg of DNA was transfected per well using Lipofectamine LTX® Reagent. 18 hours later the cells were infected with *H. pylori* strain 11638 for 3-hours. Total RNA was isolated and changes in Gene expression for *TRAF1* (A) and *FOS* (C) were evaluated by RT-qPCR using the comparative cycle threshold method. Results were normalised to *GAPDH* levels and expressed relative to uninfected cells at each time point. Two-way Anova tests with Tukey's multiple comparisons were used to calculate difference between No plasmid with *HES1* plasmid, No plasmid with Control plasmid and *HES1* plasmid with Control plasmid in the absence (uninfected) and presence of *H. pylori*. The levels of *TRAF1* (B) and *FOS* (D) in the RNA was also measured by RNAseq (Eurofins). $P \leq 0.05$, ** $P \leq 0.01$, *** $P \leq 0.001$. RT-qPCR graphs are representative of three independent experiments. RNAseq graphs represent the average of duplicate samples.

SOX9 is an important protein involved in the development of many organs (Preiss et al., 2001). *SOX9* expression has been previously shown to be upregulated in mice infected with PMSS1 strain of *H. pylori* (Serizawa et al., 2016). While SOX9 was not in the top 20 HES1 dependent *H. pylori* downregulated genes it was chosen to be validated because SOX9 is known to be a target of the Notch signalling pathway (Seymour et al., 2007), (Misiorek et al., 2021) and it was significantly downregulated in expression in *H. pylori* infected AGS HES1 overexpressing cells compared to empty vector transfected cells infected with *H. pylori* (p=1x10^{-10}). Overexpression of HES1 led to reduction in *SOX9* expression, suggesting that HES1 acts as a repressor of *SOX9* expression in AGS cells. *H. pylori* infection also led to a decrease in *SOX9* expression (Figure 4.29.A.B). However, the level of *H. pylori*-mediated SOX9 inhibition was not greater in the HES1 overexpressing cells than in the un-transfected infected cells, making it difficult to define a role for HES1 in the *H. pylori*-mediated regulation of *SOX9*.

SLX1A-SULT1A3 is a gene that encodes a long non-coding RNA (He et al., 2018). SLX1A-SULT1A3 was chosen to be validated because it was found in the list of genes with the largest decrease in expression in *H. pylori* infected HES1 overexpressing cells compared to empty vector transfected cells infected with *H. pylori* (Table 4.6). Overexpression of *HES1* in the presence and absence of *H. pylori* led to a significant reduction in expression compared to the un-transfected and control plasmid transfected samples (Figure 4.29.C.D). This suggests that *HES1* acts a repressor for *SLX1A-SULT1A3.*

RTL10 is involved in permeabilization of the mitochondrial membrane (Zhang et al., 2012a). RTL10 was chosen for validation because it was identified in Table 4.2 as being in the top 20 most downregulated genes following *H. pylori* infection. *H. pylori* infection reduced the expression of RTL10. However, un-transfected cells had a greater reduction in expression

compared to cells transfected with either the HES1 plasmid or the empty vector plasmid (Figure 4.29.E.F).

Taken together, these results show that *H. pylori* increases *TRAF1* and decreases *RTL10* expression in AGS cells. No clear role for HES1 in the *H. pylori*-mediated regulation of these genes was identified. Both *H. pylori* and HES1 could independently inhibit expression of *SOX9*. HES1 overexpression in AGS cells repressed *SLX1A-SULT1A3*. Finally, HES1 over-expression enhanced the *H. pylori*-mediated up-regulation of FOS, implying that the *H. pylori*-mediated down-regulation of HES1 under normal conditions restrains optimal FOS induction.

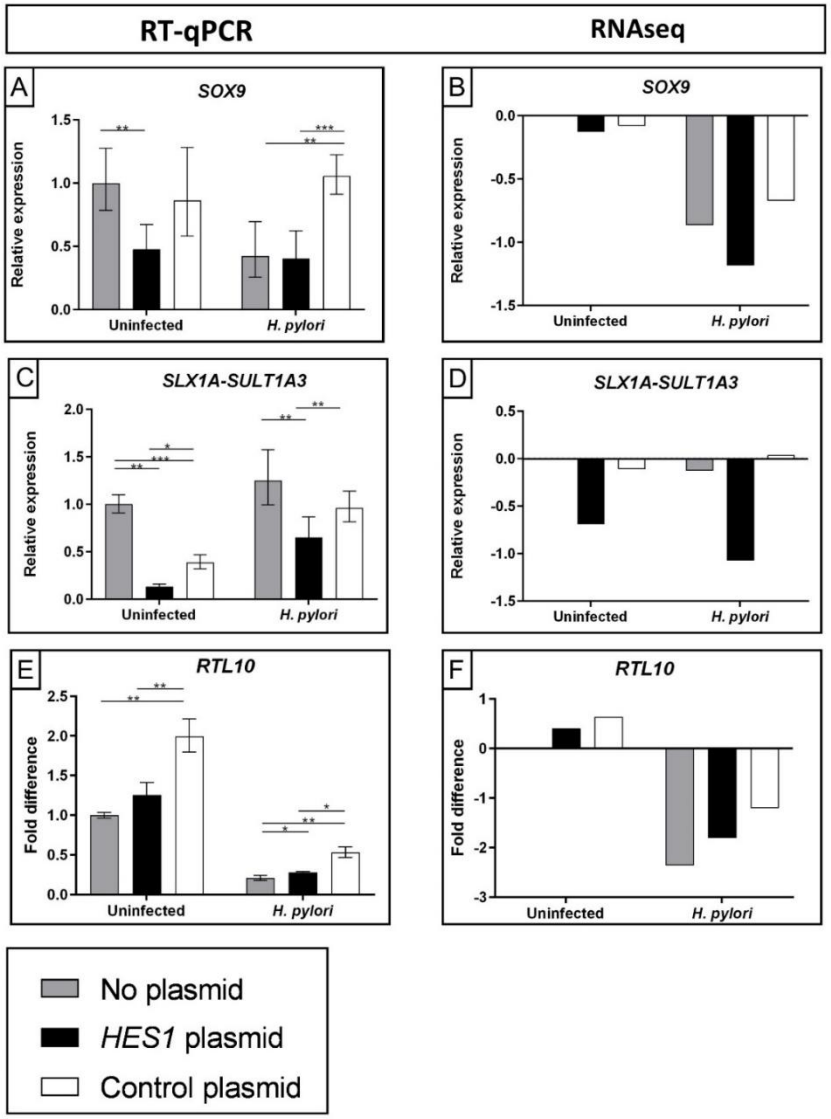

Figure 4.29 Validation of *H. pylori* downregulated genes in *HES1* overexpressing cells. AGS cells were transfected with either pCMV6-HES1 (NM_005524) Human Tagged ORF Clone or with the empty control vector, pCMV6-AC-GFP. AGS cells were seeded at $4.5x10^5$ cells per well in a 6 well plate. The following day, 2.5 µg of DNA was transfected per well using Lipofectamine LTX® Reagent. 18 hours later the cells were infected with *H. pylori* strain 11638 for 3-hours. Total RNA was isolated and changes in Gene expression for *SOX9* (A), *SLX1A-SULT1A3* (C) and *RTL10* (E) were evaluated by RT-qPCR using the comparative cycle threshold method. Results were normalised to *GAPDH* levels and expressed relative to uninfected cells at each time point. Two-way Anova tests with Tukey's multiple comparisons were used to calculate difference between No plasmid with *HES1* plasmid, No plasmid with Control plasmid and *HES1* plasmid with Control plasmid in the absence (uninfected) and presence of *H. pylori*. The levels of *SOX9* (B), *SLX1A-SULT1A3* (D) and *RTL10* (F) in the RNA was also measured by RNAseq (Eurofins). P≤0.05, ** P≤0.01, *** P≤0.001. RT-qPCR graphs are representative of three independent experiments. RNAseq graphs represent the average of duplicate samples.

4.6. *H. pylori* Infection Alters the Expression of Notch Pathway Components in Macrophages

4.6.1. Heat killed and live *H. pylori* alter the expression of *JAG1*, *DLL4* and *HEY1* in macrophages.

To identify if *H. pylori* could also mediate changes in Notch pathway expression in macrophage cells, THP-1 cells were infected with *H. pylori* or treated with heat killed *H. pylori*. All Notch receptors, ligands and associated transcription factors were measured by RT-qPCR (not shown). Across multiple experiments the genes that were consistently and significantly altered were the Notch ligands *JAG1* and *DLL4* and the Notch associated transcription factor *HEY1*, the results of which are described below. As a control for infection, significant increases in *IL-8* and *CXCL1* mRNA were observed at every time point for both heat killed and live *H. pylori* (Figure 4.30.A.B).

Regarding the Notch ligands, there were significant increases in *JAG1* seen at earlier time points with both heat killed and live bacteria (Figure 4.30.C). At 3-hours, expression of *JAG1* was increased to 1.5-fold (p=.01) in *H. pylori* infected cells and 2.2-fold (p<.001) in heat killed treated cells. However, by 24 and 48-hours, infection with live bacteria was associated with a decrease in *JAG1* expression (0.2-fold p<.001 and 0.3-fold p<.001, respectively). There is a particularly stark difference in the impact of live and heat killed *H. pylori* observed at these later time points (p=.005 and p<.001 respectively). This suggests that *H. pylori* infection leads to a transient increase in *JAG1* expression.

Both heat killed and live *H. pylori* significantly increased the expression of *DLL4* at 3- and 6-hour time points (Figure 4.30.D). Large fold differences were seen at 6-hours (549-fold, p<.001 for heat killed and 545-fold, p<.001

for live bacteria). At the 3-hour time point heat killed bacteria resulted in significantly higher *DLL4* expression compared to live bacteria ($p<.001$).

Both heat killed and live *H. pylori* also significantly increased the expression of the Notch associated transcription factor *HEY1* (Figure 4.30.E). The largest fold difference increases were seen at 3 and 6-hours (21-fold, and 17-fold for heat killed, 16-fold and 22-fold for live bacteria respectively).

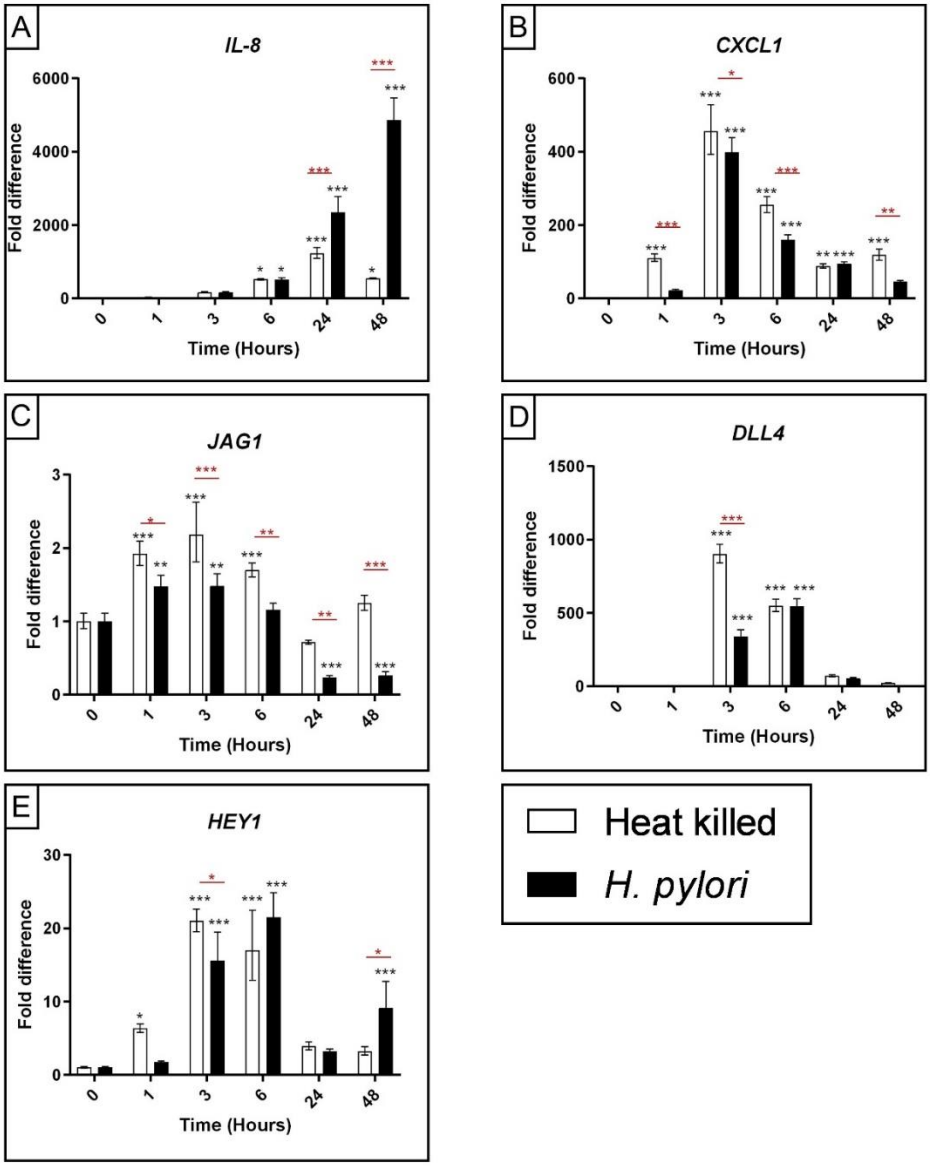

Figure 4.30 Expression of Notch pathway components in THP-1 cells treated with heat killed or infected with live *H. pylori*. THP-1 cells were seeded at $0.7x10^6$ cells per well and differentiated to macrophages following standard procedure. The cells were either infected with live *H. pylori* or treated with heat killed *H. pylori*. RNA was collected at 1, 3, 6, 24 and 48-hour intervals. The cells were infected with 100 MOI of 11638 strain of *H. pylori* or the equivalent number of heat killed *H. pylori* for the time points indicated underneath the graphs. Total RNA was isolated and changes in *IL-8* (A), *CXCL1* (B), *JAG1* (C), *DLL4* (D) and *HEY1* (E) gene expression was evaluated by RT-qPCR using the comparative cycle threshold method. Results were normalised to *GAPDH* levels and expressed relative to uninfected cells at each time point. Data shown are means ± SD. A two-way Anova was performed for each gene. Šidák multiple comparison tests were used to compare mean values of treated samples with untreated samples (black asterisk) and to compare mean values between live and heat-killed samples (red asterisk). * P≤0.05, ** P≤0.01, *** P≤0.001. Graphs are representative of three independent experiments.

4.6.2. New protein synthesis is required for *H. pylori* mediated induction of *DLL4* in THP-1 macrophages, but not for *JAG1* and *HEY1* induction.

To see the impact of blocking protein translation in the presence of *H. pylori*, THP-1 cells were treated for 1 hour with 20 μg/ml of the protein synthesis inhibitor cycloheximide and infected with *H. pylori.*

As a control for infection, *H. pylori* led to significant increase in *IL-8* and *CXCL1* expression (Figure 4.31.A,B). Cycloheximide treatment alone significantly increased the expression of *IL-8* at the 6-hour time point. Cycloheximide combined with *H. pylori* infection led to significant increases in expression of *IL-8* compared to either of these conditions alone at 3 and 6-hours. Cycloheximide combined with *H. pylori* infection led to significant increases in expression of *CXCL1* compared to either of these conditions alone at 6-hours (Figure 4.31.A,B).

Cycloheximide treatment significantly increased expression of *JAG1* at 3- and 6-hour time points. At 6 hours, combined *H. pylori* and cycloheximide led to significantly increased *JAG1* expression compared to *H. pylori* ($p<.001$) and cycloheximide ($p<.001$) alone (Figure 4.31.C). This indicates that new protein synthesis is not required for the *H. pylori*-mediated increase in *JAG1* mRNA expression.

H. pylori infection alone led to significantly increased *DLL4* expression at 3 and 6-hours (3-fold, $p<.001$ and 83-fold $p<.001$ respectively) (Figure 4.31.D). Treatment with cycloheximide significantly reduced *H. pylori* mediated *DLL4* upregulation at 3 and 6-hours ($p=.001$ and $p<.001$ respectively). Since blocking protein synthesis blocks *H. pylori* mediated upregulation of *DLL4* this would suggest that *H. pylori* induces a protein that upregulated *DLL4* expression.

H. pylori led to significantly increased *HEY1* expression at 3 and 6-hours (4.8-fold, $p<.001$ and 4.4-fold $p<.001$ respectively). Cycloheximide treatment significantly increased expression of *HEY1* at 3- and 6-hour time points. At the 6-hour time point, combined *H. pylori* and cycloheximide led to significantly increased *HEY1* expression compared to *H. pylori* treatment alone ($p<.001$). This indicates that new protein synthesis is not required for the *H. pylori*-mediated increase in *HEY1* mRNA expression.

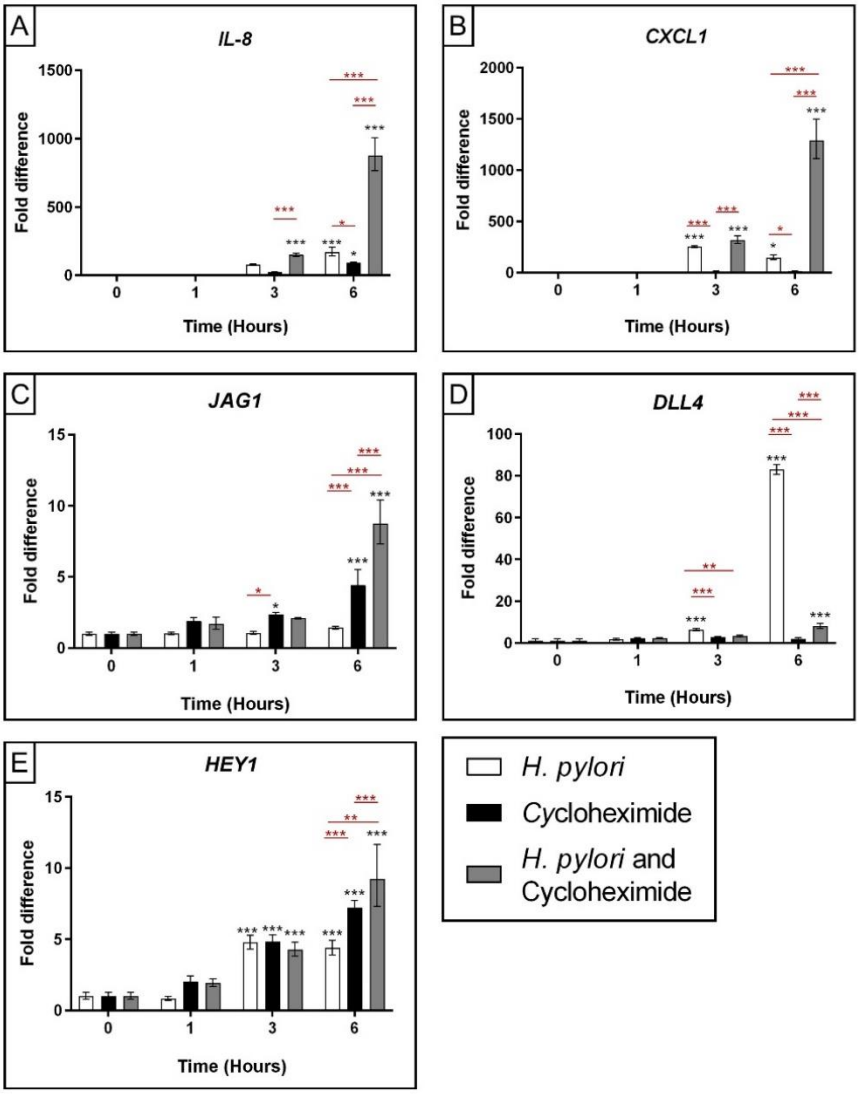

Figure 4.31 Expression of Notch pathway components in THP-1 cells treated with cycloheximide and infected with *H. pylori*. THP-1 cells were seeded at 0.75x10^6 cells per well and differentiated to macrophages following standard procedure. Subsequently, the cells were treated for 1 hour with 20 μg/ml of the protein synthesis inhibitor cycloheximide and infected with 100 MOI of *H. pylori* strain 11638 for the time points indicated underneath the graphs. Total RNA was isolated and changes in *IL-8* (A), *CXCL1* (B), *JAG1* (C), *DLL4* (D) and *HEY1* (E). Gene expression was evaluated by RT-qPCR using the comparative cycle threshold method. Results were normalised to *GAPDH* levels and expressed relative to uninfected cells at each time point. A two-way Anova was performed for each gene. Dunnett's multiple comparison test was used to compare mean values of each sample with the untreated sample (*H. pylori* 0-hour) (black asterisk). Tukey's multiple comparison test was used to compare mean values of each treatment to every other treatment at each time-point (red asterisk). P≤0.05, ** P≤0.01, *** P≤0.001. Graphs are representative of three independent experiments.

4.6.3. LPS can alter the expression *JAG1* and *DLL4* in macrophages.

To see if *H. pylori* LPS was sufficient to alter expression of Notch pathway components, THP-1 cells were treated with *H. pylori* LPS. *JAG1* and *DLL4* expression was measured by RT-qPCR. As a positive control THP-1 macrophages were treated with *E. coli* LPS which is known to trigger an innate immune response in macrophages.

Treatment with *E. coli* LPS led to significant upregulation of the cytokine *TNF* at 24-hours (Figure 4.32.A) Similar, to what was seen with live *H. pylori* infection in THP-1 cells; *H. pylori* LPS caused a significant increase in *IL-8* expression at all time points except 1-hour post treatment (Figure 4.32.B).

Significant increases in *JAG1* expression at 6-hours (2.2-fold, $p<.001$ respectively) were observed when treated with *E. coli* LPS (Figure 4.32.C). At 3-hours, significant increases in *JAG1* expression were observed following treatment with 100ng/ml and 1000ng/ml *H. pylori* LPS (2.1-fold $p=.004$ and 2.3-fold $p<.001$ respectively) (Figure 4.32.D).

Significant upregulation of *DLL4* was seen at 6 and 24-hour time points when infected with *E. coli* LPS (27.7-fold, $p<.001$ and 56-fold, $p<.001$ respectively) (Figure 4.32.E). Large increases in *DLL4* expression were observed with both concentrations of *H. pylori* LPS. The largest increase was observed at 3 hours with a fold difference of 111 for cells treated with 100ng/ml ($p<.001$) and a fold difference of 121 for cells treated with 1000ng/ml LPS, ($p<.001$) (Figure 4.32.F).

Overall, the pattern seen with *H. pylori* LPS shows a similar trend to what was seen with live, and heat killed *H. pylori.* These results indicate *H.*

pylori LPS plays a role in the *H. pylori*-mediated up-regulation of JAG1 and DLL4 in macrophages.

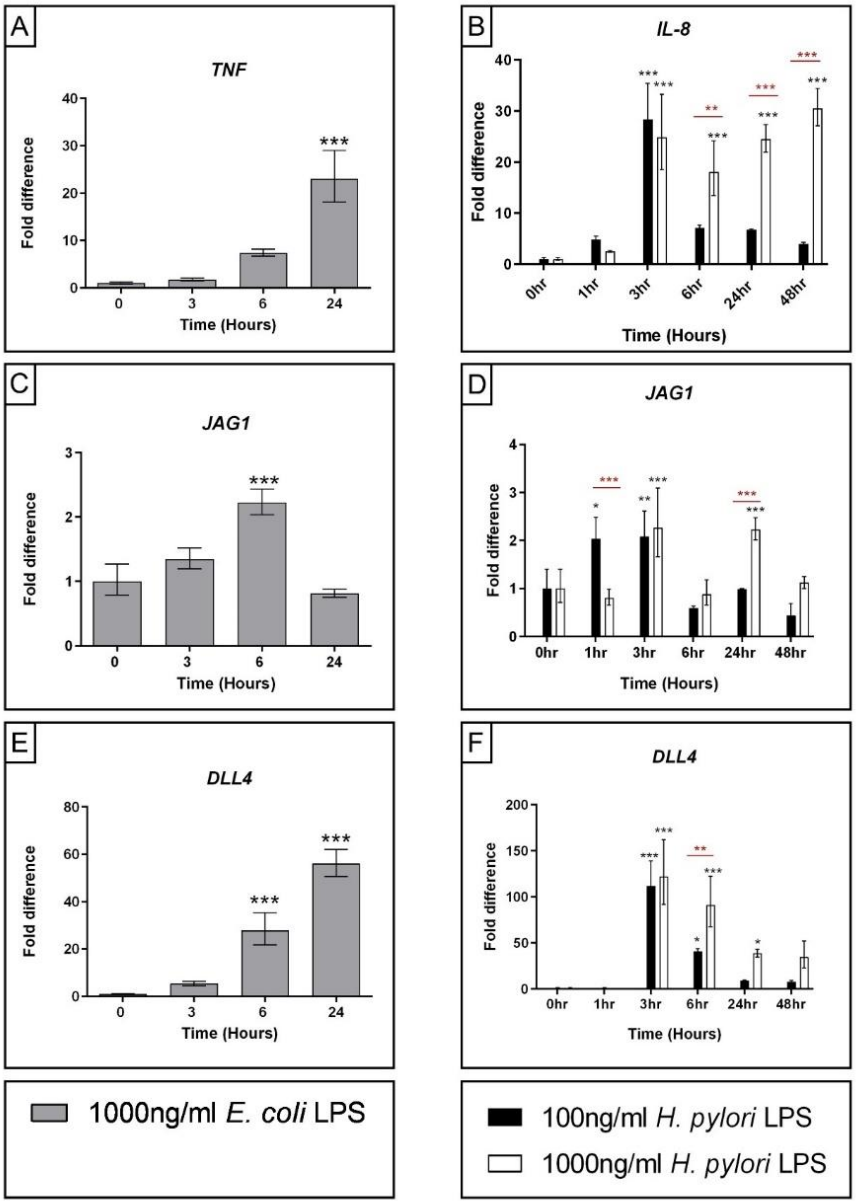

Figure 4.32 Expression of *JAG1* and *DLL4* in THP-1 cells treated with *E. coli* and *H. pylori* LPS. THP-1 cells were differentiated to macrophages with 100nM PMA. Cells were treated with 1000ng/ml E. coli LPS (Alexis) or *H. pylori* LPS from the reference strain 17874 at a concentration of 100ng/ml or 1µg/ml. RNA was collected at intervals up to 48-hours following treatment. Total RNA was isolated and changes in TNF (A), *IL-8* (B), *JAG1* (C, D) and *DLL4* (E, F) gene expression was evaluated by RT-qPCR using the comparative cycle threshold method. Results were normalised to *GAPDH* levels and expressed relative to uninfected cells. Data shown are means ± SD. One-way Anova with Dunnett's multiple comparisons were performed on the *E. coli* LPS treated cells. Two-way Anova were performed for *H. pylori* LPS treated cells. Šidák multiple comparison tests were used to compare mean values of treated samples with untreated samples (black asterisk) and to compare mean values between concentrations of LPS (red asterisk). * P≤0.05, ** P≤0.01, *** P≤0.001. Graphs are representative of three independent experiments.

4.7. Discussion

4.7.1. *H. pylori* downregulates HES1 in the gastric epithelium.

Despite the high global prevalence of *H. pylori*, much of the mechanistic pathways behind *H. pylori* virulence remains elusive. There has recently been substantial evidence that infectious agents can utilise the Notch signalling pathway to achieve or heighten pathogenesis. Both bacterial and viral pathogens of disparate nature are perceived to be associated with Notch signalling (Castro et al., 2021).

Independently, both abnormal Notch signalling, and *H. pylori* infection have been classified as risk factors for developing gastric cancer (Katoh and Katoh, 2007b, Piazzi et al., 2011, Brzozowa et al., 2013, Du et al., 2014, Hsu et al., 2016a, Sun et al., 2011, Konishi et al., 2016, McColl, 2010, Hu et al., 2020). However, there has been limited research into the potential link between these two risk factors, in particular into the associated functional consequences. *H. pylori* interacts with cells in the gastric mucosa, resulting in activation of multiple innate immune signalling pathways, subsequent production of pro-inflammatory cytokines and immune cell recruitment (Outlioua et al., 2020). Additionally, Notch signalling has been shown to influence innate immune signalling and inflammation (Shang et al., 2016b). Moreover, a few studies have emerged suggesting *H. pylori* alters expression of Notch pathway components in gastric epithelial cells (Bradley. K., 2012), (Zhang et al., 2012b), (Liu et al., 2016). For these reasons it was hypothesised that the Notch signalling pathway and its associated transcription factor HES1 are involved in *H. pylori*-mediated pathogenesis.

In this study, *H. pylori* infection increased the expression of *JAG2*, *DLL3*, *RBP-J* and *HEY1* mRNA in AGS cells. Infection transiently increased expression of *JAG1*, *DLL1*, *DLL4* and *Notch 1-3* in AGS cells at early timepoints. However, expression of *JAG1*, *DLL1*, *DLL4* and *Notch 1-3* was significantly decreased at 24-hours. *HES1* was decreased in both AGS and MKN45 gastric epithelial cells infected with *H. pylori* and the HES1 protein was shown to be downregulated in *H. pylori* infected AGS cells. For the most part, live *H. pylori* was required for these effects.

Similar to our findings, previous research has shown that *H. pylori* infection in AGS cells led to increased expression of JAG2 when measured by flow cytometry (Bradley. K., 2012). Additional evidence that *H. pylori* infection alters the Notch signalling pathway comes from Liu et al; the mRNA expression levels of *Notch1* and *Notch2* were downregulated in GES-1 cells that were infected with *H. pylori* strain NCTC11637 (Liu et al., 2016). This is in line with the decrease in *Notch1-3* observed at 24 hours in AGS cells presented herein. The reduction in *Notch1* and *Notch2* observed by Liu et al. was associated with a reduction in active NICD1 and NICD2 and a reduction in the Notch target genes *HES5* and *HEY2*. Similar to our study using AGS cells, they also observed that expression of *DLL4* was increased and that *HES1* was decreased in *H. pylori*-infected GES-1 (Liu et al., 2016). Further evidence that *H. pylori* suppresses HES1 comes from Zhang et al., who demonstrated a downregulation of HES1 using in vitro experiments in which MKN28 cells were infected with the ATCC43579 strain of *H. pylori* (Zhang et al., 2012b).

It is interesting to note that the most sustained decreases in *H. pylori* infected epithelial cells were seen in the expression of *HES1*, which may suggest altered expression of Notch receptors and ligands is causing a cumulative decrease in Notch signalling or that HES1 is being influenced by a non-canonical pathway. HES1 is activated by both canonical (the Notch signalling pathway) and non-canonical pathways such as the hedgehog

pathway (Rani et al., 2016). It was also hypothesised that the *H. pylori* mediated downregulation of Notch signalling may be inhibiting T-cell activation and leading to an environment that favours disease progression (Castro et al., 2021), (Liu et al., 2016).

In this study, there was decreased expression of *JAG2*, *HES1* and *HEY1* in the gastric mucosa of *H. pylori*-infected compared to uninfected patients. Our data is the first that we are aware of that looks at expression of Notch pathway constituents in the gastric epithelium of *H. pylori*-infected patients. Contrary to the results found in our experiments, the Notch pathway has been shown to be upregulated in gastric cancer (Piazzi et al., 2011, Sun et al., 2011, Hsu et al., 2016b, Konishi et al., 2016).
DLL1 and HES1 were found to be significantly elevated in gastric tissue from gastric cancer patients compared to healthy controls (Piazzi et al., 2011). The expression of all four Notch receptor proteins was found to be significantly higher in gastric adenocarcinoma tissue compared to normal tissue (Hu et al., 2020). Additionally, higher expression of Notch receptors correlated with worse survival rates (Hu et al., 2020). High levels of Notch receptor expression was associated with increased infiltration of immune cells, particularly macrophages and CD4+ T cells (Hu et al., 2020).

Tissue-microarray-based immunohistochemical staining and western blotting have been used to show that the expression of Notch1 was increased in intestinal metaplasia and intestinal gastric carcinoma, but not chronic gastritis or diffuse gastric carcinoma tissue (Sun et al., 2011). Notch2 was significantly associated with both intestinal and diffuse gastric cancer (Sun et al., 2011). It is likely the differences between our results and those using gastric cancer tissue are due to the stage of pathology that is under investigation. The patients involved in our study all had chronic gastritis but did not present with later disease stages. For this reason, the individuals included in our study represent only a subset of all *H. pylori* infected patients. The role of the Notch pathway varies greatly depending on

environment, cellular context and interactions with other signalling pathways (Bray, 2016). In addition, the immune and inflammatory environments encountered in the gastric epithelium differ, depending on the stages of *H. pylori* pathogenesis (Rocha et al., 2019). As a result, downregulation of Notch pathway components may be a biomarker of early stage of infection or gastritis.

From the published literature and the combined biopsy and in vitro epithelial cell results presented in this study, HES1 is downregulated in the gastric epithelium following *H. pylori* infection. Thus, it was decided that HES1 would be followed up to determine what role it plays during *H. pylori* associated pathogenesis.

An attempt to identify the *H. pylori* component(s) that control HES1 downregulation found that CagA and VacA were not required for the *H. pylori*-mediated decrease in *HES1* mRNA in AGS cells. Any significance noted between wild type and isogenic mutant strains was not replicated in repeat experiments. Additionally, *H. pylori* LPS did not inhibit *HES1* in MKN45 gastric epithelial cells. It is possible that other virulence factors are involved in *HES1* inhibition or that several virulence factors have a combined effect. It is also possible the response is triggered by another bacterial component, such as peptidoglycan. Further research will be required to identify these component(s).

Experiments using cycloheximide showed that new protein synthesis is required for the *H. pylori* -mediated down-regulation of *HES1* mRNA expression in AGS gastric epithelial cells. HES1 negatively regulates its own expression by binding to its own promotor as a transcriptional repressor (Hirata et al., 2002). Previously it was shown that cycloheximide treatment leads to increased HES1 expression (Hirata et al., 2002). This observation concurs with the results of this thesis. Moreover, it was found that in the presence of cycloheximide, *H. pylori* no longer inhibited *HES1*

mRNA expression in AGS cells and at 3 and 6-hours combined *H. pylori* and cycloheximide led to significantly higher *HES1* expression than cycloheximide alone, indicating that de novo protein synthesis is required for *HES1* repression. These results suggest that another protein regulated by *H. pylori* is required for the *H. pylori*-mediated inhibition of *HES1*. Since RBP-J is involved in transcriptional repression of *HES1*, it is possible that the increased expression of *RBP-J* mRNA observed in Figure 4.3 and its subsequent translation into its functional protein is responsible for the decrease in *HES1* expression. To address this question, future work could be performed to investigate whether increased RBP-J is present at the *HES1* promoter region following *H. pylori* infection.

Taken together, this study builds on existing evidence that *H. pylori* down-regulates HES1 expression in gastric epithelial cells. To the best of our knowledge, this is the first study to demonstrate decreased *HES1* expression in the gastric mucosa of *H. pylori*-infected patients with chronic gastritis. Neither CagA or VacA are required for the *H. pylori*-mediated down-regulation of *HES1* and *H. pylori* LPS cannot suppress *HES1*. Finally, it is likely that another *H. pylori*-mediated protein is involved in the downregulation of *HES1* in gastric epithelial cells.

4.7.2. Evaluation of genome-wide responses to *H. pylori* by RNAseq with and without HES1 overexpression.

4.7.2.1. Global changes in gene expression in AGS cells in response to *H. pylori*.

While microarrays have been previously performed investigating *H. pylori* infection in AGS cells (Sepulveda et al., 2002), (Lim et al., 2003), (Shibata et al., 2005), (Wen et al., 2004), to the best of knowledge, this is the first RNAseq analysis on *H. pylori* infection in gastric epithelial cells. Importantly, there are several advantages of using RNAseq over microarray to analyse transcriptome expression. These include, microarray associated dye-based detection problems, as well as RNAseq having the ability to detect RNA splice sites and previously unmapped genes (Mortazavi et al., 2008).

A previous microarray study found that AGS cells infected with *H. pylori* strain TN2 from 1.5-12 hours found that the number of significantly upregulated genes reached its peak at 3-hours post infection (Shibata et al., 2005). 3-hours post-infection was the time-point used in this study. Several genes identified from our RNAseq study are consistent with the previous microarray analysis in gastric epithelial cells infected with *H. pylori*, such as *IL-8* and *CCL20* (You et al., 2010), (Maeda et al., 2001). Microarray on antral biopsies from 27 *H. pylori* infected patients and 15 uninfected controls found that chemokines and their receptors make up a large proportion of upregulated genes, with *CCL20* strongly upregulated (Hofman et al., 2007). MKN45 cells infected with *H. pylori* strain TN2 for 3 hours identified *IL-8* as the most upregulated genes which is consistent with our results (Maeda et al., 2001). Additionally, microarray analysis on 12 *H. pylori* positive and 9 negative antrum biopsies found that genes could be clustered together as signatures for *H. pylori* infection. In line with the

results presented herein, cytokine and cytokine receptors was recognised as one of the key groupings (Wen et al., 2004).

Another group of genes that have previously been associated with *H. pylori* infection are mucosal matrix metalloproteinase proteins (MMPs). Previous, microarray analysis on AGS cells infected with *H. pylori* strain 26695 and MKN1 cells infected with *H. pylori* strain OHPC0016 identified MMP proteins as being substantially elevated following infection with *H. pylori* (You et al., 2010), (Kitadai et al., 2003). Similarly, microarray analysis on *H. pylori* positive gastric tissue identified MMPs as being upregulated (Wen et al., 2004). We identified MMP1 and MMP25 in the list of the top 20 genes with the largest increase following *H. pylori* infection (Table 4.1). MMPs play an important role in degrading the basement membrane and extracellular matrix which can lead to tissue remodelling, cancer cell invasion and angiogenesis (Kitadai et al., 2003). MMPs play a role in tumour invasion and metastasis and expression of MMPs has been associated with poor prognosis in gastric cancer patients (Jiang et al., 2014), (Kitadai et al., 2003). MMP-1 has previously been shown to be involved in promoting invasion and metastasis during *H. pylori* infection (Jiang et al., 2014). The expression of MMP-1 was measured using immunohistochemistry in gastric cancer patients. *H. pylori* infection was correlated with MMP-1 expression. Furthermore, MGC-803 cells infected with *H. pylori* led to significant upregulation of MMP-1 (Jiang et al., 2014). AGS cells infected with *H. pylori* strain Tx30a, which lacks CagA induced MMP-1 expression, however infection with the CagA+ strain 147C increased MMP-1 expression further. This indicates that *H. pylori* can induce MMP-1 in CagA dependent and independent manners (Pillinger et al., 2007).

When AGS cells were infected with *H. pylori* the three genes with the largest -Log10(adjusted p value) were *KDM6B*, *PHLDA1* and *PLAUR* (Figure 4.18). The impact of *H. pylori* on *KDM6B* expression will be further explored in Chapter 5. *PHLDA1* is proposed to be involved in regulating

apoptosis (Zhao et al., 2015). Increased *PHLDA1* expression has been associated with *H. pylori* infection in macrophages (Koch et al., 2016). However, decreased *PHLDA1* expression was associated with poor prognosis in gastric cancer patients (Zhao et al., 2015). *PLAUR* is a urokinase-type plasminogen activator receptor and its upregulation is associated with cell invasion, metastasis, and angiogenesis (Sheh et al., 2011). Increased *PLAUR* expression was found in the corpus of *H. pylori* infected patients and in a mouse model of *H. pylori* infection (Kenny et al., 2008), (Alpízar-Alpízar et al., 2020). Additionally *PLAUR* expression was associated with poor prognosis in gastric cancer patients (Kaneko et al., 2003).

RNAseq also revealed previously uncharacterised roles for *H. pylori* in the upregulation of Interleukin 1 Receptor Associated Kinase 2 (IRAK2) and ADP Ribosylation Factor Like GTPase 14 (ARL14) in AGS cells (Table 4.1). The four member IRAK family of proteins are comprised of an amino-terminal death domain and a serine threonine kinase domain (Kawagoe et al., 2008). When TLRs bind to PAMPs, adapter proteins such as MyD88 are recruited. IRAK family members can bind to the death domain of MyD88; this means that IRAK family members play a role in mediating TLR signalling (Su et al., 2020). It has been shown that IRAK2 is involved in sustaining TLR activation, leading to the activation of NF-κB and to the expression of cytokines (Kawagoe et al., 2008). IRAK2 signalling has been shown to regulate expression of genes such as CXCL1, TNF-α and IL6 (Su et al., 2020). This result in relation to IRAK2 may indicate a further role for *H. pylori* in the modulation of TLR signalling to influence inflammatory cytokine expression.

ARL14 is a member of the ADP ribosylation factor (ARF) family of GTP-binding proteins, which recruit cytosolic effectors to the membrane (Zhang et al., 2021). ARL14 is involved in GTP binding and signal transduction and (Zhang et al., 2021). ARL14 was shown to be overexpressed in biopsy tissue from non-small cell lung cancer patients compared to normal tissue and

correlated with poor prognosis (Zhang et al., 2021). In bladder cancer hypermethylation of ARL14 was deemed a risk factor for worse prognosis (Wang et al., 2019). ARL14 was identified as a differentially expressed gene between lymphatic metastases and non-lymphatic metastases in gastric cancer (Zhang et al., 2019). Given the links between IRAK2 and TLR signalling and ARL14 and carcinogenesis, future research into the roles of these proteins in the context of *H. pylori* infection and pathogenesis is warranted.

Table 4.2 lists the genes identified by RNAseq with the largest decrease in expression following *H. pylori* infection. Interestingly, downregulation of *SOX2* was also observed. Meta-analysis has shown *SOX2* to be downregulated in gastric cancer tissue (Li et al., 2022b). SOX2 expression has also been shown to be downregulated in AGS cells infected with Tx30a (lacking cagA) and 26695 (contains cagA) strains of *H. pylori* (Camilo et al., 2012). *H. pylori* strain 43504 was also shown to decrease SOX2 expression in MKN45 cells (Asonuma et al., 2009). Most of the other genes on this list have not previously been linked to *H. pylori* infection, which opens up additional potential future research avenues. We demonstrated via RNAseq that *HOXB3* was downregulated 1.5-fold in AGS cells infected with *H. pylori*. While there has been no previous evidence that *H. pylori* decreases HOXB3 expression, it was shown that deletion of the locus 17q21.32, which contains the *HOXB3* gene, is associated with worse prognosis in gastric cancer patients (Tomioka et al., 2010). To the best of our knowledge, we are the first to identify the zinc finger proteins (ZNF) *ZNF792* and *ZNF420* downregulation as a result of *H. pylori* infection.

In summary, it was found by RNAseq analysis that *H. pylori* increased expression of *IL-8*, *CCL20* and *MMP1* and decreased expression of SOX2, which is in line with previous studies (Yoshida et al., 2009), (Crabtree et al., 1995), (Eftang et al., 2012), (Camilo et al., 2012). RNAseq analysis allowed further novel targets of *H. pylori* infection to be uncovered, such as IRAK2,

ARL14, HOXB3, ZNF792 and ZNF420 unveiling potential novel candidates for future investigation in *H. pylori* infection.

4.7.2.2. HES1 over-expression regulates gene expression in AGS cells.

Table 4.4 lists genes that were selectively altered by HES1 overexpression in the absence of *H. pylori*. Of these FOS and EGR1 have previously been associated with Notch signalling. FOS upregulation has been previously linked to Notch signalling in B cells (Iwahashi et al., 2012). EGR1 is a transcription factor that has previously shown to be upregulated by the Notch signalling pathway coactivator MAML1 (Hansson et al., 2012). However, to the best of our knowledge there has been no previously identified link between HES1 and H4C15, HSPA6, RELN or PEX26-TUBA8. These genes may be of interest for future research in the area of gene regulation by HES1.

4.7.2.3. HES1 over-expression enhances *H. pylori*-mediated-up-regulation of *FOS*, *IL-8* and *CCL20* in AGS cells.

RNAseq analysis followed by confirmatory RT-qPCR, revealed that over-expression of HES1 enhanced the *H. pylori*-mediated induction of the cytokines *IL-8* and *CCL20*. This effect was found to be selective, as HES1 over-expression did not affect the *H. pylori*-mediated induction of the cytokines *TNF* or *CXCL1*. Interestingly, HES1 has previously been shown to reduce CXCL1 expression in BMDMs (Shang et al., 2016a). We may not have seen this in AGS cells due to the different impact HES1 has in

different cell types (human stomach epithelial cells compared to murine macrophages). In future, over-expression of HES1 could be performed in THP-1 cells to identify if HES1 can alter *CXCL1* expression in human macrophages.

Notably, the *H. pylori*-mediated induction of *FOS* was also enhanced in AGS cells as a result of HES1 over-expression, as demonstrated by both RNAseq and RT-qPCR. FOS is a subunit of the AP-1 transcription factor (Hoffmann et al., 2002). AP-1 is involved in both IL-8 and CCL20 regulation (Wolf et al., 2001), (Li et al., 2017). Mutation of the AP-1 site within the *IL-8* promoter region reduced *IL-8* reporter gene activity in UM-SCC-9 cells (Ondrey et al., 1999). Similarly, mutation of the AP-1 site within the *CCL20* promoter region reduced *CCL20* reporter gene activity in HaCaT keratinocytes (Li et al., 2017). Taken together, these findings suggest that the *H. pylori*-mediated down-regulation of HES1 selectively restrains full *IL-8* and *CCL20* induction in response to *H. pylori*. Further studies are required to confirm whether this effect is due the restrained *FOS* induction that was caused by decreased HES1 expression in response to *H. pylori*. Moreover, as IL-8 and CCL20 recruit neutrophils and monocytes respectively, it would be interesting to investigate whether the *H. pylori*-mediated down-regulation of HES1 and associated restraint of *IL-8* and *CCL20* induction is associated with attenuated neutrophil and monocyte recruitment.

Three heat shock proteins (HSP); *HSPA1A*, *HSPA1B* and *HSPA6* were significantly upregulated when HES1 was overexpressed in the context of *H. pylori* infection. Future studies could investigate HES1 mediated relation of heat shock proteins in the context of *H. pylori* infection.

A limitation of the study was the inability to investigate the impact of HES1 on *H. pylori*-mediated gene regulation using a loss-of-function approach, either using HES1 RNAi or gamma secretase inhibition of Notch signalling.

Further studies using different siRNA molecules, gamma secretase inhibitors or CRISPR/Cas9-based approaches could possibly overcome this problem and strengthen the findings presented herein.

4.7.3. *H. pylori* infection led to upregulation of *JAG1*, *DLL4* and *HEY1* in macrophages.

Macrophages are leukocytes which arise from a common precursor in the bone marrow and play a role acting as phagocytes during the innate immune response (Kumar et al., 2018). These cells can produce oxidants, chemokines and cytokines that orchestrate the immune system by regulating and recruiting other immune cells (Trehanpati et al., 2012). *H. pylori* infection is known to trigger macrophage recruitment (Cherdantseva et al., 2014), (Hua-Xiang et al., 2004), (Kaparakis et al., 2008), (Quiding-Järbrink et al., 2010), (Whitney et al., 2000), (Suzuki et al., 2002).

In this study, it was demonstrated that *H. pylori* infection increases expression of the Notch ligands *JAG1* and *DLL4* in THP-1 macrophages. Expression of the Notch target gene *HEY1* was also increased in *H. pylori*-infected THP-1 macrophages. This suggests that *H. pylori* activates Notch signalling. During the course of this research, an over-lapping study was published on the regulation of Notch signalling in macrophages in response to *H. pylori* (Wen et al., 2021). In the study by Wen et. al., mouse macrophages (RAW264.7) were infected with the mouse adapted *H. pylori* strain (SS1). This led to increased mRNA expression of *Notch1*, *Notch3*, *DLL1*, *DLL4*, *JAG1*, *JAG2* and *HES1*, as well as increased protein expression for Notch3, JAG1 and HES1. Human macrophages (THP-1) infected with the mouse adapted *H. pylori* strain SS1 exhibited upregulated protein expression for Notch1, Notch3, JAG1 and HES1 (Wen et al., 2021). Expanding on Wen et. al.'s findings, we identified another Notch ligand (*DLL4*) and another Notch target gene (*HEY1*) that are significantly

upregulated in macrophages following *H. pylori* infection. In this study, we also demonstrated that heat killed *H. pylori* and *H. pylori* LPS were sufficient to increase expression of *JAG1* and *DLL4.* There has been previous research which shows an increase in expression of *JAG1* in macrophages treated with LPS from *Salmonella minnesota* (Goh et al., 2009). However, *H. pylori* LPS has reduced endotoxicity compared to the LPS of other gram-negative bacteria such as *E. coli* (Smith, 2014). This reduced immune activation is likely due to the altered structure of the lipid A domain (Tran et al., 2005). Despite this, in macrophages *H. pylori* LPS was able to increase *JAG1* and *DLL4* to an equivalent level as *E. coli* LPS. This would suggest that *H. pylori* mediated upregulation of *JAG1* and *DLL4* is facilitated, at least in part, via LPS-TLR signalling.

Experiments using cycloheximide showed that induction of *JAG1* and *HEY1* was intact in the presence of the protein synthesis inhibitor and did not require de novo protein synthesis, implying direct transcriptional activation of *JAG1* and *HEY1* by *H. pylori*. It is possible that the induction of these genes is a direct result of *H. pylori*-mediated activation of TLR signalling, as TLR ligand stimulation of primary human macrophages has been shown to directly upregulate *HEY1* (Hu et al., 2008) and *JAG1* mRNA expression (Foldi et al., 2010). On the other hand, cycloheximide prevented the *H. pylori*-mediated up-regulation of *DLL4* mRNA in THP-1 cells, implying that another *H. pylori*-regulated protein is involved in the induction of *DLL4* by *H. pylori*. In keeping with this, TLR-ligand induced *DLL4* expression has previously been shown to require de novo protein synthesis in primary human macrophages (Foldi et al., 2010).

In summary, the findings presented here on the upregulation of *JAG1*, *DLL4* and *HEY1* in macrophages in response to *H. pylori* are in keeping with the published study by Wen et al. (Wen et al., 2021). Furthermore, the results presented show that heat killed *H. pylori* can induce these genes and that *H. pylori* LPS plays a role in the induction of *JAG1* and *DLL4*,

suggesting a role for TLR signalling in the *H. pylori*-mediated induction of these genes. *JAG1* and *HEY1*, but not *DLL4*, appear to be direct transcriptional targets of *H. pylori*. It is noteworthy that *H. pylori* infection of gastric epithelial cells appears to inhibit expression of many *H. pylori* components, whereas infection of macrophages stimulates expression of Notch components. These cell specific difference may be a result of differential PRR expression between macrophages and epithelial cells.

4.8. Summary of conlusions

Results from this chapter build on existing findings that *H. pylori* down-regulates HES1 expression in gastric epithelial cells. To the best of our knowledge, this is the first study to demonstrate decreased *HES1* expression in the gastric mucosa of *H. pylori*-infected patients with chronic gastritis. Results from RNAseq identified IRAK2, ARL14, HOXB, ZNF792 and ZNF420 as novel targets of *H. pylori* infection in gastric epithelial cells. HES1 over-expression in AGS cells augmented the *H. pylori*-mediated up-regulation of *FOS*, *IL-8* and *CCL20*, suggesting that HES1 down-regulation by *H. pylori* restrains maximum induction of these genes. Finally, *H. pylori* increased expression of *JAG1*, *HEY1* and *DLL4* in macrophages.

4.9. Future Work

The novel findings in this research open the possibility for further research if time and funding permit.

- Use chromatin immunoprecipitation to analyse the *HES1* promoter to identify if RBP-J is blocking HES1 expression in epithelial cells infected with *H. pylori*.
- Perform infections with further isogenic mutant strains of *H. pylori* or stimulation experiments with peptidoglycan to further characterise the bacterial components involved in HES1 alteration.
- Continue with the HES1 loss-of-function analysis in epithelial and macrophage cell lines using additional siRNA molecules, alternative gamma secretase inhibitors or CRISPR/Cas9 approaches. This may help confirm the downstream targets of HES1 in epithelial cells and identify new targets in macrophages.
- Investigate whether the *H. pylori*-mediated down-regulation of HES1 in AGS cells and associated attenuation of *IL-8* and *CCL20* induction inhibits neutrophil and monocyte recruitment by performing chemotaxis assays.
- Confirm the *H. pylori*-mediated Notch signalling alteration that was seen in in THP-1 cells using primary human macrophages.
- Infect gastric epithelial cells with other types of bacteria from the gastric microbiome to see if they can also alter the expression of HES1.

Chapter Five Investigating the Roles of Histone Modification Proteins and Inflammatory Caspases During *H. pylori* Infection

5.1. Intoduction

5.1.1. Introduction to epigenetics

It is essential for gene expression to be tightly regulated during both embryogenesis and throughout life. Dysregulation of gene expression is a hallmark of carcinognesis. Gene expression is tightly regulated by the interplay of two different but inter-connected mechanisms. Firstly, transcription factors can bind to specific DNA sequences and can activate or repress transcription. Secondly, chromatin cofactors can alter or maintain chromatin structure making it easier or harder for RNA polymerase and transcription factors to interact with the DNA (Cavalli and Heard, 2019). This second method is known as epigenetics. In other words, epigenetics refers to changes in gene expression that occur without altering the DNA sequence (Cavalli and Heard, 2019). The most common chromatin modification methods are i) nucleic acid methylation, ii) histone modification (methylation, acetylation, phosphorylation and ubiquitination), and iii) non-coding RNA mediated regulation (Schvartzman et al., 2018, Chen et al., 2017). This chapter will focus on proteins involved in histone methylation, which occurs at arginine or lysine residues (Burchfield et al., 2015), in particular those involved in histone methylation and demethylation at histone 3 lysine 27 (H3K27).

5.1.1.1. How is DNA packaged in the nucleus?

In order to understand how chromatin cofactors alter gene expression, it is necessary to understand how DNA is structured in each cell. Within the nucleus, DNA is organised at several complex levels resulting in tightly compacted chromosomes. Linear DNA of 147 base pairs coil around histones to form nucleosomes (Jambhekar et al., 2017). A histone is made of an octamer of proteins. Each octamer contains two of each of the four core histone proteins (H2A, H2B, H3, H4). The histones are positively charged allowing them to bind strongly to the negatively charged DNA. The nucleosomes compress further to form the higher order structures of chromatin fibres and finally chromosomes (Figure 5.1) (Chen et al., 2017). This complex organisation has two functions, firstly to compact the DNA so that it can fit into the nucleus and secondly to allow the transcription machinery to access selective regions of the genome (Chen et al., 2017).

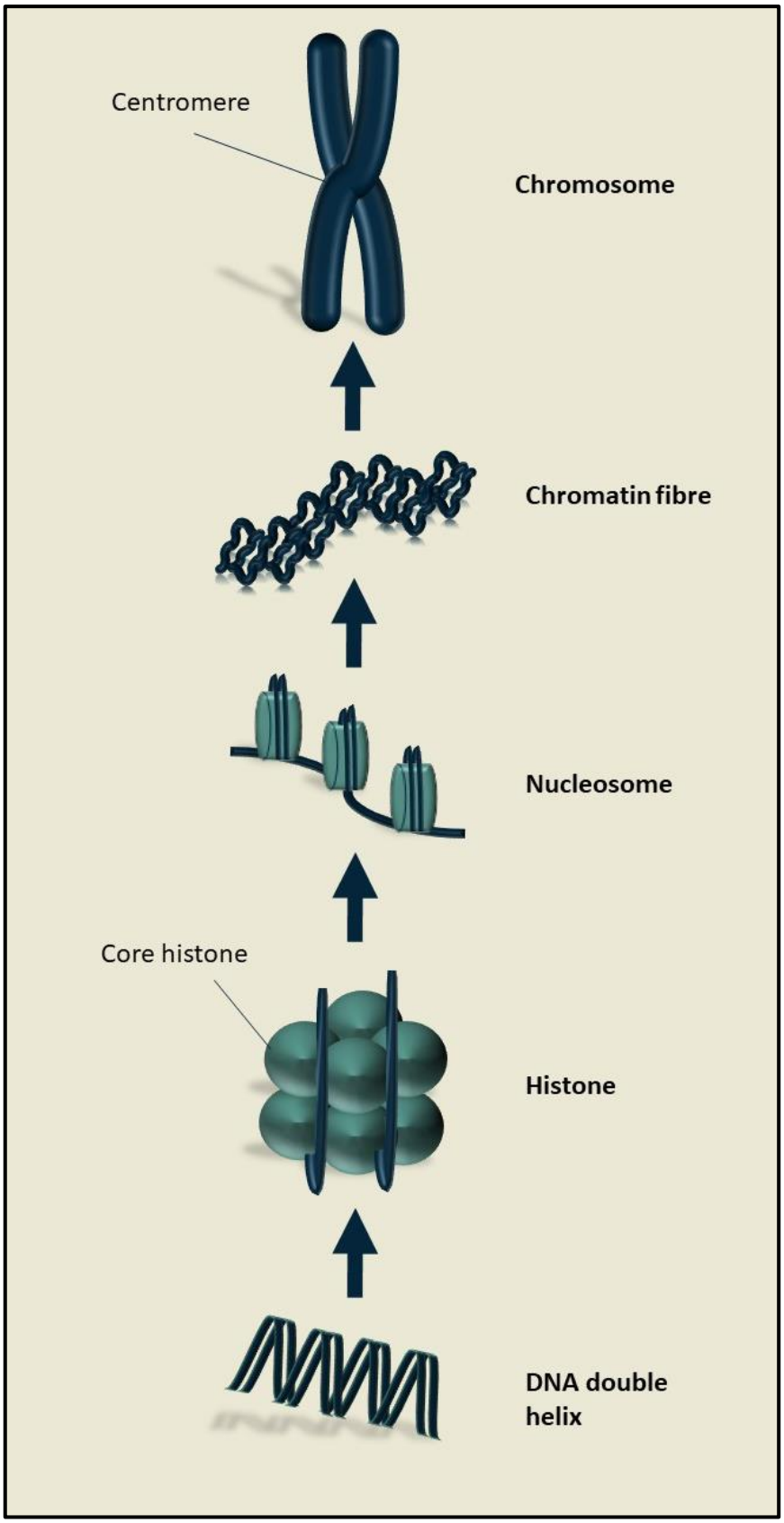

Figure 5.1 DNA is organised into levels of structural integrity. In the nucleus DNA winds around histone octamers to form nucleosomes. These fold and condense further to form chromatin fibres and finally chromosomes. (Adapted from Chen et al. 2017). Diagram created in PowerPoint.

5.1.1.2. How does chromatin arrangement impact gene expression?

The two most common histone modifications are methylation and acetylation (Burchfield et al., 2015). These modifications cause alteration to the spatial conformation of chromatin, leading to either gene expression or repression (Burchfield et al., 2015). The DNA can be organised into two conformations; euchromatin and heterochromatin (Figure 5.2). Euchromatin is associated with hypomethylation and with acetylation at H3K27. This leads to the DNA being loosley bound to the histones facilitating an open confirmation and allowing active transcription (Chen et al., 2017). Conversly, heterochromatin is associated with hypermethylation including at H3K27me3. This constricted conformation turns off active transcription since transcription factors and coactivators cannot access the DNA (Chen et al., 2017). There are several known histone methlytransferases and each lysine residue can be mono-, di-, or tri- methylated. Polycomb group proteins act as a histone methyltransferase.

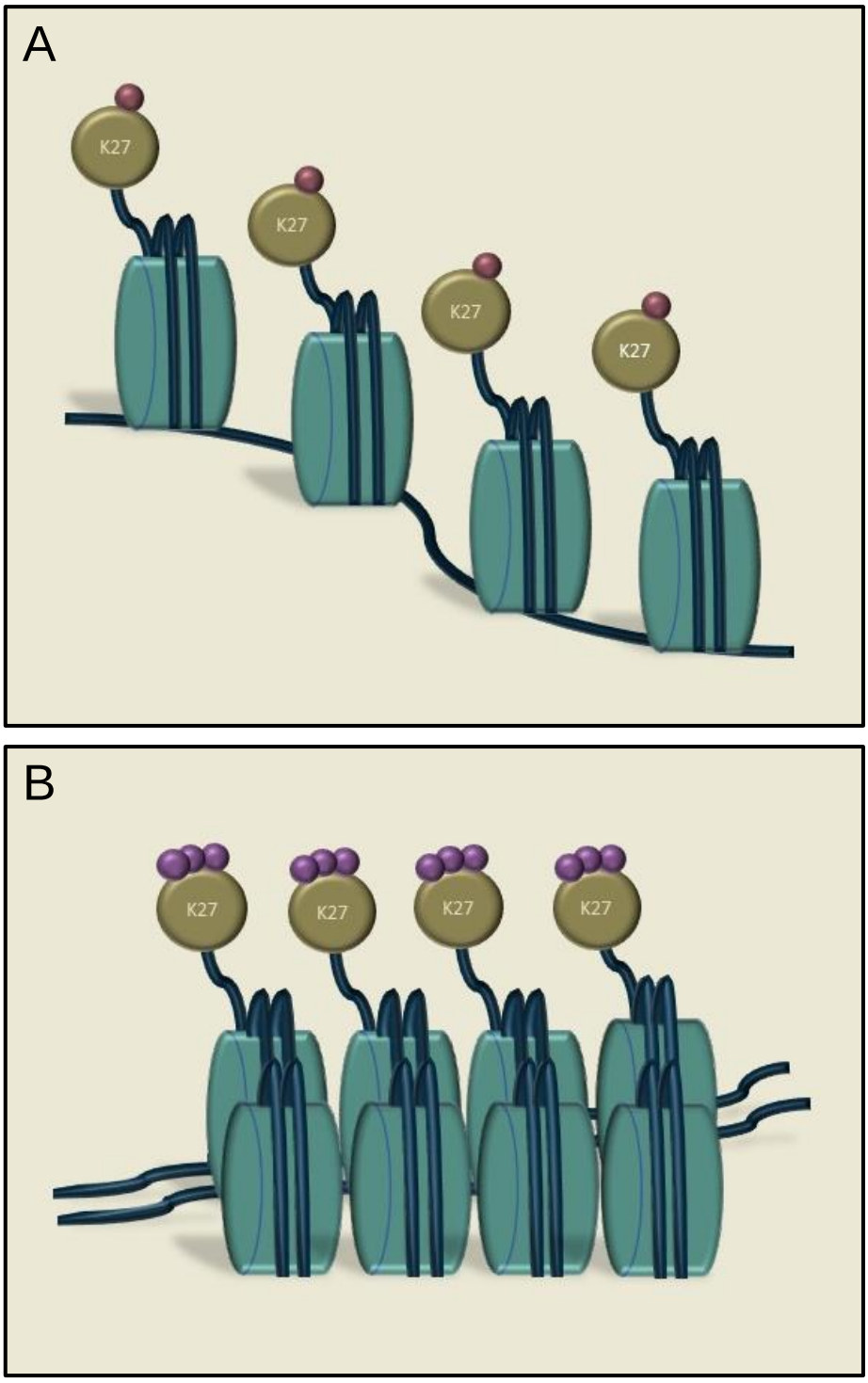

Figure 5.2 Euchromatin and heterochromatin A) Euchromatin allows for active transcription and is associated with H3K27ac (red) in the enhancer regions. B) Heterochromatin allows for silencing of genes and is marked by H3K27me3 (purple) in enhancer and promoter regions. Diagram created in PowerPoint.

5.1.1.3. Polycomb Group Proteins

Polycomb group proteins influence gene expression by regulating the structure of chromatin (Margueron and Reinberg, 2011). These proteins were first identified in Drosophila as repressors of *HOX* genes (a subset of homeobox genes which regulate embryonic development) (Conway et al., 2015). Polycomb group proteins are found in two multisubunit complexes - polycomb repressive complexes 1 and 2 (PRC1, PRC2). PRC2 componants are essential for epigenetic gene regulation during embryonic development and ensure correct gene silencing (van Mierlo et al., 2019). PRC2 is made up of the proteins Embryonic Ectoderm Development (EED), Enhancer of Zeste Homolog 2 (EZH2) and Suppressor Of Zeste 12 (SUZ12) as well as numerous substoichiometric subunits (van Mierlo et al., 2019). The core PRC2 components; SUZ12, EED and the methyltransferase EZH2 are all required for the complex's catalytic activity (Figure 5.3), (Laugesen et al., 2019). The importance of these proteins is evidenced by knockouts of EED, EZH2 and SUZ12 in mice resulting in early embryonic lethality. This also indicatates the importance of the PRC2 complex as a whole (Margueron and Reinberg, 2011). Dysregulation of PRC2 components is associated with the devlopment of numerous cancer types indicating that the PRC2 complex is important during both embryonic development and adult gene regulation (Conway et al., 2015). The PRC2 complex modifies chromatin structure by di- and tri-methalating Lysine 27 on Histone H3 (H3K27me2, H3K27me3) (Margueron and Reinberg, 2011, Laugesen et al., 2019). The mark H3K27me3 is seen as a characteristic feature of PRC2 mediated gene represssion (Laugesen et al., 2019). Notably, the H3K27me2 mark is considered the default state for H3K27. It is found ubiquitously throughout the genome including all euchromatin regions, besides actively transcribed genes which are instead marked with H3K27me1 (Conway et al., 2015).

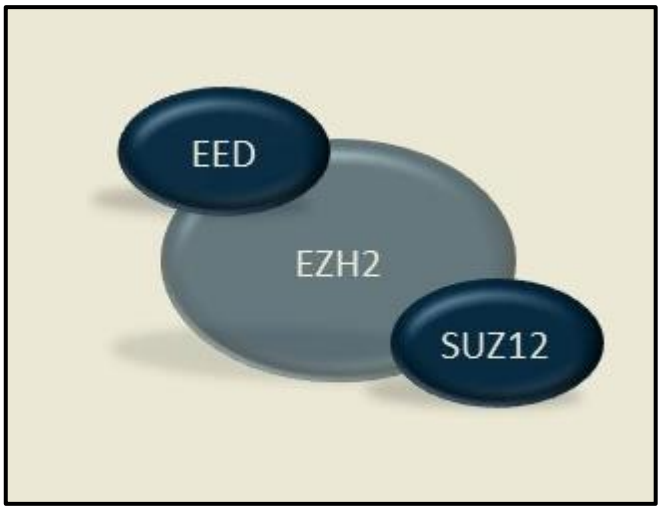

Figure 5.3 Schematic of the core PRC2 subunits. The primary components of PRC2 are EED, EZH2 and SUZ12. EZH2 is the primary cayalytic subunit of PRC2 but requires direct contact with EED and SUZ12 for catalytic activity. EED acts as an allosteric activator by changing the conformation of EZH2 increasing its catalytic activity. SUZ12 stabalises the PRC2 complex (van Mierlo et al., 2019). Diagram created in PowerPoint.

5.1.1.4. The histone lysine demethylase KDM6B

Histone methylation is a flexible process (Xiang et al., 2007). Reversal of histone methylation can be performed by several classes of enzymes (Burchfield et al., 2015). One such classification relies on the presence of a Jumonji C domain. Jumonji domain-containing protein D3 (JMJD3) also known as lysine-specific demethylase 6B (KDM6B) is a member of this classification (Burchfield et al., 2015). KDM6B can specifically remove the trimethyl group from H3K27 (Xiang et al., 2007). While trimethylated H3K27 is associated with repression of transcription, the opposite is true for monomethylated H3K27. In other words KDM6B is associated with active gene promotors (Burchfield et al., 2015). Under normal conditions the expression of KDM6B is low but cell stress and extracellular stimuli can trigger its overexpression (Liu et al., 2022).

5.1.1.5. Histone modification during *H. pylori* infection

It is widely accepted that *H. pylori* infection regulates gene expression however, the role of histone modifications in this process is not well understood. Emerging studies suggest a link between EZH2 and KDM6B and gastric cancer (Cai et al., 2010), (Purkait et al., 2022), (Liu et al., 2022). However, the expression and role of PRC2 components and KDM6B in the response to *H. pylor*i and its components is not fully explained.

5.1.2. Introduction to the Caspase Family

The Caspase family are a group of cysteine proteases that maintain homeostasis by regulating cell death and inflammation (McIlwain et al., 2013). Caspases are produced as inactive monomeric pro-caspases and are activated by dimerization or oligomerization. Additional signals are also required for processing of pro-caspases and full activation of caspase pathways (Creagh, 2014). Pro-caspases consist of an N-terminal pro-domain and a C-terminal protease domain (Creagh, 2014). Caspases are broadly broken into two groups which are dependent on their roles in either inflammation or apoptosis (Creagh, 2014). Caspases which are involved in inflammation include Caspase-1, Caspase-4, Caspase-5 and Caspase-12 in humans and Caspase-1, Caspase-11, and Caspse-12 in mice (Figure 5.4) (McIlwain et al., 2013). Caspases that are involved in apoptotic cell death are further broken down into subcategories which consist of initiator Caspases (Caspase-2, Caspase-9, Caspase-8 and Caspase-10) and executioner Caspases (Caspase-3, Caspase-6 and Caspase-7) (McIlwain et al., 2013) (Figure 5.4).

5.1.2.1. Caspases and Apoptosis

Caspases can initiate apoptosis via the intrinsic or extrinsic pathways. The intrinsic pathway is activated by cellular stressors including DNA damage and hypoxia among others (McIlwain et al., 2013). In the intrinsic pathway, cytochrome c is released from the mitochondria and forms the multimeric protein complex called the apoptosome, which consists of cytochrome c, apoptotic protease-activating factor-1 (Apaf1) and activated Caspase-9 (Creagh, 2014). In the extrinsic pathway, activation of the death receptors from the TNF superfamily results in the formation of the multimeric complex known as the death induced signalling complex (DISC), which recruits and activates Caspase-8 (Creagh, 2014). Activated Capase-9 and Caspase-8 will then process and activate the executioner caspases (Caspases-3, -6, -7) leading to apoptosis.

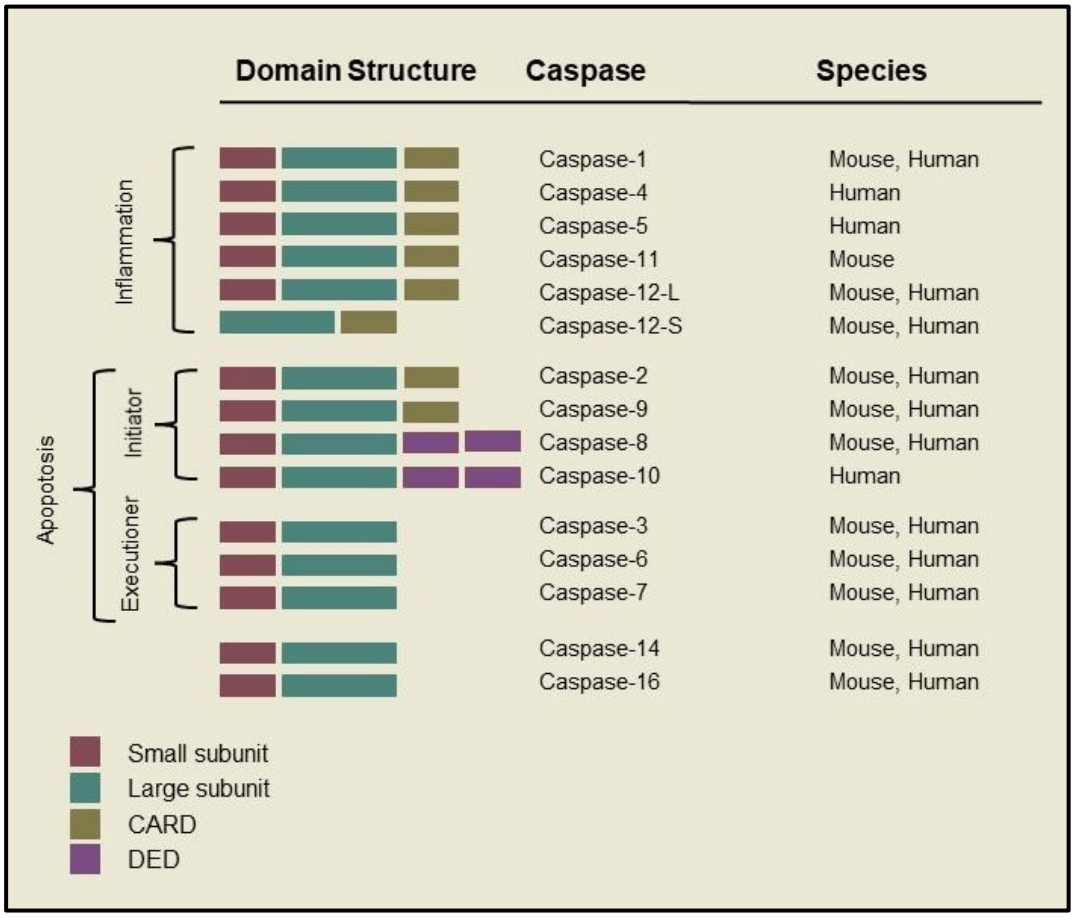

Figure 5.4 Caspase domain structure for humans and mice. Each pro-caspase consists of an N-terminal pro-domain and a C-terminal protease domain containing the catalytic cystine residue. The C-terminal is broken up into a small and large subunit. Depending on its function, a caspase may also have other conserved protein domains including Caspase-associated recruitment domains (CARDs) and death effector domains (DEDs) (Creagh, 2014). Caspases are broadly broken up into groups based on their role in either apoptosis (Caspases -2, -9, -8, -10, -3, -6, -7) or inflammation (Caspases -1, -4, -5, -11, -12) (Fernández and Lamkanfi, 2015). Diagram created in PowerPoint.

5.1.2.2. Caspases and inflammation

IL-1β is an important pro-inflammatory cytokine and because of this its expression is tightly regulated. In order to increase transcription of the *IL1B* gene, NF-κB must be first activated. The protein is then translated as pro-IL-1β and must be processed before it can be secreted (Creagh, 2014). Caspase-1 was the first inflammatory caspase to be described and is still the best categorised. It was originally known as Interleukin-1β converting enzyme (ICE) due to its ability to process pro-IL-1β into its active form (Ghayur et al., 1997). Indeed, the primary mechanism responsible for the processing of pro-IL-1β is cleavage by Caspase-1 (Creagh, 2014).

5.1.2.3. Inflammasome Complexes

Inflammasomes are multiprotein platforms of the innate immune system and are responsible for activation of Caspase-1. Activated Caspase-1 cleaves pro-IL-1β into its biologically active forms. Many bacteria can activate inflammasome production. During the innate immune response, inflammasome scaffolds consisting of intracellular nucleotide-binding oligomerization domain (NOD) like receptors (NLRs) and the adaptor apoptosis speck like protein (ASC) activate Caspase-1 and are a requirement for IL-1β production (Kayagaki et al., 2011). Nucleotide-binding oligomerization domain, Leucine rich Repeat and Pyrin domain containing Proteins (NLRPs) contain pyrin domains which bind to the pyrin domain in the adapter molecule ASC (Sanchez-Garrido et al., 2020). ASC also contains a CARD domain which recruits pro-caspase-1 into the inflammasome leading to proximity-induced activation of Caspase 1 (Sanchez-Garrido et al., 2020). The NLRP3 inflammasome is the most studied inflammasome (Pachathundikandi et al., 2020). Two signals are required to activate the NLRP3 inflammasome in myeloid cells (Sanchez-Garrido et al., 2020). The first signal upregulates expression of NLRP3 inflammasome components such as Caspase 1 and ASC. Signal one also increases expression of pro-IL-

1β (Pachathundikandi et al., 2020). The second signal causes the inflammasome scaffold to assemble (Pachathundikandi et al., 2020).

5.1.2.4. The non-canonical inflammasome

Infection with gram negative bacteria can indirectly activate the NLRP3 inflammasome via Caspase 11 in mice and Caspase4/5 in humans. This is known as non-canonical inflammasome activation (Sanchez-Garrido et al., 2020). Pro-IL-1β is the direct substrate of Caspase-1. The non-canonical inflammasome requires active Caspase-1 as Caspase-11/4/5 cannot directly process pro-IL1β (Yi, 2017) (Figure 5.5). LPS from gram negative bacteria has been shown to induce the non-canonical inflammasome (Yi, 2017). Similarly, release of IL-1β from BMDM infected with live *E. coli*, *C. rodentium* and *V. cholerae* requires the presence of Caspase-11, indicating these bacteria induce the non-canonical inflammasome (Kayagaki et al., 2011).

Mice that are deficient in Caspase-11 are developmentally normal but are resistant to endotoxic shock and do not produce IL-1β following stimulation with *E. coli* LPS (Wang et al., 1998, Kayagaki et al., 2011), implying a role for Caspase-11 in the regulation of Caspase-1 activation. Caspase-4 and Caspase-5 are duplicate human homologs of mouse Caspase-11. In total, Caspase-11 shares 60% sequence homology with Caspase-4 and 55% with Caspase-5 (Fernández and Lamkanfi, 2015).

Caspase-4 and Caspase-5 in humans and Caspase-11 in mice are activated by a process known as 'induced proximity' (Green, 2022). When these caspase monomers are triggered to form dimers, they become active enzymes. This happens when LPS (and potentially other PAMPs) from gram negative bacteria bind to the CARD domain of Caspase-4/5/11 (Green, 2022). Inflammatory caspases activate inflammation in two ways, either by causing pyroptosis or by generating an inflammasome complex.

5.1.2.5. Pyroptosis

Pyroptosis is a form of cell death associated with the release of inflammatory molecules (Man et al., 2017). In mice, pyroptosis is mediated by Caspase-1 and Caspase-11 while in humans it is mediated by Caspase-1, Caspase-4 and Caspase-5 (Man et al., 2017). The activated Caspase enzymes contribute to cell death by activating a substrate known as Gasdermin D. Activated Gasdermin D causes pores to form in the plasma membrane of the cell which ultimately causes the cell to burst (Green, 2022). Pyroptosis that is initiated by Caspase-11 releases damage-associated molecular patterns (DAMPs), which leads to a feedback loop that activates the NLRP3 inflammasome and Caspase-1, subsequently amplifying pyroptosis (Zasłona et al., 2020a) (Figure 5.5).

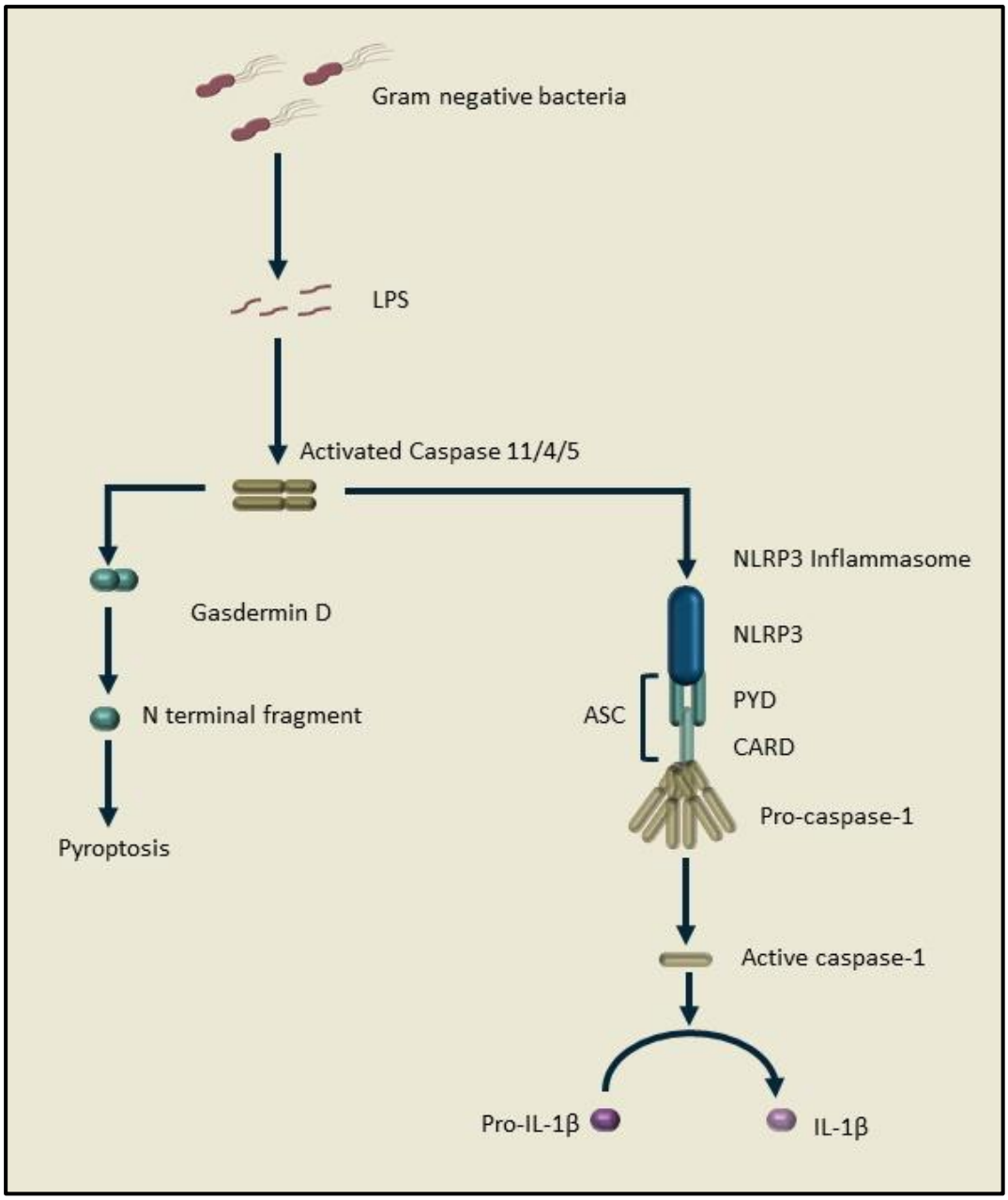

Figure 5.5 The non-canonical inflammasome. Caspase 11/4/5 can be activated by binding directly to LPS. Oligomerized Caspase 11/4/5 can i) cleave Gasdermin D which creates pores in the cell wall leading to pyroptosis. ii) trigger the assembly of the NLRP3 inflammasome that acts via Caspase 1 to induce IL-1ß maturation. Diagram created in PowerPoint.

5.1.2.6. IL-1ß and *H. pylori* infection

The production of pro-inflammatory cytokines play an important role in *H. pylori* pathogenesis. Pro-IL-1ß is upregulated during *H. pylori* infection and polymorphisms in the *IL-1ß* gene are associated with an increased risk of *H. pylori*-associated pathogenesis and carcinogenesis (Pachathundikandi et al., 2020), (El-Omar et al., 2000), (Hong et al., 2016). Furthermore, Caspase-4 has been shown to be upregulated in peptic ulcer tissue (Yaguchi et al., 2010), (Zasłona et al., 2020a). However, the role of Caspase-4 or it's murine homologue Caspase-11, in the context of *H. pylori*-mediated IL-1ß induction is not fully understood. Since Caspase 4 has been shown to play a role in IL-1 regulation in some contexts the rationale for this work was to see if Caspase 4 is regulating IL-1 during *H. pylori* infection.

5.2. Hypothesis

EZH2 and KDM6B have been linked to gastric cancer. Moreover, RNAseq analysis of *H. pylori* infected AGS cells in Chapter 4 identified *KDM6B* as a *H. pylori* target gene. It was therefore hypothesised the *H. pylori* infection leads to changes in expression of PRC2 proteins and KDM6B and that histone methylation/demethylation is involved in *H. pylori*-mediated pathogenesis.

Secondly, as Caspase 4 has been shown to play a role in IL-1 regulation in some contexts, it was hypothesised that Caspase 4 is involved in *H. pylori*-mediated IL-1β production.

5.3. Aims and Objectives

The aim of this chapter was to investigate the role of histone modifying components and inflammatory caspases in *H. pylori* infection through the objectives below.

- Objective 1: To characterise PRC2 components and KDM6B expression during *H. pylori* infection in AGS epithelial cells and in the gastric mucosa.
- Objective 2: To characterise PRC2 components and KDM6B expression during *H. pylori* infection in macrophages.
- Objective 3: To characterise Caspase-4 and IL-1β expression during *H. pylori* infection in gastric epithelial cells and the gastric mucosa.
- Objective 4: To characterise Caspase-4 and IL-1β expression during *H. pylori* infection in THP-1 macrophages.
- Objective 5: To characterise Caspase-11 and IL-1β expression during *H. pylori* infection in mouse BMDM.

5.4. *H. pylori* Alters the Expression of Histone Modifying Componants

5.4.1. *H. pylori* alters the expression of PRC2 components in MKN45 cells.

To characterise expression of histone modification proteins in *H. pylori* infection, expression of PRC2 components and *KDM6B* was firstly monitored in gastric epithelial cells infected with *H. pylori*. *IL-8* mRNA expression was monitored as a positive read-out for *H. pylori* infection.

As expected, significant upregulation of *IL-8* was observed in MKN45 cells at 3 and 6 hours post infection (8.7-fold, and 5.4-fold, respectively) (Figure 5.6.A). *H. pylori* infection led to a significant decrease in expression of all PRC2 components tested. At both 3 and 6-hours post infection *SUZ12* was decreased to 0.7-fold (p=.035 and p=.039 respectively) (Figure 5.6.B). Significant downregulation of *EZH2* was observed at 3-hours (0.5-fold, p=.008) (Figure 5.6.C). At both 3 and 6-hour time points there was a significant reduction in *EED* expression (0.4-fold, p=.001 and 0.6-fold, p=.007 respectively) (Figure 5.6.D). In contrast, *H. pylori* infection led to a significant increase in *KDM6B* expression in MKN45 cells at both 3 and 6-hours (5-fold p<.001 and 3-fold p=.007 respectively) (Figure 5.6.E).

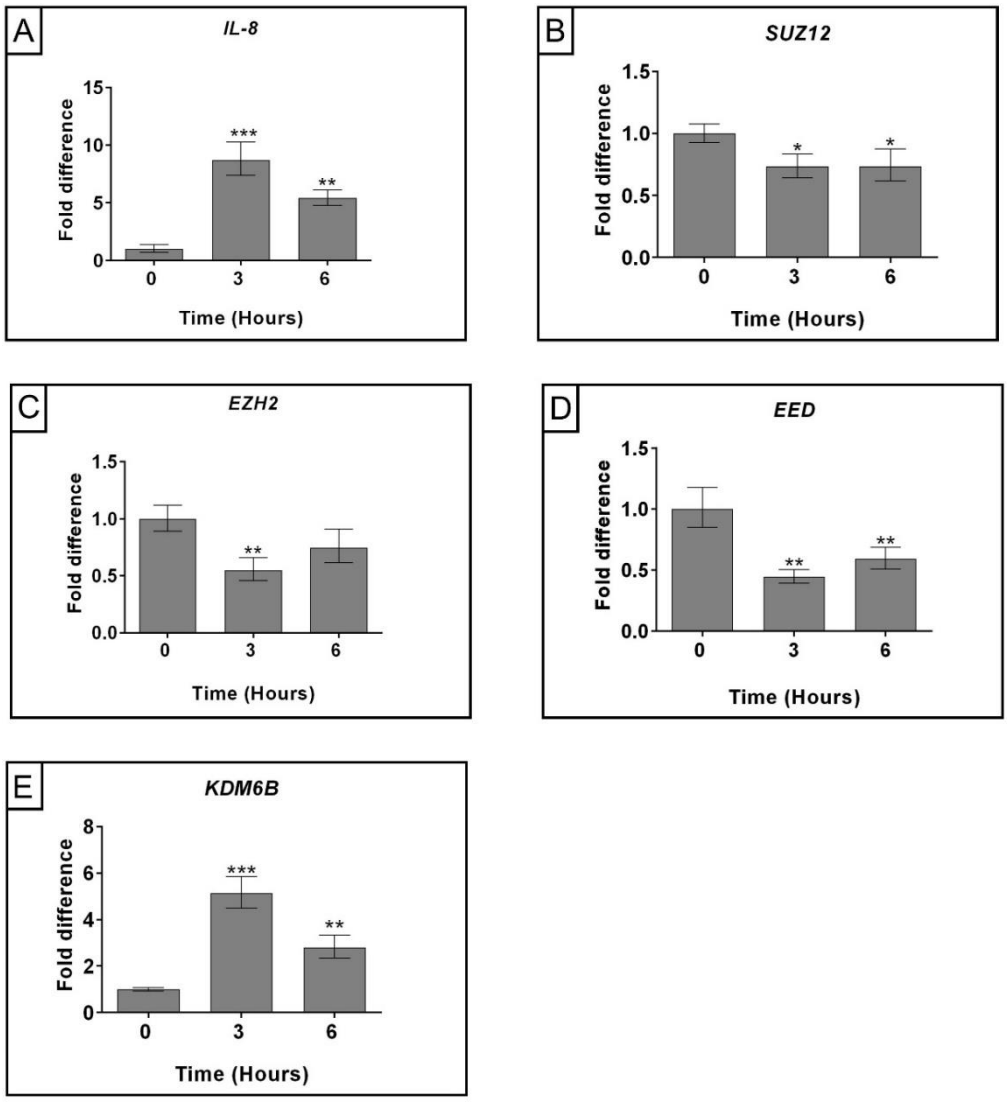

Figure 5.6 Expression of PRC2 and *KDM6B* components in MKN45 cells infected with *H. pylori*. MKN45 cells were infected with *H. pylori* strain 11638 for the time points indicated underneath the graphs. Total RNA was isolated and changes in *IL-8* (A), *SUZ12* (B), *EZH2* (C), *EED* (D) and *KDM6B* (E) gene expression were evaluated by RT-qPCR using the comparative cycle threshold method. Results were normalized to *GAPDH* levels and expressed relative to uninfected cells (time 0). Data shown are means ± SD of triplicate determinants. A one-way Anova test was performed for each gene. Dunnett's multiple comparisons test compared the untreated sample mean (0h) to the mean at each time point. * $P \leq 0.05$, ** $P \leq 0.01$, *** $P \leq 0.001$. Graphs are representative of three independent experiments. Data presented were analysed from in vitro infection experiments performed by MSc student John Hickey.

5.4.2. Live and heat-killed *H. pylori* alter the expression of the histone demethylase KDM6B in AGS cells.

Subsequently, expression of the PRC2 components and *KDM6B* was investigated in AGS cells infected with *H. pylori* or treated with heat killed *H. pylori*. As expected, significant increases in *IL-8* and *TNF* were observed following infection with live *H. pylori* (Figure 5.7.A,B). At every time point tested, live *H. pylori* led to significantly higher *IL-8,* and *TNF* expression compared to treatment with heat killed bacteria.

Both live and heat-killed bacteria led to a transient decrease in *SUZ12* expression. At three hours the heat killed treatment led to 0.5-fold expression while live bacterial infection led to 0.8-fold expression (Figure 5.7.C).

Live or heat-killed bacteria did not significantly reduce *EZH2* expression, (Figure 5.7.D). A transient significant decrease in *EED* expression was observed at 1 hour with heat-killed bacteria (0.3-fold, p=.044) (Figure 5.7.E).

Similar to the results from MKN45 cells and in line with the RNAseq findings presented in chapter 3 (Section 4.5), *H. pylori* infection led to significant increases in the expression of *KDM6B* at the 3 and 6-hour time points (Figure 5.7.F). For example, at 3-hours, live bacteria led to an increase of 6-fold (p<.001). At all-time points, live bacteria led to significantly larger increase in *KDM6B* expression compared to heat-killed *H. pylori*.

Taken together, these findings show that *H. pylori* can transiently decrease expression of *SUZ12* and *EED* in gastric epithelial cells and significantly increases *KDM6B* expression.

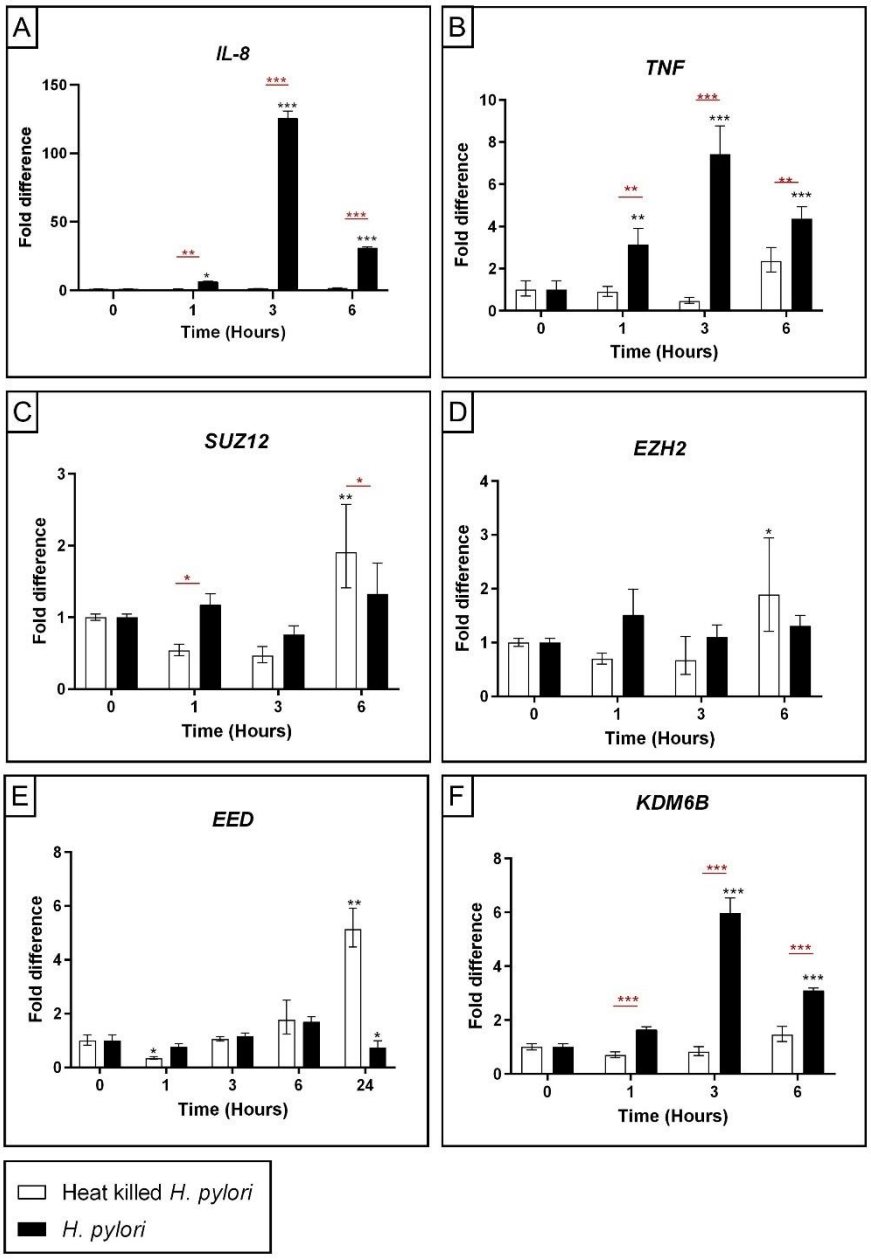

Figure 5.7 Expression of PRC2 components and KDM6B in AGS cells treated with heat killed *H. pylori* or infected with live *H. pylori*. The cells were infected with *H. pylori* strain 11638 for the time points indicated underneath the graphs. Total RNA was isolated and changes in *IL-8* (A), *TNF* (B), *SUZ12* (C), *EZH2* (D), *EED* (E) and *KDM6B* (F) gene expression was evaluated by RT-qPCR using the comparative cycle threshold method. Results were normalized to *GAPDH* levels and expressed relative to uninfected cells at each time point. A two-way Anova was performed for each gene. Šidák multiple comparison tests were used to compare mean values of treated samples with untreated samples (black asterisk) and to compare mean values between live and heat-killed samples (red asterisk). Data shown are means ± SD. * P≤0.05, ** P≤0.01, *** P≤0.001. Graphs are representative of three independent experiments.

5.4.3. *H. pylori* infection is associated with a decrease in *EED* and increase in *KDM6B* in gastric biopsy tissue.

To identify if *H. pylori* mediates gene expression changes of PRC2 components or *KDM6B* in the gastric epithelium, RT-qPCR was performed on RNA isolated from gastric biopsy tissue samples. Patients were recruited following ethical approval in Tallaght University Hospital, Dublin. Antral biopsy tissue was collected from 21 *H. pylori* infected and 9 uninfected control patients. Patients were considered infected if they tested positive for two out of three diagnostic tests. The diagnostic tests considered were the RUT, histopathologic examination of the biopsy specimen and culture of the bacteria. Patient data was collected from the Key database and stored in password protected and pseudonymised Excel files. All infected patients suffered from gastritis. The Mann-Whitney U-test was used to compare gene expression between the infected and control cohorts A significant decrease in the median expression levels of *EED* was observed in the gastric mucosa of *H. pylori* infected versus uninfected patients (p=.034) (Figure 5.8.D). A trend towards decreased median levels of *SUZ12* and *EZH2* (Figure 5.8.B,C) was observed in *H. pylori* infected compared to uninfected tissue samples, but this did not reach statistical significance. Additionally, there was a significant increase in *KDM6B* expression in samples from *H. pylori* infected versus uninfected patients (p=.031) (Figure 5.8.D).

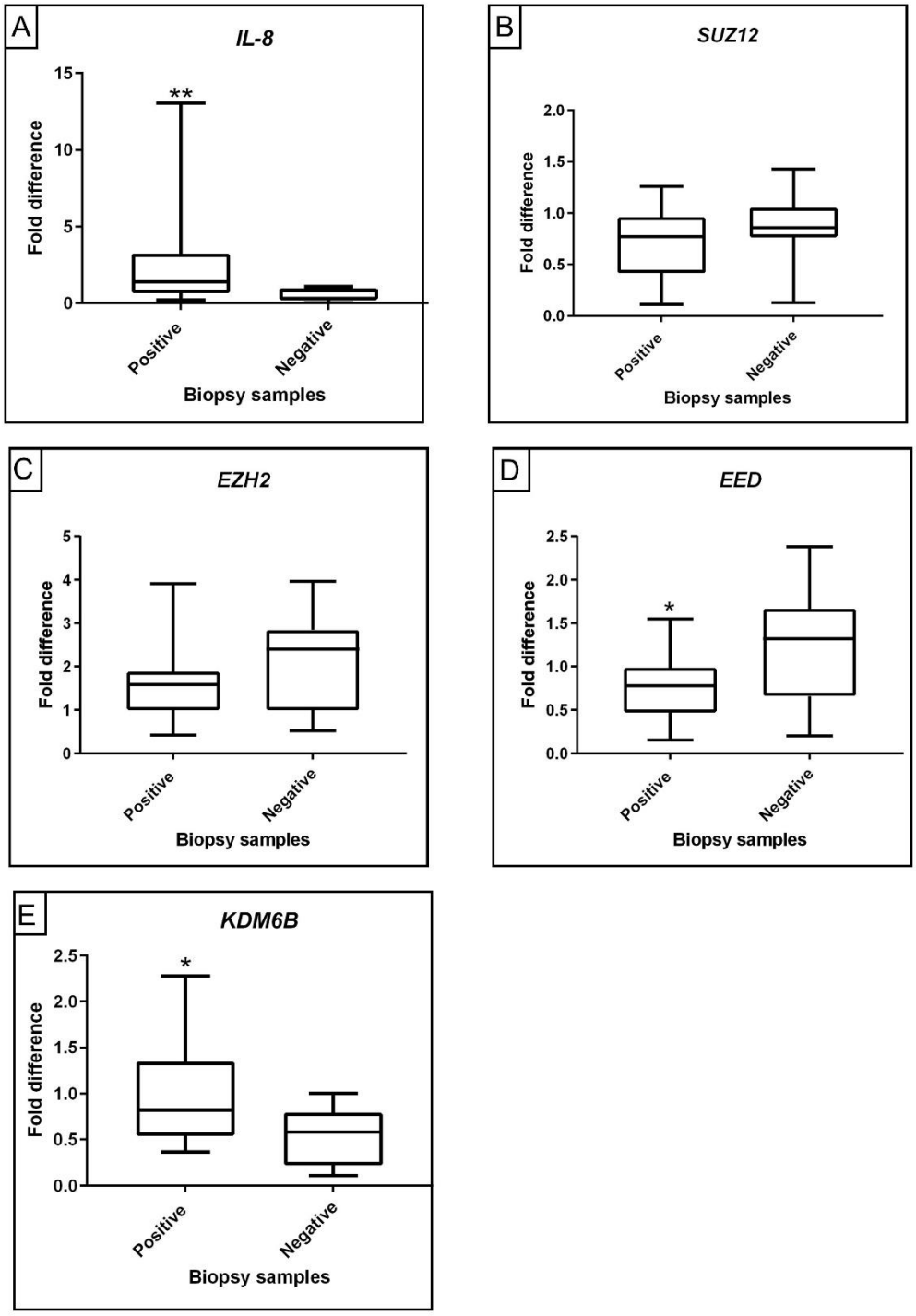

Figure 5.8 Expression of PRC2 components and *KDM6B* in gastric biopsy tissue from *H. pylori* positive and negative patients. Total RNA was purified from antral biopsies of 21 *H. pylori*-infected patients (positive) and 9 uninfected controls (negative). Changes in *IL-8* (A), *SUZ12* (B), *EZH2* (C), *EED* (D) and *KDM6B* (E) mRNA expression were evaluated by RT-qPCR using the comparative cycle threshold method. Results were normalized to *GAPDH* levels and are expressed relative to a sample in the uninfected control group. The Mann-Whitney U-test was used to compare results from positive and negative groups. * $P \leq 0.05$, ** $P \leq 0.01$.

5.4.4. New protein synthesis is not required for the *H. pylori*-mediated induction of *KDM6B* in AGS cells.

Since *KDM6B* expression was significantly and consistently increased in gastric epithelial cells (AGS and MKN45) and gastric biopsy tissue in response to *H. pylori*, it was decided to determine whether new protein synthesis was required for the *H. pylori*-mediated induction of *KDM6B* in AGS cells. The cells were treated for 1 hour with 20 μg/ml cycloheximide prior to *H. pylori* infection. As expected, infection with *H. pylori* led to increases in *IL-8* and *TNF* expression at 1, 3 and 6-hour time points (Figure 5.9.A-B). At 6-hours, Cycloheximide combined with *H. pylori* infection led to significant increases in expression of *IL-8* and *TNF* compared to either of these conditions alone. Blocking translation in the presence of *H. pylori* increased the expression of pro-inflammatory cytokines, this may suggest that a protein is synthesized in gastric epithelial cells following *H. pylori* infection that can dampen the effect of the bacteria on *IL-8* and *TNF* expression.

At 6-hours, Cycloheximide treatment statistically significantly increased the expression of *KDM6B* in AGS cells (Figure 5.9C). At 6-hours, combined *H. pylori* and cycloheximide treatment led to significantly increased expression of *KDM6B* compared to *H. pylori* infection alone ($p<.001$). Similarly, at 6-hours cycloheximide treatment combined with *H. pylori* significantly upregulated *KDM6B* expression compared to cycloheximide treatment alone ($p<.001$). These findings indicate that de novo protein synthesis is not required for the *H. pylori*-mediated induction of *KDM6B* and that *KDM6B* is a direct transcriptional target of *H. pylori* in AGS cells.

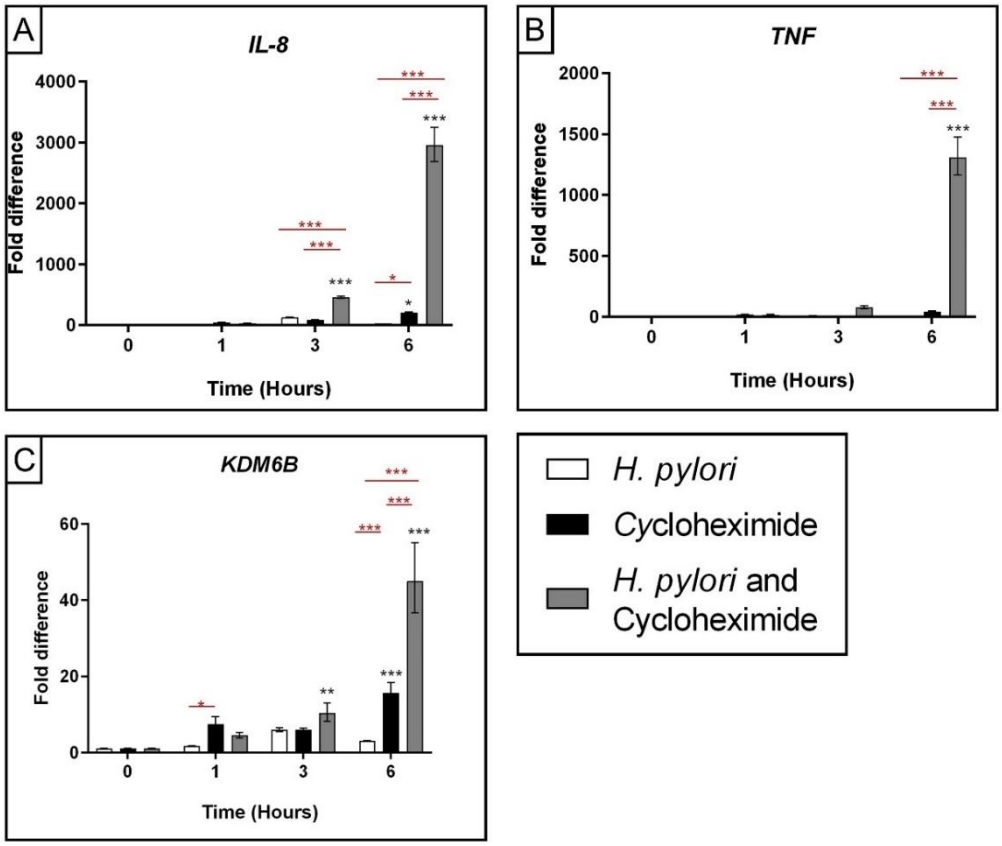

Figure 5.9 Expression of *KDM6B* in AGS cells treated with cycloheximide and infected with *H. pylori*. AGS cells were treated for 1 hour with 20 µg/ml cycloheximide and infected with 100 MOI of *H. pylori* strain 11638 for the time points indicated underneath the graphs. Total RNA was isolated and changes in *IL-8* (A), *TNF* (B), and *KDM6B* (C) gene expression were evaluated by RT-qPCR using the comparative cycle threshold method. Results were normalized to *GAPDH* levels and expressed relative to uninfected cells at each time point. A two-way Anova was performed for each gene. Dunnett's multiple comparison test was used to compare mean values of each sample with the untreated sample (*H. pylori* 0-hour) (black asterisk). Tukey's multiple comparison test was used to compare mean values of each treatment to every other treatment at each time-point (red asterisk). P≤0.05, ** P≤0.01, *** P≤0.001. Graphs are representative of three independent experiments.

5.4.5. Live and heat-killed *H. pylori* alter the expression of histone modification components in THP-1 cells.

Next, the expression of the PRC2 components and *KDM6B* was analysed in differentiated THP-1 cells. As expected, significant increases in *IL-8* and *TNF* were observed for both heat-killed and live *H. pylori* (Figure 5.10.A,B).

Heat-killed *H. pylori* transiently reduced the expression of *SUZ12* at 3 and 6-hours ($p<.001$ and $p<.001$ respectively) (Figure 5.10.C). Infection with live *H. pylori* led to sustained reduction in *SUZ12* expression, which was statistically significantly reduced at 6, 24 and 48-hours. The strongest reduction was seen at 24 and 48-hours (0.4-fold, $p<.001$, 0.2-fold, $p<.001$ respectively). At 24 and 48-hours live bacteria significantly reduced *SUZ12* expression compared to heat-killed bacteria ($p<.001$, $p<.001$ respectively).

Both live and heat-killed *H. pylori* significantly increased the expression of *EZH2* at early time points. (Figure 5.10.D). However, live bacteria statistically significantly reduced the expression of *EZH2* at both 24 and 48-hours (0.5-fold, $p=.027$, 0.3-fold, $p<001$ respectively). The different impact of live and heat killed bacteria was significant at these later time points, implying that live bacteria are required for the late reduction in *EZH2* observed.

Infection with *H. pylori* significantly decreased the expression of *EED* at 3, 6, 24 and 48-hours (Figure 5.10.E). Like *SUZ12* and *EZH2*, live *H. pylori* had a stronger effect on *EED* expression compared to heat killed bacteria. Significant differences between the effect of live and heat killed *H. pylori* were observed at 1, 6, 24 and 48-hours ($p<.001$ for all).

Both live and heat killed *H. pylori* led to significant increases in the expression of *KDM6B* (Figure 5.10.F). For example, at 3-hours, live bacteria

led to an increase of 23-fold (p<.001) while heat killed led to an increase of 26-fold (p<.001).

Taken together these data show that *H. pylori* decreases expression of PRC2 components *SUZ12* and *EED* in THP-1 cells. *H. pylori* increased *EZH2* at early points but decreased expression at 24 and 48-hours post-infection. For all PRC2 components live bacteria sustained reduction for longer than heat-killed bacteria. Both heat-killed and live bacteria significantly increased *KDM6B* expression in THP-1 cells.

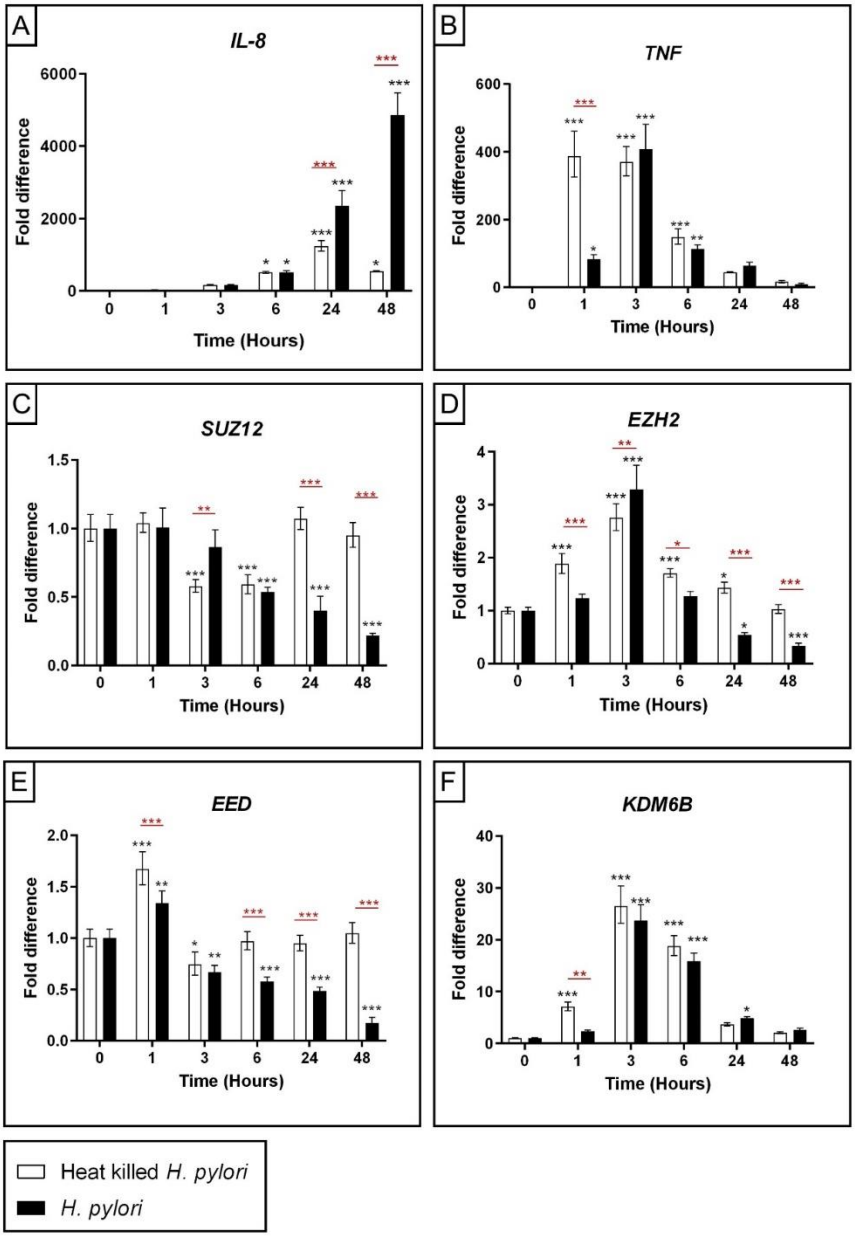

Figure 5.10 Expression of PRC2 components and *KDM6B* in THP-1 cells treated with heat killed *H. pylori* or infected with live *H. pylori*. THP-1 cells were seeded at $0.7X10^6$ cells per well and were differentiated to macrophages following standard procedure. The cells were infected with *H. pylori* strain 11638 for the time points indicated underneath the graphs. Total RNA was isolated and changes in *IL-8* (A), *TNF* (B), *SUZ12* (C), *EZH2* (D), *EED* (E) and *KDM6B* (F) gene expression was evaluated by RT-qPCR using the comparative cycle threshold method. Results were normalized to *GAPDH* levels and expressed relative to uninfected cells at each time point. Data shown are means ± SD of triplicate determinants. A two-way Anova was performed for each gene. Šidák multiple comparison tests were used to compare mean values of treated samples with untreated samples (black asterisk) and to compare mean values between live and heat-killed samples (red asterisk). * $P \leq 0.05$, ** $P \leq 0.01$, *** $P \leq 0.001$. Graphs are representative of three independent experiments.

5.4.6. Treatment of THP-1 cells with *H. pylori* LPS does not impact PRC2 expression as much as live *H. pylori.*

To investigate whether *H. pylori* LPS plays a role in the *H. pylori*-mediated effects on the expression of PRC2 components, differentiated THP-1 cells were also treated with *H. pylori* LPS from the reference strain 17874 at a concentration of 100ng/ml or 1μg/ml (Figure 5.11). At both concentrations of LPS there were significant increases in the expression of *IL-8* and *TNF* (Figure 5.11.A,B).

When treated with 100ng/ml of LPS, *SUZ12* was significantly upregulated at 48-hours (Figure 5.11.C). When treated with 100ng/ml LPS, *EZH2* was significantly downregulated at 6-hours (0.5-fold, p=.018) (Figure 5.11.D). When treated with 1μg/ml of LPS there was no significant change in *EZH2* expression. *EED* was significantly increased at the 24 and 48-hour time points when treated with 100ng/ml LPS (Figure 5.11.E). When treated with 1μg/ml LPS there was no significant change in *EED* expression. Taken together, these finding show *H. pylori* LPS does not play a strong role in the *H. pylori*-mediated changes in PRC2 component expression in THP-1 cells.

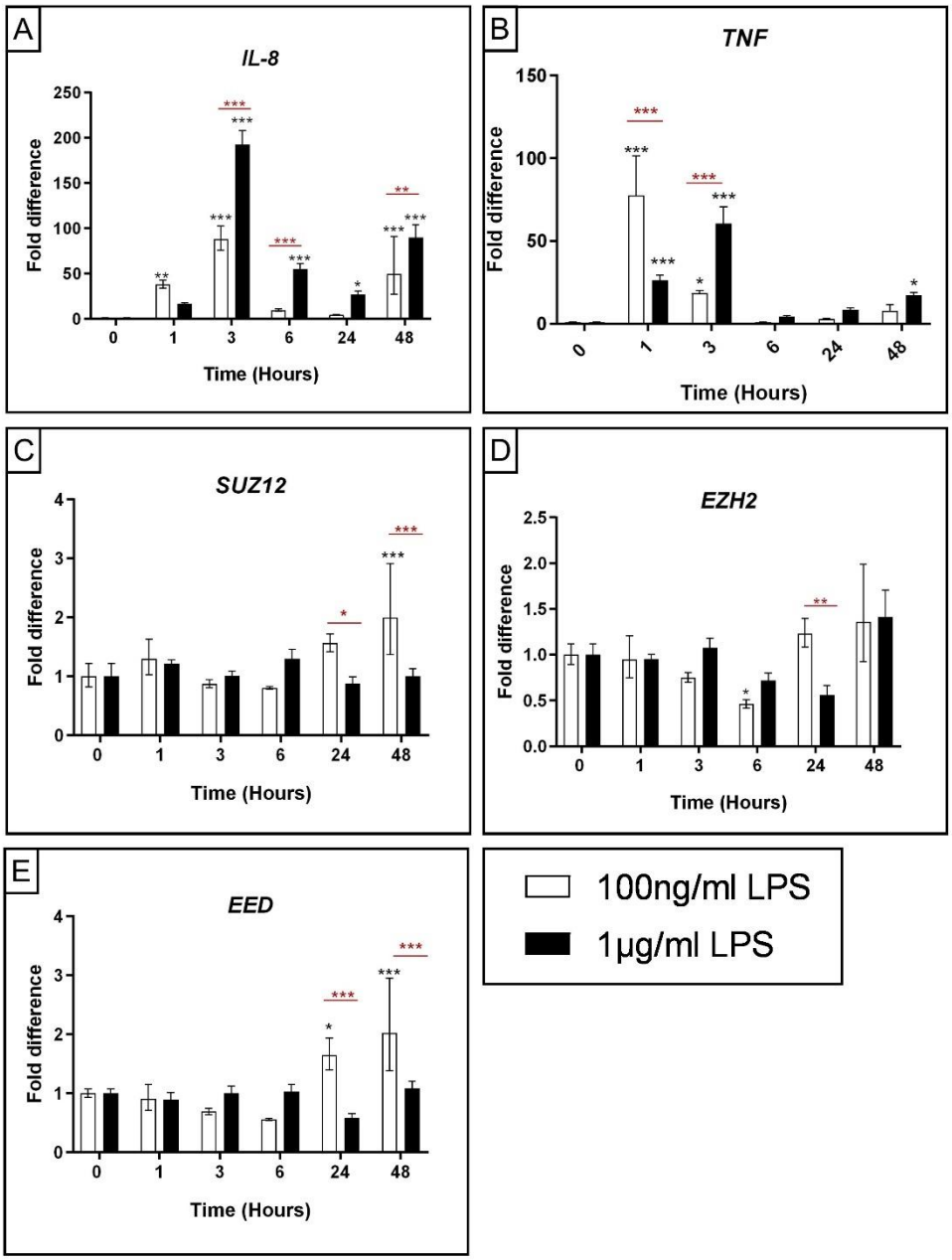

Figure 5.11 Expression of PRC2 components in THP-1 cells treated with *H. pylori* LPS. THP-1 cells were seeded at a concentration of $0.5x10^6$ cells/well in a 12 well plate and differentiated to macrophages following standard procedure. The cells were treated *H. pylori* LPS from the reference strain 17874 at a concentration of 100ng/ml or 1µg/ml for the time points indicated underneath the graphs. Total RNA was isolated and changes in *IL-8* (A), *TNF* (B), *SUZ12* (C), *EZH2* (D) and *EED* (E) gene expression was evaluated by RT-qPCR using the comparative cycle threshold method. Results were normalized to *GAPDH* levels and expressed relative to uninfected cells at 0-hour or 48-hours. Data shown are means ± SD of triplicate determinants. Two-way Anova were performed for *H. pylori* LPS treated cells. Šidák multiple comparison tests were used to compare mean values of treated samples with untreated samples (black asterisk) and to compare mean values between concentrations of LPS (red asterisk). * P≤0.05, ** P≤0.01, *** P≤0.001. Graphs are representative of three independent experiments.

5.4.7. New protein synthesis is not required for the *H. pylori*-mediated induction of *KDM6B* in THP-1 cells.

To determine whether new protein synthesis is required for the *H. pylori* mediated changes in *KDM6B* in THP-1 cells, the cells were treated for 1-hour with 20 μg/ml cycloheximide prior to *H. pylori* infection.

As expected, infection with *H. pylori* led to increases in *IL-8* and *TNF* expression in THP-1 cells (Figure 5.12.A-B). Cycloheximide treatment alone increased the expression of *IL-8* and *TNF* at all time points tested. In line with results using AGS cells (Figure 5.9), cycloheximide combined with *H. pylori* infection led to significant increases in expression of *IL-8* and *TNF* compared to either of these conditions alone. Blocking translation in the presence of *H. pylori* increased the expression of pro-inflammatory cytokines, which may suggest that a protein is synthesized in macrophages following *H. pylori* infection to dampen the effect of the bacteria on *IL-8* and *TNF* expression.

KDM6B expression was increased when THP-1 cells were infected with *H. pylori* (Figure 5.12.C). Cycloheximide treatment alone statistically significantly increased the expression of *KDM6B* in THP-1 cells at 3 and 6-hour time points. Combined treatment with cycloheximide and infection with *H. pylori* significantly increased expression of *KDM6B* compared to untreated cells. At 6 hours, *KDM6B* induction was significantly higher in the presence of both *H. pylori* and cycloheximide than with cycloheximide alone ($p<.001$) or infection with *H. pylori* alone ($p<.001$) (Figure 5.12C). As the *H. pylori*-mediated induction of *KDM6B* was intact in the presence of the protein synthesis inhibitor, this suggests *KDM6B* is a direct transcriptional target of *H. pylori* in THP-1 cells.

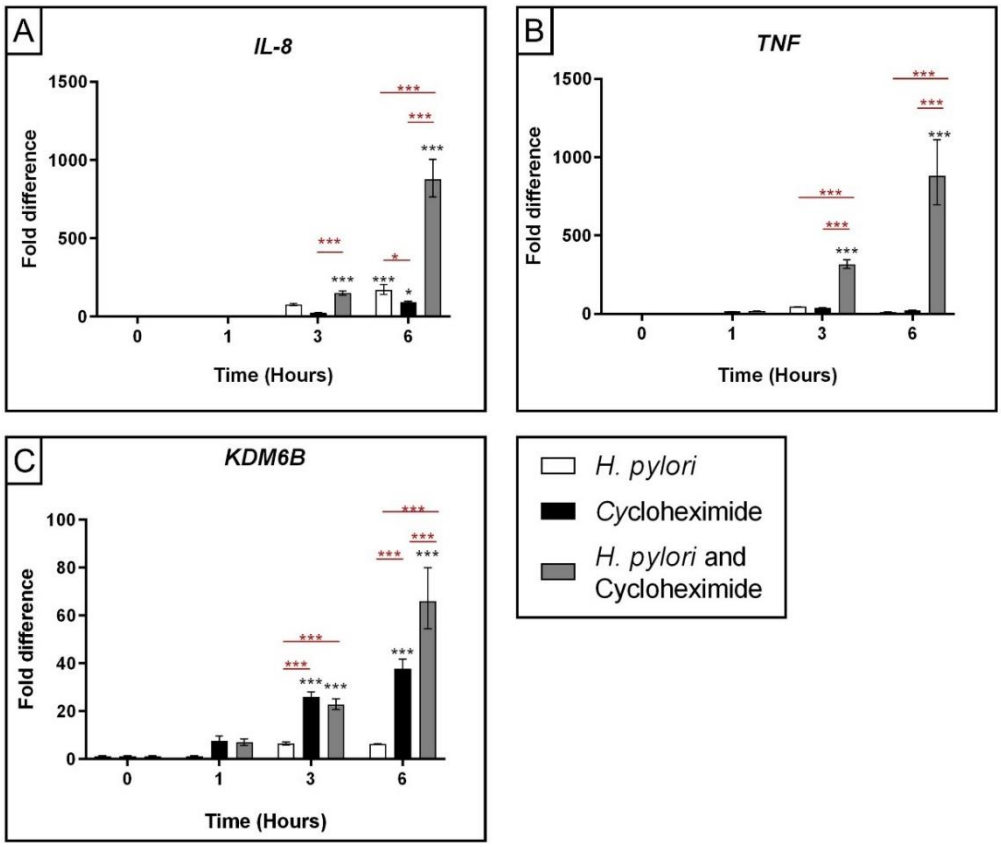

Figure 5.12 Expression of KDM6B in THP-1 cells treated with cycloheximide and infected with *H. pylori*. THP-1 cells were seeded at 0.75x10^6 cells per well and differentiated to macrophages following standard procedure. Subsequently, the cells were treated for 1-hour with 20 µg/ml cycloheximide and infected with 100 MOI of *H. pylori* strain 11638 for the time points indicated underneath the graphs. Total RNA was isolated and changes in *IL-8* (A), *TNF* (B), *KDM6B* (C) gene expression was evaluated by RT-qPCR using the comparative cycle threshold method. Results were normalized to *GAPDH* levels and expressed relative to uninfected cells at each time point. Data shown are means ± SD of triplicate determinants. A two-way Anova was performed for each gene. Dunnett's multiple comparison test was used to compare mean values of each sample with the untreated sample (*H. pylori* 0-hour) (black asterisk). Tukey's multiple comparison test was used to compare mean values of each treatment to every other treatment at each time-point (red asterisk). * P≤0.05, ** P≤0.01, *** P≤0.001. Graphs are representative of three independent experiments.

5.5. Caspase-11 contributes to IL-1ß expression in *H. pylori* infected BMDMs.

5.5.1. Caspase-4 mRNA expression in gastric epithelial cells and the gastric mucosa is not altered by H. pylori infection.

To investigate if *H. pylori* mediates changes in *Caspase-4* gene expression in gastric epithelial cells or the gastric mucosa, RT-qPCR was performed using RNA isolated from AGS cells infected with *H. pylori* or gastric biopsy tissue. For tissue analysis, antral biopsy samples were collected from 24 *H. pylori* infected and 15 uninfected control patients. Patients were considered infected if they tested positive for two out of three diagnostic tests: the RUT, histopathologic examination of the biopsy specimen and culture of the bacteria. Histology reported gastritis in all infected patients, but none of them had more developed pathology.

As expected, *H. pylori* significantly induced *IL-1B* mRNA expression in AGS cells (At 6-hours, 2-fold, p=.02) (Figure 5.13.A). However, infection did not significantly or consistently change *Caspase-4* mRNA expression across 3 independent experiments (representative image shown in Figure 5.13.B). Significant upregulation of *IL-1B* mRNA expression was also seen in stomach tissue samples from the *H. pylori* infected group compared to the uninfected control group (p=.0027, Figure 5.13.C). In line with the observations using AGS cells, there was no change in the expression of *Caspase-4* in samples from the infected versus uninfected group (p=.35, Figure 5.13.D).

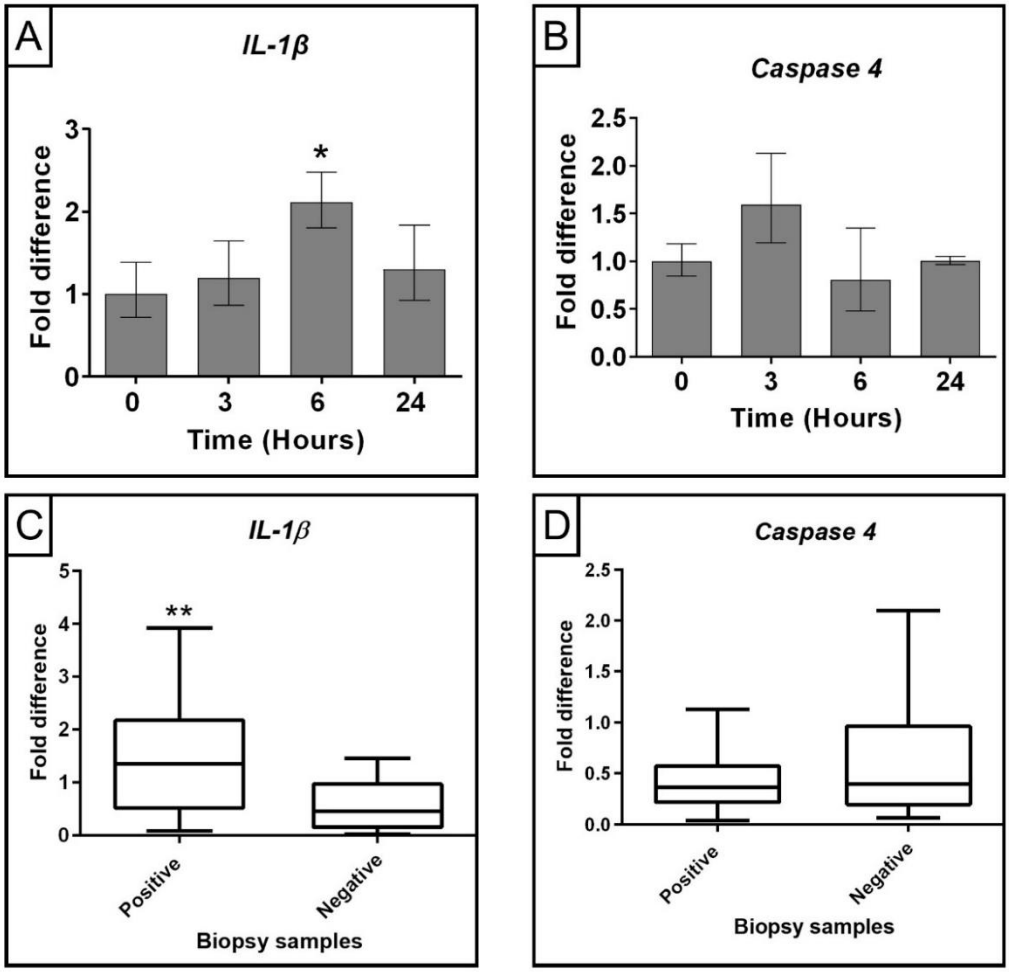

Figure 5.13 Expression of *IL1B* and *Caspase-4* in gastric epithelial cells and biopsy tissue from *H. pylori* positive patients and uninfected controls. Total RNA was purified from AGS cells infected with *H. pylori* for the time points indicated underneath the graph (A, B) and from antral biopsies of 24 *H. pylori*- infected patients (positive) and 15 uninfected controls (negative) (C, D). Changes in *IL1B* (A, C) and *Caspase-4* (B, D) mRNA expression were evaluated by RT-qPCR using the comparative cycle threshold method. Results were normalized to *GAPDH* levels and are expressed relative to uninfected cells (A, B) or a sample in the uninfected control group (C, D). A one-way Anova with Dunnett's multiple comparison-test and Mann-Whitney test were used to compare results from cell culture and biopsy experiments, respectively. Cell culture data are representative of 3 independent experiments. ***** $P \leq 0.05$. ** $P \leq 0.01$.

5.5.2. *Caspase-4* is upregulated in macrophages infected with *H. pylori.*

Next the *H. pylori*-mediated regulation of *Caspase-4* was investigated in human macrophages using PMA-differentiated THP-1 cells. As a positive control, THP-1 macrophages were treated with 1µg/ml *E. coli* LPS which is known to trigger upregulation of Caspase-4 and the non-canonical inflammasome (Sanchez-Garrido et al., 2020, Kayagaki et al., 2013). As expected, significant upregulation of the cytokine *IL1B* was seen 3-hours post LPS treatment (Figure 5.14.A). *E. coli* LPS also led to significant upregulation of *Caspase-4* at the 3-hour time point (1.5-fold, p=.006). This response was reversed at 6 and 24-hours (Figure 5.14.B).
Following infection of THP-1 cells with *H. pylori*, increased expression of *IL1ß* was observed at all time points (Figure 5.14.C). Expression increased over time, with the highest level observed at 24-hours post-infection (28-fold). Furthermore, *H. pylori* infection led to a significant upregulation of *Caspase-4*, with a maximum induction seen 3-hours following infection (1.6-fold, p=.001; Figure 5.14.D).

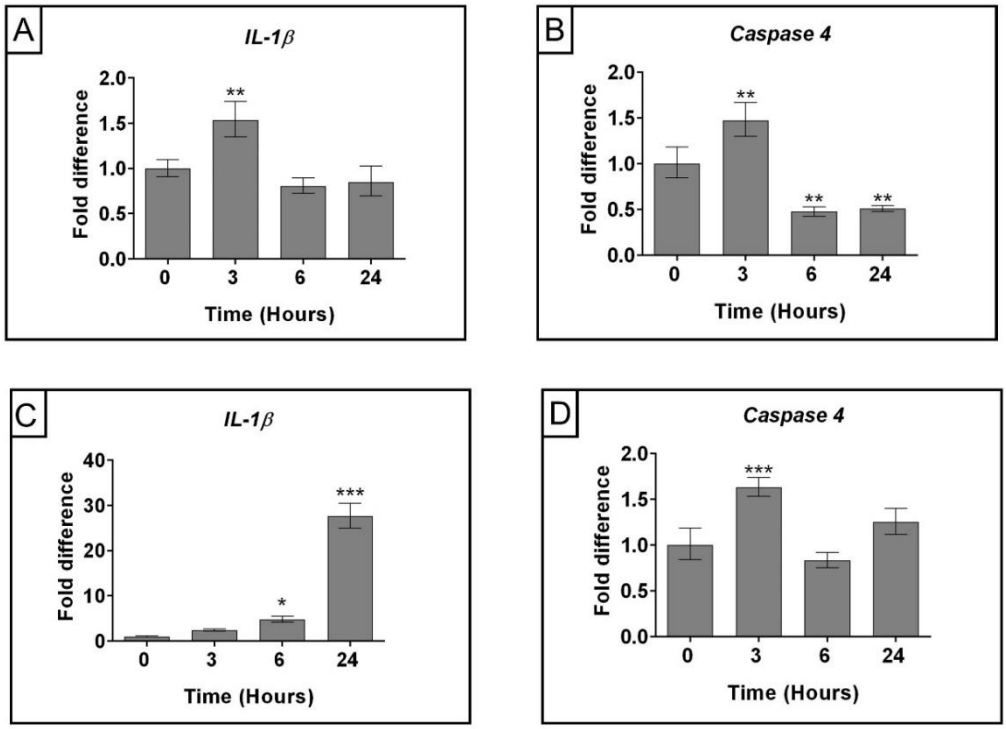

Figure 5.14 Expression of *IL1β* and *Caspase 4* in THP-1 cells treated with *E. coli* LPS or live *H. pylori.* Differentiated THP-1 macrophages were stimulated with 1 µg/ml *E. coli* LPS (A, B) or infected with *H. pylori* strain 11638 (C, D) for the time points indicated underneath the graph. Total RNA was isolated and changes in *IL1B* and *Caspase-4* gene expression were evaluated by RT-qPCR using the comparative cycle threshold method. Results were normalized to *GAPDH* levels and expressed relative to untreated or uninfected cells. Data shown are means ± SD of triplicate determinants. One-way Anova tests with Dunnett's multiple comparisons were used to compare gene expression to uninfected samples. Graphs are representative of three independent experiments. $P \leq 0.05$, ** $P \leq 0.01$, *** $P \leq 0.001$.

5.5.3. Caspase-11 contributes to IL-1ß production in murine macrophages.

This work was performed as part of a collaborative project with Dr. Emma M. Creagh, Trinity Biomedical Science Institute (TBSI), Trinity College Dublin. Isolated Bone marrow-derived macrophages (BMDMs) were provided by Ewelina Flis from the Creagh laboratory. Western blots and ELISA were performed in collaboration with Ewelina Flis.

Before commencing, prior ethical approval from the Trinity College Dublin Animal Research Ethics Committee was granted. C57BL/6J background mice were bred under sterile pathogen-free conditions at the TBSI animal facility. WT and *Casp11*$^{-/-}$ bone marrow–derived macrophages (BMDM) were isolated from the femurs and tibiae of 8-to-12-week-old female mice. BMDMs were isolated and cultured in 20% L929 for six days. Following this, cells were plated for plated for in vitro infection with *H. pylori*. Three independent in vitro infection experiments were carried out.

To identify the role of the murine Caspase-4 homolog, Caspase-11, in IL-1ß production during *H. pylori* infection, BMDM cells were isolated from wild-type (WT) and Caspase-11 deficient mice (Casp11-/-). In line with the *H. pylori* mediated increase in Caspase-4 mRNA levels observed in THP-1 cells (Figure 5.14), WT BMDM infected with *H. pylori* demonstrated an increase in Caspase-11 protein expression, particularly at 24 and 48-hours post-infection as seen by western blotting (Figure 5.15), (Figure 5.16). As anticipated, Caspase-11 was absent from the Casp11-/- cells (Figure 5.15), (Figure 5.16). *H. pylori* also induced expression of pro-IL-1ß at 6, 24, and 48-hours post infection in WT BMDM. BMDM from Casp-11-/- mice had decreased ability to upregulate pro–IL-1ß and expressed lower levels of mature Caspase-1 when compared with WT BMDM infected with *H. pylori*, demonstrating that Caspase-1 expression and pro-IL-1ß production in response to *H. pylori* infection is partially mediated by Caspase-11.

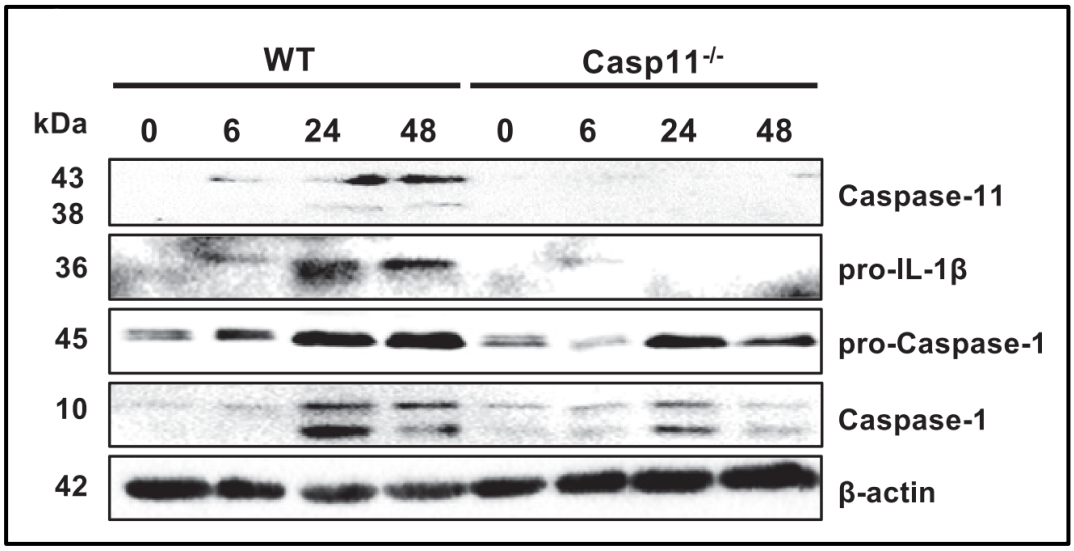

Figure 5.15 Caspase 11, pro-IL-1ß, pro-Caspase-1 and Caspase 1 expression in WT and Caspase 11$^{-/-}$ BMDMs following *H. pylori* infection. Immunoblot analysis of wild type and Caspase 11-deficient BMDM infected with *H. pylori* strain 11638 for a 48-hour time course. ß-actin was used as a control. Results representative of three independent experiments.

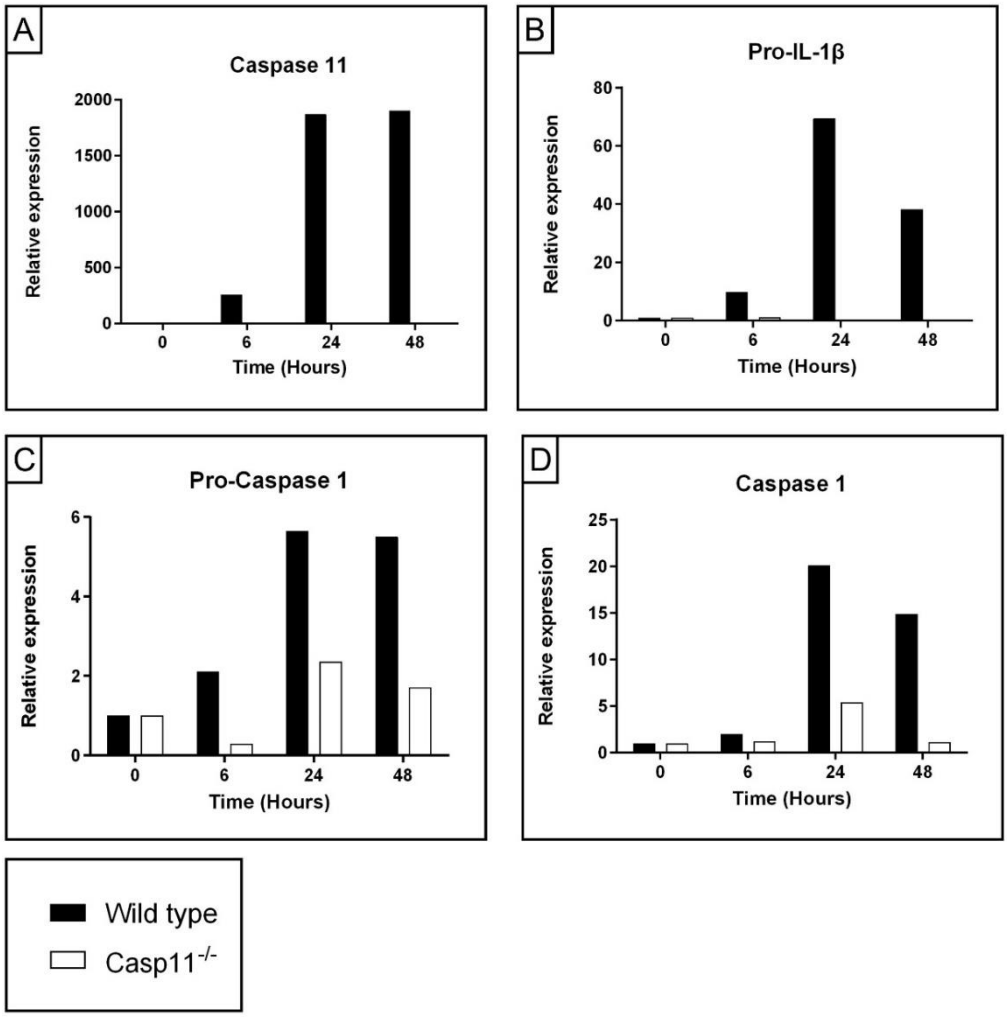

Figure 5.16 Densitometry graphs for Caspase 11, pro-IL-1ß, pro-Caspase-1 and Caspase 1 expression in WT and Caspase 11$^{-/-}$ BMDMs following *H. pylori* infection. Immunoblot analysis of wild type and Caspase 11-deficient BMDM infected with H. pylori strain 11638 for a 48-hour time course. ß-actin was used as a control. Band intensities from (Figure 5.15) were quantitated using ImageJ software. Band intensities for Caspase-11 (A), pro-IL-1B (B), pro-Caspase-1 (C) and Caspase-1 (D) were normalised to ß-actin band intensities and expressed relative to time 0. Results are representative of three independent experiments.

Activated Caspase-1 can cleave pro-IL-1ß into its mature form. IL-1ß then acts to induce the host immune response including release of inflammatory cytokines. To observe if the BMDM from WT mice were producing more enzymatically active Caspase-1 resulting in more IL-1ß maturation, release of IL-1ß was measured by ELISA in the cell supernatant of infected cells. Following 24 hours of *H. pylori* infection Casp11$^{-/-}$ BMDM cells expressed significantly less IL-1ß compared to WT cells (Figure 5.17). Taken together,

these findings suggest a role for Caspase-1 and Caspase-11 in the *H. pylori*-mediated production of IL-1ß in murine macrophages.

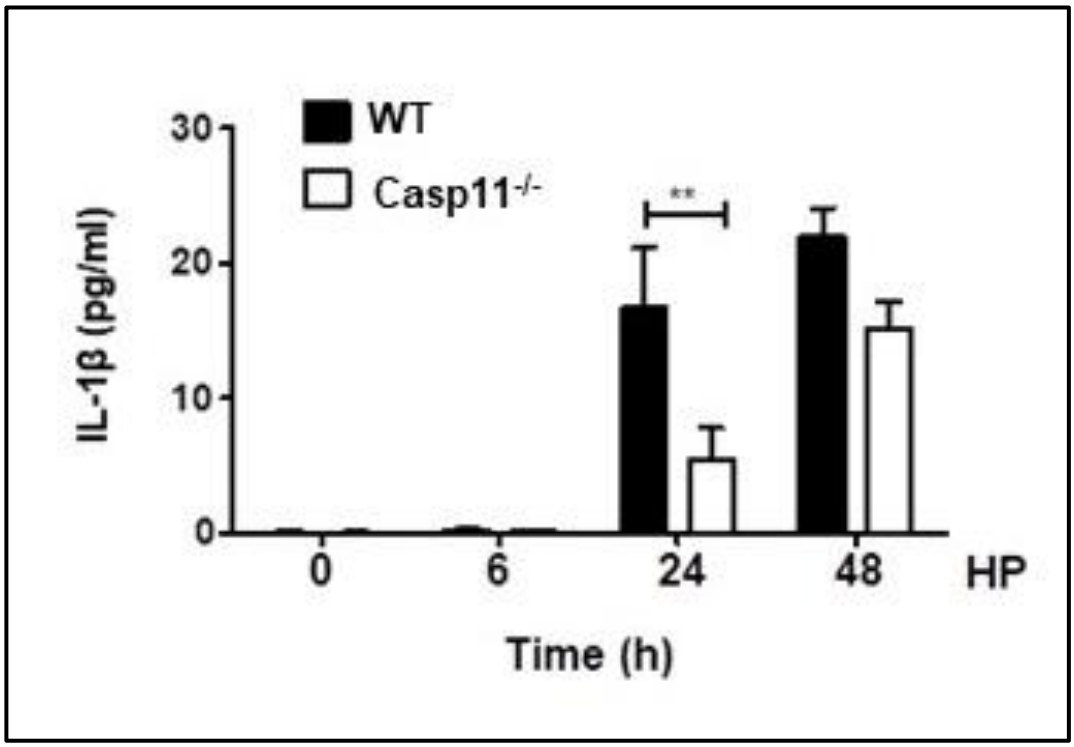

Figure 5.17 Caspase-11 is involved in *H. pylori*-mediated secretion of IL-1ß from BMDMs. Wild type and Caspase-11 deficient BMDM were infected with *H. pylori* strain 11638 for 48 hours. Cells supernatants were analysed for IL-1ß section by ELISA. The values represent the mean ± SEM. A two-way ANOVA was used to compare the mean values of WT and Caspase $11^{-/-}$ BMDM.

5.6. Discussion

5.6.1. *H. pylori* infection decreases *EED* expression in gastric epithelial cells, the gastric mucosa, and THP-1 macrophages.

H. pylori significantly decreased *SUZ12*, *EZH2* and *EED* mRNA expression in MKN45 gastric epithelial cells. In AGS cells, *SUZ12* and *EED* were reduced in a transient manner. Likewise, there was a trend of decreased *SUZ12* and *EZH2* expression in the gastric mucosa of *H. pylori* infected chronic gastritis patients, but this was not statistically significant at the numbers tested. However, in samples from *H. pylori* infected patients with chronic gastritis compared to uninfected controls, a statistically significant decrease in *EED* expression was observed.

In the past, progressive increases in EZH2 protein have been shown to correlate with disease severity in gastric biopsy tissue (Cai et al., 2010). EZH2 levels were lowest in normal control tissues followed by non-atrophic gastritis, chronic atrophic gastritis, intestinal metaplasia, and finally the largest expression was observed in dysplasia and carcinoma tissue (Cai et al., 2010). Similarly, *H. pylori* associated gastritis and carcinoma tissue were shown to be associated with higher EZH2 expression than normal mucosa (Purkait et al., 2022). Likewise, EED was shown to be upregulated in biopsy tissue from patients with gastric cancer (Bilgiç et al., 2018). However, to the best of our knowledge this is the first study to report down-regulation of *EED* in the gastric mucosa of *H. pylori* infected patients. It is possible that *EED* is only upregulated later in *H. pylori*-mediated disease progression. This may explain why our cohort of patients, who did not have severe disease at the time of endoscopy, had significantly downregulated *EED*.

Additional data from the Smith lab using ChiP-qPCR demonstrated that in line with the functional role of PRC2 in gene silencing, decreased expression of PRC2 components in AGS cells was associated with decreased accumulation of H3K27me3 and increased RNA polymerase II at the transcriptional start site of the *IL-8* gene. Low levels of polymerase II and high levels of H3K27me3 were observed at the transcriptionally silent myoglobin B gene (FitzGerald, 2021). This indicates that changes in histone methylation may be involved in the response to *H. pylori* by enabling transcription of the *IL-8* gene. It would be interesting to monitor H3K27me3 at other gene promoters by ChIP-seq to identify further targets of this pathway during *H. pylori* infection.

To the best of our knowledge, there has yet been no published data on PRC2 expression in response to *H. pylori* in macrophages. *H. pylori* infection led to a time-dependent decrease in *SUZ12* and *EED* expression in THP-1 cells and live bacteria were required for this effect. *EZH2* expression was transiently up-regulated in THP-1 cells, followed by significant reduction at 24 and 48 hours. Live *H. pylori* had a more extreme impact on *EZH2* regulation than heat killed bacteria. *H. pylori* LPS did not play a strong role in the *H. pylori*-mediated regulation of the PRC2 components in THP-1 cells. It is possible this is triggered by virulence factors such as VacA or CagA, or indeed other bacterial components. Further research into host-pathogen interactions would be needed to identify the mechanism of action.

5.6.2. *H. pylori* induces expression of *KDM6B* in gastric epithelial cells, the gastric epithelium, and macrophages.

In Chapter 4 of this study, *KDM6B* was identified by RNAseq as a gene whose expression was increased in AGS cells in response to *H. pylori*. In the published literature, KDM6B expression has been shown to be increased in gastric cancer tissue compared to normal controls and high levels of KDM6B expression were associated with a poor prognosis (Liu et al., 2022). A KDM6B inhibitor (GSK-J4) reduced the proliferation of AGS and MKN45 cells, suggesting that KDM6B is involved in gastric cancer cell proliferation and tumour formation. RNAseq on MKN45 cells comparing WT and KDM6B knockdown, and analysed by pathway enrichment analysis, demonstrated altered signalling pathways including the Wnt pathway, MAPK pathway and JAK-STAT pathway (Liu et al., 2022).

In this Chapter, RT-qPCR confirmed the RNAseq observation that *H. pylori* induces *KDM6B* in AGS cell and experiments using cycloheximide suggest *KDM6B* is a direct transcriptional target of *H. pylori*. Furthermore, *H. pylori* significantly increased *KDM6B* expression in MKN45 cells and in the gastric epithelium of infected patients with chronic gastritis. Towards the end of this research project, a paper was published showing that MKN45 and AGS cells infected with *H. pylori* for between 2 and 8 hours significantly upregulated *KDM6B* expression. Furthermore, *H. pylori* positive gastric cancer samples had significantly upregulated KDM6B compared to *H. pylori* negative tissue (Liu et al., 2022). The data in this chapter expands on the results by Liu et al. by showing that heat killed *H. pylori* can also significantly increase *KDM6B* expression in gastric epithelial cells. However, an equivalent number of live bacteria induced significantly higher levels of *KDM6B.* This would suggest that *H. pylori* may be capable of impacting *KDM6B* expression by two mechanisms, one that can be triggered by the cells recognising and responding to PAMPs such as LPS. The second

method requires the live bacteria and may be conferred via a virulence factor such as CagA that needs viable bacteria to be injected into host cells via the type IV secretion system.

To the best of our knowledge, there has yet been no published data looking at *KDM6B* expression in response to *H. pylori* in macrophages. *H. pylori*-mediated increases in *KDM6B* expression were observed in THP-1 macrophage cells, indicating that *H. pylori* can induce increased *KDM6B* expression in multiple cell types. In addition, cycloheximide experiments suggest that *KDM6B* is a direct transcriptional target in macrophages, as well as epithelial cells.

In resting myeloid cells, many loci for inflammatory genes have a closed chromatin structure associated with low levels of histone acetylation (Netea et al., 2016). Following infection, these loci develop open chromatin configuration associated with high levels of histone acetylation (Netea et al., 2016). In *E. coli* LPS treated macrophages *KDM6B* is recruited to the transcriptional start sites of thousands of genes, including those associated with an LPS triggered immune response including cytokines such as *IL6* and *TNFa* (De Santa et al., 2009). The combined reduction in PRC2 components and increase in *KDM6B* that is seen when infected with *H. pylori* would suggest infection with *H. pylori* is associated with active gene transcription. Further research would be required to identify the targets of this activated transcription. While this work is still in its preliminary stage the most compelling result from these experiments is the sharp increase in *KDM6B* expression in macrophage cells infected with *H. pylori* or treated with heat killed *H. pylori*. Future work would expand on this finding, for example, infecting cells that have had KDM6B knocked down with *H. pylori* and looking for targets via RNA sequencing or proteomics. It also puts forward questions about the downstream impacts of histone modification, such as which gene loci are altered due to *H. pylori* mediated chromatin conformational changes?

5.6.3. Caspase-11 plays a role in IL-1β expression in *H. pylori* infected BMDMs.

The innate immune system is a first line of defence against invading pathogens. A core component of the innate immune system is the generation of canonical and non-canonical inflammasome complexes (Fernández and Lamkanfi, 2015). Caspase-1 and Caspase-11 are essential for the formation of these respective complexes. As a result, Caspase-1 and Caspase-11 regulate secretion of pro-inflammatory cytokines and trigger a pro-inflammatory form of cell death known as pyroptosis (Fernández and Lamkanfi, 2015).

IL-1β is upregulated during *H. pylori* infection and has been associated with *H. pylori* associated gastritis and gastric cancer for decades (Pachathundikandi et al., 2020, El-Omar et al., 2000). Mice that are deficient in IL-1 are easily colonised by *H. pylori* due to the lack of Th1 and Th17 response (Koch and Müller, 2015). Transgenic mice that overexpress IL-1β in the gastrointestinal tract develop gastric inflammation and cancer (Koch and Müller, 2015, Tu et al., 2008). Polymorphisms in the *IL-1β* gene coincide with an increased risk of gastric cancer (El-Omar et al., 2000, Hong et al., 2016). For these reasons, it is important to fully understand how *H. pylori* regulates IL-1β.

Caspase 4 is an inflammatory caspase involved in non-canonical inflammasome production and pyroptotic cell death (Man et al., 2017). In epithelial cells and gastric biopsy tissue, *H. pylori* did not alter *Caspase-4* mRNA expression, suggesting that Caspase-4 is not involved in the *H. pylori* mediated regulation of IL-1β in the gastric epithelium. It is possible that Caspase-1 alone is contributing to IL-1β release in gastric epithelium infected with *H. pylori* that has been observed in the published literature (Koch and Müller, 2015, Pachathundikandi et al., 2020). Although there was no upregulation of Caspase-4 in the epithelial tissue of patients infected

with *H. pylori* compared to uninfected controls in the current study, increased Caspase-4 has been reported in peptic ulcer tissue (Yaguchi et al., 2010). Zasłona et. al. also found that antral biopsy tissue from peptic ulcer patients had significant upregulation of Caspase-4 (Zasłona et al., 2020a). Interestingly, and in line with the results presented in this study, analysis of a published data set by Zasłona et al. found there was no significant difference in Caspase-4 expression in patients with normal compared to mild *H. pylori*-associated gastritis, but there was a significant difference between severe *H. pylori*-associated gastritis and normal tissue (Zasłona et al., 2020a). So, it is possible that Caspase-4 and the non-canonical inflammasome are only activated later in *H. pylori*-mediated disease progression. This may explain why our cohort of patients, who did not have severe disease at the time of endoscopy, did not show significant upregulation for Caspase-4. Since macrophage cells showed a stronger signal for *H. pylori*-mediated Caspase-11/4 induction the rest of this chapter focussed on these cells.

E. coli LPS was used as a positive control for inflammatory responses in macrophages as it has previously been shown that THP-1 cells triggered by LPS will induce IL-1ß in a TRAF6-Caspase-4 dependent manner (Lakshmanan and Porter, 2007). There was comparable upregulation of *Caspase-4* mRNA expression in THP-1 cells that were treated with *E. coli* LPS or infected with *H. pylori* in the current study. Despite this, unpublished data from the Creagh laboratory showed that *H. pylori* LPS alone was not sufficient to induce Caspase-4 upregulation in THP-1 cells. *H. pylori* LPS is mutated to have a tetra-acyl lipid A moiety with long carbon fatty acid chains that can avoid the host's immune response and has less endotoxic properties compared to the LPS of other gram negative bacteria such as *E. coli* (Smith, 2014, Kayagaki et al., 2013). It is possible that other *H. pylori* components play a role in Caspase-4 upregulation in macrophages. It has been shown that activation of the Caspase-1 mediated NLRP3 inflammasome by *H. pylori* in murine dendritic cells requires VacA and

CagA virulence factors (Sanchez-Garrido et al., 2020, Zhang et al., 2022, Kim et al., 2013). Additionally, the Urease B subunit is associated with activating the NLRP3 inflammasome via TLR2 and MyD88 in dendritic cells infected with *H. pylori* (Koch and Müller, 2015).

Since pro-IL-1ß was upregulated by *H. pylori* in WT BMDM in the western blot it would suggest that *H. pylori* infection is sufficient to induce a priming signal to upregulate pro-IL-1ß. Since the ELISA measured an increase in mature IL-1ß following *H. pylori* infection this would indicate *H. pylori* can trigger inflammasome production. This means that *H. pylori* can produce both signals required for IL-1ß release. However, there have been some data pointing to a different mechanism in human macrophages where *H. pylori* could only produce a very weak second signal for canonical NLRP3 accumulation. The addition of coactivators such as Nigericin or ATP were required for substantial release of mature IL-1ß (Pachathundikandi et al., 2020). This may indicate the method which *H. pylori* induces the canonical or noncanonical inflammasome may differ depending on cell type and species.

The ELISA showed that significantly more mature IL-1ß was produced in WT compared to Casp11$^{-/-}$ cells, implying a role for Caspase-11 and the noncanonical inflammasome in *H. pylori* mediated IL-1ß release in murine macrophages. Interestingly, the western blot showed that infection with *H. pylori* in the WT cells led to an increase in pro-IL-1ß that was absent in the Casp11$^{-/-}$ cells. It is possible this may be due to a positive feedback loop where increased mature IL-1ß triggers more pro-IL-1ß to be produced.

Previous research has primarily focused on *H. pylori*-mediated induction of Caspase-1 and the canonical activation. This work shows that Caspase-11 and the non-canonical inflammasome are at least partially responsible for IL-1ß release in *H. pylori*-infected macrophages. Since IL-1ß dysregulation is associated with more severe *H. pylori* driven disease states, targeting

inflammatory caspases such as Caspase-4 may offer an avenue of research for host-directed therapies.

5.7. Summary of Conclusions

H. pylori significantly decreased the expression of the PRC2 components; *SUZ12*, *EZH2* and *EED* in MKN45 gastric epithelial cells. *H. pylori* was associated with a transient decrease of *SUZ12* and *EED* in AGS cells and a significant decrease in *EED* expression in gastric biopsy tissue. In macrophages *H. pylori* infection led to a time-dependent decrease in *SUZ12* and *EED* expression while *EZH2* expression was transiently up-regulated followed by a significant reduction at 24 and 48 hours.

KDM6B was consistently significantly upregulated with a high fold change in gastric epithelial cells, the gastric mucosa and THP-1 macrophages infected with *H. pylori*. This leads to the hypothesis that *KDM6B* histone demethylase is a key driver of *H. pylori* mediated histone modification that warrants further investigation, especially in the context of macrophage responses where data are currently lacking.

H. pylori infection led to an increase in pro-IL-1ß protein in WT BMDM. Additionally, significantly more mature IL-1ß was produced in WT compared to Casp11$^{-/-}$ BMDM cells. This suggests a role for Caspase-11 and the noncanonical inflammasome in *H. pylori* mediated IL-1ß release in murine macrophages.

5.8. Future Work

The novel findings in this research open the possibility for further research if time and funding permit.

- Perform PRC2 and *KDM6B* loss- and gain-of-function studies to identify downstream effects of histone modification during *H. pylori* infection. Pharmacological inhibitors, siRNA or CRISPR/Cas9 approaches could be utilised for loss-of-function studies and over-expression by plasmid transfection for gain-of-function studies.
- Infecting cells with various isogenic mutant strains of *H. pylori* may identify the specific virulence factor(s) that are required for alteration of PRC2 and *KDM6B*.
- Evaluating whether SNPs in PRC2 genes and/or KDM6B are associated with the risk of more-severe *H. pylori*-associated disease.
- Investigate genome-wide targets by performing H3K27me3 ChIP-sequencing before and after *H. pylori* infection.
- Confirm the *H. pylori*-mediated Caspase-11 upregulation that was seen in BMDM and the Caspase-4 upregulation observed in THP-1 cells using primary human macrophages. In addition, the role of Caspase-4 in the regulation of IL-1ß in human macrophages could be evaluated using a Caspase-4 loss-of-function approach (with either RNAi or CRISPR) in THP-1 cells or primary human macrophages.
- Generate an in vivo *H. pylori* infection model comparing WT and Casp11$^{-/-}$ mice to further investigate whether Caspase-11 plays a role in the pathogenesis of *H. pylori* infection. Experiments could include measuring the bacterial load in the stomach between *H. pylori* infected WT and casp11$^{-/-}$ mice, evaluating inflammation in the stomachs of these mice by histology and measuring IL-1ß in stomach biopsies and serum samples.

- Infect gastric epithelial cells with other types of bacteria from the gastric microbiome to see if they can also alter the expression of inflammatory caspases and histone modifying components.

Chapter Six General Discussion

6.1. Introduction

H. pylori is a gram negative bacterium that chronically infects the gastric epithelium of approximately 50% of the global population, making it one of the most prevalent bacterial infections in the world (Salama et al., 2013). Most infections are asymptomatic, however, infected individuals have a 1-10% risk of developing duodenal or gastric ulcers, a 0.1-3% risk of gastric carcinoma and a 0.01% risk of developing MALT (McColl, 2010). *H. pylori* generates both an innate and adaptive immune response. However, this is not adequate to clear the infection. Treatments for *H. pylori* typically require 1-3 antibiotics, a PPI and occasionally bismuth. Increasing antibiotic resistance has made treating *H. pylori* a more complicated task in recent years. With many different treatment combinations possible, an optimal treatment plan should take into acount the prevalence of antimicrobial resistance, local eradication rates, patient compliance, adverse effects and antimicrobial stewardship (Malfertheiner et al., 2022).

6.2. Currently the management of *H. pylori* in Ireland falls short of the recommended eradication rate.

In 1997, the first Maastricht guidelines recommended a standard Triple-C+A therapy as the first line treatment for *H. pylori* (Malfertheiner et al., 1997). However, antibiotic resistance has grown substantially in the years since. The most recent Maastricht guidelines were published in 2022 and recommended that Triple-C+A therapy should only be used in areas where primary clarithromycin resistance is known to be <15% (Malfertheiner et al., 2022). Unfortunatley, meta-analysis from 65 different countries found that, in most WHO regions, *H. pylori* resistance rates to clarithromycin are >15% (Savoldi et al., 2018). In Europe, pooled resistance from 18 countries was found to be 21.4% for clarithromycin (Megraud et al., 2021). In Ireland, the most recent primary resistance rate was 25.6% for clarithromycin (Megraud et al., 2021). In Chapter 3 an audit of prescription and eradication patterns in Ireland from 2013-2022 was performed. Despite the high rates of clarithromycin resistance in the population, the audit found that in every year of the 10-year study Triple-C+A therapy was the most prescribed first line treatment. In total, 88% of prescriptions for first line treatments were for Triple-C+A therapy. Collectively first line treatments had an eradication rate of 80.1% and Triple-C+A has an eradication rate of 81% indicating that the total first line eradication rate is largely influenced by the overwhelming usage of Triple-C+A. The aim of any *H. pylori* treatment is to achieve an eradication rate of >90% (Fallone et al., 2016b). Unfortunately, current first line treatments in Ireland are falling short of this >90% goal.

The most recent Irish guidelines for the management of *H. pylori* were published in 2017. These recommended that if bismuth is unavailable, 14 day Triple-C+A therapy with a high dose PPI can be used as first line treatment (Smith et al., 2017a). From the audit in Chapter 3 it would

appear that most clinicians are following these recommendations and prescribing high dose PPI, Triple-C+A for 14 days as a first-line therapy. We found that high dose PPI and 14-day treatment were both associated with significantly improved eradication rates, compared to low dose and 7 days respectively. Recently, the international Maastricht VI consensus report was published. It is clear in its guidance that, in areas where primary clarithromycin resistance is unknown or >15%, bismuth quadruple is recommended as the first choice of treatment with non-bismuth quadruple concomitant therapy recommended if bismuth is unavailable locally (Malfertheiner et al., 2022). In the audit of first line therapies in Ireland there were no patients who received non-bismuth quadruple concomitant therapy therefore eradication rates in the Irish population are unknown. However, data from the Hp-EuReg found that out of 3,992 patients receiving quadruple concomitant therapy (PPI, clarithromycin, amoxicillin and metronidazole) there was a mITT eradication rate of 89.9% (Nyssen et al., 2021a). When only 14-day treatments were analysed the mITT eradication rate for non-bismuth quadruple concomitant therapy jumped to 92.1% (Nyssen et al., 2021a). If we assume similar eradication rates could be achieved in the Irish population switching from Triple-C+A to non-bismuth quadruple concomitant therapy could improve eradication rates and patient outcomes. However, the rate of dual primary resistance to both clarithromycin and metronidazole needs to be considered as concomitant therapy is negatively impacted by dual resistance to these antimicrobials (Malfertheiner et al., 2022).

Auditing the Irish data found that only 17 patients received bismuth quadruple therapy as a first line treatment. However, for 16 of those *H. pylori* was successfully eradicated, giving a first line eradication rate of 94.2%. This is similar to what is observed in Europe, with the three-in-one capsule+PPI achieving a mITT eradication rate of 94.5% in a cohort of 1,124 treatment naïve patients (Nyssen et al., 2021a). The data from both the Irish and European audits show that bismuth quadruple therapy is a

substantially better first line treatment compared to Triple-C+A and efforts should be made to improve the availability of bismuth in Ireland. Overall, the audit shows that most clinicians are following the 2017 Irish recommendations. However, these recommendations may need to be updated to correspond with the more recent Maastricht VI guidelines to improve eradication rates based on local data, such as those presented herein.

6.3. *H. pylori* disease progression is correlated with inflammation.

Gastric cancer occurs in a multistep process, preceded by a cascade of precancerous lesions (Correa and Piazuelo, 2012). The first sign identified is chronic gastritis, the disease may then progress in severity in the order of atrophic gastritis, intestinal metaplasia, dysplasia and finally gastric carcinoma (Wroblewski et al., 2010) (Uemura et al., 2001) (Correa and Piazuelo, 2012). The genotypes of the host (such as polymorphisms in IL-1), the bacteria (for example virulence factor genotypes) and environmental factors (such as high salt consumption) can influence disease progression (Pachathundikandi et al., 2016). Since the diseases associated with *H. pylori* infection are progressive, this means there are multiple stages for interventions that can limit progression. Ideally host-directed therapies could be developed either to manipulate the immune response to eradicate the bacteria or to halt the progression of mild disease preventing it from developing into more serious conditions. Disease progression is correlated with the severity of the host inflammatory response (Bodger and Crabtree, 1998) (Mandell et al., 2004). The expression of cytokines is a central factor determining the extent of gastric inflammation (Bodger and Crabtree, 1998). Identifying host factors that contribute to the inflammatory response will help with understanding the mechanisms behind disease progression (Mandell et al., 2004).

6.4. *H. pylori* alters expression of Notch pathway components in a cell type specific manner.

The Notch signalling pathway is a highly conserved signalling pathway involved in cell development, proliferation and differentiation (Bray, 2016) (Shang et al., 2016b). One of the best described Notch target genes is the transcription factor HES1. In Chapter 4 it was found that *H. pylori* infection in AGS and MKN45 gastric epithelial cells resulted in a significant reduction in *HES1* expression. Additionally, the expression of HES1 protein was decreased following *H. pylori* infection in AGS cells. Furthermore, gastric biopsy tissue from a cohort of *H. pylori* infected patients had lower *HES1* expression compared to uninfected controls. Following identification of *HES1* as a gene of interest, a gain-of-function approach was used to identify the implication of HES1 downregulation during *H. pylori* infection. Transfection with a *HES1* plasmid significantly increased the expression of HES1 in AGS cells at both the mRNA and protein level. RNAseq was used to identify genes that were impacted by HES1 overexpression in the context of *H. pylori* infection. Overexpression of HES1 led to a significant increase in the cytokines *IL-8* and *CCL20* compared to un-transfected cells or cells transfected with an empty vector plasmid.

Additionally, *H. pylori* infection led to a significant increase in *FOS*, a member of the transcription factor complex AP-1 with the highest increase in the HES1 overexpression group. This would suggest that HES1 downregulation is restraining the maximum induction of *FOS*, *IL-8* and *CCL20* in response to *H. pylori* infection. As IL-8 and CCL20 are involved in the recruitment of neutrophils and monocytes respectively, it is possible that the *H. pylori*-mediated down-regulation of HES1 and associated restraint in *IL-8* and *CCL20* induction favours bacterial survival by dampening down innate immune cell recruitment to the site of infection. This will be an area of future investigation within our laboratory.

In macrophages, live and heat-killed *H. pylori,* as well as *H. pylori* LPS, led to increases in the Notch ligands *JAG1* and *DLL4* and associated transcription factor *HEY1*. Recently Wen et. al. found that *H. pylori* infection led to increased expression of the Notch ligand *JAG1* in macrophages (Wen et al., 2021). This thesis builds on the findings of Wen et. al. by showing that heat killed *H. pylori* and *H. pylori* LPS is sufficient to induce upregulation of these genes.

Taken together, Chapter 4 demonstrates that *H. pylori* can alter expression of Notch pathways and associated transcription factors in a cell type specific manner. *H. pylori* mediated downregulation of HES1 in epithelial cells is associated with altering expression of the pro-inflammatory cytokines *IL-8* and *CCL20*.

6.5. *H. pylori* infection decreases expression of *EED* and increases expression of *KDM6B.*

DNA is closely compacted so that it can fit into the nucleus (Chen et al., 2017). Gene expression must be tightly regulated at all times. To allow transcription machinery access to specific regions of the genome, chromatin can swith between two conformations. Heterochromatin is a constricted conformation that prevents active transcription. The PRC2 complex modifies chromatin structure by methalating Lysine 27 on Histone H3 (H3K27me3) (Margueron and Reinberg, 2011, Laugesen et al., 2019). The mark H3K27me3 is seen as a characteristic feature of gene represssion. The PRC2 complex is composed of the core components; SUZ12, EED and EZH2 which are all required for the complex's catalytic activity (Laugesen et al., 2019). Euchromatin is a loosely bound conformation that allows access to trascription machinery, facilitating active gene transcription (Chen et al., 2017). Euchromatin is associated with monomethylation at H3K27. KDM6B is an enzyme that can specifically remove the trimethyl group from from H3K27 (Xiang et al., 2007). This means that KDM6B is associated with active gene transcription (Burchfield et al., 2015). *KDM6B* expression was shown to be increased in gastric cancer tissue compared to normal controls, additionally high levels of *KDM6B* was associated with a poor prognosis (Liu et al., 2022).

In Chapter 5 we demonstrated that *H. pylori* infection led to significant down-regulation of *EED* and a significant upregulation of *KDM6B* in MKN45 and AGS gastric epithelial cells and in THP-1 macrophages. As well as this, a significant decrease in *EED* and a significant increase in *KDM6B* expression was observed in gastric biopsy tissue from *H. pylori* infected patients. In macrophages, a similar fold difference in *KDM6B* expression was observed with both live and heat-killed bacteria. However, in epithelial cells the impact of heat-killed bacteria was much diminished and live

infection led to significantly higher *KDM6B* expression at every time point. This would suggest that *H. pylori* can possibly alter *KDM6B* expression by two mechanisms, one that can be triggered by extracellular signals, potentially involving the cell's PRRs recognising and responding to PAMPs such as LPS. The second method requires the live bacteria and may be conferred via a virulence factor such as CagA.

Additional data from the Smith lab identified a potential downstream consequence of *H. pylori*-mediated *EED* down-regulation and *KDM6B* upregulation in AGS cells. ChIP-qPCR measured decreased accumulation of H3K27me3 and increased RNA polymerase II at the transcriptional start site of the *IL-8* gene. As a control, low levels of polymerase II and high levels of H3K27me3 were observed at the transcriptionally silent myoglobin B gene (FitzGerald, 2021).

Together, these results indicate that *H. pylori* infection is leading to down-regulated *EED* and upregulated *KDM6B* expression, causing active chromatin confirmation and transcription of genes involved in responding to *H. pylori* infection, such as *IL-8*.

6.6. Caspase-11 is involved in *H. pylori* mediated upregulation in IL-1ß.

Caspases are a family of cysteine proteases that maintain homeostasis by regulating cell death and inflammation (McIlwain et al., 2013). Infection with gram negative bacteria can indirectly activate the NLRP3 inflammasome via the inflammatory caspases, Caspase 11 in mice and Caspase4/5 in humans. This is known as non-canonical inflammasome activation (Sanchez-Garrido et al., 2020). The noncanonical inflammasome activates caspase-1 which in turn induces IL-1ß maturation (Pachathundikandi et al., 2020). Polymorphisms in the *IL-1ß* gene are associated with an increased risk of *H. pylori*-associated pathogenesis and carcinogenesis (Pachathundikandi et al., 2020) (El-Omar et al., 2000) (Hong et al., 2016). In Chapter 5, we showed that Caspase-4 expression is upregulated in THP-1 macrophages infected with *H. pylori*. Additionally, BMDM cells from WT and Casp11-/- mice were infected with *H. pylori*. Casp-11-/- cells had impaired ability to upregulate Caspase-1 and expressed significantly lower levels of IL-1ß when compared with WT BMDM. These results indicate that Caspase-11 is contributing to IL-1ß production in response to *H. pylori*.

6.7. Future directions

In Chapter 3 an audit of Irish *H. pylori* data in the HP-EuReg was performed. To improve future audits, more centres in Ireland should be encouraged to join the Hp-EuReg network and upload their data. This would give a more representative country-wide overview of *H. pylori* management instead of a Dublin centric analysis.

Chapters 4 and 5 identified *HES1*, *EED*, *KDM6B* and *Caspase 4* as potential biomarkers for *H. pylori* associated pathogenesis. Future work would focus on the downstream effects of *H. pylori* mediated changes in *HES1*, *EED, KDM6B* and *Caspase 4* expression. In vitro experiments could use loss-of-function (such as siRNA or CRISPR) or gain-of-function (such as plasmid transfection) to identify downstream effects from changing expression of these genes. In vivo murine models of infection, using mice in which these genes are knocked out, would provide valuable insight into the role of HES1, KDM6B and Caspase 4/11 in stomach inflammation and bacterial colonisation. It may be important to look at the interplay of the gastric microbiota and *H. pylori* infection in the role of *HES1*, *EED*, *KDM6B* and *Caspase 4* expression.

Since the development of *H. pylori* associated disease from gastritis to gastric cancer is a progressive multi-step process, gene expression can vary at different stages of pathology. In this thesis, gene expression was measured in vitro as a model of acute infection and in a cohort of *H. pylori* positive patients with gastritis. Future work could evaluate gene expression of Notch associated transcription factors, histone modification proteins and inflammatory caspases in several cohorts of *H. pylori* infected patients grouped by disease stage. If a consistent change in expression was associated with one or more stages, such as *H. pylori* negative controls, gastritis, intestinal metaplasia, dysplasia, or gastric carcinoma the gene in question could be used as a biomarker. These biomarkers could select for

patients for whom *H. pylori* eradication is a priority or patients who may benefit from more frequent gastric cancer screening.

6.8. Final conclusions

Chapter 3 found that current eradication rates for *H. pylori* in Ireland are insufficient. Updating Irish recommendations to include bismuth-quadruple therapy as first-line treatment as well as scaling up antimicrobial susceptibility testing are suggested to improve eradication rates. Treating *H. pylori* with currently available therapies is only going to become more difficult in the coming years and decades due to rising antibiotic resistance. Fears of a "post antibiotics era" has sparked an interest into looking for host-directed therapies. In chapters 4 and 5 potential biomarkers for *H. pylori* associated disease were identified. These included the Notch associated transcription factor *HES1* (Chapter 4), the PRC2 component *EED* and the histone demethylase *KDM6B* (Chapter 5) and the inflammatory *caspase 4* (Chapter 5). Future work will be needed to clarify the impact of *H. pylori* mediated changes in expression for these genes and if changes in their expression correspond to specific stages of disease progression.

Bibliography

AFGAN, E., BAKER, D., BATUT, B., VAN DEN BEEK, M., BOUVIER, D., ČECH, M., CHILTON, J., CLEMENTS, D., CORAOR, N. & GRÜNING, B. A. 2018. The Galaxy platform for accessible, reproducible and collaborative biomedical analyses: 2018 update. *Nucleic acids research,* 46**,** W537-W544.

ALLEN, F. & MAILLARD, I. 2021. Therapeutic Targeting of Notch Signaling: From Cancer to Inflammatory Disorders. *Frontiers in Cell and Developmental Biology,* 9.

ALPÍZAR-ALPÍZAR, W., SKINDERSOE, M. E., RASMUSSEN, L., KRIEGBAUM, M. C., CHRISTENSEN, I. J., LUND, I. K., ILLEMANN, M., LAERUM, O. D., KROGFELT, K. A. & ANDERSEN, L. P. 2020. Helicobacter pylori colonization drives urokinase receptor (uPAR) expression in murine gastric epithelium during early pathogenesis. *Microorganisms,* 8**,** 1019.

ALVARADO-ESQUIVEL, C. 2013. Seroepidemiology of Helicobacter pylori infection in pregnant women in rural Durango, Mexico. *International journal of biomedical science: IJBS,* 9**,** 224.

ANDERSEN-NISSEN, E., SMITH, K. D., STROBE, K. L., BARRETT, S. L. R., COOKSON, B. T., LOGAN, S. M. & ADEREM, A. 2005. Evasion of Toll-like receptor 5 by flagellated bacteria. *Proceedings of the National Academy of Sciences,* 102**,** 9247-9252.

ANTUNES, R., OLEASTRO, M., NOGUEIRA, J. P. & LOPES, A. I. 2023. Time trend prevalence of helicobacter pylori infection and endoscopic findings in symptomatic children in Portugal: A retrospective study based on three time points in 2009, 2014, and 2019. *Helicobacter***,** e12963.

ARGUETA, E. A., ALSAMMAN, M. A., MOSS, S. F. & D'AGATA, E. M. 2021. Impact of antimicrobial resistance rates on eradication of Helicobacter pylori in a United States population. *Gastroenterology*.

ASONUMA, S., IMATANI, A., ASANO, N., OIKAWA, T., KONISHI, H., IIJIMA, K., KOIKE, T., OHARA, S. & SHIMOSEGAWA, T. 2009. Helicobacter pylori induces gastric mucosal intestinal metaplasia through the inhibition of interleukin-4-mediated HMG box protein Sox2 expression. *American Journal of Physiology-Gastrointestinal and Liver Physiology,* 297**,** G312-G322.

AZIZ, R. K., KHALIFA, M. M. & SHARAF, R. R. 2015. Contaminated water as a source of Helicobacter pylori infection: A review. *Journal of advanced research,* 6**,** 539-547.

BAGHERI, N., SALIMZADEH, L. & SHIRZAD, H. 2018. The role of T helper 1-cell response in Helicobacter pylori-infection. *Microbial Pathogenesis*.

BASTOS, J., PELETEIRO, B., BARROS, R., ALVES, L., SEVERO, M., DE FÁTIMA PINA, M., PINTO, H., CARVALHO, S., MARINHO, A. & GUIMARÃES, J. T. 2013. Sociodemographic determinants of prevalence and incidence of Helicobacter pylori infection in Portuguese adults. *Helicobacter,* 18**,** 413-422.

BIK, E. M., ECKBURG, P. B., GILL, S. R., NELSON, K. E., PURDOM, E. A., FRANCOIS, F., PEREZ-PEREZ, G., BLASER, M. J. & RELMAN, D. A. 2006. Molecular analysis of the bacterial microbiota in the human stomach. *Proceedings of the National Academy of Sciences,* 103**,** 732-737.

BILGIÇ, F., GERÇEKER, E., BOYACıOĞLU, S. Ö., KASAP, E., DEMIRCI, U., YıLDıRıM, H., BAYKAN, A. R. & YÜCEYAR, H. 2018. Potential role of chromatin remodeling factor genes in atrophic gastritis/gastric cancer risk. *The Turkish Journal of Gastroenterology,* 29**,** 427.

BLOSSE, A., LEHOURS, P., WILSON, K. T. & GOBERT, A. P. 2018. Helicobacter: Inflammation, immunology, and vaccines. *Helicobacter,* 23**,** e12517.

BODGER, K. & CRABTREE, J. E. 1998. Helicobacter pylori and gastric inflammation. *British medical bulletin,* 54**,** 139-150.

BOLTIN, D., BENIASHVILI, Z., LAHAT, A., HIRSCH, J., NYSSEN, O. P., MÉGRAUD, F., O'MORAIN, C., GISBERT, J. P. & NIV, Y. 2021. European Registry on Helicobacter pylori management (Hp-EuReg): First-line Therapy in Israel. *The Israel Medical Association Journal: IMAJ,* 23**,** 38-42.

BRADLEY. K., L. T. T., PINCHUCK. I. V., REYES. V. E. H. pylori affects gastric epithelial expression of novel receptors involved in effector T cell regulation. TAMHSC SUMMER RESEARCH PROGRAM, 2012 Health Professions Education Building Bryan, Texas. 10.

BRAY, S. J. 2016. Notch signalling in context. *Nature reviews Molecular cell biology,* 17**,** 722.

BRENNAN, D., O'MORAIN, C., MCNAMARA, D. & SMITH, S. M. 2021. Molecular detection of antibiotic-resistant helicobacter pylori. *Helicobacter Pylori.* Springer.

BRENNAN, D. E., OMOROGBE, J., HUSSEY, M., TIGHE, D., HOLLERAN, G., O'MORAIN, C., SMITH, S. M. & MCNAMARA, D. 2016. Molecular detection of Helicobacter pylori antibiotic resistance in stool vs biopsy samples. *World journal of gastroenterology,* 22**,** 9214.

BRZOZOWA, M., MIELAŃCZYK, Ł., MICHALSKI, M., MALINOWSKI, Ł., KOWALCZYK-ZIOMEK, G., HELEWSKI, K., HARABIN-SŁOWIŃSKA, M. & WOJNICZ, R. 2013. Role of Notch signaling pathway in gastric cancer pathogenesis. *Contemporary oncology,* 17**,** 1.

BUCKLEY, M. J., O'SHEA, J., GRACE, A., ENGLISH, L., KEANE, C., HOURIHAN, D. & O'MORAIN, C. A. 1998. A community-based study of the epidemiology of Helicobacter pylori infection and associated asymptomatic gastroduodenal pathology. *European journal of gastroenterology & hepatology,* 10**,** 375-380.

BUI, D., BROWN, H. E., HARRIS, R. B. & OREN, E. 2016. Serologic evidence for fecal–oral transmission of Helicobacter pylori. *The American journal of tropical medicine hygiene,* 94**,** 82-88.

BURCHFIELD, J. S., LI, Q., WANG, H. Y. & WANG, R.-F. 2015. JMJD3 as an epigenetic regulator in development and disease. *The international journal of biochemistry & cell biology,* 67**,** 148-157.

BURGOS-SANTAMARÍA, D., NYSSEN, O. P., GASBARRINI, A., VAIRA, D., PÉREZ-AISA, Á., RODRIGO, L., PELLICANO, R., KECO-HUERGA, A., PABÓN-CARRASCO, M. & CASTRO-FERNANDEZ, M. 2022. Empirical rescue treatment of Helicobacter pylori infection in third and subsequent lines: 8-year experience in 2144 patients from the European Registry on H. pylori management (Hp-EuReg). *Gut*.

BUTLER TJ, M. S., COSTIGAN C, VAN DER MERWE K, SEMENOV S, HOUGH S, TIGHE D, KEVANS D, PARIHAR V, MCNAMARA D, SMITH S. 2023. A MULTICENTRE SURVEY OF HELICOBACTER PYLORI ANTIMICROBIAL RESISTANCE IN IRELAND. *European Helicobacter and Microbiota Study Group (EHMSG)*

Abstracts.

CAI, G. H., WANG, K., MIAO, Q., PENG, Y. S. & CHEN, X. Y. 2010. Expression of polycomb protein EZH2 in multi-stage tissues of gastric carcinogenesis. *Journal of digestive diseases,* 11**,** 88-93.

CAI, W., ZHOU, L., REN, W., DENG, L. & YU, M. 2009. Variables influencing outcome of Helicobacter pylori eradication therapy in South China. *Helicobacter,* 14**,** 443-448.

CALDAS, M., PEREZ-AISA, A., CASTRO-FERNANDEZ, M., BUJANDA, L., LUCENDO, A. J., RODRIGO, L., HUGUET, J. M., PEREZ-LASALA, J., MOLINA-INFANTE, J. & BARRIO, J. 2020. European registry on Helicobacter pylori management: effectiveness of first and second-line treatment in Spain. *Antibiotics,* 10**,** 13.

CAMILO, V., BARROS, R., SOUSA, S., MAGALHÃES, A. M., LOPES, T., MÁRIO SANTOS, A., PEREIRA, T., FIGUEIREDO, C., DAVID, L. & ALMEIDA, R. 2012. Helicobacter pylori and the BMP pathway regulate CDX2 and SOX2 expression in gastric cells. *Carcinogenesis,* 33**,** 1985-1992.

CAPITANI, N., CODOLO, G., VALLESE, F., MINERVINI, G., GRASSI, A., CIANCHI, F., TROILO, A., FISCHER, W., ZANOTTI, G. & BALDARI, C. T. 2019. The lipoprotein HP1454 of

Helicobacter pylori regulates T-cell response by shaping T-cell receptor signalling. *Cellular Microbiology,* 21**,** e13006.

CARDENAS, V. M., MENA, K. D., ORTIZ, M., KARRI, S., VARIYAM, E., BEHRAVESH, C. B., SNOWDEN, K. F., FLISSER, A., BRISTOL, J. R. & MAYBERRY, L. F. 2010. Hyperendemic H. pylori and tapeworm infections in a US-Mexico border population. *Public Health Reports,* 125**,** 441-447.

CASTAÑO-RODRÍGUEZ, N., KAAKOUSH, N. O., GOH, K.-L., FOCK, K. M. & MITCHELL, H. M. 2014. The NOD-like receptor signalling pathway in Helicobacter pylori infection and related gastric cancer: a case-control study and gene expression analyses. *J PloS one,* 9**,** e98899.

CASTRO, R. C., GONÇALES, R. A., ZAMBUZI, F. A. & FRANTZ, F. G. 2021. Notch signaling pathway in infectious diseases: role in the regulation of immune response. *Inflammation Research***,** 1-14.

CAVALLI, G. & HEARD, E. 2019. Advances in epigenetics link genetics to the environment and disease. *Nature,* 571**,** 489-499.

CHAKRANI, Z., ROBINSON, K. & TAYE, B. 2018. Association Between ABO Blood Groups and Helicobacter pylori Infection: A Meta-Analysis. *Scientific reports,* 8**,** 17604.

CHANG, Y. W., KO, W. J., OH, C. H., PARK, Y. M., OH, S. J., MOON, J. R., CHO, J.-H., KIM, J.-W. & JANG, J.-Y. 2019. Clarithromycin resistance and female gender affect Helicobacter pylori eradication failure in chronic gastritis. *The Korean journal of internal medicine,* 34**,** 1022.

CHEN, S., ZHOU, Y., CHEN, Y. & GU, J. 2018. fastp: an ultra-fast all-in-one FASTQ preprocessor. *Bioinformatics,* 34**,** i884-i890.

CHEN, Z., LI, S., SUBRAMANIAM, S., SHYY, J. Y.-J. & CHIEN, S. 2017. Epigenetic regulation: a new frontier for biomedical engineers. *Annual review of biomedical engineering,* 19**,** 195-219.

CHERDANTSEVA, L. A., POTAPOVA, O. V., SHARKOVA, T. V., BELYAEVA, Y. Y. & SHKURUPIY, V. A. 2014. Association of Helicobacter pylori and iNOS production by macrophages and lymphocytes in the gastric mucosa in chronic gastritis. *Journal of immunology research,* 2014.

CONWAY, E., HEALY, E. & BRACKEN, A. P. 2015. PRC2 mediated H3K27 methylations in cellular identity and cancer. *Current opinion in cell biology,* 37**,** 42-48.

CORREA, P. & PIAZUELO, M. B. 2012. The gastric precancerous cascade. *Journal of digestive diseases,* 13**,** 2-9.

CRABTREE, J., COVACCI, A., FARMERY, S., XIANG, Z., TOMPKINS, D., PERRY, S., LINDLEY, I. & RAPPUOLI, R. 1995. Helicobacter pylori induced interleukin-8 expression in gastric epithelial cells is associated with CagA positive phenotype. *Journal of clinical pathology,* 48**,** 41-45.

CREAGH, E. M. 2014. Caspase crosstalk: integration of apoptotic and innate immune signalling pathways. *Trends in immunology,* 35**,** 631-640.

DE SANTA, F., NARANG, V., YAP, Z. H., TUSI, B. K., BURGOLD, T., AUSTENAA, L., BUCCI, G., CAGANOVA, M., NOTARBARTOLO, S. & CASOLA, S. 2009. Jmjd3 contributes to the control of gene expression in LPS-activated macrophages. *The EMBO journal,* 28**,** 3341-3352.

DOBIN, A., DAVIS, C. A., SCHLESINGER, F., DRENKOW, J., ZALESKI, C., JHA, S., BATUT, P., CHAISSON, M. & GINGERAS, T. R. 2013. STAR: ultrafast universal RNA-seq aligner. *Bioinformatics,* 29**,** 15-21.

DOMANOVICH-ASOR, T., CRADDOCK, H. A., MOTRO, Y., KHALFIN, B., PERETZ, A. & MORAN-GILAD, J. 2021. Unraveling antimicrobial resistance in Helicobacter pylori: Global resistome meets global phylogeny. *Helicobacter***,** e12782.

DU, X., CHENG, Z., WANG, Y.-H., GUO, Z.-H., ZHANG, S.-Q., HU, J.-K. & ZHOU, Z.-G. 2014. Role of Notch signaling pathway in gastric cancer: a meta-analysis of the literature. *World Journal of Gastroenterology: WJG,* 20**,** 9191.

EDILOVA, M. I., ABDUL-SATER, A. A. & WATTS, T. H. 2018. TRAF1 signaling in human health and disease. *Frontiers in immunology,* 9**,** 2969.

EFTANG, L. L., ESBENSEN, Y., TANNÆS, T. M., BUKHOLM, I. R. & BUKHOLM, G. 2012. Interleukin-8 is the single most up-regulated gene in whole genome profiling of H. pylori exposed gastric epithelial cells. *BMC microbiology,* 12**,** 1-15.

EL-OMAR, E. M., CARRINGTON, M., CHOW, W.-H., MCCOLL, K. E., BREAM, J. H., YOUNG, H. A., HERRERA, J., LISSOWSKA, J., YUAN, C.-C. & ROTHMAN, N. 2000. Interleukin-1 polymorphisms associated with increased risk of gastric cancer. *Nature,* 404**,** 398.

EMA. 2018. *Disabling and potentially permanent side effects lead to suspension or restrictions of quinolone and fluoroquinolone antibiotics* [Online]. European Medicines Agency. [Accessed 27/02/2023 2023].

EUSEBI, L. H., ZAGARI, R. M. & BAZZOLI, F. 2014. Epidemiology of Helicobacter pylori infection. *Helicobacter,* 19**,** 1-5.

FALLONE, C. A., CHIBA, N., VAN ZANTEN, S. V., FISCHBACH, L., GISBERT, J. P., HUNT, R. H., JONES, N. L., RENDER, C., LEONTIADIS, G. I. & MOAYYEDI, P. 2016a. The Toronto consensus for the treatment of Helicobacter pylori infection in adults. *Gastroenterology,* 151**,** 51-69. e14.

FALLONE, C. A., CHIBA, N., VAN ZANTEN, S. V., FISCHBACH, L., GISBERT, J. P., HUNT, R. H., JONES, N. L., RENDER, C., LEONTIADIS, G. I., MOAYYEDI, P. & MARSHALL, J. K. 2016b. The Toronto Consensus for the Treatment of Helicobacter pylori Infection in Adults. *Gastroenterology,* 151**,** 51-69.e14.

FERNÁNDEZ, D. J. & LAMKANFI, M. 2015. Inflammatory caspases: key regulators of inflammation and cell death. *Biological chemistry,* 396**,** 193-203.

FITZGERALD, R. & SMITH, S. M. 2021. An Overview of Helicobacter pylori Infection. *Methods in Molecular Biology (Clifton, NJ),* 2283**,** 1-14.

FITZGERALD, R. D., M. SAINI, V. HICKEY, J. MCNAMARA, D. SMITH, S. 2021. Helicobacter pylori infection inhibits expression and function of the Polycomb Repressive Complex 2. . *In:* DRENTH, J. P. (ed.) *29th United European Gastroenterology Week Virtual 2021.* Virtual Wiley.

FOLDI, J., CHUNG, A. Y., XU, H., ZHU, J., OUTTZ, H. H., KITAJEWSKI, J., LI, Y., HU, X. & IVASHKIV, L. B. J. T. J. O. I. 2010. Autoamplification of Notch signaling in macrophages by TLR-induced and RBP-J–dependent induction of Jagged1. 185**,** 5023-5031.

FORD, A. C., YUAN, Y. & MOAYYEDI, P. 2020. Helicobacter pylori eradication therapy to prevent gastric cancer: systematic review and meta-analysis. *Gut,* 69**,** 2113-2121.

FREED, D., ALDANA, R., WEBER, J. A. & EDWARDS, J. S. 2017. The Sentieon Genomics Tools–A fast and accurate solution to variant calling from next-generation sequence data. *BioRxiv***,** 115717.

GALL, A., GAUDET, R. G., GRAY-OWEN, S. D. & SALAMA, N. R. 2017. TIFA signaling in gastric epithelial cells initiates the cag type 4 secretion system-dependent innate immune response to Helicobacter pylori infection. *MBio,* 8**,** e01168-17.

GAN, H.-Y., PENG, T.-L., HUANG, Y.-M., SU, K.-H., ZHAO, L.-L., YAO, L.-Y. & YANG, R.-J. 2018. Efficacy of two different dosages of levofloxacin in curing Helicobacter pylori infection: A Prospective, Single-Center, randomized clinical trial. *Scientific reports,* 8**,** 1-5.

GATTA, L., NYSSEN, O. P., FIORINI, G., SARACINO, I. M., PAVONI, M., ROMANO, M., GRAVINA, A. G., GRANATA, L., PELLICANO, R. & GASBARRINI, A. 2023. Effectiveness of first and second-line empirical treatment in Italy: Results of the European registry on Helicobacter pylori management. *United European Gastroenterology Journal,* 11**,** 103-113.

GATTA, L., VAKIL, N., RICCI, C., OSBORN, J. F., TAMPIERI, A., PERNA, F., MIGLIOLI, M. & VAIRA, D. 2004. Effect of proton pump inhibitors and antacid therapy on 13C urea breath tests and stool test for Helicobacter pylori infection. LWW.

GEBEYEHU, E., NIGATU, D. & ENGIDAWORK, E. 2021. Complete symptom resolution as predictor of Helicobacter pylori eradication and factors affecting symptom resolution: Prospective follow up study. *Plos one,* 16**,** e0246624.

GHAYUR, T., BANERJEE, S., HUGUNIN, M., BUTLER, D., HERZOG, L., CARTER, A., QUINTAL, L., SEKUT, L., TALANIAN, R. & PASKIND, M. 1997. Caspase-1 processes IFN-γ-inducing factor and regulates LPS-induced IFN-γ production. *Nature,* 386**,** 619-623.

GIAKOUSTIDIS, A., GIAKOUSTIDIS, D., MUDAN, S., SKLAVOS, A., WILLIAMS, R. & HEPATOLOGY 2015. Molecular signalling in hepatocellular carcinoma: Role of and crosstalk among WNT/β-catenin, sonic hedgehog, notch and dickkopf-1. 29**,** 209-217.

GISBERT, J. P., DE LA MORENA, F. & ABRAIRA, V. 2006. Accuracy of monoclonal stool antigen test for the diagnosis of H. pylori infection: a systematic review and meta-analysis. *American Journal of Gastroenterology,* 101**,** 1921-1930.

GODBOLE, G., MÉGRAUD, F. & BESSÈDE, E. 2020. Diagnosis of Helicobacter pylori infection. *Helicobacter,* 25**,** e12735.

GOH, F., IRVINE, K. M., LOVELACE, E., DONNELLY, S., JONES, M. K., BRION, K., HUME, D. A., KOTZE, A. C., DALTON, J. P. & INGHAM, A. 2009. Selective induction of the Notch ligand Jagged-1 in macrophages by soluble egg antigen from Schistosoma mansoni involves ERK signalling. *Immunology,* 127**,** 326-337.

GRAHAM, D. Y., LEE, Y. C. & WU, M. S. 2014. Rational Helicobacter pylori therapy: evidence-based medicine rather than medicine-based evidence. *Clinical Gastroenterology and Hepatology,* 12**,** 177-186. e3.

GREEN, D. R. 2022. Inflammasomes and other caspase-activation platforms. *Cold Spring Harbor Perspectives in Biology,* 14**,** a041061.

GUO, L., CHEN, W., ZHU, H., CHEN, Y., WAN, X., YANG, N., XU, S., YU, C. & CHEN, L. 2014. Helicobacter pylori Induces Increased Expression of the Vitamin D Receptor in Immune Responses. *Helicobacter,* 19**,** 37-47.

HAIDER, R. B., BRENNAN, D. E., OMOROGBE, J., HOLLERAN, G., HALL, B., O'MORAIN, C., BRESLIN, N., O'CONNOR, H. J., SMITH, S. M. & MCNAMARA, D. 2015. A randomized–controlled study to compare the efficacy of sequential therapy with standard triple therapy for Helicobacter pylori eradication in an Irish population. *European journal of gastroenterology,* 27**,** 1265-1269.

HANSSON, M. L., BEHMER, S., CEDER, R., MOHAMMADI, S., PRETA, G., GRAFSTRÖM, R. C., FADEEL, B. & WALLBERG, A. E. 2012. MAML1 acts cooperatively with EGR1 to activate EGR1-regulated promoters: implications for nephrogenesis and the development of renal cancer.

HATAKEYAMA, M. 2014. Helicobacter pylori CagA and gastric cancer: a paradigm for hit-and-run carcinogenesis. *Cell host & microbe,* 15**,** 306-316.

HE, Y., YUAN, C., CHEN, L., LEI, M., ZELLMER, L., HUANG, H. & LIAO, D. J. 2018. Transcriptional-readthrough RNAs reflect the phenomenon of "a gene contains gene (s)" or "gene (s) within a gene" in the human genome, and thus are not chimeric RNAs. *Genes,* 9**,** 40.

HIRATA, H., YOSHIURA, S., OHTSUKA, T., BESSHO, Y., HARADA, T., YOSHIKAWA, K. & KAGEYAMA, R. 2002. Oscillatory expression of the bHLH factor Hes1 regulated by a negative feedback loop. *Science,* 298**,** 840-843.

HOFFMANN, E., DITTRICH-BREIHOLZ, O., HOLTMANN, H. & KRACHT, M. 2002. Multiple control of interleukin-8 gene expression. *Journal of leukocyte biology,* 72**,** 847-855.

HOFMAN, V. J., MOREILHON, C., BREST, P. D., LASSALLE, S., LE BRIGAND, K., SICARD, D., RAYMOND, J., LAMARQUE, D., HÉBUTERNE, X. A. & MARI, B. 2007. Gene expression profiling in human gastric mucosa infected with Helicobacter pylori. *Modern Pathology,* 20**,** 974-989.

HONG, J.-B., ZUO, W., WANG, A.-J. & LU, N.-H. 2016. Helicobacter pylori infection synergistic with IL-1β gene polymorphisms potentially contributes to the carcinogenesis of gastric cancer. *International journal of medical sciences,* 13**,** 298.

HOOI, J. K., LAI, W. Y., NG, W. K., SUEN, M. M., UNDERWOOD, F. E., TANYINGOH, D., MALFERTHEINER, P., GRAHAM, D. Y., WONG, V. W. & WU, J. C. 2017. Global prevalence of Helicobacter pylori infection: systematic review and meta-analysis. *Gastroenterology,* 153**,** 420-429.

HOOTON, C., KEOHANE, J., CLAIR, J., AZAM, M., O'MAHONY, S., CROSBIE, O. & LUCEY, B. 2006. Comparison of three stool antigen assays with the 13C–urea breath test for the primary diagnosis of Helicobacter pylori infection and monitoring treatment outcome. *European journal of gastroenterology & hepatology,* 18**,** 595-599.

HSU, K.-W., FANG, W.-L., HUANG, K.-H., HUANG, T.-T., LEE, H.-C., HSIEH, R.-H., CHI, C.-W. & YEH, T.-S. 2016a. Notch1 pathway-mediated microRNA-151-5p promotes gastric cancer progression. *Oncotarget,* 7**,** 38036.

HSU, K. W., FANG, W. L., HUANG, K. H., HUANG, T. T., LEE, H. C., HSIEH, R. H., CHI, C. W. & YEH, T. S. 2016b. Notch1 pathway-mediated microRNA-151-5p promotes gastric cancer progression. *Oncotarget*.

HU, J., YU, J., GAN, J., SONG, N., SHI, L., LIU, J., ZHANG, Z. & DU, J. 2020. Notch1/2/3/4 are prognostic biomarker and correlated with immune infiltrates in gastric cancer. *Aging (Albany NY),* 12**,** 2595.

HU, X., CHUNG, A. Y., WU, I., FOLDI, J., CHEN, J., JI, J. D., TATEYA, T., KANG, Y. J., HAN, J. & GESSLER, M. 2008. Integrated regulation of Toll-like receptor responses by Notch and interferon-γ pathways. *Immunity,* 29**,** 691-703.

HUA-XIANG, H., LAM, S.-K., HUANG, X.-R., WONG, W.-M., LEUNG, S.-Y., YUEN, S.-T., LAN, H.-Y. & WONG, C.-Y. 2004. Helicobacter pylori infection is associated with increased expression of macrophage migratory inhibitory factor—by epithelial cells, T cells, and macrophages—in gastric mucosa. *The Journal of infectious diseases,* 190**,** 293-302.

IWAHASHI, S., MAEKAWA, Y., NISHIDA, J., ISHIFUNE, C., KITAMURA, A., ARIMOCHI, H., KATAOKA, K., CHIBA, S., SHIMADA, M. & YASUTOMO, K. 2012. Notch2 regulates the development of marginal zone B cells through Fos. *Biochemical and Biophysical Research Communications,* 418**,** 701-707.

JAMBHEKAR, A., ANASTAS, J. N. & SHI, Y. 2017. Histone lysine demethylase inhibitors. *Cold Spring Harbor perspectives in medicine,* 7**,** a026484.

JASOVSKÝ, D., LITTMANN, J., ZORZET, A. & CARS, O. 2016. Antimicrobial resistance—a threat to the world's sustainable development. *Upsala journal of medical sciences,* 121**,** 159-164.

JAUVAIN, M. & BESSÈDE, E. 2023. GASTRIC MICROBIOME. *Microb Health Dis,* 5.

JIANG, H., ZHOU, Y., LIAO, Q. & OUYANG, H. 2014. Helicobacter pylori infection promotes the invasion and metastasis of gastric cancer through increasing the expression of matrix metalloproteinase-1 and matrix metalloproteinase-10. *Experimental and therapeutic medicine,* 8**,** 769-774.

KALIA, N., BARDHAN, K., ATHERTON, J. & BROWN, N. 2002. Toxigenic Helicobacter pylori induces changes in the gastric mucosal microcirculation in rats. *Gut,* 51**,** 641-647.

KAMEOKA, S., KAMEYAMA, T., HAYASHI, T., SATO, S., OHNISHI, N., HAYASHI, T., MURATA-KAMIYA, N., HIGASHI, H., HATAKEYAMA, M. & TAKAOKA, A. 2016. Helicobacter pylori induces IL-1β protein through the inflammasome activation in differentiated macrophagic cells. *Biomedical Research,* 37**,** 21-27.

KANEKO, T., KONNO, H., BABA, M., TANAKA, T. & NAKAMURA, S. 2003. Urokinase-type plasminogen activator expression correlates with tumor angiogenesis and poor outcome in gastric cancer. *Cancer science,* 94**,** 43-49.

KAO, C.-Y., SHEU, B.-S. & WU, J.-J. 2016. Helicobacter pylori infection: An overview of bacterial virulence factors and pathogenesis. *Biomedical journal,* 39**,** 14-23.

KAPARAKIS, M., WALDUCK, A. K., PRICE, J. D., PEDERSEN, J. S., VAN ROOIJEN, N., PEARSE, M. J., WIJBURG, O. L. & STRUGNELL, R. A. 2008. Macrophages are mediators of gastritis in acute Helicobacter pylori infection in C57BL/6 mice. *Infection and immunity,* 76**,** 2235-2239.

KATOH, M. & KATOH, M. 2007a. Integrative genomic analyses on HES/HEY family: Notch-independent HES1, HES3 transcription in undifferentiated ES cells, and Notch-dependent HES1, HES5, HEY1, HEY2, HEYL transcription in fetal tissues, adult tissues, or cancer. *International journal of oncology,* 31**,** 461-466.

KATOH, M. & KATOH, M. 2007b. Notch signaling in gastrointestinal tract. 30**,** 247-251.

KAWAGOE, T., SATO, S., MATSUSHITA, K., KATO, H., MATSUI, K., KUMAGAI, Y., SAITOH, T., KAWAI, T., TAKEUCHI, O. & AKIRA, S. 2008. Sequential control of Toll-like receptor–dependent responses by IRAK1 and IRAK2. *Nature immunology,* 9**,** 684-691.

KAYAGAKI, N., WARMING, S., LAMKANFI, M., WALLE, L. V., LOUIE, S., DONG, J., NEWTON, K., QU, Y., LIU, J. & HELDENS, S. 2011. Non-canonical inflammasome activation targets caspase-11. *Nature,* 479**,** 117-121.

KAYAGAKI, N., WONG, M. T., STOWE, I. B., RAMANI, S. R., GONZALEZ, L. C., AKASHI-TAKAMURA, S., MIYAKE, K., ZHANG, J., LEE, W. P. & MUSZYŃSKI, A. 2013. Noncanonical inflammasome activation by intracellular LPS independent of TLR4. *Science,* 341**,** 1246-1249.

KENNY, S., DUVAL, C., SAMMUT, S. J., STEELE, I., PRITCHARD, D. M., ATHERTON, J. C., ARGENT, R. H., DIMALINE, R., DOCKRAY, G. J. & VARRO, A. 2008. Increased expression of the urokinase plasminogen activator system by Helicobacter pylori in gastric epithelial cells. *American Journal of Physiology-Gastrointestinal and Liver Physiology,* 295**,** G431-G441.

KIM, D.-J., PARK, J.-H., FRANCHI, L., BACKERT, S. & NÚÑEZ, G. 2013. The Cag pathogenicity island and interaction between TLR2/NOD2 and NLRP3 regulate IL-1β production in Helicobacter pylori infected dendritic cells. *European Journal of Immunology,* 43**,** 2650-2658.

KITADAI, Y., SASAKI, A., ITO, M., TANAKA, S., OUE, N., YASUI, W., AIHARA, M., IMAGAWA, K., HARUMA, K. & CHAYAMA, K. 2003. Helicobacter pylori infection influences expression of genes related to angiogenesis and invasion in human gastric carcinoma cells. *Biochemical and biophysical research communications,* 311**,** 809-814.

KOCH, K. N. & MÜLLER, A. 2015. Helicobacter pylori activates the TLR2/NLRP3/caspase-1/IL-18 axis to induce regulatory T-cells, establish persistent infection and promote tolerance to allergens. *Gut Microbes,* 6**,** 382-387.

KOCH, M., MOLLENKOPF, H. J. & MEYER, T. F. 2016. Macrophages recognize the Helicobacter pylori type IV secretion system in the absence of toll-like receptor signalling. *Cellular microbiology,* 18**,** 137-147.

KONISHI, H., ASANO, N., IMATANI, A., KIMURA, O., KONDO, Y., JIN, X., KANNO, T., HATTA, W., ARA, N. & ASANUMA, K. 2016. Notch1 directly induced CD133 expression in human diffuse type gastric cancers. *Oncotarget,* 7**,** 56598.

KUMAR, K. P., NICHOLLS, A. J. & WONG, C. H. 2018. Partners in crime: neutrophils and monocytes/macrophages in inflammation and disease. *Cell and tissue research,* 371**,** 551-565.

LAKSHMANAN, U. & PORTER, A. G. 2007. Caspase-4 interacts with TNF receptor-associated factor 6 and mediates lipopolysaccharide-induced NF-κB-dependent production of IL-8 and CC chemokine ligand 4 (macrophage-inflammatory protein-1β). *The Journal of Immunology,* 179**,** 8480-8490.

LAUGESEN, A., HØJFELDT, J. W. & HELIN, K. 2019. Molecular mechanisms directing PRC2 recruitment and H3K27 methylation. *Molecular cell,* 74**,** 8-18.

LEJA, M., AXON, A. & BRENNER, H. 2016. Epidemiology of Helicobacter pylori infection. *Helicobacter,* 21**,** 3-7.

LI, B. & DEWEY, C. N. 2011. RSEM: accurate transcript quantification from RNA-Seq data with or without a reference genome. *BMC bioinformatics,* 12**,** 1-16.
LI, H., LI, H., HUO, R., WU, P., SHEN, Z., XU, H., SHEN, B. & LI, N. 2017. Cyr61/CCN1 induces CCL20 production by keratinocyte via activating p38 and JNK/AP-1 pathway in psoriasis. *Journal of Dermatological Science,* 88**,** 46-56.
LI, H., SHEN, Y., SONG, X., TANG, X., HU, R., MARSHALL, B. J., TANG, H. & BENGHEZAL, M. 2022a. Need for standardization and harmonization of Helicobacter pylori antimicrobial susceptibility testing. *Helicobacter,* 27**,** e12873.
LI, N., PANG, Y., SANG, J., SUN, Y. & HOU, W. 2022b. The controversial expression of SOX2 in gastric cancer and its correlation with Helicobacter pylori infection: A meta-analysis. *Medicine,* 101**,** e30886.
LIATSOS, C., PAPAEFTHYMIOU, A., KYRIAKOS, N., GALANOPOULOS, M., DOULBERIS, M., GIAKOUMIS, M., PETRIDOU, E., MAVROGIANNIS, C., ROKKAS, T. & KOUNTOURAS, J. 2022. Helicobacter pylori, gastric microbiota and gastric cancer relationship: unrolling the tangle. *World Journal of Gastrointestinal Oncology,* 14**,** 959.
LIM, J. W., KIM, H. & KIM, K. H. 2003. Cell adhesion-related gene expression by Helicobacter pylori in gastric epithelial AGS cells. *The international journal of biochemistry & cell biology,* 35**,** 1284-1296.
LIM, S. H., KWON, J.-W., KIM, N., KIM, G. H., KANG, J. M., PARK, M. J., YIM, J. Y., KIM, H. U., BAIK, G. H. & SEO, G. S. 2013. Prevalence and risk factors of Helicobacter pylori infection in Korea: nationwide multicenter study over 13 years. *BMC gastroenterology,* 13**,** 104.
LIU, F., WANG, Y., YANG, Z., CUI, X., ZHENG, L., FU, Y., SHAO, W., ZHANG, L., YANG, Q. & JIA, J. 2022. KDM6B promotes gastric carcinogenesis and metastasis via upregulation of CXCR4 expression. *Cell Death & Disease,* 13**,** 1068.
LIU, T., HE, W. & LI, Y. 2016. Helicobacter pylori Infection of Gastric Epithelial Cells Affects NOTCH Pathway In Vitro. *Digestive diseases and sciences,* 61**,** 2516-2521.
LIVAK, K. J. & SCHMITTGEN, T. D. 2001. Analysis of relative gene expression data using real-time quantitative PCR and the 2− ΔΔCT method. *methods,* 25**,** 402-408.
LOVE, M. I., HUBER, W. & ANDERS, S. 2014. Moderated estimation of fold change and dispersion for RNA-seq data with DESeq2. *Genome biology,* 15**,** 1-21.
LUO, W. & BROUWER, C. 2013. Pathview: an R/Bioconductor package for pathway-based data integration and visualization. *Bioinformatics,* 29**,** 1830-1.
LUO, W., FRIEDMAN, M. S., SHEDDEN, K., HANKENSON, K. D. & WOOLF, P. J. 2009. GAGE: generally applicable gene set enrichment for pathway analysis. *BMC bioinformatics,* 10**,** 1-17.
MAEDA, S., OTSUKA, M., HIRATA, Y., MITSUNO, Y., YOSHIDA, H., SHIRATORI, Y., MASUHO, Y., MURAMATSU, M.-A., SEKI, N. & OMATA, M. 2001. cDNA microarray analysis of Helicobacter pylori-mediated alteration of gene expression in gastric cancer cells. *Biochemical and biophysical research communications,* 284**,** 443-449.
MAKRISTATHIS, A., HIRSCHL, A. M., MÉGRAUD, F. & BESSÈDE, E. 2019. Diagnosis of Helicobacter pylori infection. *Helicobacter,* 24**,** e12641.
MALFERTHEINER, P., MEGRAUD, F., O'MORAIN, C., BELL, D., PORRO, B. G., DELTENRE, M., FORMAN, D., GASBARRINI, G., JAUP, B., MISIEWICZ, J. J. E. J. O. G. & HEPATOLOGY 1997. Current European concepts in the management ofHelicobacter pyloriinfection-the Maastricht Consensus Report. 9**,** 1-2.
MALFERTHEINER, P., MEGRAUD, F., O'MORAIN, C., GISBERT, J., KUIPERS, E., AXON, A., BAZZOLI, F., GASBARRINI, A., ATHERTON, J. & GRAHAM, D. Y. 2016. Management of Helicobacter pylori infection—the Maastricht V/Florence consensus report. *Gut***,** gutjnl-2016-312288.
MALFERTHEINER, P., MEGRAUD, F., O'MORAIN, C. A., GISBERT, J. P., KUIPERS, E. J., AXON, A. T., BAZZOLI, F., GASBARRINI, A., ATHERTON, J., GRAHAM, D. Y., HUNT, R., MOAYYEDI, P.,

ROKKAS, T., RUGGE, M., SELGRAD, M., SUERBAUM, S., SUGANO, K., EL-OMAR, E. M. & PANEL, E. H. A. M. S. G. A. C. 2017. Management of Helicobacter pylori infection-the Maastricht V/Florence Consensus Report. *Gut,* 66**,** 6-30.

MALFERTHEINER, P., MEGRAUD, F., ROKKAS, T., GISBERT, J. P., LIOU, J.-M., SCHULZ, C., GASBARRINI, A., HUNT, R. H., LEJA, M. & O'MORAIN, C. 2022. Management of Helicobacter pylori infection: the Maastricht VI/Florence consensus report. *Gut,* 71**,** 1724-1762.

MAN, S. M., KARKI, R. & KANNEGANTI, T.-D. 2017. Molecular mechanisms and functions of pyroptosis, inflammatory caspases and inflammasomes in infectious diseases. *Immunological Reviews,* 277**,** 61-75.

MANDELL, L., MORAN, A. P., COCCHIARELLA, A., HOUGHTON, J., TAYLOR, N., FOX, J. G., WANG, T. C. & KURT-JONES, E. A. 2004. Intact gram-negative Helicobacter pylori, Helicobacter felis, and Helicobacter hepaticus bacteria activate innate immunity via toll-like receptor 2 but not toll-like receptor 4. *Infection and immunity,* 72**,** 6446-6454.

MARGUERON, R. & REINBERG, D. 2011. The Polycomb complex PRC2 and its mark in life. *Nature,* 469**,** 343-349.

MARINI, F. & BINDER, H. 2019. pcaExplorer: an R/Bioconductor package for interacting with RNA-seq principal components. *BMC bioinformatics,* 20**,** 1-8.

MARSHALL, B. & WARREN, J. R. 1984. Unidentified curved bacilli in the stomach of patients with gastritis and peptic ulceration. *The Lancet,* 323**,** 1311-1315.

MARSHALL, B. J., ARMSTRONG, J. A., MCGECHIE, D. B. & GLANCY, R. J. 1985. Attempt to fulfil Koch's postulates for pyloric Campylobacter. *The medical journal of Australia,* 142**,** 436-439.

MATHEWOS, B., MOGES, B. & DAGNEW, M. 2013. Seroprevalence and trend of Helicobacter pylori infection in Gondar University Hospital among dyspeptic patients, Gondar, North West Ethiopia. *BMC research notes,* 6**,** 346.

MATOS, J. I., DE SOUSA, H. A., MARCOS-PINTO, R. & DINIS-RIBEIRO, M. 2013. Helicobacter pylori CagA and VacA genotypes and gastric phenotype: a meta-analysis. *Eur J Gastroenterol Hepatol,* 25**,** 1431-41.

MCCLAIN, M., BECKETT, A. & COVER, T. 2017. Helicobacter pylori vacuolating toxin and gastric cancer. *Toxins,* 9**,** 316.

MCCOLL 2010. Helicobacter pylori infection. *New England Journal of Medicine,* 362**,** 1597-1604.

MCCOLL, K., EL-NUJUMI, A., MURRAY, L., EL-OMAR, E., DICKSON, A., KELMAN, A. & HILDITCH, T. 1998. Assessment of symptomatic response as predictor ofHelicobacter pylori status following eradication therapy in patients with ulcer. *Gut,* 42**,** 618-622.

MCILWAIN, D. R., BERGER, T. & MAK, T. W. 2013. Caspase functions in cell death and disease. *Cold Spring Harbor perspectives in biology,* 5**,** a008656.

MCNICHOLL, A. G., O'MORAIN, C. A., MEGRAUD, F., GISBERT, J. P. & COORDINATORS, A. S. C. O. T. H. E. O. B. O. T. N. 2019. Protocol of the European registry on the management of Helicobacter pylori infection (Hp-EuReg). *Helicobacter,* 24**,** e12630.

MEGRAUD, F., BRUYNDONCKX, R., COENEN, S., WITTKOP, L., HUANG, T.-D., HOEBEKE, M., BÉNÉJAT, L., LEHOURS, P., GOOSSENS, H. & GLUPCZYNSKI, Y. 2021. Helicobacter pylori resistance to antibiotics in Europe in 2018 and its relationship to antibiotic consumption in the community. *Gut,* 70**,** 1815-1822.

MEGRAUD, F., COENEN, S., VERSPORTEN, A., KIST, M., LOPEZ-BREA, M., HIRSCHL, A. M., ANDERSEN, L. P., GOOSSENS, H. & GLUPCZYNSKI, Y. J. G. 2013. Helicobacter pylori resistance to antibiotics in Europe and its relationship to antibiotic consumption. 62**,** 34-42.

MELESE, A., GENET, C., ZELEKE, B. & ANDUALEM, T. 2019. Helicobacter pylori infections in Ethiopia; prevalence and associated factors: a systematic review and meta-analysis. *BMC gastroenterology,* 19**,** 1-15.

MIRZAEI, N., POURSINA, F., MOGHIM, S., RASHIDI, N. & GHASEMIAN SAFAEI, H. 2017. The study of H. pylori putative candidate factors for single-and multi-component vaccine development. *Critical reviews in microbiology,* 43**,** 631-650.

MISIOREK, J. O., PRZYBYSZEWSKA-PODSTAWKA, A., KAŁAFUT, J., PAZIEWSKA, B., ROLLE, K., RIVERO-MÜLLER, A. & NEES, M. 2021. Context Matters: NOTCH Signatures and Pathway in Cancer Progression and Metastasis. *Cells,* 10**,** 94.

MOLINARI, M., SALIO, M., GALLI, C., NORAIS, N., RAPPUOLI, R., LANZAVECCHIA, A. & MONTECUCCO, C. 1998. Selective inhibition of Ii-dependent antigen presentation by Helicobacter pylori toxin VacA. *The Journal of experimental medicine,* 187**,** 135-140.

MORAN, A. P., KNIREL, Y. A., SOF'YA, N. S., WIDMALM, G., HYNES, S. O. & JANSSON, P.-E. 2002. Phenotypic Variation in Molecular Mimicry betweenHelicobacter pylori Lipopolysaccharides and Human Gastric Epithelial Cell Surface Glycoforms: ACID-INDUCED PHASE VARIATION IN LEWISXAND LEWISY EXPRESSION BY H. PYLORILIPOPOLYSACCHARIDES. *Journal of Biological Chemistry,* 277**,** 5785-5795.

MORILLA, A. M., ÁLVAREZ-ARGÜELLES, M. E., DUQUE, J. M., ARMESTO, E., VILLAR, H. & MELÓN, S. 2019. Primary antimicrobial resistance rates and prevalence of Helicobacter pylori infection in the north of Spain. A 13-year retrospective study. *Gastroenterología y Hepatología (English Edition),* 42**,** 476-485.

MORTAZAVI, A., WILLIAMS, B. A., MCCUE, K., SCHAEFFER, L. & WOLD, B. 2008. Mapping and quantifying mammalian transcriptomes by RNA-Seq. *Nature methods,* 5**,** 621-628.

MOSS, S. F., DANG, L. P., CHUA, D., SOBRADO, J., ZHOU, Y. & GRAHAM, D. Y. 2022. Comparable results of Helicobacter pylori antibiotic resistance testing of stools vs gastric biopsies using next-generation sequencing. *Gastroenterology,* 162**,** 2095-2097. e2.

MURRAY, L. J., MCCRUM, E. E., EVANS, A. E. & BAMFORD, K. B. 1997. Epidemiology of Helicobacter pylori infection among 4742 randomly selected subjects from Northern Ireland. *International journal of epidemiology,* 26**,** 880-887.

NAGY, P., JOHANSSON, S. & MOLLOY-BLAND, M. 2016. Systematic review of time trends in the prevalence of Helicobacter pylori infection in China and the USA. *Gut pathogens,* 8**,** 1-14.

NETEA, M. G., JOOSTEN, L. A., LATZ, E., MILLS, K. H., NATOLI, G., STUNNENBERG, H. G., O'NEILL, L. A. & XAVIER, R. J. 2016. Trained immunity: a program of innate immune memory in health and disease. *Science,* 352**,** aaf1098.

NYSSEN, O. P., BORDIN, D., TEPES, B., PÉREZ-AISA, Á., VAIRA, D., CALDAS, M., BUJANDA, L., CASTRO-FERNANDEZ, M., LERANG, F. & LEJA, M. 2021a. European Registry on Helicobacter pylori management (Hp-EuReg): patterns and trends in first-line empirical eradication prescription and outcomes of 5 years and 21 533 patients. *Gut,* 70**,** 40-54.

NYSSEN, O. P., MOREIRA, L., GARCÍA-MORALES, N., CANO-CATALÀ, A., PUIG, I., MÉGRAUD, F., O'MORAIN, C. & GISBERT, J. P. 2022. European Registry on Helicobacter pylori Management (Hp-EuReg): Most relevant results for clinical practice. *Frontiers in Gastroenterology,* 1**,** 965982.

NYSSEN, O. P., VAIRA, D., AÍSA, Á. P., RODRIGO, L., CASTRO-FERNANDEZ, M., JONAITIS, L., TEPES, B., VOLOGZHANINA, L., CALDAS, M. & LANAS, A. 2021b. Empirical Second-Line Therapy in 5000 Patients of the European Registry on Helicobacter pylori Management (Hp-EuReg). *Clinical Gastroenterology and Hepatology*.

O'CONNOR, A. 2021. The urea breath test for the noninvasive detection of Helicobacter pylori. *Helicobacter pylori.* Springer.

OHNISHI, N., YUASA, H., TANAKA, S., SAWA, H., MIURA, M., MATSUI, A., HIGASHI, H., MUSASHI, M., IWABUCHI, K. & SUZUKI, M. 2008. Transgenic expression of Helicobacter pylori CagA induces gastrointestinal and hematopoietic neoplasms in mouse. *Proceedings of the National Academy of Sciences,* 105**,** 1003-1008.

ONDREY, F. G., DONG, G., SUNWOO, J., CHEN, Z., WOLF, J. S., CROWL-BANCROFT, C. V., MUKAIDA, N. & VAN WAES, C. 1999. Constitutive activation of transcription factors NF-

κB, AP-1, and NF-IL6 in human head and neck squamous cell carcinoma cell lines that express pro-inflammatory and pro-angiogenic cytokines. *Molecular Carcinogenesis: Published in cooperation with the University of Texas MD Anderson Cancer Center,* 26**,** 119-129.

OPHORI, E., ISIBOR, C., ONEMU, S. & JOHNNY, E. 2011. Immunological response to Helicobacter pylori among healthy volunteers in Agbor, Nigeria. *Asian Pacific Journal of Tropical Disease,* 1**,** 38-40.

OSATO, M. S., REDDY, R., REDDY, S. G., PENLAND, R. L., MALATY, H. M. & GRAHAM, D. Y. 2001. Pattern of primary resistance of Helicobacter pylori to metronidazole or clarithromycin in the United States. *Archives of internal medicine,* 161**,** 1217-1220.

OUTLIOUA, A., BADRE, W., DESTERKE, C., ECHARKI, Z., EL HAMMANI, N., RABHI, M., RIYAD, M., KARKOURI, M., ARNOULT, D. & KHALIL, A. 2020. Gastric IL-1β, IL-8, and IL-17A expression in Moroccan patients infected with Helicobacter pylori may be a predictive signature of severe pathological stages. *Cytokine,* 126**,** 154893.

ÖZTÜRK, K., KURT, Ö., ÇELEBI, G., ŞARLAK, H., KARAKAYA, M. F., DEMIRCI, H., KILIÇ, A. & UYGUN, A. 2020. High-dose dual therapy is effective as first-line treatment for Helicobacter pylori infection. *The Turkish Journal of Gastroenterology,* 31**,** 234.

PACHATHUNDIKANDI, S. K., BLASER, N., BRUNS, H. & BACKERT, S. 2020. Helicobacter pylori Avoids the Critical Activation of NLRP3 Inflammasome-Mediated Production of Oncogenic Mature IL-1β in Human Immune Cells. *Cancers,* 12**,** 803.

PACHATHUNDIKANDI, S. K., BRANDT, S., MADASSERY, J. & BACKERT, S. 2011. Induction of TLR-2 and TLR-5 expression by Helicobacter pylori switches cagPAI-dependent signalling leading to the secretion of IL-8 and TNF-α. *J PLoS One,* 6**,** 1-11.

PACHATHUNDIKANDI, S. K., MÜLLER, A. & BACKERT, S. 2016. Inflammasome activation by Helicobacter pylori and its implications for persistence and immunity. *Inflammasome Signaling and Bacterial Infections.* Springer.

PAN, K.-F., ZHANG, L., GERHARD, M., MA, J.-L., LIU, W.-D., ULM, K., WANG, J.-X., ZHANG, L., ZHANG, Y. & BAJBOUJ, M. 2015. A large randomised controlled intervention trial to prevent gastric cancer by eradication of Helicobacter pylori in Linqu County, China: baseline results and factors affecting the eradication. *Gut,* 65**,** 9-18.

PANDEYA, N., WHITEMAN, D. C. & STUDY, A. C. 2011. Prevalence and determinants of Helicobacter pylori sero-positivity in the Australian adult community. *Journal of gastroenterology and hepatology,* 26**,** 1283-1289.

PARIHAR, V. & MCNAMARA, D. 2021. Endoscopic Detection of Helicobacter pylori by the Rapid Urease Test. *Helicobacter Pylori.* Springer.

PATTERSON, T., STRATEN, E. & JIMENEZ, S. 2012. The prevalence of Helicobacter pylori antibody in different age groups in Central Texas. *American Society for Clinical Laboratory Science,* 25**,** 102-106.

PEEK, R. M., WIRTH, H. P., MOSS, S. F., YANG, M., ABDALLA, A., THAM, K. T., ZHANG, T., TANG, L. H., MODLIN, I. M. & BLASER, M. J. 2000. Helicobacter pylori alters gastric epithelial cell cycle events and gastrin secretion in Mongolian gerbils. *Gastroenterology,* 118**,** 48-59.

PÉREZ-PÉREZ, G. I., SHEPHERD, V. L., MORROW, J. D. & BLASER, M. J. 1995. Activation of human THP-1 cells and rat bone marrow-derived macrophages by Helicobacter pylori lipopolysaccharide. *Infection and immunity,* 63**,** 1183-1187.

PIAZZI, G., FINI, L., SELGRAD, M., GARCIA, M., DAOUD, Y., WEX, T., MALFERTHEINER, P., GASBARRINI, A., ROMANO, M. & MEYER, R. L. 2011. Epigenetic regulation of Delta-Like1 controls Notch1 activation in gastric cancer. *Oncotarget,* 2**,** 1291.

PILLINGER, M. H., MARJANOVIC, N., KIM, S.-Y., LEE, Y.-C., SCHER, J. U., ROPER, J., ABELES, A. M., IZMIRLY, P. I., AXELROD, M. & PILLINGER, M. Y. 2007. Helicobacter pylori stimulates gastric epithelial cell MMP-1 secretion via CagA-dependent and-independent ERK activation. *Journal of Biological Chemistry,* 282**,** 18722-18731.

PINCOCK, S. 2005. Nobel prize winners robin warren and barry marshall. *The Lancet,* 366**,** 1429.

PLUMMER, M., FRANCESCHI, S., VIGNAT, J., FORMAN, D. & DE MARTEL, C. 2015. Global burden of gastric cancer attributable to Helicobacter pylori. 136**,** 487-490.

PREISS, S., ARGENTARO, A., CLAYTON, A., JOHN, A., JANS, D. A., OGATA, T., NAGAI, T., BARROSO, I., SCHAFER, A. J. & HARLEY, V. R. 2001. Compound effects of point mutations causing campomelic dysplasia/autosomal sex reversal upon SOX9 structure, nuclear transport, DNA binding, and transcriptional activation. *Journal of Biological Chemistry,* 276**,** 27864-27872.

PURKAIT, S., PATRA, S., MITRA, S., BEHERA, M. M., PANIGRAHI, M. K., KUMAR, P., KAR, M., HALLUR, V. & SAMAL, S. C. 2022. Elevated expression of DNA methyltransferases and enhancer of Zeste homolog 2 in Helicobacter pylori-gastritis and gastric carcinoma. *Digestive Diseases,* 40**,** 156-167.

QUIDING-JÄRBRINK, M., RAGHAVAN, S. & SUNDQUIST, M. 2010. Enhanced M1 macrophage polarization in human helicobacter pylori-associated atrophic gastritis and in vaccinated mice. *PloS one,* 5.

RAND, M. D., GRIMM, L. M., ARTAVANIS-TSAKONAS, S., PATRIUB, V., BLACKLOW, S. C., SKLAR, J. & ASTER, J. C. 2000. Calcium depletion dissociates and activates heterodimeric notch receptors. *Molecular and cellular biology,* 20**,** 1825-1835.

RANGARAJAN, A., TALORA, C., OKUYAMA, R., NICOLAS, M., MAMMUCARI, C., OH, H., ASTER, J. C., KRISHNA, S., METZGER, D. & CHAMBON, P. 2001. Notch signaling is a direct determinant of keratinocyte growth arrest and entry into differentiation. *The EMBO journal,* 20**,** 3427-3436.

RANI, A., GREENLAW, R., SMITH, R. A. & GALUSTIAN, C. 2016. HES1 in immunity and cancer. *Cytokine & growth factor reviews,* 30**,** 113-117.

RAZAVI, A., BAGHERI, N., AZADEGAN-DEHKORDI, F., SHIRZAD, M., RAHIMIAN, G., RAFIEIAN-KOPAEI, M. & SHIRZAD, H. 2015. Comparative immune response in children and adults with H. pylori infection. *Journal of immunology research,* 2015.

REIMAND, J., ISSERLIN, R., VOISIN, V., KUCERA, M., TANNUS-LOPES, C., ROSTAMIANFAR, A., WADI, L., MEYER, M., WONG, J. & XU, C. 2019. Pathway enrichment analysis and visualization of omics data using g: Profiler, GSEA, Cytoscape and EnrichmentMap. *Nature protocols,* 14**,** 482-517.

REVOLLO, J. R., OAKLEY, R. H., LU, N. Z., KADMIEL, M., GANDHAVADI, M. & CIDLOWSKI, J. A. 2013. HES1 is a master regulator of glucocorticoid receptor–dependent gene expression. *Sci. Signal.,* 6**,** ra103-ra103.

ROBINSON, K. & LEHOURS, P. 2020. Review-Helicobacter, inflammation, immunology and vaccines. *Helicobacter,* 25**,** e12737.

ROCHA, G. A., DE MELO, F. F., CABRAL, M. M., DE BRITO, B. B., DA SILVA, F. A. & QUEIROZ, D. M. 2019. Interleukin-27 is abrogated in gastric cancer, but highly expressed in other Helicobacter pylori-associated gastroduodenal diseases. *Helicobacter*.

ROKKAS, T., GEORGOPOULOS, S., MICHOPOULOS, S., NTOULI, V., LIATSOS, C., PUIG, I., NYSSEN, O. P., MÉGRAUD, F., O'MORAIN, C. & GISBERT, J. P. 2022. Assessment of first-line eradication treatment in Greece: data from the European Registry on Helicobacter pylori management (Hp-EuReg). *Annals of Gastroenterology,* 35**,** 42.

SABBAGH, P., MOHAMMADNIA-AFROUZI, M., JAVANIAN, M., BABAZADEH, A., KOPPOLU, V., VASIGALA, V. R., NOURI, H. R. & EBRAHIMPOUR, S. 2019. Diagnostic methods for Helicobacter pylori infection: ideals, options, and limitations. *European Journal of Clinical Microbiology & Infectious Diseases,* 38**,** 55-66.

SALAMA, N. R., HARTUNG, M. L. & MÜLLER, A. 2013. Life in the human stomach: persistence strategies of the bacterial pathogen Helicobacter pylori. *Nat Rev Microbiol,* 11**,** 385-99.

SALIMZADEH, L., BAGHERI, N., ZAMANZAD, B., AZADEGAN-DEHKORDI, F., RAHIMIAN, G., HASHEMZADEH-CHALESHTORI, M., RAFIEIAN-KOPAEI, M., SANEI, M. H. & SHIRZAD, H.

2015. Frequency of virulence factors in Helicobacter pylori-infected patients with gastritis. *Microbial pathogenesis,* 80**,** 67-72.
SANCHEZ-GARRIDO, J., SLATER, S. L., CLEMENTS, A., SHENOY, A. R. & FRANKEL, G. 2020. Vying for the control of inflammasomes: The cytosolic frontier of enteric bacterial pathogen–host interactions. *Cellular Microbiology,* 22.
SAVOLDI, A., CARRARA, E., GRAHAM, D. Y., CONTI, M. & TACCONELLI, E. 2018. Prevalence of antibiotic resistance in Helicobacter pylori: a systematic review and meta-analysis in World Health Organization regions. *Gastroenterology,* 155**,** 1372-1382. e17.
SCHVARTZMAN, J. M., THOMPSON, C. B. & FINLEY, L. W. 2018. Metabolic regulation of chromatin modifications and gene expression. *Journal of Cell Biology,* 217**,** 2247-2259.
SEPULVEDA, A., TAO, H., CARLONI, E., SEPULVEDA, J., GRAHAM, D. & PETERSON, L. 2002. Screening of gene expression profiles in gastric epithelial cells induced by Helicobacter pylori using microarray analysis. *Alimentary pharmacology & therapeutics,* 16**,** 145-157.
SERIZAWA, T., HIRATA, Y., HAYAKAWA, Y., SUZUKI, N., SAKITANI, K., HIKIBA, Y., IHARA, S., KINOSHITA, H., NAKAGAWA, H. & TATEISHI, K. 2016. Gastric metaplasia induced by Helicobacter pylori is associated with enhanced SOX9 expression via interleukin-1 signaling. *Infection and immunity,* 84**,** 562-572.
SEYMOUR, P. A., FREUDE, K. K., TRAN, M. N., MAYES, E. E., JENSEN, J., KIST, R., SCHERER, G. & SANDER, M. 2007. SOX9 is required for maintenance of the pancreatic progenitor cell pool. *Proceedings of the National Academy of Sciences,* 104**,** 1865-1870.
SHANG, Y., COPPO, M., HE, T., NING, F., YU, L., KANG, L., ZHANG, B., JU, C., QIAO, Y. & ZHAO, B. 2016a. The transcriptional repressor Hes1 attenuates inflammation by regulating transcription elongation. *Nature immunology,* 17**,** 930.
SHANG, Y., SMITH, S. & HU, X. 2016b. Role of Notch signaling in regulating innate immunity and inflammation in health and disease. *Protein & Cell,* 7**,** 159-174.
SHEH, A., GE, Z., PARRY, N. M., MUTHUPALANI, S., RAGER, J. E., RACZYNSKI, A. R., MOBLEY, M. W., MCCABE, A. F., FRY, R. C. & WANG, T. C. 2011. 17β-estradiol and tamoxifen prevent gastric cancer by modulating leukocyte recruitment and oncogenic pathways in helicobacter pylori–infected INS-GAS male mice. *Cancer prevention research,* 4**,** 1426-1435.
SHIBATA, W., HIRATA, Y., YOSHIDA, H., OTSUKA, M., HOSHIDA, Y., OGURA, K., MAEDA, S., OHMAE, T., YANAI, A. & MITSUNO, Y. 2005. NF-kB and ERK-signaling pathways contribute to the gene expression induced by cag PAI-positive-Helicobacter pylori infection. *World Journal of Gastroenterology: WJG,* 11**,** 6134.
SHIOTA, S., SUZUKI, R. & YAMAOKA, Y. J. J. O. D. D. 2013. The significance of virulence factors in H elicobacter pylori. 14**,** 341-349.
SMITH, M. F., MITCHELL, A., LI, G., DING, S., FITZMAURICE, A. M., RYAN, K., CROWE, S. & GOLDBERG, J. B. 2003. Toll-like receptor (TLR) 2 and TLR5, but not TLR4, are required for Helicobacter pylori-induced NF-κB activation and chemokine expression by epithelial cells. *Journal of Biological Chemistry,* 278**,** 32552-32560.
SMITH, S. 2015. An update on the treatment of Helicobacter pylori infection.
SMITH, S., BOYLE, B., BRENNAN, D., BUCKLEY, M., CROTTY, P., DOYLE, M., FARRELL, R., HUSSEY, M., KEVANS, D. & MALFERTHEINER, P. 2017a. The Irish Helicobacter pylori Working Group consensus for the diagnosis and treatment of H. pylori infection in adult patients in Ireland. *European Journal of Gastroenterology & Hepatology,* 29**,** 552-559.
SMITH, S. M. 2014. Role of Toll-like receptors in Helicobacter pylori infection and immunity. *World J Gastrointest Pathophysiology,* 5**,** 133-46.
SMITH, S. M., FREELEY, M., MOYNAGH, P. N. & KELLEHER, D. P. 2017b. Differential modulation of Helicobacter pylori lipopolysaccharide-mediated TLR 2 signaling by individual Pellino proteins. *Helicobacter,* 22**,** e12325.

SMITH, S. M., HAIDER, R. B., O'CONNOR, H., MCNAMARA, D. & O'MORAIN, C. 2014a. Practical treatment of Helicobacter pylori: a balanced view in changing times. *Eur J Gastroenterol Hepatol,* 26**,** 819-25.

SMITH, S. M., HAIDER, R. B., O'CONNOR, H., MCNAMARA, D., O'MORAIN, C. J. E. J. O. G. & HEPATOLOGY 2014b. Practical treatment of Helicobacter pylori: a balanced view in changing times. 26**,** 819-825.

SMITH, S. M., MORAN, A. P., DUGGAN, S. P., AHMED, S. E., MOHAMED, A. S., WINDLE, H. J., O'NEILL, L. A. & KELLEHER, D. P. 2011. Tribbles 3: a novel regulator of TLR2-mediated signaling in response to Helicobacter pylori lipopolysaccharide. *The Journal of Immunology,* 186**,** 2462-2471.

SU, L.-C., XU, W.-D. & HUANG, A.-F. 2020. IRAK family in inflammatory autoimmune diseases. *Autoimmunity reviews,* 19**,** 102461.

SU, Y.-L., HUANG, H.-L., HUANG, B.-S., CHEN, P.-C., CHEN, C.-S., WANG, H.-L., LIN, P.-H., CHIEH, M.-S., WU, J.-J. & YANG, J.-C. 2016. Combination of OipA, BabA, and SabA as candidate biomarkers for predicting Helicobacter pylori-related gastric cancer. *Scientific reports,* 6**,** 36442.

SUN, Y., GAO, X., LIU, J., KONG, Q.-Y., WANG, X.-W., CHEN, X.-Y., WANG, Q., CHENG, Y.-F., QU, X.-X. & LI, H. 2011. Differential Notch1 and Notch2 expression and frequent activation of Notch signaling in gastric cancers. *Archives of pathology & laboratory medicine,* 135**,** 451-458.

SUZUKI, T., KATO, K., OHARA, S., NOGUCHI, K., SEKINE, H., NAGURA, H. & SHIMOSEGAWA, T. 2002. Localization of antigen-presenting cells in Helicobacter pylori-infected gastric mucosa. *Pathology international,* 52**,** 265-271.

SZALÓKI, N., KRIEGER, J. W., KOMÁROMI, I., TÓTH, K. & VÁMOSI, G. 2015. Evidence for homodimerization of the c-Fos transcription factor in live cells revealed by fluorescence microscopy and computer modeling. *Molecular and cellular biology,* 35**,** 3785-3798.

TERRY, K., WILLIAMS, S. M., CONNOLLY, L. & OTTEMANN, K. M. 2005. Chemotaxis plays multiple roles during Helicobacter pylori animal infection. *Infection and immunity,* 73**,** 803-811.

THORELL, K., BENGTSSON-PALME, J., LIU, O. H.-F., PALACIOS GONZALES, R. V., NOOKAEW, I., RABENECK, L., PASZAT, L., GRAHAM, D. Y., NIELSEN, J. & LUNDIN, S. B. 2017. In vivo analysis of the viable microbiota and Helicobacter pylori transcriptome in gastric infection and early stages of carcinogenesis. *Infection and immunity,* 85**,** 10.1128/iai. 00031-17.

THUNG, I., ARAMIN, H., VAVINSKAYA, V., GUPTA, S., PARK, J., CROWE, S. & VALASEK, M. 2016. the global emergence of Helicobacter pylori antibiotic resistance. *Alimentary pharmacology & therapeutics,* 43**,** 514-533.

TOMIOKA, N., MORITA, K., KOBAYASHI, N., TADA, M., ITOH, T., SAITOH, S., KONDO, M., TAKAHASHI, N., KATAOKA, A. & NAKANISHI, K. 2010. Array comparative genomic hybridization analysis revealed four genomic prognostic biomarkers for primary gastric cancers. *Cancer genetics and cytogenetics,* 201**,** 6-14.

TOSELLO, V. & FERRANDO, A. A. 2013. The NOTCH signaling pathway: role in the pathogenesis of T-cell acute lymphoblastic leukemia and implication for therapy. *Therapeutic advances in hematology,* 4**,** 199-210.

TRAN, A. X., STEAD, C. M. & TRENT, M. S. 2005. Remodeling of Helicobacter pylori lipopolysaccharide. *Journal of endotoxin research,* 11**,** 161-166.

TREHANPATI, N., SHRIVASTAV, S., SHIVAKUMAR, B., KHOSLA, R., BHARDWAJ, S., CHATURVEDI, J., KUMAR, B., BOSE, S., TRIPATHI, D. M. & DAS, T. 2012. Analysis of Notch and TGF-β signaling expression in different stages of disease progression during hepatitis B virus infection. *Clinical and translational gastroenterology,* 3**,** e23.

TRIPEPI, G., CHESNAYE, N. C., DEKKER, F. W., ZOCCALI, C. & JAGER, K. J. 2020. Intention to treat and per protocol analysis in clinical trials. *Nephrology,* 25**,** 513-517.

TU, S., BHAGAT, G., CUI, G., TAKAISHI, S., KURT-JONES, E. A., RICKMAN, B., BETZ, K. S., PENZ-OESTERREICHER, M., BJORKDAHL, O. & FOX, J. G. 2008. Overexpression of interleukin-1β induces gastric inflammation and cancer and mobilizes myeloid-derived suppressor cells in mice. *Cancer cell,* 14**,** 408-419.

UEDA, J., GOSHO, M., INUI, Y., MATSUDA, T., SAKAKIBARA, M., MABE, K., NAKAJIMA, S., SHIMOYAMA, T., YASUDA, M. & KAWAI, T. 2014. Prevalence of H elicobacter pylori Infection by Birth Year and Geographic Area in Japan. *Helicobacter,* 19**,** 105-110.

UEMURA, N., OKAMOTO, S., YAMAMOTO, S., MATSUMURA, N., YAMAGUCHI, S., YAMAKIDO, M., TANIYAMA, K., SASAKI, N. & SCHLEMPER, R. J. J. N. E. J. O. M. 2001. Helicobacter pylori infection and the development of gastric cancer. 345**,** 784-789.

VALLVE, M., VERGARA, M., GISBERT, J. & CALVET, X. 2002. Single vs. double dose of a proton pump inhibitor in triple therapy for Helicobacter pylori eradication: a meta-analysis. *Alimentary pharmacology & therapeutics,* 16**,** 1149-1156.

VAN BLANKENSTEIN, M., VAN VUUREN, A. J., LOOMAN, C. W., OUWENDIJK, M. & KUIPERS, E. J. 2013. The prevalence of Helicobacter pylori infection in the Netherlands. *Scandinavian journal of gastroenterology,* 48**,** 794-800.

VAN MIERLO, G., VEENSTRA, G. J. C., VERMEULEN, M. & MARKS, H. 2019. The complexity of PRC2 subcomplexes. *Trends in cell biology,* 29**,** 660-671.

VÁZQUEZ-ULLOA, E., LIZANO, M., SJÖQVIST, M., OLMEDO-NIEVA, L. & CONTRERAS-PAREDES, A. 2018. Deregulation of the Notch pathway as a common road in viral carcinogenesis. *Reviews in medical virology,* 28**,** e1988.

VIALA, J., CHAPUT, C., BONECA, I. G., CARDONA, A., GIRARDIN, S. E., MORAN, A. P., ATHMAN, R., MÉMET, S., HUERRE, M. R. & COYLE, A. 2004. Nod1 responds to peptidoglycan delivered by the Helicobacter pylori cag pathogenicity island. *Nature immunology,* 5**,** 1166.

VILLORIA, A., GARCIA, P., CALVET, X., GISBERT, J. & VERGARA, M. 2008. Meta-analysis: high-dose proton pump inhibitors vs. standard dose in triple therapy for Helicobacter pylori eradication. *Alimentary pharmacology & therapeutics,* 28**,** 868-877.

WANG, L., SHI, J., HUANG, Y., LIU, S., ZHANG, J., DING, H., YANG, J. & CHEN, Z. 2019. A six-gene prognostic model predicts overall survival in bladder cancer patients. *Cancer cell international,* 19**,** 1-15.

WANG, S., MIURA, M., JUNG, Y.-K., ZHU, H., LI, E. & YUAN, J. 1998. Murine caspase-11, an ICE-interacting protease, is essential for the activation of ICE. *Cell,* 92**,** 501-509.

WANG, Y.-K., KUO, F.-C., LIU, C.-J., WU, M.-C., SHIH, H.-Y., WANG, S. S., WU, J.-Y., KUO, C.-H., HUANG, Y.-K. & WU, D.-C. 2015. Diagnosis of Helicobacter pylori infection: Current options and developments. *World Journal of Gastroenterology: WJG,* 21**,** 11221.

WEI, X., WANG, J.-P., HAO, C.-Q., YANG, X.-F., WANG, L.-X., HUANG, C.-X., BAI, X.-F., LIAN, J.-Q. & ZHANG, Y. 2016. Notch signaling contributes to liver inflammation by regulation of interleukin-22-producing cells in hepatitis B virus infection. *Frontiers in cellular and infection microbiology,* 6**,** 132.

WEN, J., CHEN, C., LUO, M., LIU, X., GUO, J., WEI, T., GU, X., GU, S., NING, Y. & LI, Y. 2021. Notch Signaling Ligand Jagged1 Enhances Macrophage-Mediated Response to Helicobacter pylori. *Frontiers in Microbiology,* 12**,** 1741.

WEN, S., FELLEY, C. P., BOUZOURENE, H., REIMERS, M., MICHETTI, P. & PAN-HAMMARSTRÖM, Q. 2004. Inflammatory gene profiles in gastric mucosa during Helicobacter pylori infection in humans. *The Journal of Immunology,* 172**,** 2595-2606.

WHITNEY, A. E., EMORY, T. S., MARTY, A. M., O'SHEA, P. A., NEWMAN, G. W. & GOLD, B. D. 2000. Increased macrophage infiltration of gastric mucosa in Helicobacter pylori-infected children. *Digestive diseases and sciences,* 45**,** 1337-1342.

WINDLE, H. J., FOX, A., NíEIDHIN, D. I. & KELLEHER, D. 2000. The thioredoxin system of Helicobacter pylori. *Journal of Biological Chemistry,* 275**,** 5081-5089.

WOLF, J. S., CHEN, Z., DONG, G., SUNWOO, J. B., BANCROFT, C. C., CAPO, D. E., YEH, N. T., MUKAIDA, N. & WAES, C. V. 2001. IL (interleukin)-1α promotes nuclear factor-κB and AP-1-induced IL-8 expression, cell survival, and proliferation in head and neck squamous cell carcinomas. *Clinical Cancer Research,* 7**,** 1812-1820.

WONG, W. M., GU, Q., WANG, W. H., FUNG, F. M.-Y., BERG, D. E., LAI, K. C., XIA, H. H.-X., HU, W. H. C., CHAN, C. K., CHAN, A. O.-O., YUEN, M.-F., HUI, C.-K., LAM, S. K. & WONG, B. C.-Y. 2003. Effects of Primary Metronidazole and Clarithromycin Resistance to Helicobacter pylori on Omeprazole, Metronidazole, and Clarithromycin Triple-Therapy Regimen in a Region with High Rates of Metronidazole Resistance. *Clinical Infectious Diseases,* 37**,** 882-889.

WROBLEWSKI, L. E., PEEK JR, R. M. & WILSON, K. T. 2010. Helicobacter pylori and gastric cancer: factors that modulate disease risk. *Clinical microbiology reviews,* 23**,** 713-739.

XIANG, Y., ZHU, Z., HAN, G., LIN, H., XU, L. & CHEN, C. D. 2007. JMJD3 is a histone H3K27 demethylase. *Cell research,* 17**,** 850-857.

YAGUCHI, T., SAITO, M., YASUDA, Y. & NISHIZAKI, T. 2010. Caspase-4 activation in association with decreased adenosine deaminase activity may be a factor for gastric ulcer. *Digestion,* 81**,** 62-67.

YAHIRO, K., SATOH, M., NAKANO, M., HISATSUNE, J., ISOMOTO, H., SAP, J., SUZUKI, H., NOMURA, F., NODA, M. & MOSS, J. 2012. Low-density lipoprotein receptor-related protein-1 (LRP1) mediates autophagy and apoptosis caused by Helicobacter pylori VacA. *Journal of Biological Chemistry,* 287**,** 31104-31115.

YANG, T., ARSLANOVA, D., GU, Y., AUGELLI-SZAFRAN, C. & XIA, W. 2008. Quantification of gamma-secretase modulation differentiates inhibitor compound selectivity between two substrates Notch and amyloid precursor protein. *Molecular brain,* 1**,** 1-13.

YAP, T. W.-C., GAN, H.-M., LEE, Y.-P., LEOW, A. H.-R., AZMI, A. N., FRANCOIS, F., PEREZ-PEREZ, G. I., LOKE, M.-F., GOH, K.-L. & VADIVELU, J. 2016. Helicobacter pylori eradication causes perturbation of the human gut microbiome in young adults. *PloS one,* 11**,** e0151893.

YI, Y. S. 2017. Caspase-11 non-canonical inflammasome: a critical sensor of intracellular lipopolysaccharide in macrophage-mediated inflammatory responses. *Immunology,* 152**,** 207-217.

YOSHIDA, A., ISOMOTO, H., HISATSUNE, J., NAKAYAMA, M., NAKASHIMA, Y., MATSUSHIMA, K., MIZUTA, Y., HAYASHI, T., YAMAOKA, Y. & AZUMA, T. 2009. Enhanced expression of CCL20 in human Helicobacter pylori-associated gastritis. *Clinical Immunology,* 130**,** 290-297.

YOU, Y.-H., SONG, Y.-Y., MENG, F.-L., HE, L.-H., ZHANG, M.-J., YAN, X.-M. & ZHANG, J.-Z. 2010. Time-series gene expression profiles in AGS cells stimulated with Helicobacter pylori. *World Journal of Gastroenterology: WJG,* 16**,** 1385.

ZAGARI, R. M., RABITTI, S., EUSEBI, L. H. & BAZZOLI, F. E. J. O. C. I. 2018. Treatment of Helicobacter pylori infection: A clinical practice update. *European journal of clinical investigation,* 48**,** e12857.

ZASŁONA, Z., FLIS, E., NULTY, C., KEARNEY, J., FITZGERALD, R., DOUGLAS, A. R., MCNAMARA, D., SMITH, S., O'NEILL, L. A. J. & CREAGH, E. M. 2020a. Caspase-4: A Therapeutic Target for Peptic Ulcer Disease. *ImmunoHorizons,* 4**,** 627-633.

ZASŁONA, Z., FLIS, E., WILK, M. M., CARROLL, R. G., PALSSON-MCDERMOTT, E. M., HUGHES, M. M., DISKIN, C., BANAHAN, K., RYAN, D. G., HOOFTMAN, A., MISIAK, A., KEARNEY, J., LOCHNIT, G., BERTRAMS, W., GREULICH, T., SCHMECK, B., MCELVANEY, O. J., MILLS, K. H. G., LAVELLE, E. C., WYGRECKA, M., CREAGH, E. M. & O'NEILL, L. A. J. 2020b. Caspase-11 promotes allergic airway inflammation. *Nat Commun,* 11**,** 1055.

ZHANG, B., XU, A., WU, D., XIA, W., LI, P., WANG, E., HAN, R., SUN, P., ZHOU, S. & WANG, R. 2021. ARL14 as a prognostic biomarker in non-small cell lung cancer. *Journal of Inflammation Research,* 14**,** 6557.

ZHANG, C., JING, L.-W., LI, Z.-T., CHANG, Z.-W., LIU, H., ZHANG, Q.-M. & ZHANG, Q.-Y. 2019. Identification of a prognostic 28-gene expression signature for gastric cancer with lymphatic metastasis. *Bioscience Reports,* 39.

ZHANG, X., LI, C., CHEN, D., HE, X., ZHAO, Y., BAO, L., WANG, Q., ZHOU, J. & XIE, Y. 2022. H. pylori CagA activates the NLRP3 inflammasome to promote gastric cancer cell migration and invasion. *Inflammation Research,* 71**,** 141-155.

ZHANG, X., WENG, C., LI, Y., WANG, X., JIANG, C., LI, X., XU, Y., CHEN, Q., PAN, L. & TANG, H. 2012a. Human Bop is a novel BH3-only member of the Bcl-2 protein family. *Protein & cell,* 3**,** 790-801.

ZHANG, X., YANG, Y., ZHU, R., BAI, J., TIAN, Y., LI, X., PENG, Z., HE, Y., CHEN, L. & FANG, D. 2012b. H. pylori induces the expression of Hath1 in gastric epithelial cells via interleukin-8/STAT3 phosphorylation while suppressing Hes1. *Journal of cellular biochemistry,* 113**,** 3740-3751.

ZHAO, P., LU, Y. & LIU, L. 2015. Correlation of decreased expression of PHLDA1 protein with malignant phenotype of gastric adenocarcinoma. *International journal of clinical and experimental pathology,* 8**,** 5230.

ZHAO, T.-X. & WANG, Z.-L. 2022. GraphBio: a shiny web app to easily perform popular visualization analysis for omics data. *bioRxiv*.

ZHU, Y., ZHOU, X., WU, J., SU, J., ZHANG, G. J. G. R. & PRACTICE 2014. Risk factors and prevalence of Helicobacter pylori infection in persistent high incidence area of gastric carcinoma in Yangzhong city. 2014.

ZUMLA, A., RAO, M., WALLIS, R. S., KAUFMANN, S. H., RUSTOMJEE, R., MWABA, P., VILAPLANA, C., YEBOAH-MANU, D., CHAKAYA, J. & IPPOLITO, G. J. T. L. I. D. 2016. Host-directed therapies for infectious diseases: current status, recent progress, and future prospects. 16**,** e47-e63.

Appendices

Appendix A: Aseptic technique

Strict aseptic technique was maintained to ensure sterility of cultured bacterial and mammalian cells. Bacterial and mammalian cell culture work was carried out in dedicated Class 2 laminar flow hood biological Safety cabinets which passes air through a high efficiency particle air (HEPA) filter preventing contamination from external airborne contaminants. As standard, the fans in both cabinets were maintained switched on or allowed to run for 20-30 minutes before work commenced. Each time a laminar flow hood was used it was disinfected, first with 2% Trigene followed by 70% industrial methylated spirit (IMS) before commencing work and again after work had been completed. The grate allowing air flow was kept clear in both hoods and any work took place away from the grate. Work surfaces were kept clear of clutter and organised with labelled reagents. Liquid waste from cell culture, such as used media, was decontaminated in a sealed container containing overnight, in an equal volume of Sodium NaDCC solution. This was prepared by adding 4 X 2.5g Presept tablets (Johnson and Johnson) to 5L of water. Since NaDCC is inactivated by contact with organic material, fresh disinfectant was used each day. Only one cell line was used at a time in the cabinet. This prevented overcrowding and cross-contamination of cell lines. Separate bottles of media were used for each cell line to prevent cross-contamination. Cultures and media were examined regularly to check for gross bacterial or fungal contamination.

Liquid and plastic waste, such as pipette tips and flasks that were contaminated with bacteria were decontaminated in NaDCC solution overnight. This was prepared by adding 2 X 2.5g Presept tablets (Johnson and Johnson) to 1L of water. The plastics were then put in yellow biohazard bins. Used agar plates were sealed with parafilm (Bemis), put in an

autoclavable bag and autoclaved before disposal. Disposable Nitrile gloves (sprayed with 70% IMS) were always worn when working with cell cultures or bacteria and changed regularly as required.

Appendix B: Bacteria Culture Media

Preparation of Columbia blood agar (CBA) plates

19.5g of Columbia blood agar base (Oxoid; CM0331) was dissolved in 500ml of distilled water and sterilized by autoclaving on a liquid cycle (121°C for 15 min). The mixture was cooled to 45-50°C and 25ml (5%) laked horse blood (Fisher) was added to the agar in a laminar air flow cabinet. If selective plates were required, 500µl of a 1:1000 stock of kanamycin was added to make a final kanamycin concentration of 50µg/ml. 15-20ml of agar was poured into each petri dish (Fisher). The plates were left to cool and stored upside down at 4°C until required.

Preparation of Brain-Heart infusion medium

3.7g of Brain-Heart infusion broth base powder (Sigma; 53286-100G) was dissolved in 100ml of distilled water and sterilized by autoclaving on a liquid cycle (121°C for 15 min). The medium was cooled and stored at 4°C until required.

Preparation of Selective Agar Lysogeny broth plates

18.5g lysogeny broth (LB) agar base powder (Sigma L3147) was dissolved in 500ml of distilled water and autoclaved on a liquid cycle (121°C for 15 minutes). The medium was cooled to approximately 50°C and Ampicillin was added to a final concentration of 100µg/ml. Approximately 20ml was poured into each sterile Petri dish. The plates were cooled until solid and stored upside down at 4°C until required.

Preparation of Selective LB broth

12.5 g LB broth base powder (Sigma L3522) was dissolved in 500ml of distilled water and sterilized by autoclaving on a liquid cycle (121°C for 15 min). The medium was cooled to approximately 50°C and Ampicillin was added to a final concentration of 100µg/ml. The medium was stored at 4°C until required.

Appendix C: Qiagen RNA purification protocol

If the cell culture samples were purified using the RNeasy Mini Kit (Qiagen, Cat No./ID: 74104) the cells were collected using 500µl of RLT lysis buffer (Qiagen) per well in a 6 well plate or 350µl of RLT lysis buffer (Qiagen) per well in a 12 well or 24 well plate. 600 µl of RLT lysis buffer was added each biopsy sample and homogenised using the TissueRuptor (Qiagen).

Before commencing, the lyophilized DNase I (RNase-Free DNase Set (Qiagen; 79254)) was dissolved in 550µl of RNase-free water by injecting the water into the vial and mixing gently. The DNase I was aliquoted and stored at -20°C. Buffer RPE (RNeasy Mini Kit (Qiagen)) was diluted in 4 volumes of 98% Ethanol. Samples were defrosted on ice and a solution of 70% ethanol was prepared.

A 1:1000 dilution of ß-Mercaptoethanol was added to each sample. 1 volume of 70% ethanol was added to the lysate and mixed by pipetting up and down. Up to 700µl of the sample was transferred at a time to an RNA mini spin column which was placed into a 2ml collection tube and centrifuged for 30 seconds at 8,000 RCF. The flow through was discarded and this was repeated until all the lysate was gone. 350µl of buffer RW1 was added to the spin column and centrifuged for 30 seconds at 8,000 RCF, and the flow through was discarded. The RNase-Free Dnase Set (Qiagen) was used to digest DNA during RNA purification. A master mix was made containing

10µl of Dnase1 and 70µl of buffer RDD per sample. 75µl of master mix was added to each column and incubated at room temperature for 15 minutes. The columns were spun in the centrifuge for 30 seconds at 8,000 RCF and the flow through was discarded. Another 350µl of buffer RW1 was added to the spin column and spun for 30 seconds at 8,000 RCF and the flow through was discarded. 500µl of buffer RPE was added to each column and spun for 30 seconds at 8,000 RCF and the flow through was discarded. A further 500µl of buffer RPE was added and spun in the centrifuge for 2 minutes at 8,000 RCF. The spin columns were placed into clean collection tubes and spun in the centrifuge for 60 seconds at full speed to dry the membrane. The columns were placed into labelled Eppendorf tubes and 30-50µl of RNase free water was added directly onto each membrane. The columns were spun for 60 seconds at 8,000 RCF. To ensure a high yield of RNA the eluate was re-filtered through the column followed by centrifugation for 60 seconds at 8,000 RCF. The samples were kept at -80°C until required.

Appendix D: The number of prescriptions for each first line treatment each year

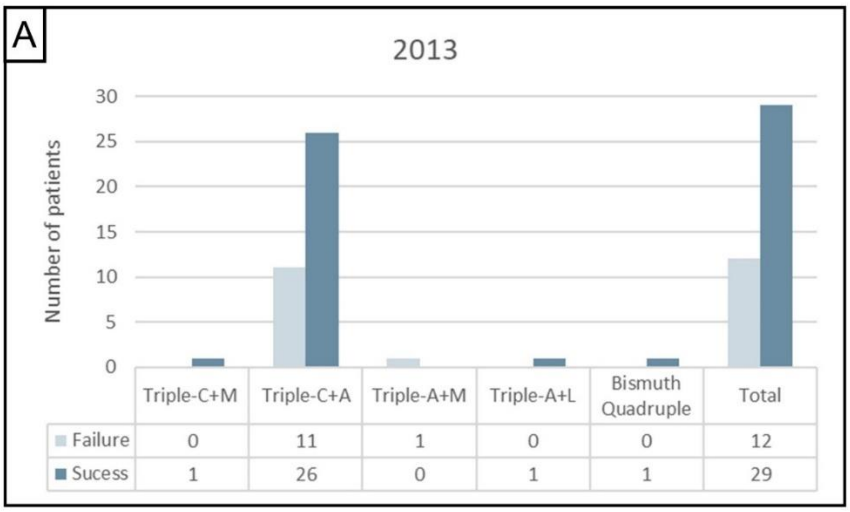

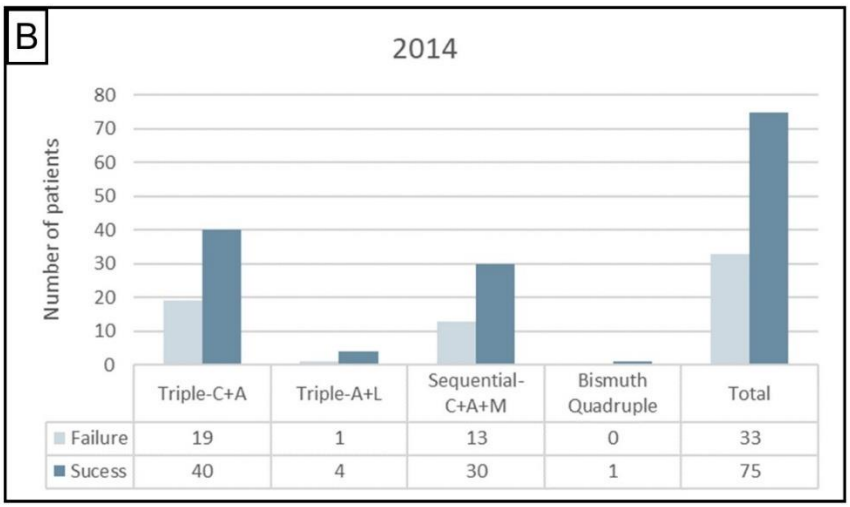

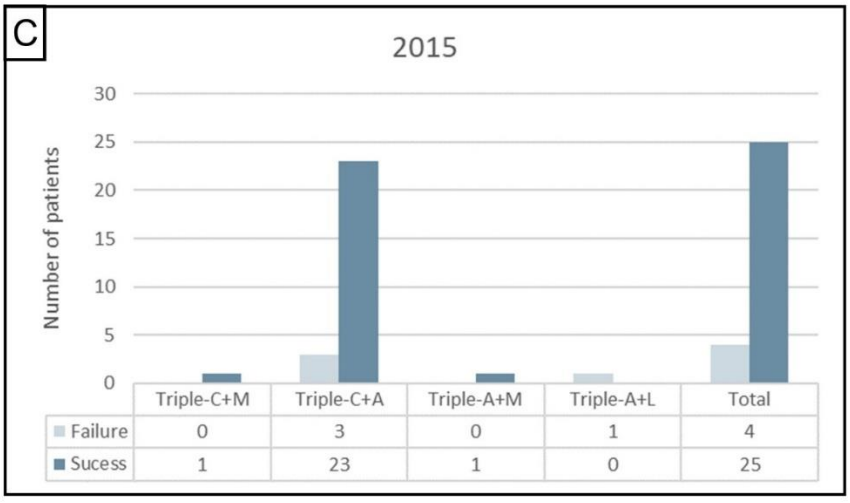

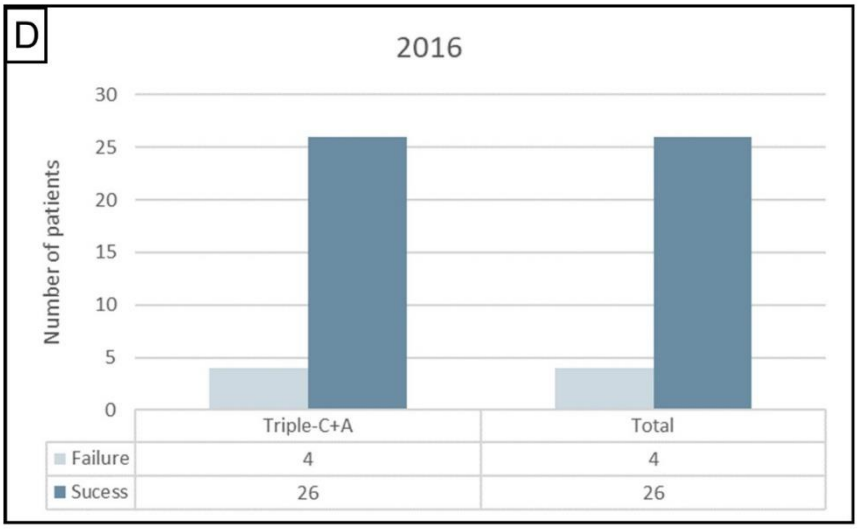
D
2016
Number of patients
30
25
20
15
10
5
0
Triple-C+A
Total
Failure
4
4
Sucess
26
26

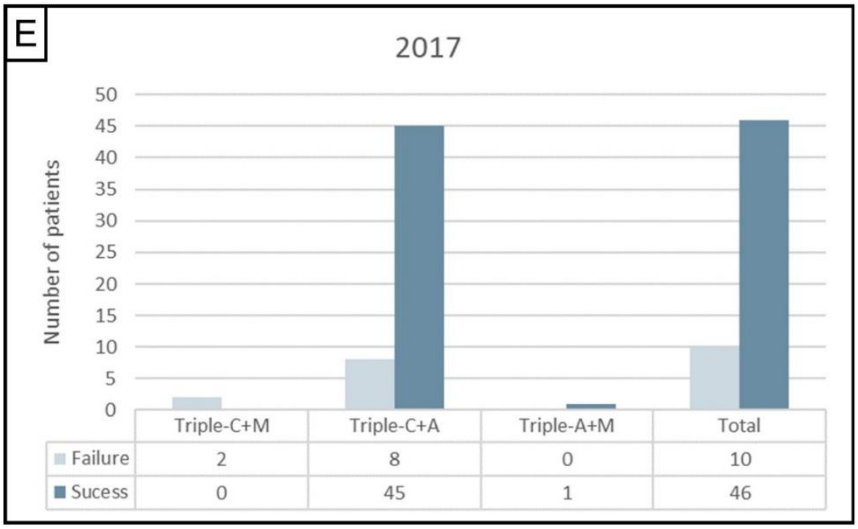
E
2017
Number of patients
50
45
40
35
30
25
20
15
10
5
0
Triple-C+M
Triple-C+A
Triple-A+M
Total
Failure
2
8
0
10
Sucess
0
45
1
46

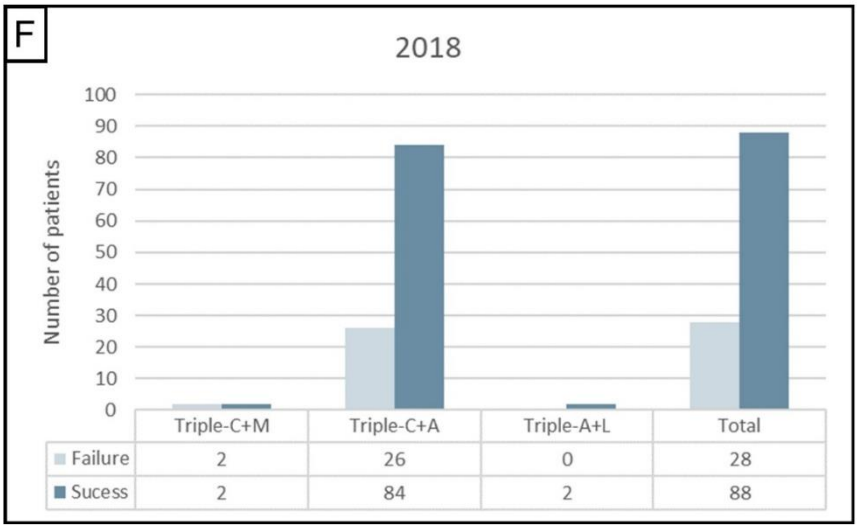
F
2018
Number of patients
100
90
80
70
60
50
40
30
20
10
0
Triple-C+M
Triple-C+A
Triple-A+L
Total
Failure
2
26
0
28
Sucess
2
84
2
88

G

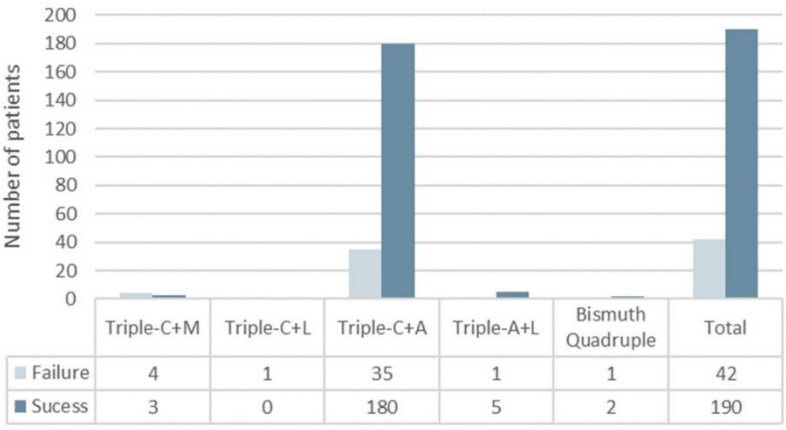

	Triple-C+M	Triple-C+L	Triple-C+A	Triple-A+L	Bismuth Quadruple	Total
Failure	4	1	35	1	1	42
Sucess	3	0	180	5	2	190

H

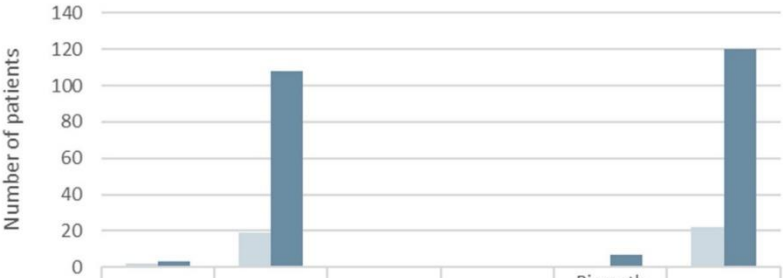

	Triple-C+M	Triple-C+A	Triple-A+M	Triple-A+L	Bismuth Quadruple	Total
Failure	2	19	0	1	0	22
Success	3	108	1	1	7	120

I

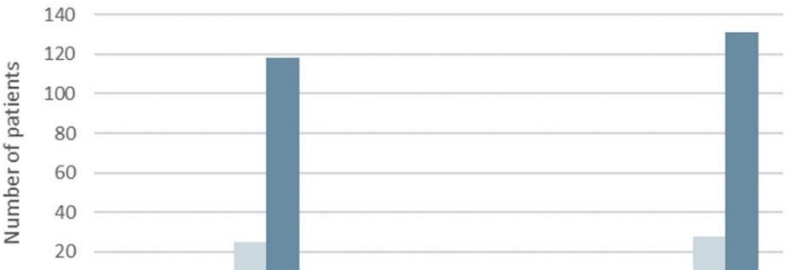

	Triple-C+M	Triple-C+A	Triple-A+M	Triple-A+L	Bismuth Quadruple	Total
Failure	2	25	1	0	0	28
Sucess	3	118	5	1	4	131

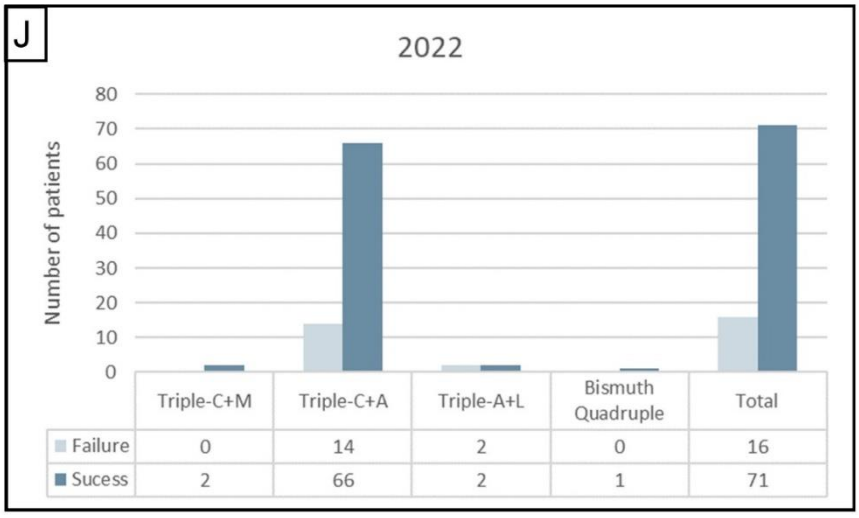

Number of patients treated with each regime broken down per year. A) 2013, B) 2014, C) 2015, D) 2016, E) 2107, F) 2018, G) 2019, H) 2020, I) 2021, J) 2022.